

# **Novel Phosphaalkene-Based Late Transition Metal Complexes: Synthesis and Applications**

Cumulative Dissertation

in partial fulfillment for the degree of

***doctor rerum naturalium (Dr. rer. nat.)***

at the University of Rostock

Faculty for Mathematics and Natural Sciences

submitted by

**M.Sc. Priyanka Gupta**

Born 09. 26. 1995, India.

**Leibniz Institute for Catalysis**

**2022**



# **Selbstständigkeitserklärung**

Ich versichere hiermit an Eides statt, dass ich die vorliegende Arbeit selbständig angefertigt und ohne fremde Hilfe verfasst habe, keine außer die von mir angegebenen Hilfsmittel und Quellen dazu verwendet habe und die den benutzten Werken inhaltlich und wörtlich entnommenen Stellen als solche kenntlich gemacht habe.

Rostock, den 03.05.2023

Priyanka Gupta





# Reviewers

**First reviewer:** Prof. Dr. Torsten Beweries

Modern Concepts in Molecular Catalysis

Leibniz Institute for Catalysis

**Second reviewer:** Dr. Christian Hering-Junghans

Catalysis of Phosphorus Materials

Leibniz Institute for Catalysis

**Third reviewer:** Prof. Dr. Robert wolf

Institute of Inorganic Chemistry

University of Regensburg

**Fourth reviewer:** Prof. Dr. Jarl Ivar van der Vlugt

Institute for Chemistry

University of Oldenburg

**Submitted on:** 12<sup>th</sup> December, 2022

**Defense date:** 4<sup>th</sup> April, 2023



## **Acknowledgements**

First and foremost, I am extremely grateful to my supervisors, Prof. Dr. Torsten Beweries and Dr. Christian Hering-Junghans for providing me this wonderful opportunity to carry out my doctoral studies under their guidance. Their immense knowledge and plentiful experience have encouraged me in all the time of my academic research and daily life. I deeply value their work ethics and supervision skills. It is their constant motivation and support that have made my student life in Germany a wonderful time. I am extremely thankful for believing in me and allowing me to grab all the opportunities coming my way. Undoubtedly, I could not have a better Ph.D. experience.

I would like to offer my special thanks to Dr. Fabian Reiß for his insightful lecture series on DFT calculations and Dr. Hans-Joachim Drexler for patiently performing SC-XRD experiments on all of my crystals and for valuable suggestions during group meetings.

I would like to extend my thanks to LIKAT, Rostock for providing financial support that allowed me to conduct the research for this thesis. Also, my appreciation goes out to Dr. Anke Spannenberg, Dr. Wolfgang Baumann, Mr. Andreas Koch, Mrs. Astrid Lehmann, Mrs. Susann Buchholz, and the other colleagues of the analytic department for their precise analysis and generous support.

I am indebted to wonderful members of my group, Alexander Linke, Jan-Erik Siewert, Tim Wellnitz, Andre Schumann, Dr. Xinzhe Shi, Kevin Lindenau, David Decker, Benjamin Andres, Laura Tadiello, Nora Jannsen, Sihan Li, Dr. Tobias Täufer, Thea Mayer, Mirko Rippke, Hanan Maher Alhamwi, Carmen Selle, Cornelia Pribbenow and Prof. Dr. Detlef Heller for being so accommodating and providing a pleasant working atmosphere. It was so easy working with all of you and I will always cherish the time that we spent together.

I would also like to sincerely thank all my friends and colleagues in Germany, Pratik Deshmukhe, Neerja Jaishankar, Shital Kale, Vishwas Chandrashekhar, Rajesh Dasi, Fairoosa

## *Acknowledgements*

---

Poovan, Sara Kopf, Weiheng Huang, Trang Pham, Vishal Budhija, Vishal Chugh, Soumyashree Jena, for all the good time that we had together.

A big share of my gratitude goes to all the teachers whose positive influence have shaped my life. My special thanks go to Mr. Ankur Goyal, my first chemistry teacher, for teaching exceptionally well and developing my interest in chemistry. It was his classes where my love for chemistry actually began.

I am immensely thankful to the biggest cheerleader of my life, my best friend and my partner for life, Abhishek Rastogi, for always being there for me through thick and thin. I would like to extend my thanks to my dearest friends, Isha Yadav, Megha Goel, Deven Kakran, Komal Bajaj, Poonam Silori, Anand Swaroop, Khushboo Gupta, Manisha Gupta, for being my moral support and celebrating every small victory of mine.

Last but not least, I would like to thank the most important people in my life, my parents, Mr. Vinod Kumar Gupta, and Mrs. Rajni Gupta. I am grateful to God for giving me such supportive and loving parents. I could not have done this without you. Additionally, I would like to thank my siblings, Garima Dua and Shivam Gupta, and my brother-in-law, Kunal Dua, for backing me up in all my decisions and loving me unconditionally.

My gratitude to all the mentioned people knows no boundaries. Thankyou!

## Abstract

The content of this thesis is presented into four parts. The first part mainly focuses on describing the electronic structure of phosphalkenes and their synthesis. Generally, phosphalkenes are synthesized using the following routes: The “phospha-Peterson reaction” and the “phospha-Wittig reaction”. Phosphalkenes prepared as a part of this thesis were synthesized using phospha-Wittig reagents in the reaction with suitable aldehydes. Phospha-Wittig reagents have been discussed in detail in the second chapter. Phosphanylidene phosphoranes or phospha-Wittig reagents can be considered as phosphine-stabilized phosphinidenes. Apart from their structural characterization, the synthetic potential of phospha-Wittig reagents in phosphinidene-transfer reactions has been explored. Phosphalkenes possess unique electronic properties (poor  $\sigma$ -donor, strong  $\pi$ -acceptor) which make them particularly attractive as ligands for application in late transition metal catalysis. The last two chapters comprise of the selected examples to illustrate the strong  $\pi$  accepting properties of phosphalkene ligands in coordination chemistry and late transition metal catalysis. These ligands have stabilized late transition metals like Ir, Rh and Pd in unusual geometries showcasing interesting E–H (E = C, N) activation reactions and reactivity in catalysis. The use of phosphalkene ligands in catalytic transformations like ethylene polymerization, cross-coupling and cycloisomerization have been discussed along with some other examples.

Diese Arbeit ist in vier Teile gegliedert. Im ersten Teil wird die elektronische Struktur von Phosphalkenen und deren Synthese. Im Allgemeinen werden Phosphalkene über die folgenden Wege synthetisiert: Die "Phospha-Peterson-Reaktion" und die "Phospha-Wittig-Reaktion". Die im Rahmen dieser Arbeit hergestellten Phosphalkene wurden unter Verwendung von Phospha-Wittig-Reagenzien in der Reaktion mit geeigneten Aldehyden synthetisiert. Die Eigenschaften und Reaktivitäten von Phospha-Wittig-Reagenzien werden im zweiten Kapitel ausführlich besprochen. Phosphanylidene phosphorane oder Phospha-Wittig-Reagenzien können als Phosphin-stabilisierte Phosphinidene angesehen werden. Neben ihrer strukturellen Charakterisierung wurde auch das synthetische Potenzial von Phospha-Wittig-Reagenzien in Phosphinidin-Transferreaktionen untersucht. Phosphalkene besitzen einzigartige elektronische Eigenschaften (schlechter  $\sigma$ -Donor, starker  $\pi$ -Akzeptor), die sie als Liganden für die Anwendung in der späten Übergangsmetallkatalyse besonders attraktiv machen. Die letzten beiden Kapitel enthalten ausgewählte Beispiele zur

Veranschaulichung der starken  $\pi$ -akzeptierenden Eigenschaften von Phosphaalken-Liganden in der Koordinationschemie und der späten Übergangsmetallkatalyse. So werden Ir, Rh und Pd in ungewöhnlichen Koordinationsgeometrien stabilisiert, was in interessanten E–H (E = C, N) Aktivierungsreaktionen und vielfältigen Reaktivitäten in der Katalyse resultiert. Die Verwendung von Phosphaalken-Liganden in katalytischen Umwandlungen wie der Ethylenpolymerisation, Kreuzkupplungsreaktionen und Cycloisomerisationen wird zusammen mit einigen anderen Beispielen diskutiert.

---

## Table of Contents

<b>1 Introduction.....</b>	<b>1</b>
<b>1.1 Phosphaalkenes.....</b>	<b>1</b>
<b>1.2 Electronic structure of phosphaalkenes .....</b>	<b>2</b>
<b>1.3 Synthesis of phosphaalkenes.....</b>	<b>3</b>
1.3.1 The phospho-Peterson reaction .....	4
1.3.2 The phospho-Wittig reaction .....	5
<b>2 Phosphanylidene phosphoranes.....</b>	<b>7</b>
<b>2.1 Introduction .....</b>	<b>7</b>
<b>2.2 Structural characterization of phosphanylidene phosphoranes .....</b>	<b>8</b>
<b>2.3 Phosphanylidene phosphoranes as phosphinidene transfer agents.....</b>	<b>8</b>
<b>3 Phosphaalkenes and their coordination chemistry .....</b>	<b>14</b>
<b>3.1 Coordination properties .....</b>	<b>14</b>
<b>3.2 Phosphaalkene complexes.....</b>	<b>15</b>
<b>4 Applications in homogeneous catalysis .....</b>	<b>20</b>
<b>4.1 Introduction .....</b>	<b>20</b>
<b>4.2 Ethylene polymerization .....</b>	<b>20</b>
<b>4.3 Cross-coupling reactions.....</b>	<b>22</b>
4.3.1 Sonogashira reactions.....	22
4.3.2 Suzuki-Miyaura reactions .....	23
4.3.3 Stille cross-coupling reactions.....	23
4.3.4 Cyanation reactions .....	23
4.3.5 C–N cross-coupling reactions .....	24
<b>4.4 Hydro- and dehydrosilylation .....</b>	<b>25</b>
4.4.1 Hydrosilylation.....	25
4.4.2 Dehydrogenative silylation.....	25
<b>4.5 Hydroamination and hydroamidation.....</b>	<b>26</b>
4.5.1 Hydroamination.....	26
4.5.2 Hydroamidation.....	27

4.6	Isomerization reactions .....	27
4.7	Allylic substitution.....	28
4.8	Asymmetric catalysis.....	30
5	Objectives of this work.....	31
6	List of publications .....	33
6.1	Reactivity of phospho-Wittig reagents towards NHCs and NHOs.....	35
6.2	Synthesis, coordination chemistry, and mechanistic studies of P,N-type phosphalkene-based Rh(I) complexes .....	43
6.3	Metal-free N-H bond activation by phospho-Wittig reagents .....	57
6.4	Deoxygenation of chalcogen oxides EO <sub>2</sub> (E = S, Se) with phospho-Wittig reagents..	65
6.5	P,N-Type phosphalkene-based Ir(I) complexes: synthesis, coordination chemistry, and catalytic applications .....	77
7	References .....	89
8	Curriculum vitae .....	93



## List of Abbreviations

AgOTf	silver triflate	<i>m</i>	<i>meta</i>
aq.	aqueous	[M]	metal
ar	aryl	Me	methyl
BPEP	2,6-bis(2-phosphaethenyl)pyridine	MeCN	acetonitrile
Bu	n-butyl	MeO	methoxy
calcd.	calculated	MeOH	methanol
Cat.	catalytic	Mes	mesityl
DBU	1,8-diazabicyclo[5,4,0]undec-7-ene	Mes*	2,4,6- <i>t</i> Bu <sub>3</sub> C <sub>6</sub> H <sub>2</sub>
DCM	dichloromethane	<sup>Mes</sup> Ter	2,6-(2,4,6-Me <sub>3</sub> C <sub>6</sub> H <sub>2</sub> )-C <sub>6</sub> H <sub>3</sub>
DFT	density function theory	M <sub>w</sub>	molecular weight
DMF	dimethylformamide	NBO	natural bond orbital
DPCB	1,2-diphenyl-3,4-diphosphinidene cyclobutene	NHO	<i>N</i> -heterocyclic olefin
e.g.	example	NHC	<i>N</i> -heterocyclic carbene
EIND	1,1,3,3,5,5,7,7-octaethyl-1,2,3,5,6,7-hexahydro- <i>s</i> -indacen-4-yl	NMP	<i>N</i> -methyl-2-pyrrolidone
equiv.	equivalent	NMR	nuclear magnetic resonance
Et	ethyl	Nuc	nucleophile
g	gramm	<i>o</i>	ortho
<i>gem</i>	geminal	OAc	acetate
h	hours	OEt	ethoxy
HCl	hydrochloric acid	PA	phosphaalkene
HOMO	highest occupied molecular orbital	PDI	polydispersity index
Hz	Hertz	PhAk-Ox	phosphaalkene-oxazoline
IBO	intrinsic bond orbital	PhNH <sub>2</sub>	phenyl aniline
<i>iPr</i>	isopropyl	PPEP	2-(phospholanylmethyl)-6-(2-phosphaethenyl)pyridine
IR	infrared spectroscopy	ppm	parts per million
KOtBu	potassium <i>tert</i> -butoxide	PPV	polyphenylene vinylenes
L	ligand	S <sub>N</sub> 2	bimolecular nucleophilic substitution
		THF	tetrahydrofuran
		TOF	turn over frequency
		<i>t</i> -Bu	<i>tert</i> -butyl
		<i>tert</i>	tertiary



# 1 Introduction

## 1.1 Phosphaalkenes

Phosphorus is ubiquitous in ligands. As noted by Mathey and co-workers, phosphorus can actually be regarded as multi-faceted element which can mimic either carbon or silicon or nitrogen depending on its coordination number.<sup>[1-2]</sup> Undoubtedly, the discovery of low coordinate phosphorus species featuring multiple bonding between phosphorus and other elements such as carbon and nitrogen will probably remain one of the most significant landmarks in this area. Prior to this breakthrough, it was generally accepted that heavier elements of the p-block would not form stable (3p–2p) $\pi$  bonds due to the well-known difficulty of heavier main group elements to achieve  $sp^2$  ( $\lambda^3\sigma^2$ ) (trivalent phosphorus atom with the coordination number 2) and  $sp$  ( $\lambda^3\sigma^1$ ) hybridization apart from their usual oxidation state, mainly  $\lambda^3\sigma^3$  and  $\lambda^5\sigma^4$  (Figure 1.1).

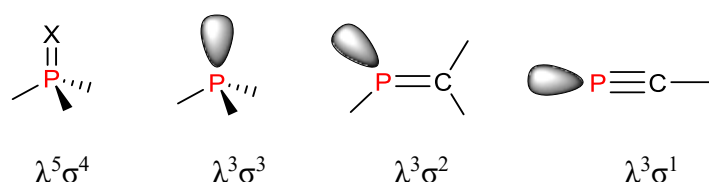


**Figure 1.1** Some coordination states of phosphorus.

The starting point for the chemistry of low-coordinated phosphorus compounds was in 1961, when Gier *et al.* reported that the phosphaacetylene  $H-C\equiv P$ , characterized in the gas phase using spectroscopic methods, could not be isolated in condensed form.<sup>[3]</sup> The first isolable compounds containing phosphorus–carbon multiple bonds were the phosphamethine cyanine<sup>[4]</sup> cations (**1**) and the phosphinines<sup>[5-6]</sup> (**2**, **3**) each benefiting from the delocalization of the  $P=C$  bond over multiple centers (Figure 1.2). The first isolable compounds with localized  $P=C$  bonds (**4**), phosphaalkenes, were prepared in 1976 by Becker and co-workers (Figure 1.3).<sup>[7]</sup> In 1978, Bickelhaupt and co-workers reported the first phosphaalkene bearing solely carbon substituents,  $MesP=CPh_2$  (**5**;  $Mes=2,4,6$ -trimethylphenyl) (Figure 1.3).<sup>[8]</sup> These early discoveries laid a foundation for the widespread growth that has occurred in the field of phosphaalkene chemistry as evidenced by the number of recent reviews dedicated to the subject.<sup>[9-15]</sup>

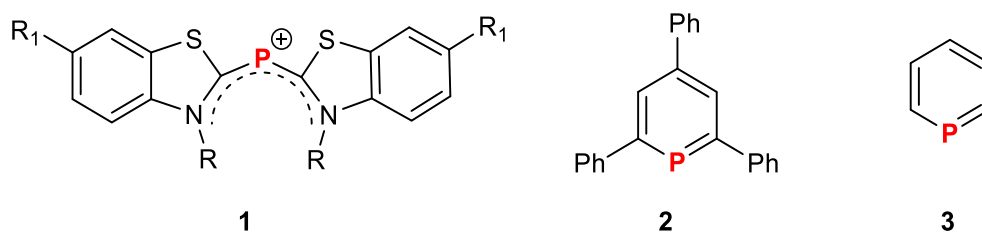


**Figure 1.2** The first isolable compounds containing phosphorus–carbon multiple bonds.

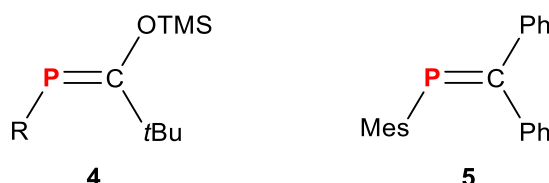


**Figure 1.3** The first isolable phosphalkenes.

## 1.2 Electronic structure of phosphalkenes

Phosphalkenes possess unique electronic properties which make them particularly attractive as ligands for applications in late transition metal catalysis. Phosphalkenes are often compared to their lighter group congener, imines ( $\text{HN}=\text{CH}_2$ ), in terms of their coordinating properties, however, there are significant electronic differences between these systems. Calculations on  $\text{HP}=\text{CH}_2$  have shown that the lone pair on phosphorus is not the highest in energy, but rather the HOMO-1, and features a very high 3s character (66%) (Figure 1.4).<sup>[16]</sup> On the contrary, in imines ( $\text{HN}=\text{CH}_2$ ), the HOMO describes the lone pair at nitrogen and features an inverted orbital distribution (39% s character), indicative of  $\text{sp}^2$  hybridization at N. The degree of the s-character affects the directionality of the lone pair and, consequently, the higher the s-character, the lower is the  $\sigma$  donation capacity. Experimentally, the high s-character of the lone pair, and therefore the low s-character of the  $\sigma$ -bonds, is supported by the reduced angle (between  $100^\circ$  and  $107^\circ$ ) formed by the substituent at phosphorus and the carbon atom compared to classical  $\text{sp}^2$  C- and N-based systems.<sup>[17]</sup> The P=C bond length within a phosphalkene is typically between 1.63 Å and 1.71 Å.

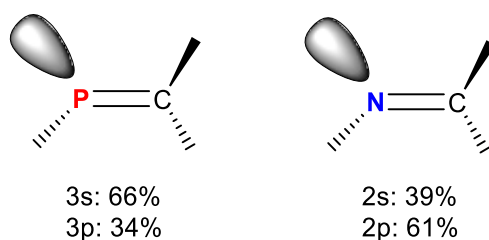


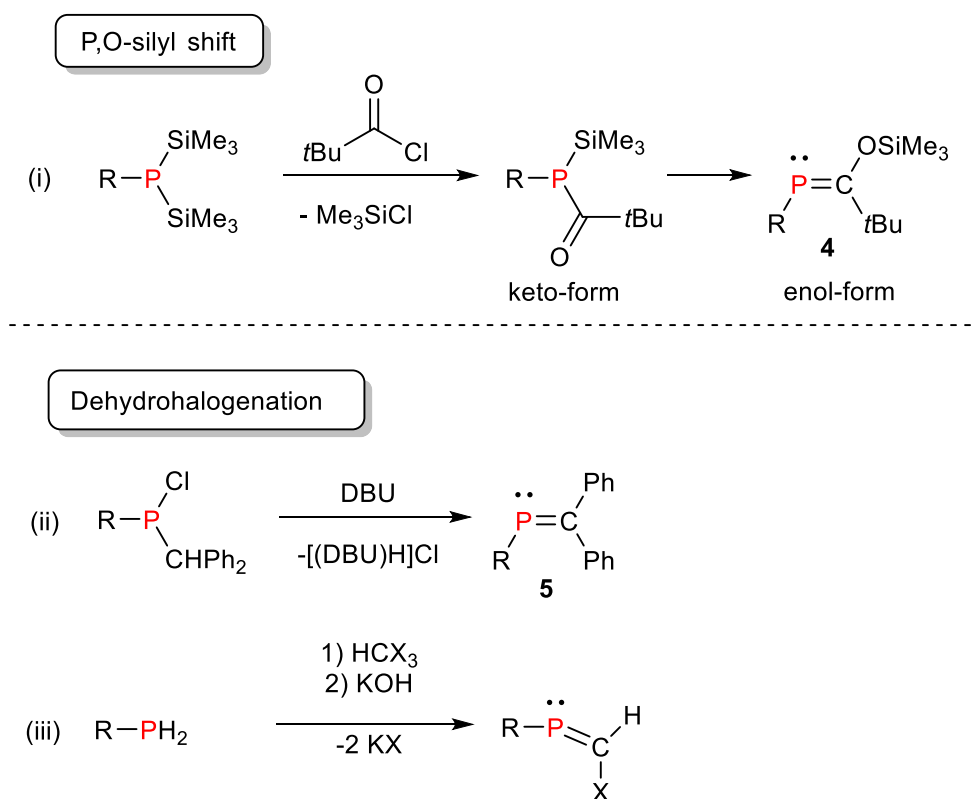
**Figure 1.4** Calculated lone pair molecular orbital compositions in  $\text{HP}=\text{CH}_2$  and  $\text{HN}=\text{CH}_2$ .

The electronegativity difference is a second major effect that helps to rationalize the differences observed in the respective reactivities of C=C-, N=C- and P=C-based systems. On the Pauling scale, phosphorus (2.1) is more electropositive than carbon (2.5) and nitrogen (3.0), suggesting that the P–C  $\sigma$ -bond is polarized slightly toward carbon. NBO calculations on HP=CH<sub>2</sub> reveal that a positive charge of +0.42 e resides at phosphorus, whereas HN=CH<sub>2</sub> has the reverse polarization with a build-up of negative charge on nitrogen (–0.59 e).<sup>[11]</sup> This polarization, combined with the high p-character of the lone pair on nitrogen, imparts better  $\sigma$ -donating properties to HN=CH<sub>2</sub> when compared to HP=CH<sub>2</sub>. Moreover, the P=C  $\pi$ -bond strength (45 kcal/mol in HP=CH<sub>2</sub>) is weaker than that of olefinic systems (65 kcal/mol for CH<sub>2</sub>=CH<sub>2</sub>) and as a result,<sup>[18-19]</sup> most of these phosphalkene derivatives only exist as isolable species upon significant kinetic stabilization. Due to the high s-character of the lone pair in phosphalkenes, their properties as  $\sigma$ -donors might be better compared to carbon monoxide rather than to imines. The lone pair on carbon in C≡O is formally in an sp-hybrid orbital (50% 2 s), which is similar in s-character to the lone pair of HP=CH<sub>2</sub> (66% 3s). The analogy between phosphalkenes and carbonyls can be further extended to their excellent  $\pi$ -accepting ability.<sup>[20]</sup> The electropositive character of phosphorus makes the  $\pi^*$  orbital in phosphalkenes rather low in energy and thus enhances their acceptor properties in transition-metal complexes, resulting in more effective back-bonding similar to CO. The characteristic  $\pi$ -acceptor and  $\sigma$ -donor properties of phosphalkenes combined with the potential to fine-tune the steric and electronic properties of the substituents in phosphalkenes have led to considerable excitement about the potential of P=C-based ligands in transition metal catalyzed reactions.

### 1.3 Synthesis of phosphalkenes

Numerous synthetic pathways toward phosphalkenes have been presented in the literature, offering a variety of methods to construct these systems. The first acyclic phosphalkene (**4**) was formed in the isomerization of silylacylphosphines R–P(SiMe<sub>3</sub>)–(COCR<sub>3</sub>) (obtained from bis-silylphosphines and acylchlorides) into its enol-form at room temperature with the concomitant formation of a P=C double bond facilitated by a silyl shift to the oxygen of the keto-function (Scheme 1.1, i).<sup>[21]</sup> Two years later, the synthesis of the first phosphalkene, MesP=CPh<sub>2</sub> (**5**), with localized P=C double bond was achieved by dehydrochlorination of a benzhydryl-substituted chlorophosphine R<sub>2</sub>PCl(CHPh<sub>2</sub>) in the presence of DBU as a scavenger of HCl (Scheme 1.1, ii).<sup>[8]</sup> In an alternative pathway, Mes\*PH<sub>2</sub> (Mes\* = 2,4,6-*t*Bu<sub>3</sub>C<sub>6</sub>H<sub>2</sub>) can be converted to the phosphalkene using strong alkaline solutions of chloroform or

dichloromethane (Scheme 1.1, iii). A carbene addition mechanism is most likely for this reaction.<sup>[22]</sup> More recently, P=C double bonds have been constructed using the phosphorus-variants of two famous synthetic pathways: The “phospha-Peterson route” and the “phospha-Wittig route”. In the next section, both of these synthetic routes will be discussed in detail.

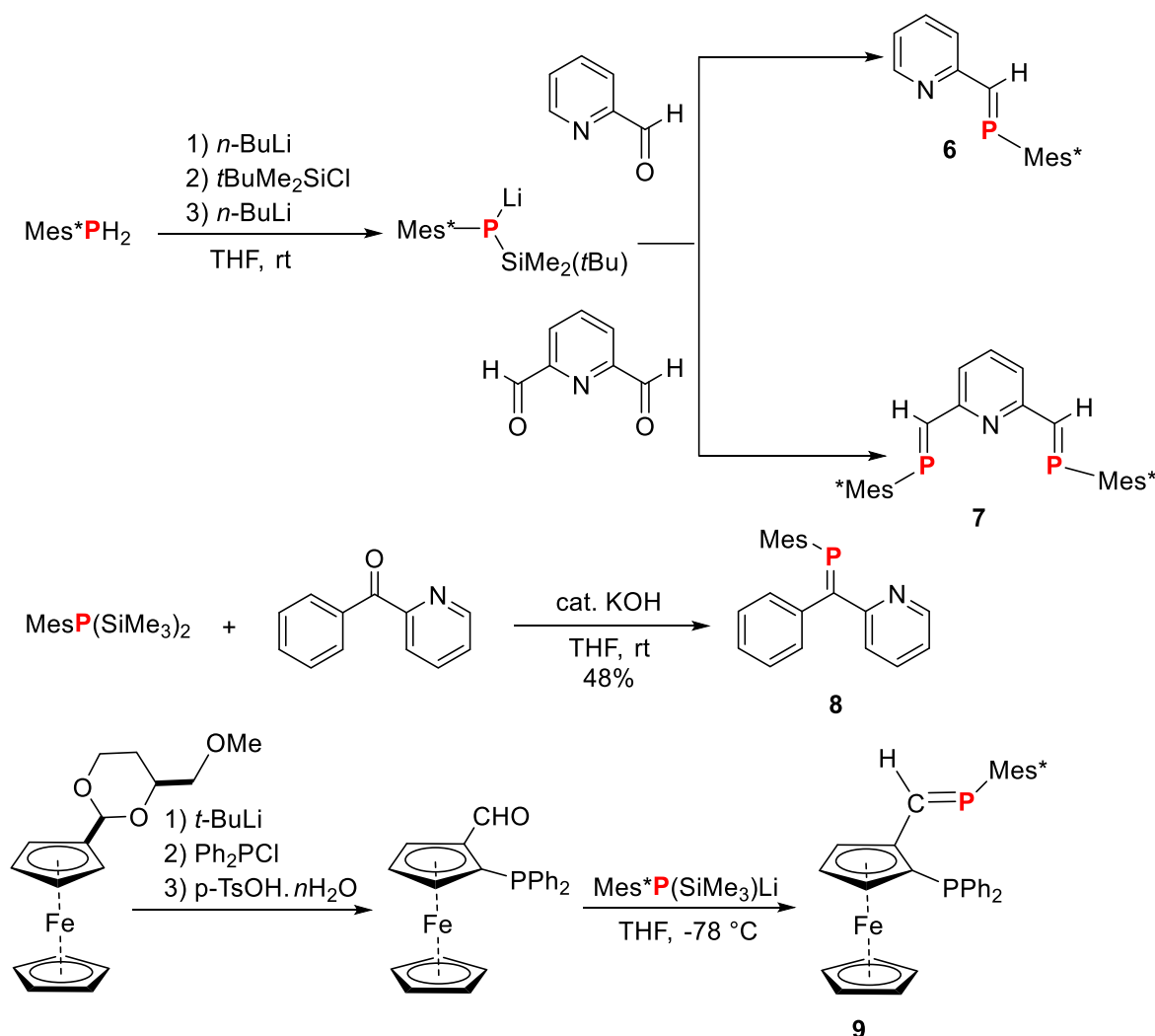


**Scheme 1.1** Different synthetic strategies towards phosphalkenes.

### 1.3.1 The phospha-Peterson reaction

Geoffroy and co-workers<sup>[23]</sup> and Yoshifuji and co-workers<sup>[24]</sup> reported a series of interesting kinetically protected mono-, di- (**6**) and tridentate (**7**) phosphalkene ligands following the Phospha-Petersen route that involves the reaction of a silylated anion of the type  $\text{RP}^{(-)}\text{Si}(t\text{-Bu})\text{Me}_2$  with an aldehyde (Scheme 1.2, top). The Gates group has further developed this synthetic route, using bis(silyl)phosphines as a starting material in a room temperature reaction with MeLi (1 equiv.) for the generation of reactive silyl phosphides. They have shown that starting from  $\text{MesP}(\text{SiMe}_3)_2$ , a variety of mesityl-substituted phosphalkenes could be isolated, among them the P,N-type ligand  $\text{MesP}=\text{C}(\text{Ph})(2\text{-pyridyl})$  (**8**).<sup>[25]</sup> P,N-chelating, chiral phosphalkenes have also been prepared using the Phospha-Peterson methodology. The development of chiral phosphalkene ligands for their use in asymmetric catalysis is an exciting prospect. The first examples of chiral, enantiomerically pure ferrocene-based phosphalkenes have recently appeared in the literature (**9**).<sup>[26]</sup> In some cases,

due to the difficulty in preparing the phospho-Peterson reagents, like EIND-P(SiMe<sub>3</sub>)Li (EIND = 1,1,3,3,5,5,7,7-octaethyl-1,2,3,5,6,7-hexahydro-*s*-indacen-4-yl), the phospho-Wittig pathway is considered a better approach.<sup>[27]</sup>

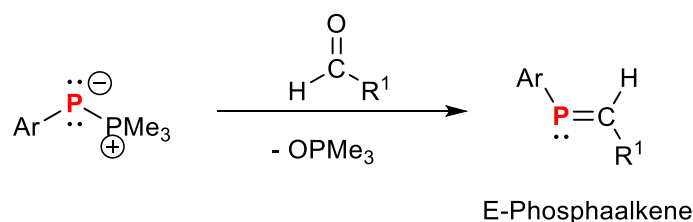


**Scheme 1.2** Synthesis of pyridyl phosphoalkenes (**6**, **7** and **8**) and chiral 1-phosphoethenyl-2-phosphanylferrocenes (**9**) via the phospho-Peterson route.

### 1.3.2 The Phospha-Wittig Reaction

In 1998, Protasiewicz *et al.* outlined the so-called “phospha-Wittig” reaction, using phosphanylidene-σ<sup>4</sup>-phosphoranes of the type Ar-P(PMe<sub>3</sub>) (Mes\*, <sup>Mes</sup>Ter = 2,6-(2,4,6-Me<sub>3</sub>C<sub>6</sub>H<sub>2</sub>)-C<sub>6</sub>H<sub>3</sub>)<sup>[28]</sup> to construct a variety of phosphoalkenes in the reaction with aldehydes in an *E*-selective manner (Scheme 1.3).<sup>[29]</sup> The “phospha-Wittig” concept has since been used to prepare a variety of P,N,P-,<sup>[30]</sup> P,P-,<sup>[31]</sup> and P,P,P,P-type (**11**) phosphoalkene ligands.<sup>[32]</sup> For example, Ozawa and co-workers presented various P,N,P-phosphoalkene systems with a pyridine backbone and sterically demanding Mes\* or EIND (**12**) substituents (Figure 1.5).<sup>[33]</sup>

Unlike PPEP (PPEP = 2-(phospholanylmethyl)-6-(2-phosphaethenyl)pyridine), bearing Mes\* as a steric protecting group of the P=C bond, EIND-PPEP (**12**) protected by a fused-ring bulky EIND group was sufficiently stable against C–H addition/cyclization.<sup>[33]</sup> Apart from that, phosphine-phosphaalkenes<sup>[31]</sup> (**10**, **11**) and a series of pyridine based P,N-phosphaalkenes (**13**) were reported by Cain and co-workers<sup>[34]</sup> and very recently, we have reported the synthesis and characterization of the novel P,N-type quinoline-based phosphaalkene ligand (2-quin)(H)C=PMes\* using the phospha-Wittig route.<sup>[35]</sup>



**Scheme 1.3** Synthesis of phosphaalkenes *via* “phospha-Wittig” route.

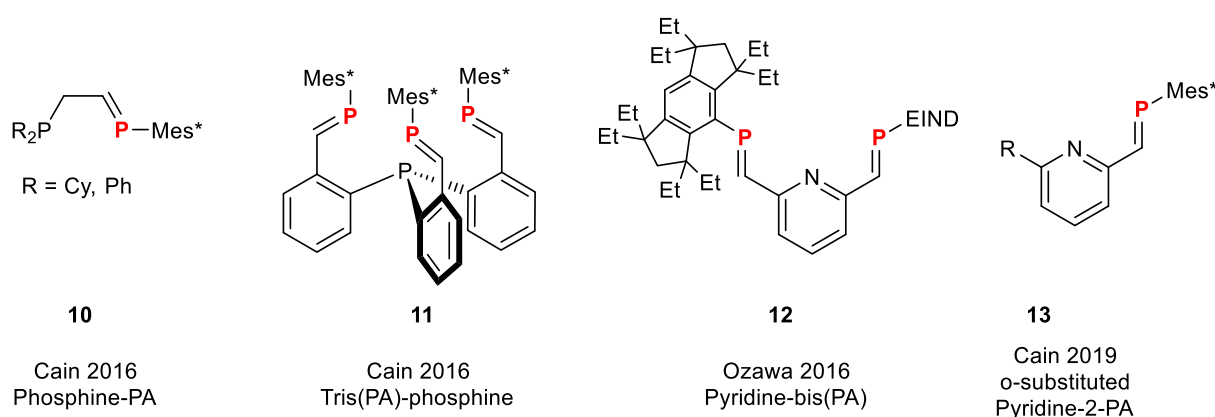


**Figure 1.5** Variety of phosphaalkene (PA) ligands prepared using a “phospha-Wittig” approach.

Phosphanylidenephosphoranes R—P(PR'<sub>3</sub>) have emerged as a powerful tool in synthetic inorganic chemistry and have found applications in the formation of phosphaalkenes using the so-called phospha-Wittig reaction, as well as a valuable phosphinidene-transfer reagents. The next chapter of this thesis is dedicated to the chemistry of phospha-Wittig reagents beyond the formation of phosphaalkenes.

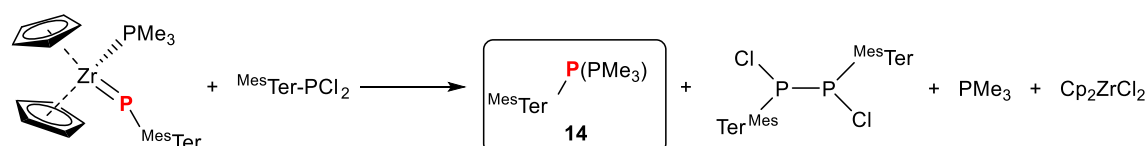


## 2 Phosphanylidene phosphoranes

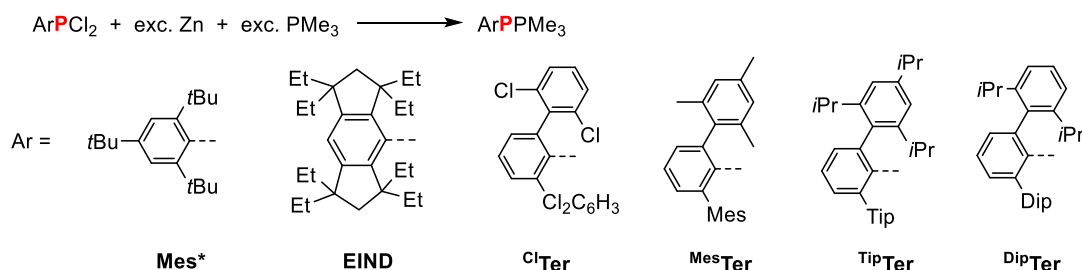
### 2.1 Introduction

In general, compounds of the type  $RP=PR'_3$  are referred to as phospho-Wittig reagents or phosphanylidene phosphoranes by isolobal replacement of the  $CR_2$  in  $R_2C=PR'_3$  with a phosphinidene fragment  $PR$ .<sup>[28]</sup> Burg and Mahler investigated the action of an excess of  $PMe_3$  on the cyclophosphanes  $(PCF_3)_4$  and  $(PCF_3)_5$ , noting the reversible formation of  $F_3CP=PMe_3$ , a phosphanylidene phosphorane. The concentration-dependent  $^1H$  NMR shift of  $PMe_3$  was later detected, indicating exchange of coordinated  $PMe_3$ . Investigating the reactivity of  $[Cp_2Zr(PR_3)P^{Mes}Ter]$  ( $R = Me, nBu$ ), Protasiewicz and co-workers noted the formation of the phospho-Wittig reagent  $^{Mes}TerP=PR_3$  instead of the anticipated formation of  $(^{Mes}TerP)_2$  and  $Cp_2ZrCl_2$  (Scheme 2.1, top).

First evidence for stable aryl-substituted phosphanylidene phosphoranes



Rational Synthesis



**Scheme 2.1** Coincidental finding of  $^{Mes}Ter-P(PMe_3)_2$  (**14**, top) and rational synthesis of  $Ar-P(PMe_3)_2$  along with different aryl-substituents commonly used to obtain stable phospho-Wittig reagents (bottom).

The term “phospho-Wittig” reaction was originally introduced by Mathey for the reaction of  $[(RO)_2P(O)-P\{W(CO)_5\}R']^{-}$  with ketones to give  $(CO)_5W$ -coordinated phosphalkenes.<sup>[36]</sup> The Protasiewicz group then showed that unsupported phospho-Wittig reagents can be isolated when the group  $R$  on phosphorus is kinetically stabilizing. Phospho-Wittig reagents are generally obtained by the combination of the respective dichlorophosphine  $Ar-PCl_2$  with zinc powder and an excess of  $PMe_3$ , whereby  $PMe_3$  acts as the active reductant (with concomitant formation of  $Cl_2PMe_3$ ),<sup>[37-38]</sup> and stabilizing base (Scheme 2.1, bottom). Zinc

dust seems to be redundant here, however, high yields are not obtained when only using  $\text{PMe}_3$ . Several examples of  $\text{ArP}=\text{PMe}_3$  ( $\text{Ar} = \text{Mes}^*$ ,<sup>[29]</sup>  $\text{EIND}$ ,<sup>[33]</sup>  $\text{Cl}^t\text{Ter}$ ,<sup>[39]</sup>  $\text{Mes}^t\text{Ter}$ ,<sup>[29]</sup>  $\text{Tip}^t\text{Ter}$ ,<sup>[40]</sup> Scheme 2.1) have been reported in the literature and only recently, we have reported the synthesis of  $^{\text{Dip}}\text{TerP}=\text{PMe}_3$  obtained in the reduction of  $^{\text{Dip}}\text{TerPCl}_2$  with an excess of  $\text{PMe}_3$  and Zn dust in THF.<sup>[41]</sup>

## 2.2 Structural Characterization of Phosphanylidenephosphoranes

Phosphanylidenephosphoranes can be discussed using three major resonance structures (Figure 2.1). These species are characterized by electron-rich dicoordinate P atoms, as indicated by their shielded signal in the  $^{31}\text{P}$  NMR spectrum. In addition, a rather large  $^1J_{\text{PP}}$  coupling constant between 430 and 700 Hz points to significant multiple bonding between the P atoms, resembling that of diphosphenes (cf.  $\text{Mes}^*\text{P}=\text{PMes}$   $^1J_{\text{PP}} = 574$  Hz).<sup>[42-43]</sup> Additionally, in the structurally characterized examples, the P–P bond between the dicoordinate and tetra-coordinated P atoms is rather short with values ranging from ca. 2.06 to 2.15 Å, which is considerably shorter as the theoretically predicted value for a P–P single bond (cf.  $\Sigma r_{\text{cov}}(\text{P}-\text{P}) = 2.22$  Å) and closer to the value of a double bond (cf.  $\Sigma r_{\text{cov}}(\text{P}=\text{P}) = 2.04$  Å).<sup>[44]</sup> All these experimental observations and the three plausible Lewis structures shown in Figure 2.1 clearly indicate a certain degree of multiple bond character. A closer look at the ylidic form **II** (Figure 2.1) shows that phosphanylidenephosphoranes are related to the ubiquitously used alkylidenephosphoranes, the classic Wittig-reagents of the type  $\text{R}_2\text{C}^{(+)}-\text{P}^{(-)}\text{R}'_3$ .

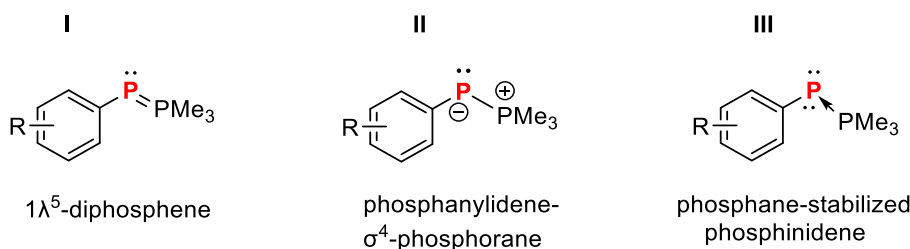
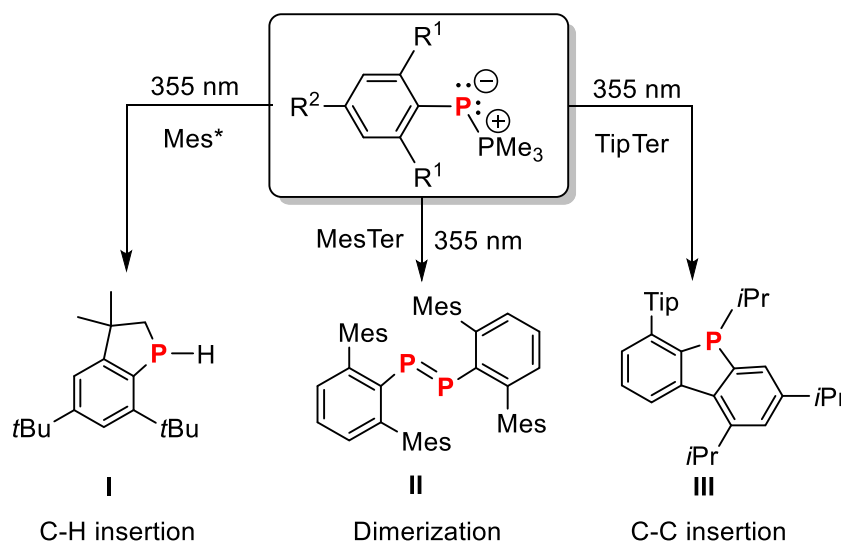


**Figure 2.1** Three plausible Lewis structures of aryl-substituted phosphanylidenephosphoranes.

## 2.3 Phosphanylidenephosphoranes as Phosphinidene Transfer Agents

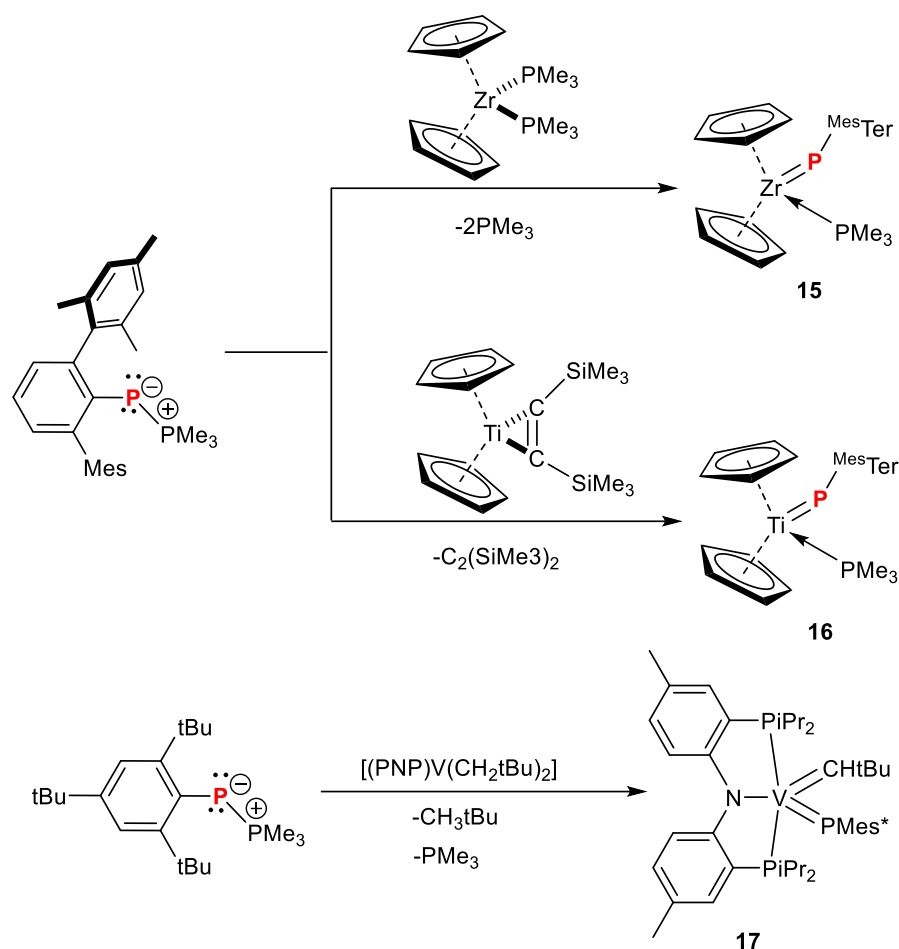
Phospha-Wittig reagents can be considered as phosphine-stabilized phosphinidenes. The LUMO of the parent phosphanylidenephosphorane  $\text{HP}(\text{PH}_3)$  has significant  $\sigma^*$  character and thus photolysis or addition of a stronger nucleophile should facilitate P–P bond scission and phosphinidene release. Phosphanylidenephosphoranes have been shown to display

phosphinidenoid reactivity. Upon laser irradiation of  $\text{Ar-P}(\text{PMe}_3)$ , aryl-substituted phosphanylidenephosphoranes with bulky substituents at the phosphanylidene P atom, at 355 nm in  $\text{C}_6\text{D}_6$  solution were shown to generate the phosphinidene  $\text{Ar-P}$  ( $\text{Ar} = \text{Mes}^*$ ,  $^{\text{Mes}}\text{Ter}$ ,  $^{\text{Tip}}\text{Ter}$ ).<sup>[40]</sup>  $^{31}\text{P}$  NMR spectroscopy revealed free  $\text{PMe}_3$  and the known 3,3-dimethyl-5,7-di-*tert*butylphosphaindane **I** (Scheme 2.2, left), which is a decomposition product of  $\text{Mes}^*\text{-P}$ , forming through insertion of the phosphinidene P atom into a vicinal CH bond of the *o*-*t*Bu-group.<sup>[45]</sup>  $^{\text{Mes}}\text{Ter-P}(\text{PMe}_3)$  gives the diphosphene  $(^{\text{Mes}}\text{TerP})_2$  **II** upon photolysis with the release of  $\text{PMe}_3$  and the photolytic stability of this diphosphene inhibits further photochemical degradation. Using the phospho-Wittig reagent  $^{\text{Tip}}\text{Ter-P}(\text{PMe}_3)$ , phosphafluorene **III** was observed as the main product of photolytic P-P bond cleavage.



**Scheme 2.2** Photolytic cleavage of  $\text{Ar-P}(\text{PMe}_3)$  ( $\text{Ar} = \text{Mes}^*$ ,  $^{\text{Mes}}\text{Ter}$ ,  $^{\text{Tip}}\text{Ter}$ ) and the products of intra- and intermolecular phosphinidene quenching.

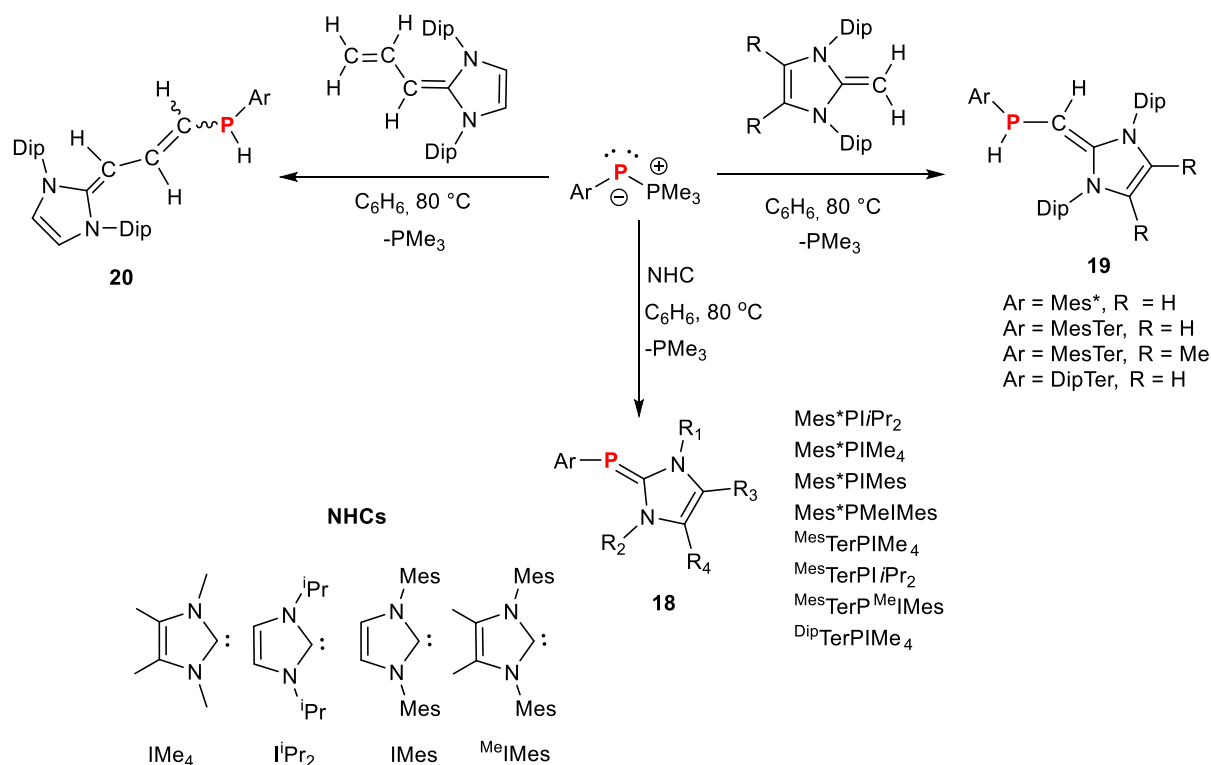
Another report by Protasiewicz and co-workers shows that the combination of the Zr(II) synthon  $[\text{Cp}_2\text{Zr}(\text{PMe}_3)_2]$  and  $^{\text{Mes}}\text{Ter-P}(\text{PMe}_3)$  afforded  $[(\text{Cp})_2(\text{PMe}_3)\text{Zr}=\text{P}^{\text{Mes}}\text{Ter}]$  with a characteristic deshielded phosphinidene P atom with a  $^{31}\text{P}$  NMR signal at 762 ppm (Scheme 2.3, top).<sup>[46]</sup> Likewise, the first terminal titanocene phosphinidene complex  $[(\text{Cp})_2(\text{PMe}_3)\text{Ti}=\text{P}^{\text{Mes}}\text{Ter}]$  (**16**) was afforded when combining the Ti(II) precursor  $\text{Cp}_2\text{Ti}(\text{C}_2(\text{SiMe}_3)_2)$  with  $^{\text{Mes}}\text{Ter-P}(\text{PMe}_3)$  and heating the mixture to 80 °C.<sup>[47]</sup> The first vanadium(V) phosphinidine complex  $(\text{PNP})\text{V} = \text{PMe}^*(\text{CH}t\text{Bu})$  was furnished upon treatment of  $(\text{PNP})\text{V}(\text{CH}_2t\text{Bu})_2$  ( $\text{PNP} = \text{N}[2\text{-P}(\text{CHMe}_2)_2\text{-4-methylphenyl}]_2$ ) with  $\text{Mes}^*\text{-P}(\text{PMe}_3)$  at 50 °C for 12 h (Scheme 2.3, bottom).<sup>[46]</sup>



**Scheme 2.3** Phospha-Wittig reagents as phosphinidene-transfer reagent to access a variety of terminal transition metal phosphinidene complexes.

Phospha-Wittig reagents are moreover isovalence-electronic to carbene phosphinidene adducts,<sup>[48]</sup> an emerging compound class in main group and transition metal chemistry<sup>[49]</sup> and thus, phosphanylidenephosphoranes should be easily converted into such by replacement of the phosphine with a carbene. Recently, we have reported the facile synthesis of a variety of NHC phosphinidene adducts derived from  $\text{Ar-P}(\text{PMe}_3)$  ( $\text{Ar} = \text{Mes}^*$ ,  $^{\text{Mes}}\text{Ter}$ ,  $^{\text{Dip}}\text{Ter}$ ) and show that in case of *N*-heterocyclic olefins (NHOs),  $\text{PMe}_3$  release is followed by an intramolecular  $\text{C}(\text{sp}^2)\text{-H}$  activation to afford phosphine-substituted NHOs.<sup>[41]</sup> A clean conversion into the corresponding NHC-phosphinidene adducts ( $\text{NHC}=\text{PAr}$ ) was observed upon heating a variety of NHCs ( $\text{NHC} = \text{IMe}_4$ ,  $\text{IiPr}_2$ ,  $\text{IMes}$ ,  $^{\text{Me}}\text{IMes}$ ) and  $\text{Ar-P}(\text{PMe}_3)$  ( $\text{Ar} = \text{Mes}^*$ ,  $^{\text{Mes}}\text{Ter}$ ,  $^{\text{Dip}}\text{Ter}$ ) in  $\text{C}_6\text{D}_6$  at 80 °C or 105 °C ( $\text{Ar} = \text{Mes}^*$ ;  $\text{NHC} = \text{IMes}$ ,  $^{\text{Me}}\text{IMes}$ ) (**18**, Scheme 2.4, bottom). Theoretical studies revealed a T-shaped transition state with a free energy barrier of 23.8 kcal mol<sup>-1</sup> for the reaction of  $\text{Mes}^*\text{-P}(\text{PMe}_3)$  with  $\text{IiPr}_2$  and an overall exergonic process ( $\Delta_{\text{R}}G^0 = -17.9$  kcal mol<sup>-1</sup>) for the formation of  $(\text{IiPr}_2)=\text{PMes}^*$  and release of  $\text{PMe}_3$ . Inspection of the intrinsic bond orbitals (IBOs) along the intrinsic reaction coordinate showed that the IBO

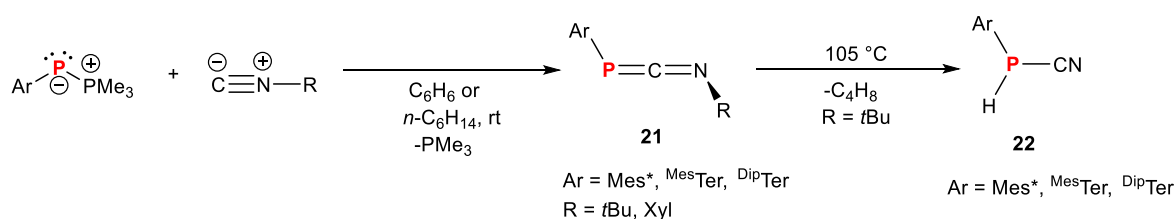
representing the  $\text{LiPr}_2$  lone pair transforms into the C–P  $\sigma$ -bond in  $(\text{LiPr}_2)=\text{PMes}^*$ , and the IBO of the P–P bond in  $\text{Mes}^*-\text{P}(\text{PMe}_3)$  converts into the  $\text{PMe}_3$  lone pair of electrons. These details are in line with an initial nucleophilic attack of the NHC at the  $\sigma^*$  P–P orbital and thus, an  $\text{S}_{\text{N}}2$ -type substitution is proposed. The scope of this protocol is outlined in Scheme 2.4, and it adds to the various pathways toward NHC phosphinidene adducts,<sup>[48]</sup> which have been shown to be versatile ligands in transition metal chemistry.<sup>[49]</sup> In contrast to NHCs, NHOs are strongly  $\sigma$ -donating, and their  $\pi$ -accepting properties are neglectable.<sup>[50–51]</sup> When  $\text{IDipCH}_2$  was combined with  $\text{Mes}^*-\text{P}(\text{PMe}_3)$ , a new species with a PH group was detected in the  $^1\text{H}$  NMR spectrum, which pointed to the formation of the P-substituted NHO  $\text{IDipC(H)P(H)Mes}^*$  (**19**, Scheme 2.4, right). To elucidate whether this C–H activation pathway is more general, allyl-appended NHO  $\text{IDipC}_3\text{H}_4$ <sup>[52]</sup> was heated to 80 °C with  $\text{Ar}-\text{P}(\text{PMe}_3)$  ( $\text{Ar} = \text{Mes}^*, {}^{\text{Mes}}\text{Ter}$ ) in  $\text{C}_6\text{H}_6$ . By means of  $^{31}\text{P}$  NMR spectroscopy conversion into the new species  $\text{Mes}^*\text{PHC}_3\text{H}_3\text{IDip}$  and  ${}^{\text{Mes}}\text{TerPHC}_3\text{H}_3\text{IDip}$  (**20**) and release of  $\text{PMe}_3$  were noted (Scheme 2.4, left). In solution,  $\text{IDipC}_3\text{H}_3\text{P(H)Ar}$  are mainly *E*-configured 1,3-dienes, while the *Z*-configured diene  $\text{IDipC}_3\text{H}_3\text{P(H)Mes}^*$  was observed in the crystal.



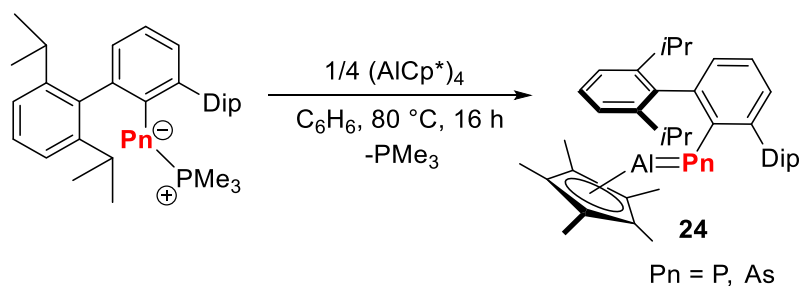
**Scheme 2.4** Phospha-Wittig reagents as precursors for NHC–phosphinidene adducts (bottom) and  $\text{C}(\text{sp}^2)\text{--H}$  activation in the reaction with NHOs (right) and enediamines to give P-substituted NHOs or butadienes, respectively (left), see chapter 6.1.<sup>[41]</sup>

The Hering-Junghans group has also shown the facile  $\text{PMe}_3$  for  $\text{CN-R}$  exchange to furnish 1,3-phosphaazaallenes.<sup>[53]</sup> Combination of  $\text{Ar-P}(\text{PMe}_3)$  ( $\text{Ar} = \text{Mes}^*, \text{MesTer}, \text{DipTer}$ ) with the isocyanides  $\text{CN}t\text{Bu}$  and  $\text{CNXyl}$  ( $\text{Xyl} = 2,6\text{-Me}_2\text{C}_6\text{H}_3$ ) gave six examples of  $\text{ArPCNR}$  (**21**) after heating 1:1 mixtures of the phospho-Wittig reagent and the respective isocyanide to 80 °C for a period of 16 h (Scheme 2.5, top). In case of the  $\text{CN}t\text{Bu}$ -derivatives, these were further transformed into the corresponding cyanophosphines  $\text{ArP}(\text{H})\text{CN}$  (**22**) when heated to 105 °C for a prolonged period with the concomitant elimination of *iso*-butene. In another work, the group also presented the synthesis of phospho- and arsaalumenes using the  $\text{Al}(\text{I})$  species  $(\text{Cp}^*\text{Al})_4$ <sup>[54]</sup> or  $\text{Cp}^{3t}\text{Al}$  ( $\text{Cp}^{3t} = 1,2,4\text{-}t\text{Bu}_3\text{C}_5\text{H}_2$ )<sup>[55]</sup> in combination with  $\text{Ar-Pn}(\text{PMe}_3)$  ( $\text{Pn} = \text{P}, \text{As}$ ) where  $\text{PMe}_3$  acts as innocent and volatile leaving group (Scheme 2.6). Although the reaction of  $\text{MesTer-P}(\text{PMe}_3)$  does not afford phosphaalumemes,<sup>[56]</sup> heating 4:1 mixtures of  $\text{DipTer-Pn}(\text{PMe}_3)$  ( $\text{Pn} = \text{P}, \text{As}$ ) and  $(\text{Cp}^*\text{Al})_4$  afforded the phospho- and arsaalumenes  $\text{DipTerPnAlCp}^*$  (**24**,  $\text{Pn} = \text{P}, \text{As}$ ), which are thermally stable in solution as well as in the solid state under an inert gas atmosphere. This reactivity clearly underlines the synthetic potential of phospho-Wittig reagents in phosphinidene-transfer reactions, to access previously challenging types of heterodiatomic multiple bond systems between main group elements.<sup>[57]</sup>

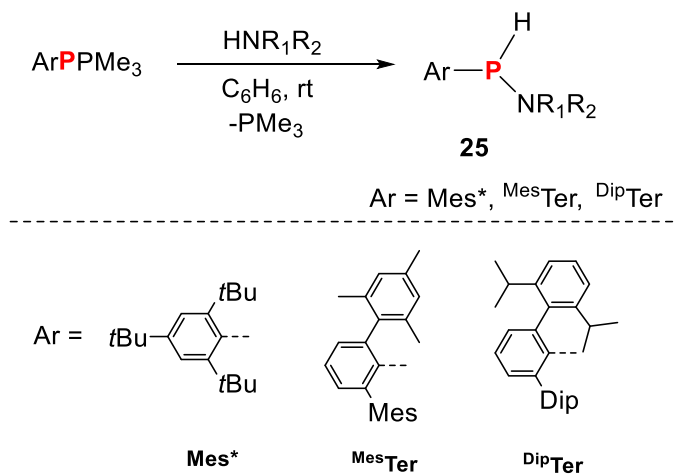
Later, the metal-free  $\text{NH}_3$  activation using  $\text{Ar-P}(\text{PMe}_3)$  was demonstrated, affording for the first time isolable secondary aminophosphines  $\text{ArP}(\text{H})\text{NH}_2$  (**25**, Scheme 2.7).<sup>[58]</sup> The activation of primary and secondary amines was likewise achieved. This novel reactivity of phospho-Wittig reagents is a straightforward way towards  $\text{P-N}$ -bonds from a variety of substrates, including chiral amines. DFT studies revealed that two molecules of  $\text{NH}_3$  act in concert to facilitate an  $\text{NH}_3$  for  $\text{PMe}_3$  exchange.



**Scheme 2.5** Reaction of  $\text{Ar-P}(\text{PMe}_3)$  with isocyanides to give 1,3-phosphaazaallenes, which upon heating affords cyanophosphines ( $\text{R} = t\text{Bu}$ ).



**Scheme 2.6**  $\text{PMe}_3$  for  $\text{Cp}^*\text{Al}$ -exchange to afford phospho- and arsaaluminenes.



**Scheme 2.7** N-H bond activation in  $\text{HNR}_1\text{R}_2$  using phospho-Wittig reagents ( $\text{ArPPMe}_3$ ), see chapter 6.3.<sup>[58]</sup>

### 3 Phosphaalkenes and their coordination chemistry

#### 3.1 Coordination Properties

Phosphaalkenes have different binding properties than traditional  $sp^3$  hybridized phosphines. Five different coordination modes are possible in phosphaalkenes due to the presence of a phosphorus lone pair and a  $\pi$  bond (Figure 3.1). The most common metal binding motif reported for phosphaalkenes is the  $\eta^1(\text{P})$ -coordination (**A**).<sup>[59]</sup> The second most common motif is the  $\eta^2(\text{P,C})$ -coordination (**B**). Due to the small energy difference between the lone pair and the  $\pi$  bond, a phosphaalkene can interconvert between  $\eta^1$ - and  $\eta^2$ -coordination.<sup>[60]</sup> More interesting mono- and multimetallic coordination modes can sometimes be observed (Figure 3.1, **C**, **D**, **E**).  $\eta^1, \eta^2$ -coordination has been reported when an excess of metal is present (**C**).<sup>[59, 61]</sup> Another unusual mode is  $\eta^1, (\mu_2\text{-P})$ -coordination due to the capacity of phosphorus to become tetravalent (**D**).<sup>[59, 62]</sup> Phosphaalkenes incorporated into a metal cluster have led to the characterization of the very unusual  $\eta^1, \eta^2, \mu_3$ -binding mode (**E**).<sup>[63]</sup> The first coordination complexes of a phosphaalkene were characterized by NMR spectroscopy as *cis*- $\text{M}(\text{CO})_4(\eta^1\text{-MesP=CPh}_2)_2$  ( $\text{M}=\text{Cr, Mo, W}$ ), *trans*- $\text{RhCl}(\text{PPh}_3)_2(\eta^1\text{-MesP=CPh}_2)$ , *trans*- $\text{RhCl}(\eta^1\text{-MesP=CPh}_2)_2(\text{CO})$ ,  $\text{Rh}(\eta^5\text{-C}_9\text{H}_7)(\eta^1\text{-MesP=CPh}_2)_2$ , *cis*- $\text{PtX}_2(\eta^1\text{-MesP=CPh}_2)_2$  ( $\text{X}=\text{Cl, I, Me}$ ), and *cis*- and *trans*- $\text{PtCl}_2(\text{PEt}_3)(\eta^1\text{-MesP=CPh}_2)$ .<sup>[64]</sup> Each of these complexes exhibited binding of the type  $\eta^1(\text{P})$  through the phosphorus lone pair, and this was crystallographically confirmed with the structural characterization of  $\text{Cr}(\text{CO})_5(\text{MesP=CPh}_2)$  and *cis*- $\text{PtCl}_2(\text{PEt}_3)(\text{MesP=CPh}_2)$ .<sup>[65-66]</sup> This field has grown considerably and now includes examples of some very unusual binding modes of phosphaalkenes.

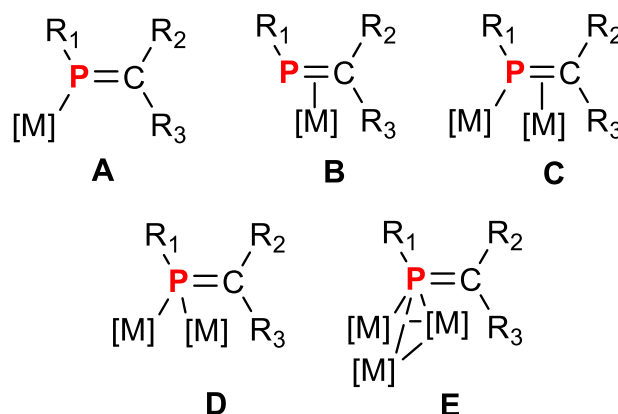


**Figure 3.1** Different coordination modes of phosphaalkene ligands.

Phosphaalkenes bind to metals in the following fashion (Figure 3.2): the phosphorus lone pair donates into an empty metal  $d$  orbital (**I**) and a filled metal  $d$  orbital back-donates into the



$\pi^*$  orbital of the P=C bond (**II**). Upon metal binding, phosphaalkenes become closer to the ideal  $sp^2$  hybridized geometry, which can be observed by an increase of the C–P=C angle to around  $115^\circ$  (**III**).

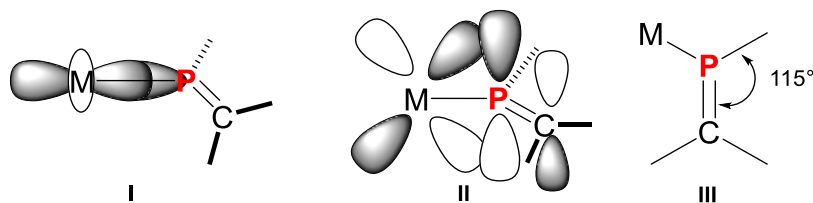


**Figure 3.2** Molecular orbital depiction of phosphaalkenes binding to metals.

### 3.2 Phosphaalkene Complexes

This section illustrates a few selected examples of phosphaalkene coordination complexes rather than discussing all of them exhaustively. Representative examples of phosphaalkene ligands include 1,2-diphenyl-3,4-diphosphinidenecyclobutene derivatives (DPCB-Y, **26**),<sup>[67]</sup> which possess a 1,6 diphospha-1,3,5-hexatriene skeleton and 2,6-bis[2-(2,4,6-tri-*tert*-butylphenyl)-2 phosphaethenyl]pyridines (BPEP-Y, **27**) which are phosphorus analogues of 2,6-bis(imino)pyridines (NNN, **28**).<sup>[68–69]</sup> These compounds are also analogous to nowadays ubiquitously used pyridine-based PNP-pincer-type phosphine ligands (PNP, **29**) (Figure 3.3).

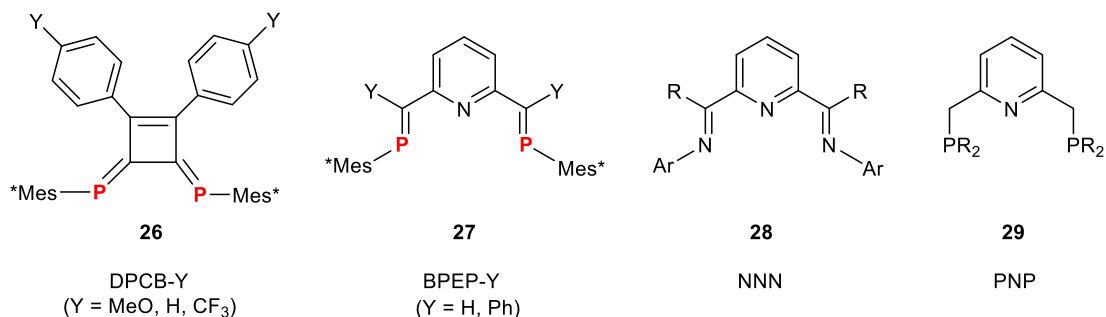
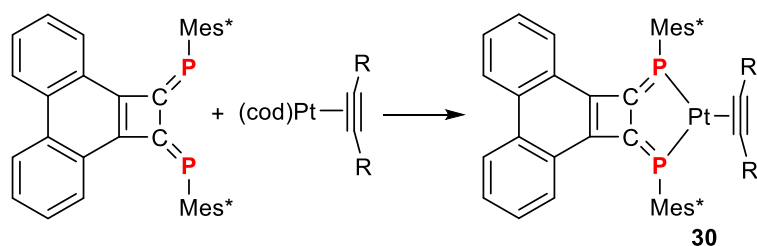


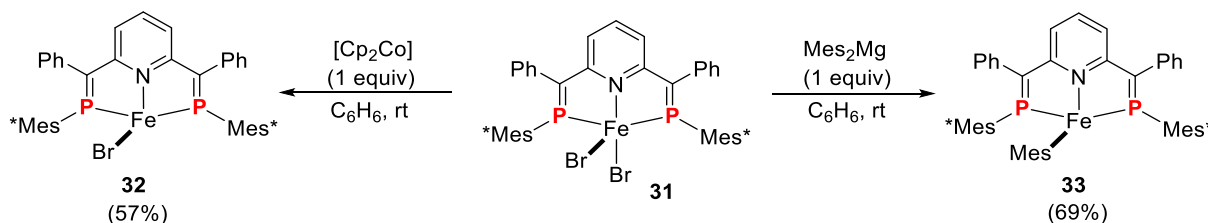
**Figure 3.3** Phosphaalkene and related ligands.

DPCB-Ys are stable towards air and moisture and undergo bidentate coordination with transition metals to form highly active catalysts. Ozawa and co-workers reported platinum(0) alkyne complexes containing a DPCB ligand (**30**) having interesting conjugative properties (Scheme 3.1).<sup>[70]</sup> DFT calculations revealed that the  $\pi$ -accepting nature of the phosphaalkene ligand generates an extended  $\pi$ -conjugated system that has HOMO-LUMO gaps within the visible region of the electromagnetic spectrum.<sup>[71]</sup> This phenomenon has not been observed with other ligands for similar Pt(alkyne) complexes.



**Scheme 3.1**  $\pi$ -Conjugation of DPCB Pt(alkyne) complexes.

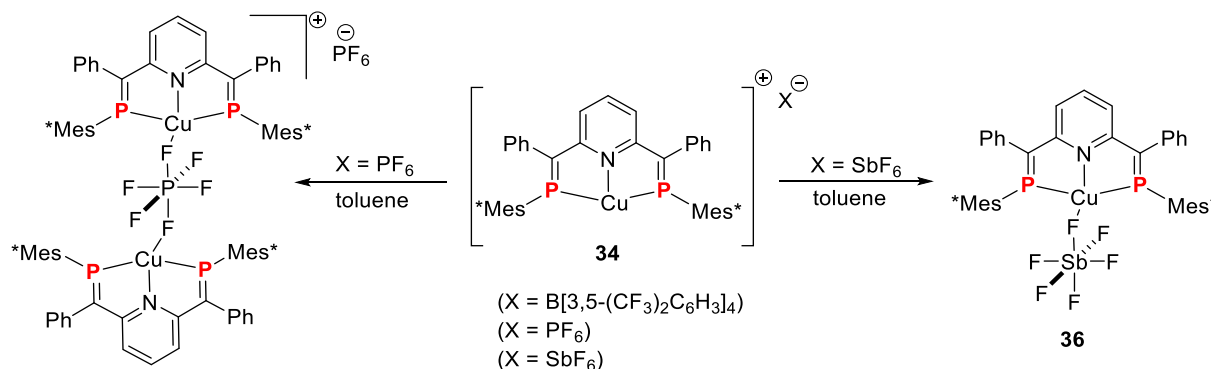
Geoffrey et al. prepared the parent bisphosphaethinylpyridines (BPEP) in the early 1990's by applying a synthetic protocol that utilizes Mes\*PH<sub>2</sub> as a starting material and intermediate formation of a silylated phosphide in a Peterson-analogous reaction.<sup>[23]</sup> Ozawa and co-workers followed that path to prepare Fe, Cu and Ir complexes of these BPEP's. One electron reduction of FeBr<sub>2</sub>[BPEP-Ph] with CoCp<sub>2</sub> or Mes<sub>2</sub>Mg yielded the Fe(I) species FeBr[BPEP-Ph] (**32**) and FeMes[BPEP-Ph], respectively. FeBr[BPEP-Ph] (**33**) was characterized as Fe(I) (S=3/2) complex, on the basis of Mössbauer and broken-symmetry DFT calculations (Scheme 3.2).<sup>[72]</sup> Analysis of the bonding properties by NBO analysis revealed an effective d<sub>π</sub>-p<sub>π</sub> metal-phosphaalkene interaction due to the low-lying π\* orbital of the phosphaalkene ligand. The Fe(I) center was found to be in the rare distorted trigonal monopyramidal geometry. It needs to be noted that an Fe(I) complex was not formed when a pyridinediimine ligand was used. In this case reduction of the ligand backbone occurred, while Fe remained as Fe(II).<sup>[72]</sup>



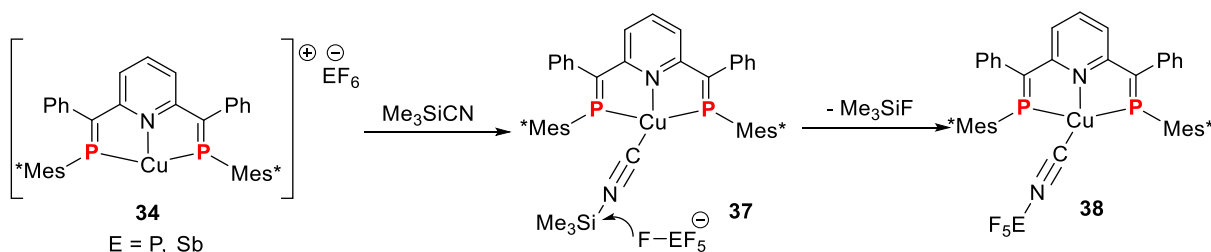
**Scheme 3.2** Reduction of [FeBr<sub>2</sub>(BPEP-Ph)] to give Fe(I) complexes

Cationic Cu(I) complexes were obtained by treatment of the CuBr[BPEP-Ph] (**34**) systems with Ag[EF<sub>6</sub>] (E = P, Sb) or Ag[B(C<sub>6</sub>H<sub>3</sub>(CF<sub>3</sub>)<sub>2</sub>)<sub>4</sub>], which were identified as ion-separated salts in polar solvents by <sup>31</sup>P NMR spectroscopy and in the solid state by means of X-ray crystallography.<sup>[73]</sup> Interestingly, in non-polar solvents such as toluene or benzene contact ion pairs formed through Cu-F interactions, which in the case of PF<sub>6</sub> yielded a dinuclear complex with a bridging PF<sub>6</sub>-ligand (**35**), with Cu-F distances in the range of typical Cu(I) fluorides (ca. 2.1 Å) and the dimeric structure is retained in solution even in the presence of MeCN or CO (Scheme 3.3). The authors rationalized the unexpected F-affinity of the BPEP-Cu systems to originate in the strong  $\pi$ -accepting abilities of the ligand.<sup>[74]</sup> Complexes [Cu(BPEP-

Ph)][EF<sub>6</sub>] (E = P, Sb (**36**)) were shown to cause bond-activation of Me<sub>3</sub>SiCN under mild-conditions (Scheme 3.4).

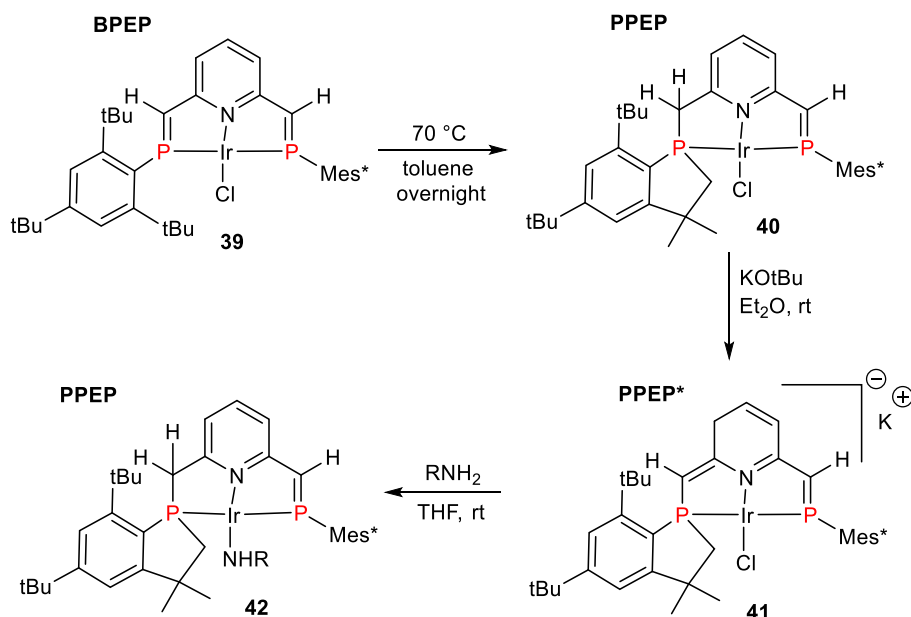


**Scheme 3.3** Cu(I) BPEP-Ph complexes.



**Scheme 3.4** Bond activation of Me<sub>3</sub>SiCN promoted by Cu(I) BPEP-Ph complexes

In another work by Ozawa and co-workers, metal–ligand cooperativity was observed for a mixed Ir(I) P,N,P-complex with phosphalkene<sup>[75]</sup> and phosphaindane units. Iridium(I)-complex [ClIr(BPEP-H)] (**39**) can be converted into the unsymmetrical complex by heating a toluene solution overnight, resulting in ring closure of one of the *t*Bu-groups of the Mes\* unit with phosphorus affected by the presence of iridium. Oxidative C–H addition and reductive P–C elimination occurs selectively on only one side of the ligand, affording a PPEP-type ligand (**40**). In a second step dearomatization of the central pyridine ring was initiated by addition of KO<sup>*t*</sup>Bu, resulting in the deprotonation of the benzylic position and anionic complexes of the type K[ClIr(PPEP\*)] (**41**).<sup>[76]</sup> In the anionic iridium complex **41** a considerable elongation of the P–C bond is observed (*d*(P–C) 1.701(12)Å), which hints at enhanced  $\pi$ -backdonation when compared to the neutral BPEP. This species exhibits extremely high reactivity towards metal–ligand cooperative activation of the N–H bonds of NH<sub>3</sub> (1 atm), *n*-C<sub>6</sub>H<sub>13</sub>NH<sub>2</sub>, and *p*-YC<sub>6</sub>H<sub>4</sub>NH<sub>2</sub> (Y = functional group, Scheme 3.5).<sup>[76]</sup> All reactions proceed rapidly at room temperature to form amido complexes (**42**) quantitatively. On the other hand, analogues Rh(I) complexes could not be obtained due to the occurrence of successive C–H addition/cyclization at both Mes\*P=C(R)H groups, giving rise to complete loss of the P=C bonds.



**Scheme 3.5** Synthesis of Ir(I) PPEP and PPEP\* complexes and N–H bond cleavage.

A series of Ru P,N-phosphaalkene complexes were reported by Cain and co-workers just recently.<sup>[34]</sup> The latter complexes showed intramolecular C–H bond activation at the Mes\* groups to produce phosphaindane structures. Only very recently, we have presented the synthesis and characterization of the novel P,N-type quinoline-based phosphaalkene ligand [2-quin](H)C=PMes\* (**43**) (Figure 3.4).<sup>[35]</sup> When coordinated to Rh(I), this ligand showed a diverse coordination chemistry, ranging from simple twofold coordination, to give complex **44**. A selective cyclization of one or two of the P,N-ligands was achieved by using sub- or superstoichiometric amounts of AgOTf (**45**, **46**). DFT studies show an oxidative proton shift from one *t*Bu-group to Rh giving a Rh(III) intermediate with a dearomatized quinoline. Selective dearomatization of the phosphaindane complexes was achieved by deprotonation of the benzylic position with KO<sup>t</sup>Bu, giving neutral complexes with a distorted square planar coordination at Rh(I). This study showed for the first time that Rh(I) can be coordinated by two PN-type phosphaalkene units.

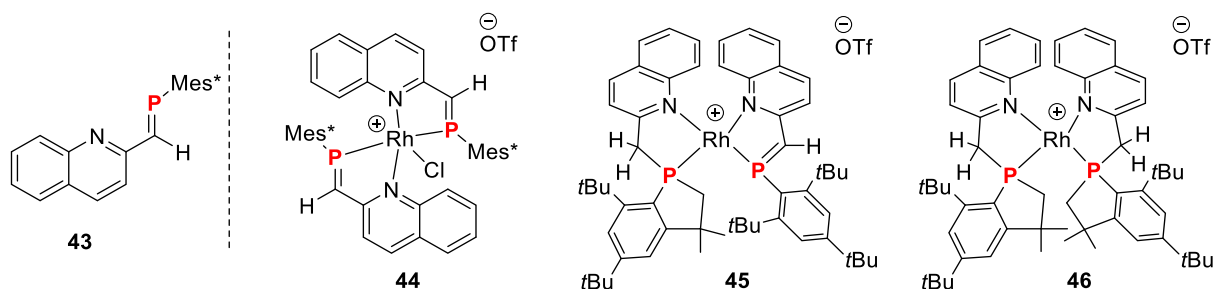


**Figure 3.4** P,N-type phosphaalkene ligand and Rh P,N-phosphaalkene complexes, see chapter 6.2.<sup>[77]</sup>

In summary, these selected examples serve to illustrate the diverse coordination chemistry of phosphaalkene ligands.<sup>[11]</sup> These ligands have stabilized metals in unusual coordination geometries,<sup>[72]</sup> have increased conjugative properties<sup>[70]</sup> and have undergone electrochemical processes.<sup>[78]</sup> Such novel coordination chemistry can yield fruitful and exciting reactivity in catalysis which will be discussed in detail in the next chapter.

## 4 Applications in Homogeneous Catalysis

### 4.1 Introduction

Over the past 15 years there has been growing interest to incorporate phosphalkenes in transition metal catalysts.<sup>[11, 79]</sup> Phosphine based ligands have been extensively studied, and their applicability in catalytic processes has been demonstrated on numerous occasions. In contrast, reports on related phosphalkene based P,N,P- and P,N-ligands and their applications in coordination chemistry are less common, thus, many groups have been interested over the last few years in evaluating the potential of such ligands and their respective transition metal complexes in homogeneous catalysis. Non-kinetically stabilized phosphalkenes were found to be too reactive to be efficiently used as ligands and most studies logically focused on sterically protected molecules such as 1,2-disubstituted-3,4-diphosphinidenecyclobutenes (Scheme 3.1). The first known report of a catalytic transformation to use a phosphalkene ligand was a Sonogashira coupling in 1995 and no further examples were reported until the early 2000s. The following sections of this chapter summarize the use of phosphalkene ligands in catalysis and the following reactions will be discussed: ethylene polymerization, followed by cross-coupling, hydro- and dehydrosilylation, hydroamination and hydroamidation, *N*-Alkylation of amines, cycloisomerizations and allylic substitutions.

### 4.2 Ethylene polymerization

The metal complexes containing  $\alpha$ -diimine ligands have been proven successful in promoting ethylene polymerization.<sup>[80]</sup> Phosphalkenes, structurally similar to  $\alpha$ -diimine ligands, have also been investigated for this application and appear to be more stable than the comparable  $\alpha$ -diimine complexes under typical polymerization conditions.

Ozawa and co-workers reported neutral DPCB palladium(II) complexes **47–49** that are active toward ethylene polymerization upon acid activation with  $[\text{H}(\text{OEt}_2)_2][\text{B}(\text{Ar}^{\text{F}})_4]$  to afford catalytically active cationic complexes (Figure 4.1).<sup>[81]</sup> Complex **47** ( $\text{Ar} = \text{Ph}$ ), upon activation, is more active than **48** and **49** and polymerizes ethylene (turnover frequency (TOF) =  $4,600 \text{ h}^{-1}$ , pressure =  $10 \text{ kg}\cdot\text{cm}^{-2}$ ) to give polyethylene with a molecular weight ( $M_w$ ) of  $18,700 \text{ g}\cdot\text{mol}^{-1}$  and polydispersity indexes (PDIs) of 1.48. Interestingly, these DPCB complexes will polymerize ethylene at  $100^\circ\text{C}$ , a temperature at which  $\alpha$ -diimine catalysts are not stable.<sup>[81]</sup> Further studies on the electronic properties of DPCB ligands found generally that electron withdrawing aryl groups were more active ( $\text{Ar} = 4\text{-MeOC}_6\text{H}_4 < \text{Ar} = \text{Ph} < \text{Ar} =$

3,5-(CF<sub>3</sub>)<sub>2</sub>C<sub>6</sub>H<sub>3</sub> < Ar = 4-(CF<sub>3</sub>)-C<sub>6</sub>H<sub>4</sub>).<sup>[82]</sup> The most active catalyst **47** (Ar = 4-(CF<sub>3</sub>)-C<sub>6</sub>H<sub>4</sub>) gave the best results with an activity of 210 kg·h<sup>-1</sup>·(mol cat)<sup>-1</sup> and molecular weights of 43 kg·mol<sup>-1</sup> and PDIs of 23.7.

The mixed P,N-catalyst **50** (Ar = Mes) synthesized by Brookhart and co-workers is also an effective catalyst for the polymerization of ethylene with low turnover frequency (TOF = 94 h<sup>-1</sup>) compared with  $\alpha$ -diimine Pd(II) complexes (TOF of 4,500 h<sup>-1</sup>).<sup>[83]</sup> The low TOF can be attributed to slow rates of ethylene migratory insertion, and calculations of the energy barrier supported this hypothesis.

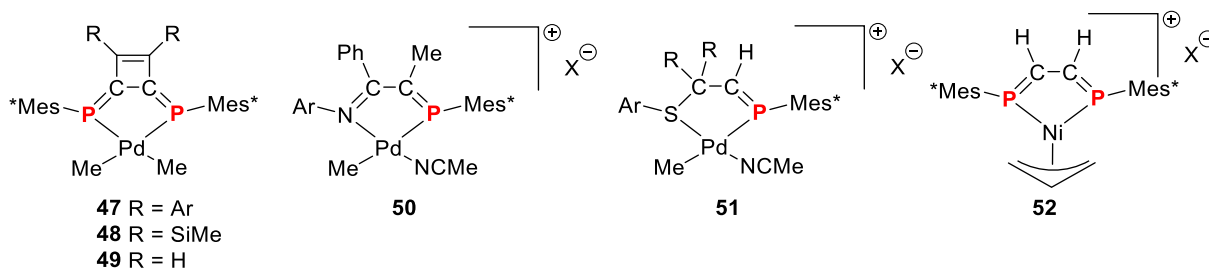


**Figure 4.1** Phosphaalkene complexes used in ethylene polymerization.

Therefore, a P,S-phosphaalkene complex **51** (Ar = Tip = 2,4,6-(iPr)C<sub>6</sub>H<sub>2</sub>; R = H) was synthesized in an attempt to lower the migratory insertion energy barrier. Remarkably, **51** polymerizes ethylene with activities comparable to  $\alpha$ -diimine ligands (TOF = 4,300 h<sup>-1</sup> for a 3 h run). Complex **51** also has greater stability (TOF of 3,000 h<sup>-1</sup> for a 15 h run) under polymerization conditions than systems that featured  $\alpha$ -diimine ligands but generated oligomers rather than polymers ( $M_n$  = 215 g·mol<sup>-1</sup>). Modification of the ligand structure by the addition of a methyl group to the backbone generated catalyst **51** (Ar = Tip, R = Me) that showed high activity (TOF 3,100 h<sup>-1</sup>) and gave higher molecular weight polyethylene ( $M_n$  = 2,300-2,500 g·mol<sup>-1</sup>) with extensive branching.

Ionkin and Marshall also investigated the use of phosphaalkene ligands for ethylene polymerization and reported that nickel(II) complexes such as **52** have also successfully been utilized as catalysts for the polymerization of ethylene to afford polymers ( $M_w$  = 58,000 g·mol<sup>-1</sup>; PDI = 3.19) with less branching.<sup>[84]</sup> Overall, the phosphaalkene-based metal complexes seem to have a greater thermal stability than  $\alpha$ -diimine complexes in palladium- and nickel-catalyzed polymerizations of ethylene, which might be an advantage for industrial applications.

### 4.3 Cross-Coupling Reactions

Phosphaalkene based metal complexes have also been investigated in cross-coupling reactions. These reactions are well established and offer a useful benchmark to compare catalytic efficiencies.<sup>[85]</sup> Complexes containing phosphaalkene-based ligands are active in a variety of different cross-coupling reactions such as the Sonogashira,<sup>[86]</sup> Suzuki–Miyaura,<sup>[87]</sup> Stille,<sup>[88]</sup> Buchwald–Hartwig,<sup>[89–90]</sup> and Ullmann couplings.<sup>[91]</sup> The complexes shown in Figure 4.2 are active in the Sonogashira and Suzuki–Miyaura coupling.

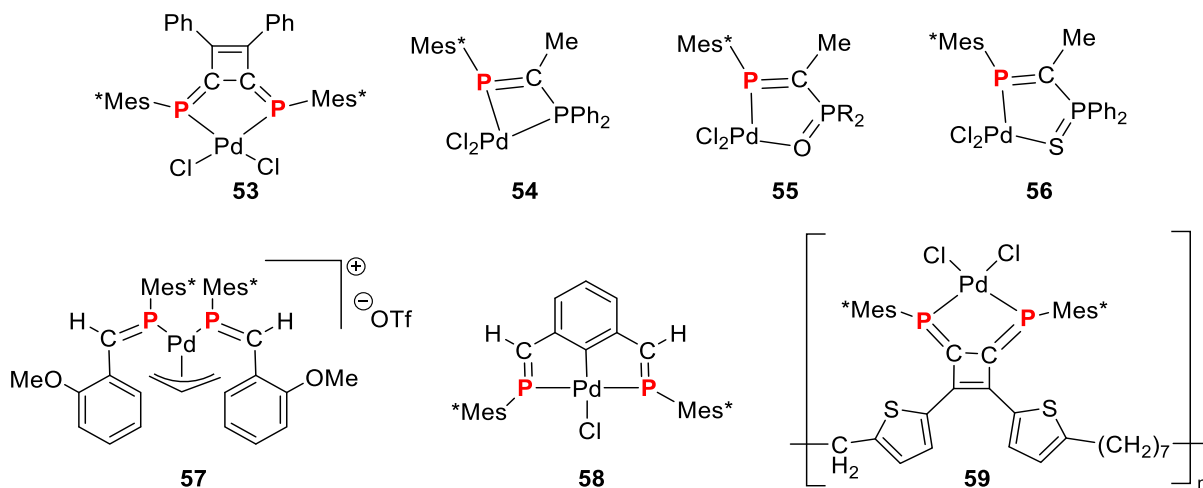


Figure 4.2 Complexes used in Sonogashira and Suzuki–Miyaura coupling.

#### 4.3.1 Sonogashira Reactions

Yoshifuji and co-workers were the first to use a phosphaalkene ligand in catalysis. Complex **53** effectively couples 1-bromo-4-nitrobenzene with trimethylsilylacetylene in 77% yield.<sup>[92]</sup> Interestingly, the 1,3-diphenylphosphaalkene complex **54** is a more active catalyst for the coupling of phenylacetylene and iodobenzene in high yields.<sup>[93]</sup> However, the limitations of complex **54** are its inability to couple 1-bromo-4-nitrobenzene and its sensitivity toward air and moisture.<sup>[94]</sup> To rectify the sensitivity of **54**, the oxidized complex **55** can be employed, but lower yields of cross-coupled products are obtained.<sup>[95]</sup> The more electron-rich phosphine sulfide complex **56** tolerates air and moisture and gives synthetically useful yields of diphenylacetylene.<sup>[94]</sup> Complex **56** will not cross-couple bromobenzene with phenylacetylene but rather dimerizes phenylacetylene quantitatively to afford diphenylbutadiyne ( $\text{Ph}-\text{C}\equiv\text{C}-\text{C}\equiv\text{C}-\text{Ph}$ ).<sup>[96]</sup> The authors of this work suggest that the dimerization product results from the formation of a dialkynylpalladium(II) complex. Le Floch and co-workers found that monodentate phosphaalkene complex **57** and tridentate phosphaalkene complex **58** can effectively couple bromoarenes with phenylacetylene with low catalyst loadings (0.1 mol %).<sup>[97]</sup> Complex **59**, which is incorporated into a polymer, showed good activity in the cross-



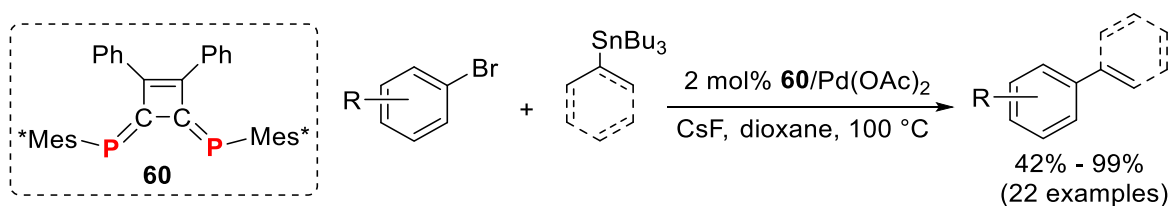
coupling of 1-bromo-4-nitrobenzene with trimethylsilylacetylene<sup>[98]</sup> and the catalyst could easily be removed from the crude reaction mixture and recycled.

### 4.3.2 Suzuki-Miyaura Reactions

The coupling of aryl halides with aryl boronic acids or esters is an important class of C–C bond forming reactions that has found many applications. The Suzuki–Miyaura coupling of aryl halides with aryl boronic acids can be catalyzed using phosphalkene complexes **55**, **56**, **57**, and **58**. Phosphine oxide complex **55** efficiently catalyzes the cross-coupling of iodobenzene and phenylboronic acid.<sup>[95]</sup> Although the electron-rich phosphine sulfide complex **56** efficiently cross-couples iodobenzene and phenylboronic acid, its use could not be extended to less reactive electrophiles such as bromobenzene or 4-iodoanisole.<sup>[94]</sup> Remarkably, cross-coupling of bromoarenes with phenylboronic acid is achieved rapidly (2 h) and quantitatively with very low catalyst loadings ( $10^{-5}$  mol %) of complexes **57** and **58**.<sup>[97]</sup>

### 4.3.3 Stille Cross-Coupling Reactions

In the above-mentioned work, the complexes used for catalysis were isolated prior to use but in the following example the catalyst was generated *in situ*. Addition of ligand **60** to  $\text{Pd}(\text{OAc})_2$  was efficient towards Stille cross-coupling reaction of aryl bromides with vinyl-, allyl- and aryl tin reagents (Scheme 4.3).<sup>[99]</sup> The cross-coupling conditions were general for a variety of different bromoarenes containing a variety of different electronic and steric properties. The cross-coupling reactions also tolerated the presence of unprotected alcohols and heteroaromatics.

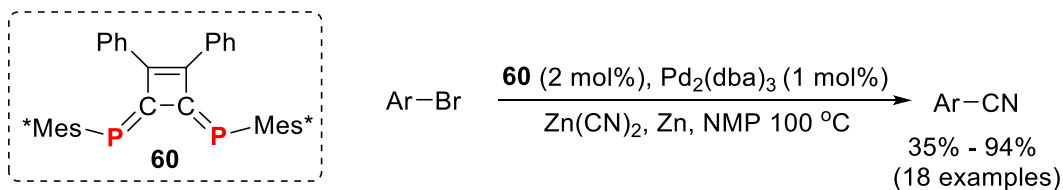


Scheme 4.3 Stille coupling using ligand **60**.

### 4.3.4 Cyanation Reactions

The cyanation of aryl bromides is another reaction that was effectively catalyzed by generating the phosphalkene metal complex *in situ*. Addition of  $\text{Pd}_2(\text{dba})_3$  to **60** in the presence of Zn and  $\text{Zn}(\text{CN})_2$  effectively catalyzed the cyanation of aryl bromides at 100 °C (Scheme 4.4).<sup>[100]</sup> The catalysts loading of 2 mol % is low for cyanation reactions, that are normally plagued by the deactivation of the palladium catalyst by cyanides.<sup>[101]</sup> However, it

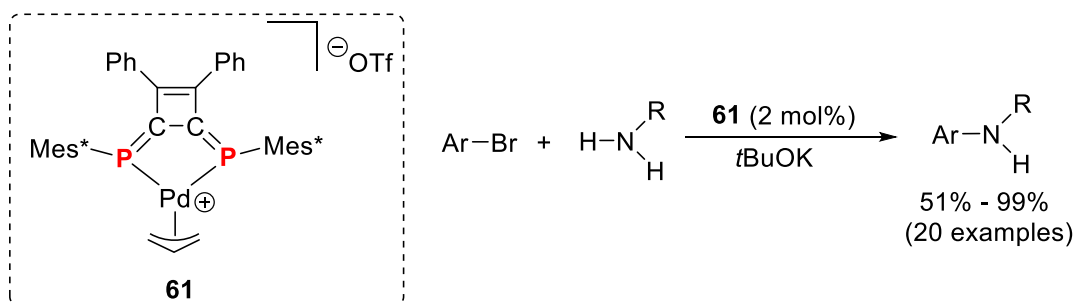
was previously found that the addition of Zn dust is an important additive to reduce catalyst loadings.<sup>[102]</sup> The yields obtained for the reaction were generally high and were used to synthesize the bulky 2,4,6-trimethylbenzonitrile in synthetically useful yields.



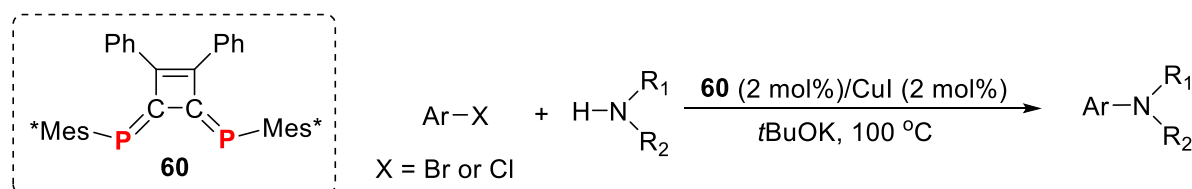
**Scheme 4.4** Cyanation of aryl bromides with **60**.

### 4.3.5 C–N Cross-Coupling Reactions

Anilines can be coupled to bromoarenes (Buchwald–Hartwig coupling) in synthetically useful yields using palladium allyl complex **61** and potassium *tert*-butoxide (Scheme 4.5).<sup>[103]</sup> It is noteworthy that amination proceeds at room temperature without solvent. Interestingly, monoarylated anilines are the observed products at room temperature even in the presence of excess bromobenzene. Disubstitution reactions of aniline using two equivalents of bromobenzene or the cross-coupling of secondary aromatic amines such as *N*-methyl aniline could be performed at high temperature (100 °C). In contrast, aliphatic secondary amines such as piperidine and morpholine couple readily at room temperature. Aryl bromides and chlorides can also be coupled with anilines in an Ullman coupling process using DPCB **60**, copper iodide, and potassium *tert*-butoxide (Scheme 4.6).<sup>[104]</sup> These reactions usually require higher temperatures (100 °C) relative to the palladium catalysis shown in Scheme 4.5. The yields of products obtained from both the palladium- and copper-catalyzed processes were similar.



**Scheme 4.5** Buchwald–Hartwig coupling using **61**.

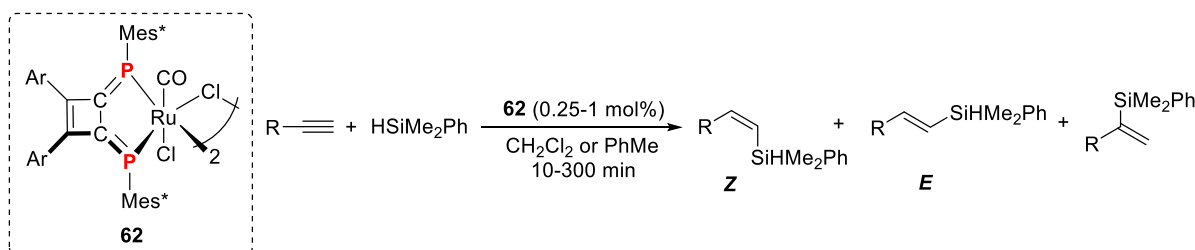
Scheme 4.6 Ullman coupling using **60**.

## 4.4 Hydro- and dehydrosilylation

The following section discusses the use of phosphalkene ligands in reactions with silanes. Two types of reactions have been catalyzed by phosphalkene-based ligands to date:

### 4.4.1 Hydrosilylation

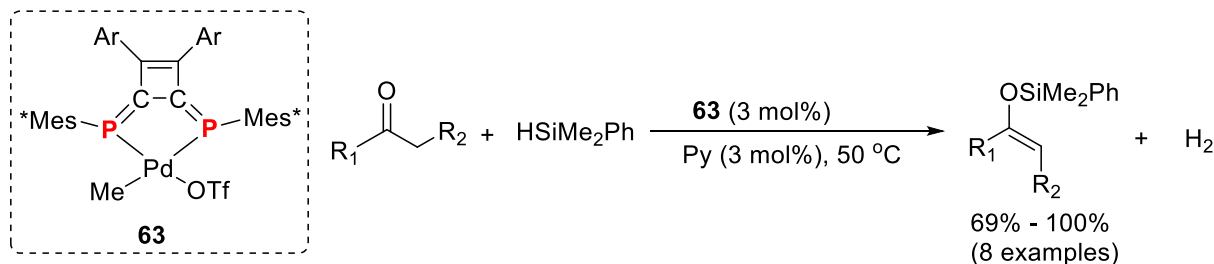
The hydrosilylation of alkynes mediated by a metal catalyst generates preferentially the *E*-vinyl silane. Dimeric ruthenium complex **62** (Ar = 4-MeOC<sub>6</sub>H<sub>4</sub>) however, is selective for the formation of the *Z*-vinyl silane (Scheme 4.7).<sup>[105]</sup> A wide range of substrates are tolerated. For example, terminal alkynes with either electron donating or withdrawing aryl groups, as well as aliphatic groups, are hydrosilylated in high yields. The low catalyst loading, and short reaction times are also noteworthy features of using **62** (Ar = 4-MeOC<sub>6</sub>H<sub>4</sub>). Mechanistic studies of the reaction suggested that the strong  $\pi$ -accepting properties of **62** (Ar = 4-MeOC<sub>6</sub>H<sub>4</sub>) are responsible for the *Z*-selectivity.<sup>[105]</sup> Complex **62** (Ar = 4-MeOC<sub>6</sub>H<sub>4</sub>) outperformed all other catalysts to generate bifunctional *Z*-vinyl silanes *en route* to all-*cis* poly(phenylene vinylenes) (PPVs).

Scheme 4.7 *Z*-selective hydrosilylation of alkynes.

### 4.4.2 Dehydrogenative silylation

It is quite remarkable that phosphalkene based transition metal complex **63** (Ar = Ph) catalyzes the dehydrosilylation of ketones to silyl enol ethers (Scheme 4.8).<sup>[106]</sup> Electronic perturbations of ligand **63** (Ar = 4-MeOC<sub>6</sub>H<sub>4</sub> or Ar = 4-CF<sub>3</sub>C<sub>6</sub>H<sub>4</sub>) lead to different reactivity profiles. These solvent-free reactions generally form the *E*-isomer of the most substituted silyl

enol ether. It was proposed that the  $\pi$ -accepting properties of the DPCB ligand in **63** were responsible for the selectivity of ketone dehydrogenative silylation over hydrosilylation.



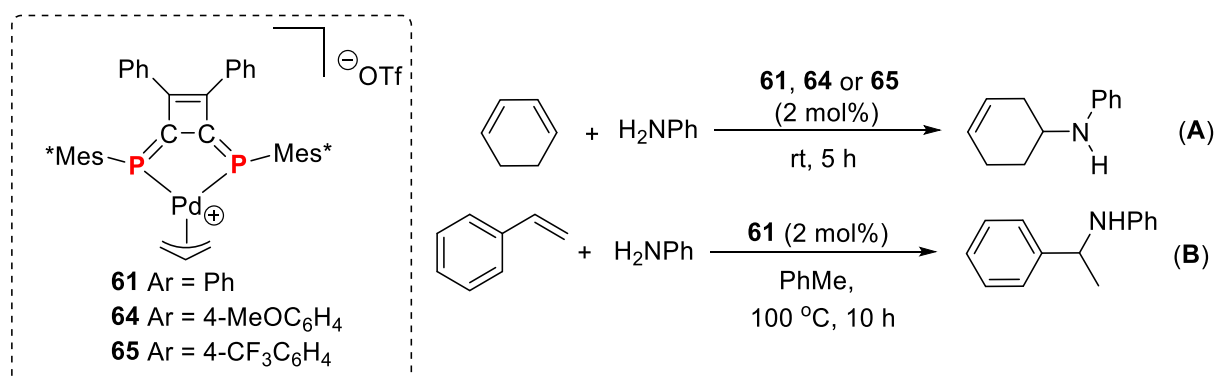
**Scheme 4.8** Dehydrogenative silylation of ketones using **63**.

## 4.5 Hydroamination and hydroamidation

The below described section discusses the use of palladium and rhodium phosphaaalkene complexes in the formal addition of N–H across dienes and enones.<sup>[107]</sup> The first set of examples are of a palladium catalyzed hydroamination of 1,3 dienes and the second set of examples are of a rhodium and a palladium catalyzed hydroamidation of enones.

### 4.5.1 Hydroamination

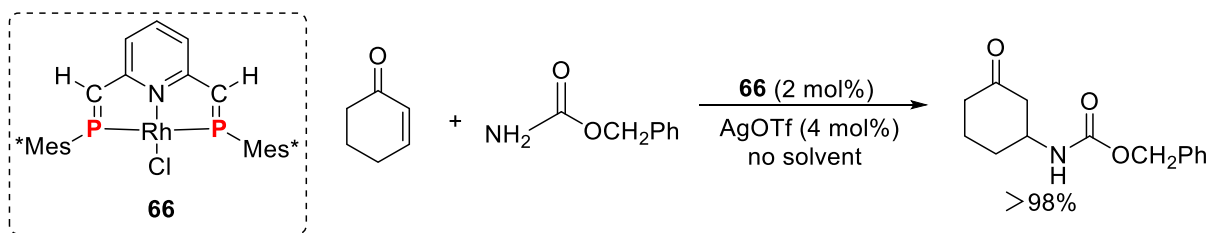
Palladium allyl DPCB complexes **61**, **64**, and **65** are effective for the 1,4-hydroamination of 1,3-dienes with aniline (Scheme 4.9).<sup>[107]</sup> An interesting solvent effect is observed: reactions in toluene (nonpolar) give high yields (91%), but there is no reaction observed using otherwise identical conditions in DMF (polar) (equation A). The incorporation of electron-withdrawing substituents on the DPCB ligand results in lower isolated yields [**65** (58%) < **61** (89%) < **64** (91%)]. Catalyst **61** also effectively mediates the hydroamination of styrene (equation B).



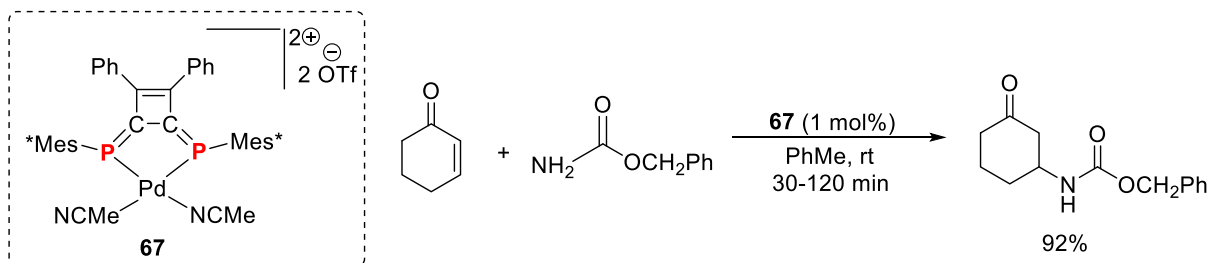
**Scheme 4.9** Hydroamination of 1,3-dienes.

### 4.5.2 Hydroamidation

P,N,P-complex **66** is active in the conjugative addition of carbamates to enones (Scheme 4.10) in excellent yields without solvent. The addition of silver triflate (AgOTf) is essential for catalytic activity. Prior exchange of the chloride counterion in **66** with a triflate counterion did not generate an active catalyst without the further addition of a catalytic amount of AgOTf. Importantly, control experiments demonstrated that AgOTf alone is not a competent catalyst for this conjugate addition, but that both **66** and AgOTf are required to achieve activity. Dicationic complex **67** actively catalyzes the conjugate addition of carbamates to enones (Scheme 4.11).<sup>[108]</sup> Although complex **67** shows higher activity than PdCl<sub>2</sub>(MeCN)<sub>2</sub>, its activity was comparable to the dicationic complex [Pd(MeCN)<sub>4</sub>](BF<sub>4</sub>)<sub>2</sub>. A possible advantage of using **67** as a catalyst is that palladium black is not observed. Palladium black is known to catalyze the undesirable disproportionation of cyclohexenone to cyclohexanone and phenol. Palladium black is generated when [Pd(MeCN)<sub>4</sub>](BF<sub>4</sub>)<sub>2</sub> is used as the catalyst.<sup>[108]</sup>



Scheme 4.10 Conjugate addition of benzyl carbamate to enones using **66**.

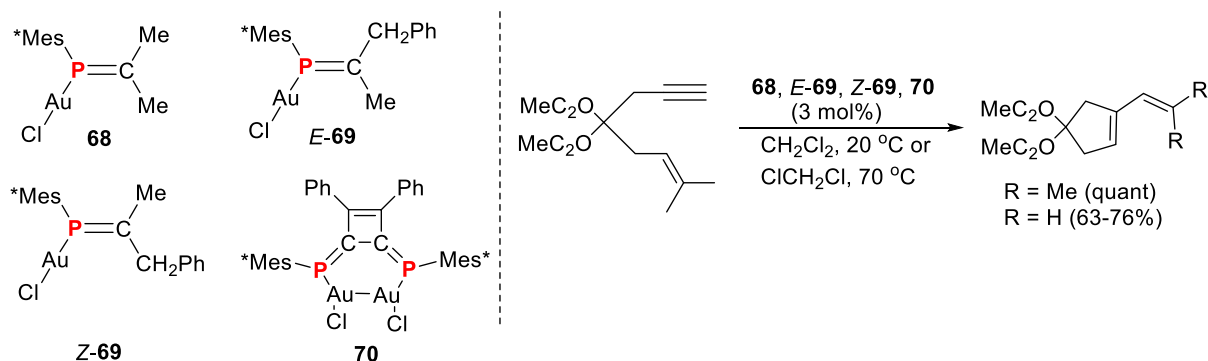


Scheme 4.11 Conjugate addition of benzyl carbamate to enones using **67**.

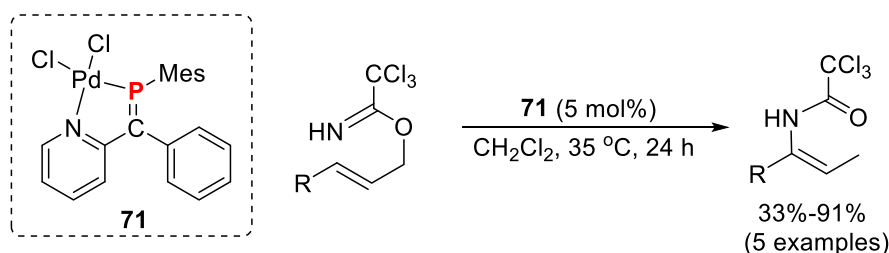
## 4.6 Isomerization reactions

Mostly, catalysis with phosphalkene ligands has used transition metals from the first and second rows. The following example of gold catalyzed cycloisomerization of enynes has expanded the use of phosphalkene ligands to the third row of the transition metals. Gold chloride complexes **68**, *E*-**69**, *Z*-**69**, and **70** effectively catalyze the isomerization of enynes to cyclopentenes in high yields (Figure 4.12). Interestingly, the phosphalkene–gold complexes do not require the addition of a silver co-catalyst as is often the case in these types of reactions. Mesityl-substituted phosphalkene Pd complex **71** is an effective catalyst for the

Overman–Claisen rearrangement (Scheme 4.13).<sup>[109]</sup> The substrate scope was investigated, and complex **71** catalyzes the conversion of linear allylic trichloroacetimidates containing linear aliphatic chains to branched allylic trichloroamides. Phosphaalkene-gold complexes showed potent catalytic activity in gold catalyzed cycloisomerization reactions.



**Scheme 4.12** Gold-catalyzed cycloisomerization of enynes.



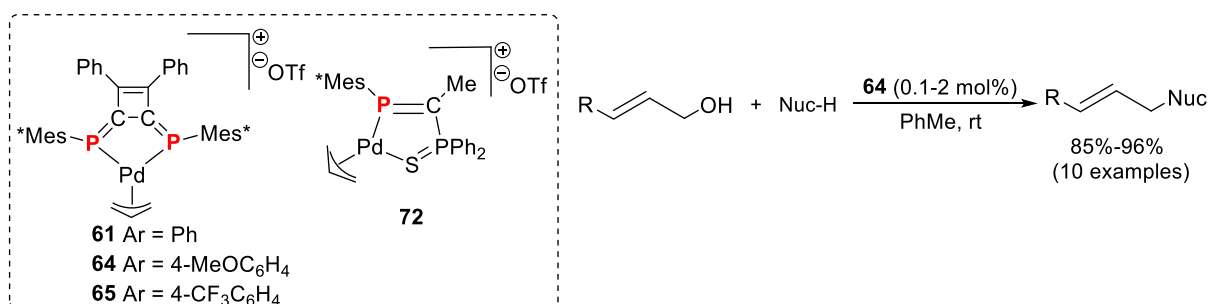
**Scheme 4.13** Overman–Claisen rearrangement using **71**.

## 4.7 Allylic substitution

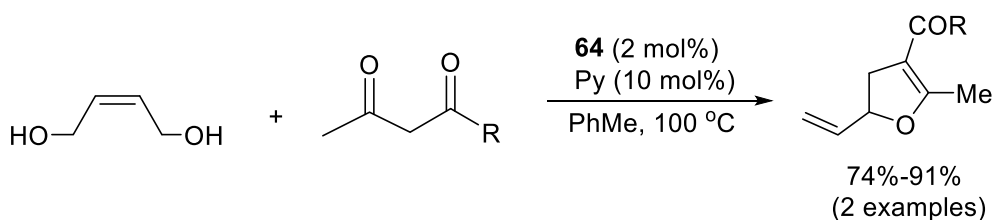
Allyl alcohols are usually converted to allyl acetates before metal-catalyzed allylic substitution can take place. Therefore, the direct substitution of allylic alcohols improves synthetic efficiency as the hydroxyl activation step is rendered unnecessary. The reaction of aniline with substituted allyl alcohols is catalyzed by complexes **61** (91%), **64** (96%), **65** (82%), and **72** (63%) (Scheme 4.14).<sup>[94, 96, 110]</sup> Superior results are obtained with the electron-rich complex **64**. Expanding upon the direct substitution of allyl alcohols, the cyclodehydration of *cis*-2-butene-1,4-diols can be employed to synthesize dihydrofuranes (Scheme 4.15).<sup>[111]</sup> The methodology involves mixing the diol and  $\beta$ -dicarbonyl compounds with a catalytic amount of base and **64** in toluene at 100 °C. Acetylacetone and ethyl acetoacetate generated dihydrofuranes in synthetically useful yields (91% and 74%, respectively).

Complex **64** is also an effective catalyst for the deallylation of a variety of allylic phenol ethers in the presence of aniline (Scheme 4.16). Deallylation reactions using **64** may be

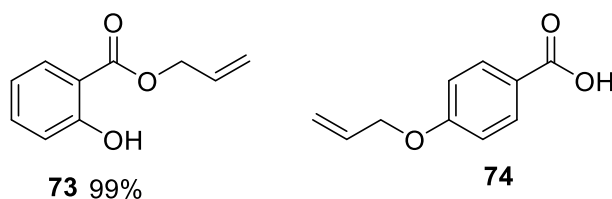
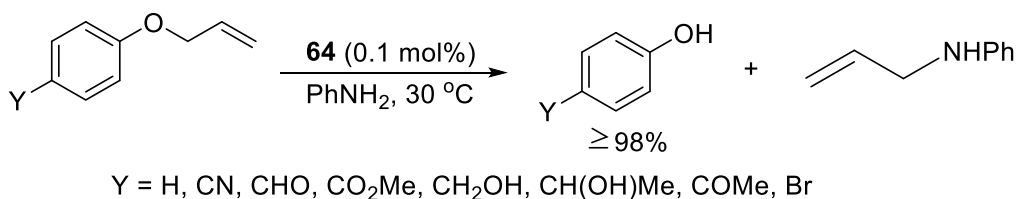
performed in air and in the presence of a variety of different functionalities such as vinyl, alkynyl, hydroxy, acetoxy, silyloxy, and acetonide groups.<sup>[112]</sup> An unusual selectivity is observed in the deallylation of bis-allylated hydroxybenzoic acid derivatives. Complex **64** removed only one allyl group, although two were present in the substrates. Allyl O-allyl-2-hydroxybenzoate reacts under identical conditions at only its allyl ether function to generate ester **73**. Allyl benzoate esters having allyl ether substitution at the *meta* or *para* positions react only at the ester function to afford products such as **74**. The use of Pd(PPh<sub>3</sub>)<sub>4</sub> as the catalyst resulted in complete, global deallylation. The authors speculated that coordination effects are responsible for the observed selectivities.



**Scheme 4.14** Allylic alkylation of allyl alcohols using phosphalkene complexes.



**Scheme 4.15** Cyclodehydration using **64**.

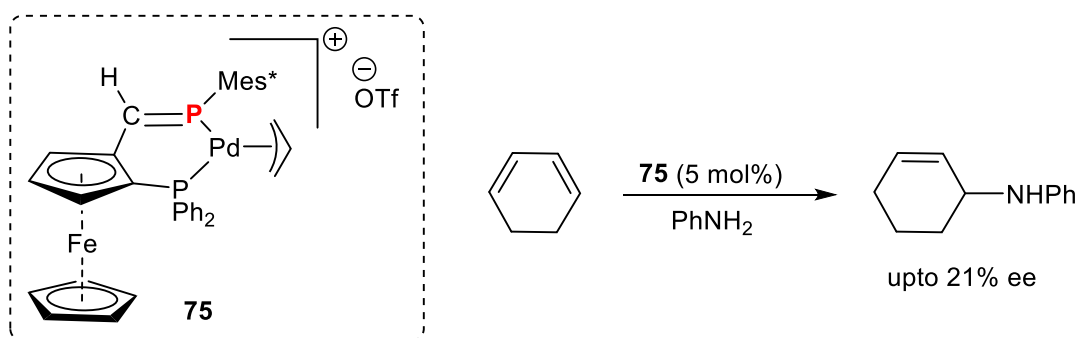


**Scheme 4.16** Deallylation reactions using **64**.

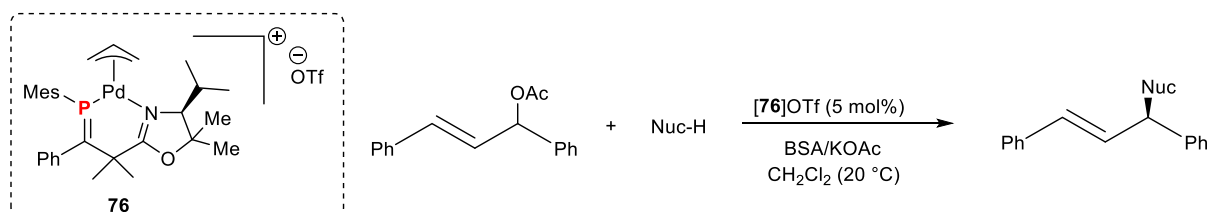
## 4.8 Asymmetric Catalysis

Recently, the development of chiral phosphalkene-based ligands and utilizing them within enantioselective processes has been an interesting area of research. Ozawa and co-workers utilized complex **75** in an asymmetric 1,4-addition of cyclobutadiene with aniline. The process resulted in low enantioselectivity (Scheme 4.17).<sup>[113]</sup>

The development of a novel class of phosphalkene–oxazoline (PhAk–Ox) ligands for use in asymmetric catalysis has given promising results. Allylic alkylation reactions can be performed in high yields and enantioselectivities using palladium(II) complexes supported by PhAk–Ox ligands (Scheme 4.18).<sup>[114]</sup> The use of complex **[76]OTf** bearing a ligand having *gem*-dimethyl substitution on the oxazoline ring was important in acquiring enantioselectivities above 90%. A variety of substituted malonate nucleophiles can be used in reactions catalyzed by a palladium PhAk–Ox complex **[76]OTf**.



**Scheme 4.17** Enantioselective hydroamination using **75**.



**Scheme 4.18** Allylic alkylation using complex **76**.



## 5 Objectives of this work

Phosphaalkenes are emerging as a new class of phosphorus ligands endowed with specific electronic properties. Their unique donor–acceptor properties offer interesting perspectives in coordination chemistry and catalysis. Phosphaalkenes are accessible via a variety of synthetic routes but in the past decade, the phospha-Wittig reaction has appeared as the most promising pathway to afford phosphaalkenes. Phosphanylidene phosphoranes or phospha-Wittig reagents  $R-P(PR'_3)$  are a powerful tool in synthetic inorganic chemistry and have found applications in the formation of phosphaalkenes using the so-called phospha-Wittig reaction, as well as valuable phosphinidene-transfer reagents.

Therefore, the main objective of this work was divided into two parts. First, we aimed to further study the potential of phosphanylidene phosphoranes as phosphinidene-transfer reagents to access bulky NHC phosphinidene adducts. In addition, the electron-rich dicoordinate phosphanylidene P-atom was utilized in reactions with nucleophiles and the activation of E–H bonds. The facile activation of E–H bonds gave straightforward access to species of interest for materials chemistry as well as to ligands for homogenous catalysis. Next, we attempted to exploit the reactivity of phospha-Wittig reagents toward carbonyl compounds to make a variety of phosphaalkene based ligands. As a part of this thesis, we targeted to synthesize a number of P,N-type phosphaalkene based Rh and Ir complexes to study their reactivity and application in homogenous catalysis. When preparing these complexes, special attention is required with respect to reaction conditions as otherwise, C–H bond activated phosphaindane based metal complexes are obtained. Theoretical investigations on the mechanism of such C–H bond activation were a part of this thesis.



## **6 List of publications**

The following chapter contains the original papers in which the presented results were published. The own contribution of the author of the dissertation to each publication is highlighted separately.

In paper 6.1, the work I carried out all experiments and analyzed the characterization data. In addition, a major part of the supporting information corresponding to the paper was written by me.

In paper 6.2, the work I undertook is synthesizing the ligand and the metal complexes along with the reported DFT study. In addition, I have drafted the manuscript.

In paper 6.3, the work I undertook is carrying out experiments and analyzing the characterization data of parts of the substrate scope.

In paper 6.4, I have contributed to the synthesis and characterization of parts of the compounds.

In paper 6.5, the work I undertook is carrying out all the synthetic as well as catalytic experiments and analyzing the characterization data. In addition, a major part of the manuscript corresponding to the paper was written by me.



## **6.1 Reactivity of phospho–Wittig reagents towards NHCs and NHOs**

Priyanka Gupta, Jan-Erik Siewert, Tim Wellnitz, Malte Fischer, Wolfgang Baumann, Torsten Beweries and Christian Hering-Junghans

*Dalton Trans.*, **2021**, 50, 1838–1844

DOI: 10.1039/d1dt00071c

Reprinted (adapted) with permission from *Dalton Trans.*

© The Royal Society of Chemistry 2021

Contribution to this paper is 50%





Cite this: *Dalton Trans.*, 2021, **50**, 1838

Received 8th January 2021,  
Accepted 12th January 2021

DOI: 10.1039/d1dt00071c

rsc.li/dalton

## Reactivity of phospho–Wittig reagents towards NHCs and NHOs†‡

Priyanka Gupta,<sup>ID</sup> Jan-Erik Siewert, Tim Wellnitz, Malte Fischer, Wolfgang Baumann, Torsten Beweries<sup>ID</sup>\* and Christian Hering-Junghans<sup>ID</sup>\*

Phospha–Wittig reagents,  $\text{RPPMe}_3$  ( $\text{R} = \text{Mes}^* 2,4,6\text{-}t\text{Bu}_3\text{-C}_6\text{H}_2$ ;  $\text{Mes}^*\text{Ter}$  2,6-(2,4,6- $\text{Me}_3\text{C}_6\text{H}_2$ )- $\text{C}_6\text{H}_3$ ;  $\text{DipTer}$  2,6-(2,6- $\text{iPr}_2\text{C}_6\text{H}_3$ )- $\text{C}_6\text{H}_3$ ), can be considered as phosphine-stabilized phosphinidenes. In this study we show that  $\text{PMe}_3$  can be displaced by NHCs or NHOs. Interestingly, phosphinidene-like reactivity results in a subsequent  $\text{C}(\text{sp}^2)\text{-H}$  activation of the exocyclic  $\text{CH}_2$  group in NHOs. This concept was further extended to allyl-aped NHOs, which resulted in phosphine-substituted allyl species.

In 1953 Wittig and Geisler reported the olefination of carbonyl groups with the aid of phosphorus ylides, the so-called Wittig reaction.<sup>1,2</sup> This protocol allows the chemo- and regioselective conversion of carbonyl functionalities into olefins and has been widely utilized, even on large industrial scale.<sup>3–5</sup> Phosphorus ylides of the type  $\text{R}_3\text{P}^{(+)}\text{-C}^{(-)}\text{R}_2$  are generated by the alkylation of phosphines and subsequent treatment with stoichiometric amounts of base. The reaction with a carbonyl compound then furnishes the desired alkene and phosphine oxides, which are the driving force of this transformation.

Burg and Mahler investigated the action of an excess of  $\text{PMe}_3$  on the cyclophosphanes  $(\text{PCF}_3)_4$  and  $(\text{PCF}_3)_5$ , noting the reversible formation of  $\text{F}_3\text{CP}=\text{PMe}_3$ , a phosphanylidene phosphorane,<sup>6</sup> and the concentration-dependent exchange of  $\text{PMe}_3$  was later detected, indicating exchange of coordinated  $\text{PMe}_3$ .<sup>7</sup> Investigating the reactivity of  $[\text{Cp}_2\text{Zr}(\text{PR}_3)\text{P}^{\text{Mes}^*\text{Ter}}]$  ( $\text{R} = \text{Me}$ ,  $n\text{Bu}$ ;  $\text{Mes}^*\text{Ter} = 2,6\text{-}\{2,4,6\text{-}\text{Me}_3\text{C}_6\text{H}_2\}_2\text{-C}_6\text{H}_3$ ) Protasiewicz and co-workers noted the formation of  $\text{Mes}^*\text{TerP}=\text{PR}_3$ .<sup>8</sup> In general compounds of the type  $\text{RP}=\text{PR}'_3$  are referred to as phospho–Wittig reagents by isolobal replacement of the  $\text{CR}_2$  in  $\text{R}_2\text{C}=\text{PR}'_3$  with a phosphinidene fragment  $\text{PR}$ .<sup>9</sup> The term “phospho–Wittig” reaction was originally introduced by Mathey for the reaction of  $(\text{RO})_2\text{P}(\text{O})\text{-P}^{(-)}[\text{W}(\text{CO})_5]\text{R}'$  with ketones to give  $(\text{CO})_5\text{W}$ -coordinated phosphoalkenes.<sup>10</sup> The Protasiewicz group then showed that unsupported phospho–

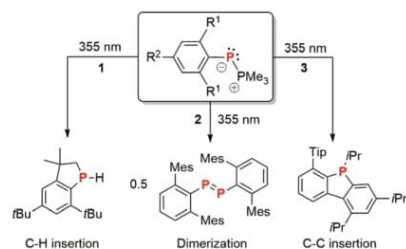
Wittig reagents can be isolated when the group  $\text{R}$  on phosphorus is kinetically stabilizing and to date four examples of  $\text{ArP}=\text{PMe}_3$  ( $\text{Ar} = 2,4,6\text{-}t\text{Bu}_3\text{-C}_6\text{H}_2$ ,  $\text{Mes}^*$  (1);  $\text{Mes}^*\text{Ter}$  (2);<sup>11</sup> 2,6- $\{2,4,6\text{-}\text{iPr}_3\text{C}_6\text{H}_2\}_2\text{-C}_6\text{H}_3$ ,  $\text{TipTer}$  (3);<sup>12</sup> 1,1,3,3,5,5,7,7-octaethyl-1,2,3,5,6,7-hexahydro-*s*-indacen-4-yl,  $\text{EIND}^{13}$ ) have been described in the literature. In addition, the difunctional phospho–Wittig material  $(E),(E)\text{-1,4-bis-(Me}_3\text{P}=\text{P})\text{-(3,5-dimesitylstyryl)-2,5-di-}n\text{-hexyloxybenzene}$  was shown to afford diphosphene containing polymers upon photolysis or thermolysis.<sup>14</sup> Phospho–Wittig reagents are generally obtained by the combination of the respective dichlorophosphine  $\text{Ar-PCl}_2$  with zinc powder and an excess of  $\text{PMe}_3$ , whereby  $\text{PMe}_3$  acts as the active reductant (with concomitant formation of  $\text{Cl}_2\text{PMe}_3$ ),<sup>15,16</sup> and stabilizing base. Zinc dust seems to be redundant here, however, high yields are not obtained when only using  $\text{PMe}_3$ , *vide infra*. The role of  $\text{PR}_3$  and  $\text{PR}_3\text{Cl}_2$  was studied in detail and it was shown that  $\text{PMe}_3$  can catalyse the chlorine atom transfer between  $\text{ArPPMe}_3$  and  $\text{Ar'PCl}_2$ .<sup>15</sup> Using  $\text{ArP}=\text{PMe}_3$  in the reaction with aldehydes (note ketones cannot be converted using this methodology) phosphoalkenes,  $\text{RP}=\text{CR'H}$ , are obtained, with the concomitant formation of  $\text{Me}_3\text{P}=\text{O}$ . Thus, this reactivity can be classified as Wittig-type, as the driving force in the classical Wittig reaction is the formation of  $\text{R}_3\text{P}=\text{O}$  as well. Furthermore, phosphanylidene phosphoranes have been shown to display phosphinidenoid reactivity. For example, laser irradiation of 1–3 at 355 nm facilitates  $\text{PMe}_3$  cleavage,<sup>12</sup> and in case of 1 a C–H activation of one *o*-*t*Bu-group of  $\text{Mes}^*$  results in the formation of a phosphaindane (Scheme 1).<sup>17–19</sup> For 2 phosphinidene recombination and formation of  $(\text{PTer})_2$  prevails, whereas C–C bond activation and phosphoalkene formation is the major pathway for 3 (Scheme 1, middle and right).<sup>20</sup> Moreover, the cyclo-addition of 1 and 2 with quinones affords 1,3,2-dioxophospholanes rather than producing the expected 1,2-diphosphoalkenes.<sup>21</sup> Phosphinidene transfer was shown for 2 when combined with  $\text{Cp}_2\text{Zr}(\text{PMe}_3)_2$  yielding

Leibniz-Institut für Katalyse e.V. (LIKAT Rostock), Albert-Einstein-Straße 29a, 18059 Rostock, Germany. E-mail: torsten.beweries@catalysis.de, christian.hering-junghans@catalysis.de

†Dedicated to Prof. Dr Paul Kamer for his achievements in Phosphorus Chemistry.

‡Electronic supplementary information (ESI) available: Synthesis and characterization of compounds, NMR spectra, crystallographic, and computational details. CCDC 2046859–2046869. For ESI and crystallographic data in CIF or other electronic format see DOI: 10.1039/d1dt00071c





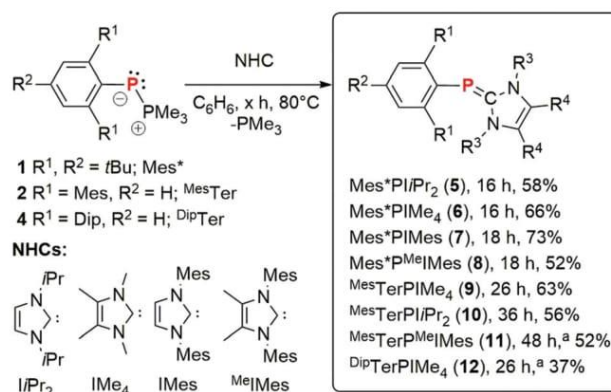
**Scheme 1** Photolytic cleavage of **1** ( $R^1, R^2 = t\text{Bu}$ ), **2** ( $R^1 = \text{Mes}, R^2 = \text{H}$ ) and **3** ( $R^1 = \text{Tip}, R^2 = \text{H}$ ) and the products of phosphinidene quenching.

$\text{Cp}_2\text{Zr}(\text{P}^{\text{Mes*Ter}})(\text{PMe}_3)$ , while combination of **1** with (PNP)V( $\text{CH}_2t\text{Bu}$ )<sub>2</sub> (PNP =  $\text{N}[\text{C}_6\text{H}_4\text{P}(\text{CHMe}_2)_2-4\text{-methylphenyl}]_2$ ) furnished the first V(v) terminal phosphinidene complex.<sup>22</sup>

Recently, phosphanylphosphaketenes  $\text{R}_2\text{P-PCO}$  have emerged as a synthetic surrogate for phosphinidenes, which unlocked a pathway towards an isolable room-temperature stable singlet phosphinidene  $[\text{P}]\text{P}$  ( $[\text{P}] = (\text{H}_2\text{CNAr}^{**})_2\text{P}$ ,  $\text{Ar}^{**} = 2,6\text{-bis}[(4\text{-tert-butylphenyl)methyl]-4-methylphenyl}$ ).<sup>23</sup> In addition, Bertrand and co-workers showed facile ligand exchange of CO in  $[\text{S}^{\text{P}}]\text{PCO}$  ( $[\text{S}^{\text{P}}] = (\text{H}_2\text{CNDip})_2\text{P}$ ) for  $\text{PR}_3$ , CNAd,  $\text{I}^t\text{Pr}_2$  and  $\text{Et}^t\text{CAAC}$ , with calculations supporting an associative mechanism with a T-shaped transition state.<sup>24</sup> Just recently, the decarbonylation of  $[\text{S}^{\text{P}}]\text{PCO}$  in the presence of  $(\text{Dip}^t\text{Nacnac})\text{Ga}$  afforded a phosphagallene with a  $\text{P=Ga}$  double bond.<sup>25</sup> Gallium phosphaketenes also show CO for  $\text{PMe}_3$  exchange, affording gallium-substituted phospho-Wittig reagents.<sup>26</sup>

Phospha-Wittig reagents are moreover isovalence-electronic to carbene phosphinidene adducts,<sup>27</sup> an emerging compound class in main group and transition metal chemistry<sup>28</sup> and thus, phosphanylidene phosphoranes should be easily converted into such by replacement of the phosphine with a carbene. In addition, the NHC phosphinidene adduct  $\text{PhP=IME}_2$  has been shown to be transferred onto organic substrates in the presence of  $\text{ZnCl}_2$ ,<sup>29</sup> furthermore underlining the potential of this compound class. We now report on the facile synthesis of a variety of NHC phosphinidene adducts derived from  $\text{ArPPR}_3$  and show that in case of N-heterocyclic olefins (NHOs)  $\text{PMe}_3$  release is followed by an intramolecular  $\text{C}(\text{sp}^2)\text{-H}$  activation to afford phosphine-substituted NHOs.

Phospha-Wittig reagents are usually synthesized *in situ* and directly used in subsequent reactions, mostly with aldehydes in the synthesis of phosphalkenes. Herein, modified literature procedures were used to allow for the isolation of the phospho-Wittig reagents **1** and **2** in up to a multigram scale (Scheme 2, for detailed synthetic procedures please refer to the ESI p.S4ff†).<sup>30</sup>  $\text{Dip}^t\text{TerPPMe}_3$  (**4**), has not been reported previously and was synthesized by reduction of  $\text{Dip}^t\text{TerP}(\text{Cl})_2$  with  $\text{Zn}/\text{PMe}_3$  in a 1:2:10 ratio in THF. Full conversion was achieved after stirring the mixture for 24 h and after filtration and removal of the solvent **4** was afforded as a yellow, thermally stable solid in 50% yield. In the  $^{31}\text{P}$  NMR spectrum **4** is characterized by two doublet signals at  $-116.5$  ppm ( $\text{P}^{\text{Dip}^t\text{Ter}}$ )



**Scheme 2** Synthesis of NHC phosphinidene adducts **5–12** in the reaction of various NHCs with **1**, **2** or **4**, respectively. (<sup>a</sup>Mixture was heated to 115 °C in toluene- $d_8$ ).

and  $-3.1$  ( $\text{PMe}_3$ ) ppm, respectively and a  $^1\text{J}_{\text{PP}}$  coupling constants of 560 Hz. X-ray quality crystals of **4** were grown from a saturated *n*-hexane solution at  $-30$  °C (Fig. S13†). The P1–P2 distance [ $2.0955(7)$  Å] is significantly shorter than typical P–P single bonds ( $\sum r_{\text{cov}}(\text{P–P}) = 2.22$  Å)<sup>31</sup> and slightly elongated compared to typical  $\text{P=P}$  double bonds ( $\sum r_{\text{cov}}(\text{P=P}) = 2.04$  Å),<sup>31</sup> thus being, as expected, in good accordance to the other structurally characterized phospho-Wittig reagent **2** [ $2.084(2)$  Å].<sup>32</sup> With **1**, **2** and **4** available on a gram-scale we systematically studied their reactivity.

In a first sequence  $\text{Mes}^*\text{PPMe}_3$  (**1**) was combined with  $\text{I}^t\text{Pr}_2$  in  $\text{C}_6\text{D}_6$  at room temperature, resulting in a color change from yellow to orange and the appearance of a signal at  $-62.6$  ppm for free  $\text{PMe}_3$  in the  $^{31}\text{P}$  NMR spectrum and at  $-50.7$  ppm suggested formation of the corresponding NHC phosphinidene adduct  $\text{Mes}^*\text{P=I}^t\text{Pr}_2$  (**5**) (Scheme 2).<sup>27,33</sup> Clean conversion to **5** is achieved upon heating to 80 °C over a period of 16 h. To gauge the scope of the substitution reaction, carbenes with different steric profiles were tested. Complete  $\text{PMe}_3$  for NHC exchange in **1** at 80 °C was achieved for  $\text{IME}_4$ ,  $\text{IMes}$  and  $\text{MeI}^t\text{Mes}$ , while no conversion was achieved with  $\text{I}^t\text{Pr}_2\text{Me}_2$ , which is most likely due to steric reasons.  $\text{Mes}^*\text{P=IME}_4$  (**6**),  $\text{Mes}^*\text{P=IMes}$  (**7**) and  $\text{Mes}^*\text{P=MeI}^t\text{Mes}$  (**8**) are deep yellow thermally stable (melting points  $>138$  °C) solids and X-Ray quality crystals of **5**, **6** and **8** were grown from saturated *n*-hexane solutions at  $-30$  °C. **6** shows a  $^{31}\text{P}$  NMR signal at  $-47.5$  ppm, while **7** and **8** appear less shielded at  $-29.8$  and  $-33.2$  ppm, respectively. In the  $^1\text{H}$  NMR spectrum three signals are detected for the  $\text{Mes}^*$  group and two sets of signals for the *N*-substituents of the NHCs as well as for the backbone protons (**5**, **7**) or methyl groups (**6**, **8**), respectively, indicating  $\text{C}_2$  symmetry on the NMR time-scale. The molecular structures of **6** and **8** display P– $\text{C}_{\text{NHC}}$  distances [**6**  $1.7709(12)$ , **8**  $1.7630(19)$  Å] (Fig. 1) similar to that reported in  $(\text{EIND})\text{P=IME}_4$  [ $d(\text{P–C}_{\text{NHC}})$   $1.767(3)$  Å],<sup>34</sup> and  $\text{MesP=IMes}$  [ $d(\text{P–C}_{\text{NHC}})$   $1.769(3)$  Å].<sup>35</sup> The  $\text{CPC}_{\text{NHC}}$  angles [**6**  $102.58(5)$ , **8**  $106.38(8)$  °] are in the expected range for NHC phosphinidene adducts and the planes of the central phenyl group in  $\text{Mes}^*$  and the imidazolidine unit are offset from a



## Paper

perpendicular arrangement by 10–15°. One of the *N*-mesityl substituents in **8** is parallel to the Mes\* group indicating arene–arene interactions. The concept of NHC for  $\text{PMe}_3$  exchange could be extended to **2** and  $\text{Mes}^*\text{TerP}=\text{IME}_4$  (**9**),<sup>36</sup> and  $\text{Mes}^*\text{TerP}=\text{IiPr}_2$  (**10**) were afforded as yellow crystalline solids in moderate isolated yields solids after heating **2** and the respective NHC at 80 °C overnight (Scheme 2). The combination of **2** and  $\text{Me}^*\text{IMes}$  gave only minimal conversion at 80 °C, however, heating the mixture to 115 °C in toluene-*d*<sub>8</sub> for 48 h facilitated full conversion to  $\text{Mes}^*\text{TerP}=\text{Me}^*\text{IMes}$  (**11**). Again, no conversion was observed with  $\text{IiPr}_2\text{Me}_2$ , even though  $\text{Mes}^*\text{TerP}=\text{IiPr}_2\text{Me}_2$  has been previously reported by Ragogna *et al.* through the desulfurization of  $[\text{SP}^{\text{Mes}^*}\text{Ter}]_2$  with 2 equivalents of  $\text{IiPr}_2\text{Me}_2$ . With **4** only the reaction with  $\text{IME}_4$  yielded the corresponding  $\text{Dip}^{\text{Ter}}\text{P}=\text{IME}_4$  (**12**) in low isolated yields of 37% (Scheme 2). The  $\text{P}-\text{C}_{\text{NHC}}$  distances in **10** [1.786(2) Å] and **12** [1.8074(11) Å] are minimally longer compared to **6** and **8**, the  $\text{CPC}_{\text{NHC}}$  angles are similar [**10** 104.21(5), **12** 102.90°] and the imidazolidine and central phenyl plane deviate from a perpendicular arrangement by *ca.* 35° (Fig. 1). This indicates a more electron-rich phosphorus center compared to the Mes\* substituted derivatives **5–8** as further evidenced by the <sup>31</sup>P NMR shift of **9** [−76.9 ppm], **10** [−79.8 ppm], **11** [−45.1 ppm] and **12** [−63.2 ppm]. In addition, the <sup>13</sup>C NMR signal of the  $\text{C}_{\text{NHC}}$  atom is detected at *ca.* 170 ppm with a <sup>1</sup>*J*<sub>PC</sub> coupling constant that directly corresponds to the P–C bond lengths,<sup>33</sup> with *J*<sub>PC</sub> values being smaller when the P–C bond is longer.

To elucidate the reaction mechanism we conducted DFT calculations at the B3LYP/6-311G(d,p) gd3 smd(C<sub>6</sub>H<sub>6</sub>) level of theory, which reproduced the metrical parameters of **1**, **2**, **4** and **5–12** well with respect to their molecular structures.<sup>30</sup> In addition, the calculated <sup>31</sup>P NMR shifts are in good agreement with experimental values and reflect the trends observed for **5–12**.<sup>30</sup> Starting from **1** a T-shaped transition state in the reaction with  $\text{IiPr}_2$  was found, in line with the observed exchange of  $\text{PMe}_3$  for a NHC in **1** to afford **5–8**.<sup>24</sup> The activation barrier was determined to be  $\Delta_R G^\ddagger = 23.8 \text{ kcal mol}^{-1}$  for  $\text{IiPr}_2$  and overall the formation of **5** and release of  $\text{PMe}_3$  is exergonic by  $\Delta_R G^0 = -17.9 \text{ kcal mol}^{-1}$ . A lower barrier was found for the reaction with  $\text{IME}_4$  [ $\Delta_R G^\ddagger = 20.4 \text{ kcal mol}^{-1}$ ], whereas for  $\text{IMes}$  and  $\text{Me}^*\text{IMes}$  the barriers are the highest. Furthermore, the

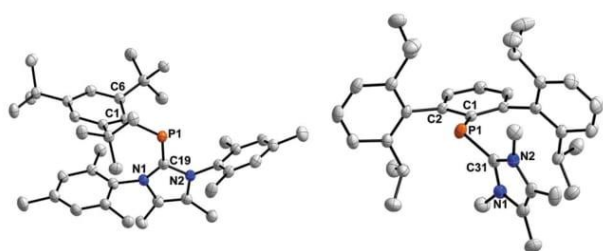
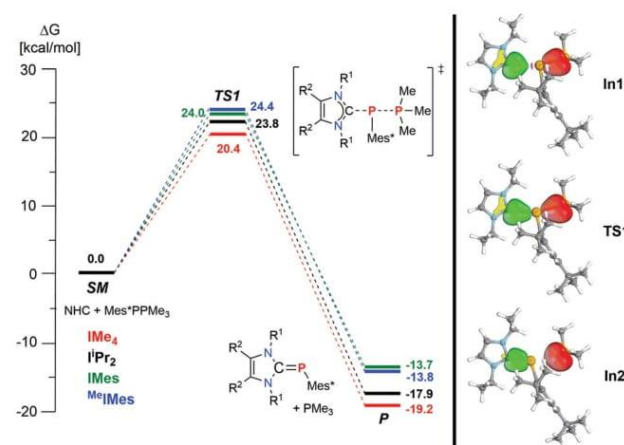


Fig. 1 POV-ray depiction of the molecular structure of **8** and **12**. ORTEPs drawn at 50% probability, all H-atoms are omitted for clarity. Selected bond lengths (Å) and angles (°) of **8** (values from 2<sup>nd</sup> molecule in the asymmetric unit): P1–C19 1.7630(19) (1.7594(19)), P1–C1 1.8683 (18) (1.8639(18)), C19–P1–C1 106.38(8) (105.22(8)); **12**: P1–C19 1.8074 (11), P1–C1 1.8280(10), C31–P1–C1 104.21(5).

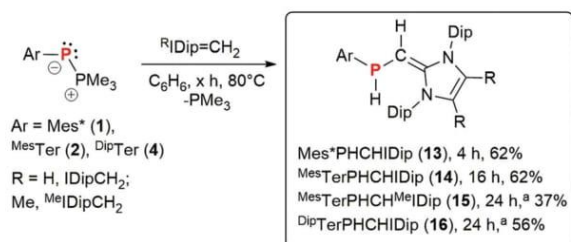
associative transition state explains that the formation of the C–H-activated phosphaindane is not detected.<sup>30</sup> In accordance with experimental findings, the exchange in **2** was shown to possess higher  $\Delta_R G^\ddagger$  energy barriers, with a similar exergonic overall reaction. The reaction of **2** with  $\text{Me}^*\text{IMes}$  only proceeded at 115 °C, which is clearly reflected by a high activation barrier of 35.9 kcal mol<sup>−1</sup> for this reaction, while the overall reaction is exergonic by −5.0 kcal mol<sup>−1</sup>. To achieve a better understanding of this substitution reaction, IBO analyses of stationary points of selected species along the intrinsic reaction coordinate (IRC) from **1** with  $\text{IiPr}_2$  leading to **5** were performed (Scheme 3, right). IBOs have been shown to illustrate electronic structure changes in intuitive terms.<sup>37,38</sup> In the case of **5**, the IBO associated with the  $\text{IiPr}_2$  lone pair (LP; Scheme 3, **IN1**, green/yellow) is transformed into a newly formed C–P  $\sigma$ -bond (Scheme 3, **IN2**, green/yellow), and the IBO for the P–P bonds converts into the  $\text{PMe}_3$  lone pair of electrons (Scheme 3, **IN2**, red). The transformation clearly involves initial nucleophilic attack by the NHC LP onto the  $\sigma^*$ -antibonding orbital of the P–P bond in **1**, **2** and **4** (Scheme 3, **TS1**), concurrent with the proposed S<sub>N</sub>2-type substitution.

Having shown the facile  $\text{PMe}_3$  for NHC exchange in **1**, **2** and **4** we wanted to investigate whether strongly  $\sigma$ -donating NHOs could also facilitate  $\text{PMe}_3$  exchange to give more labile phosphinidene NHO adducts. NHOs are characterized by a highly polarized exocyclic double bond,<sup>39,40</sup> placing considerable electron density on the terminal =CH<sub>2</sub> group, and determinations of their TEP values have shown that they are strong donors.<sup>33,41,42</sup> In contrast to NHCs however, they are not  $\pi$ -accepting, facilitating the formation of Pd nanoparticles when using [ $\text{Me}^*\text{IDipCH}_2$ ] $\text{PdCl}(\text{Cin})$  as a precatalyst in Buchwald–Hartwig aminations.<sup>43</sup> Beller and coworkers introduced 2-phosphanylmethyl-*N,N'*-biaryl-imidazolium salts as ligand precursors in palladium-catalysed C–O and C–N coupling reactions, which under the respective reaction conditions (*e.g.* CsOH as a base) should be deprotonated to give P-substituted NHOs.<sup>44,45</sup> Moreover, isolable P-substituted



Scheme 3 DFT predicted free energy profile for the reaction of Mes\*PPMe<sub>3</sub> with NHCs (left). Selected IBOs along the reaction coordinate (right).





**Scheme 4** Synthesis of P-substituted NHOs (**13–16**) starting from **1**, **2** or **4** in the reaction with IDipCH<sub>2</sub> or MeIDipCH<sub>2</sub>, respectively. (<sup>a</sup>Sample was heated to 105 °C).

NHOs have been reported and Ghadwal *et al.* showed facile access to <sup>R</sup>IDip=C(Ph)PCL<sub>2</sub>,<sup>46</sup> whereas IDipCH(PR<sub>2</sub>) (R = *i*Pr, Ph) was reported by Rivard *et al.*<sup>47</sup> Using a bis(NHO)-ligand Kinjo and co-workers reported on aromatic isophosphindolium derivatives.<sup>48</sup> Combining **1** with IDipCH<sub>2</sub> in C<sub>6</sub>D<sub>6</sub> and heating the 1:1 mixture to 80 °C overnight resulted in consumption of **1** and formation of a new species with a doublet of doublets in the <sup>1</sup>H NMR spectrum centred at 5.20 ppm (<sup>1</sup>J<sub>PH</sub> = 216.2 Hz, <sup>3</sup>J<sub>HH</sub> = 1.0 Hz) indicating the formation of Mes\*PHCHIDip (**13**) (Scheme 4). This assignment was confirmed by SC-XRD experiments on crystals grown from saturated *n*-hexane solutions at –30 °C (Fig. 2, left). The P–H protons in **13** could be located on the Fourier map and a 1:1 ratio between *R* and *S* configurations was identified.

**13** can be considered as a P-substituted NHO with a C=C<sub>NHC</sub> [1.360(2), *cf.*  $\sum r_{\text{cov}}(\text{C}=\text{C}) = 1.34 \text{ \AA}$ ]<sup>31</sup> double bond and a P–C<sub>NHO</sub> [1.8013(18), *cf.*  $\sum r_{\text{cov}}(\text{P}=\text{C}) = 1.86 \text{ \AA}$ ]<sup>31</sup> single bond in accord with the related IDipCH(P*i*Pr<sub>2</sub>) [*cf.*  $d(\text{C}=\text{C}_{\text{NHC}}) 1.364(4)$ ,  $d(\text{P}=\text{C}_{\text{NHO}}) 1.780(3) \text{ \AA}$ ].<sup>47</sup> To show that this reactivity is not only restricted to Mes\*PPMe<sub>3</sub>, **2** was treated with one equivalent

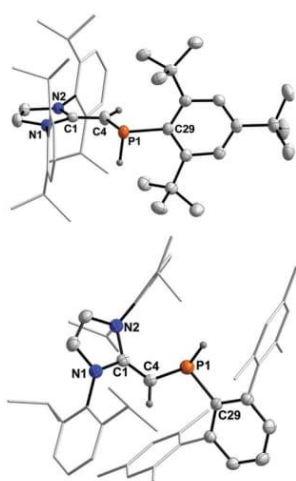
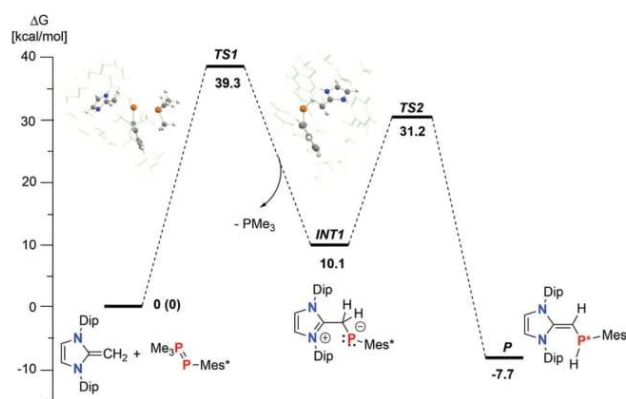


**Fig. 2** POV-ray depiction of the molecular structure of **13** and **14**. ORTEPs drawn at 50% probability, all H atoms are omitted for clarity. Selected bond lengths (Å) and angles (°) of **13**: P1–C4 1.8013(18), P1–C29 1.8679(17), C1–C4 1.360(2); C1–C4–P1 126.51(14), C4–P1–C29 105.12(8); **14**: P1–C4 1.8540(13), P1–C29 1.8540(13), C1–C4 1.3580(18); C1–C4–P1 126.93(10), C4–P1–C29 100.59(6).

IDipCH<sub>2</sub> or MeIDipCH<sub>2</sub>, and after heating to 80 °C or 105 °C the corresponding P-substituted NHOs Mes\*TerPHCHIDip (**14**) and Mes\*TerPHCHMeIDip (**15**) were afforded in 62 and 37% yield, respectively (Scheme 4). In addition, DipTerPHCHIDip (**16**) was afforded when utilizing **4** as a starting material. As mentioned above, the formation of **13–16** can be clearly identified by the appearance of a doublet of doublets between 4.11–5.29 ppm with a characteristic <sup>1</sup>J<sub>PH</sub> and <sup>3</sup>J<sub>HH</sub> coupling constant of *ca.* 210 Hz and *ca.* 2 Hz, respectively. Additionally, the <sup>13</sup>C NMR signal of the vinyl C-atom appears as a characteristic doublet (<sup>1</sup>J<sub>PC</sub> = 7–15 Hz) at *ca.* 42 ppm (**14–16**) and 52.5 ppm (**13**) [*cf.* IDipCH(P*i*Pr<sub>2</sub>)  $\delta(^{13}\text{C}) = 51.4 \text{ ppm}$ ].<sup>47</sup> Moreover, IR spectroscopy revealed characteristic P–H stretching modes at *ca.* 2300 cm<sup>–1</sup>.<sup>30</sup> A similar C–H activation process was discussed by Ghadwal *et al.* for IDipCH(SiCl<sub>2</sub>H), readily accessible from the combination of two equivalents IDipCH<sub>2</sub> with HSiCl<sub>3</sub>, with concomitant formation of [IDipCH<sub>3</sub>]Cl. Interestingly, IDipCH(SiCl<sub>2</sub>H) is also formed when IDipSiCl<sub>2</sub> is reacted with IDipCH<sub>2</sub>, with a formal insertion of the silylene SiCl<sub>2</sub> into the exocyclic CH<sub>2</sub> group of IDipCH<sub>2</sub>.<sup>49</sup>

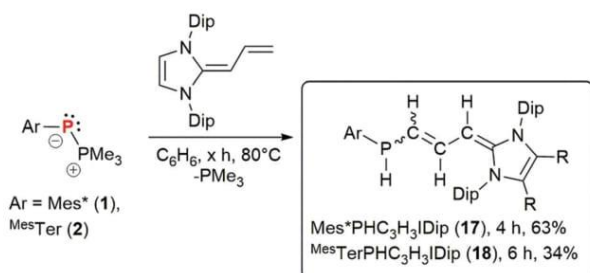
This C(sp<sup>2</sup>)–H bond activation in NHOs with the aid of the phosphinidenoid species **1**, **2** and **4** was theoretically investigated by DFT studies. A potential energy surface scan was carried out for the reaction of **1** with IDipCH<sub>2</sub> and a first T-shaped transition state was located with a high barrier of  $\Delta_R G^\ddagger = 39.3 \text{ kcal mol}^{-1}$  (Scheme 5), in line with these reactions going to completion only after prolonged heating at 80 °C. The intermediate **INT1**, an NHO–phosphinidene adduct through release of PMe<sub>3</sub> is endergonic and in a second reaction step an H-Shift from IDipCH<sub>2</sub> to PMes\* occurs with a barrier (TS2,  $\Delta_R G^\ddagger = 21.1 \text{ kcal mol}^{-1}$ ) that is lower than TS1. Therefore, the NHO for PMe<sub>3</sub> substitution is the rate-determining step, in line with **INT1** not being observed in this transformation. It needs to be pointed out that the energy barrier TS1 is rather high, however, the full model was used for these calculations and the trends observed experimentally are clearly supported.

Having observed this C(sp<sup>2</sup>)–H activation we turned to the allyl-appended NHO IDipC<sub>3</sub>H<sub>4</sub>, to elucidate whether the C–H activation pathway is more general. Enediamine IDipC<sub>3</sub>H<sub>4</sub> was



**Scheme 5** DFT predicted free energy profile for the reaction of Mes\*PPMe<sub>3</sub> with IDipCH<sub>2</sub>. The free enthalpies are given in kcal mol<sup>–1</sup>.

## Paper



**Scheme 6** Synthesis of P-substituted enediamines **17** and **18** starting from **1** or **2** in the reaction with IDipC<sub>3</sub>H<sub>4</sub>.

first reported by Jacobi von Wangelin *et al.* and has two potential nucleophilic sites in  $\alpha$  and  $\gamma$  position.<sup>50,51</sup> Rivard and co-workers have shown coordination to Pd(II),<sup>43</sup> and AlMe<sub>3</sub>,<sup>52</sup> through the  $\gamma$ -position. Heating a mixture of **1** or **2** with IDipC<sub>3</sub>H<sub>4</sub> in C<sub>6</sub>H<sub>6</sub> to 80 °C, conversion into the new species Mes\*PHC<sub>3</sub>H<sub>3</sub>IDip (**17**) and TerPHC<sub>3</sub>H<sub>3</sub>IDip (**18**) and release of PMe<sub>3</sub> were noted by <sup>31</sup>P{<sup>1</sup>H} NMR spectroscopy (Scheme 6). Pale yellow X-ray quality crystals of **17** and **18** could be grown from saturated *n*-hexane solutions at –30 °C and revealed in case of **17** a *Z*-configuration of the C5–C6 double bond, so that the vinylic proton on C4 and the PH point into one direction, even though they are not in one plane (Fig. 3, note that in solution *E*-**17** is the major component, but *Z*-**17** is detected as well). In solution a spatial correlation *via* dipolar couplings, in particular homonuclear NOE, between C(4)–H and P(1)–H in *Z*-**17** is detected.

For **18** a *E*-configuration is observed for the C5–C6 bond, which in solution was corroborated by dipolar coupling of C(4)–H and C(6)–H.<sup>30</sup> The bonding parameters of **17** and **18** correspond with P-substituted enediamines [C1–C4 1.376(2) (**17**), 1.3734(16) (**18**); C4–C5 1.422(2) (**17**), 1.4309(15) (**18**); C5–C6 1.355(2) (**17**), 1.3483(16) (**18**) Å] with trigonal pyramidal P atoms. The C<sub>4</sub>P unit minimally deviates from a planar arrange-

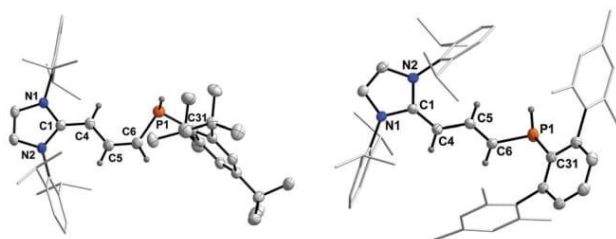
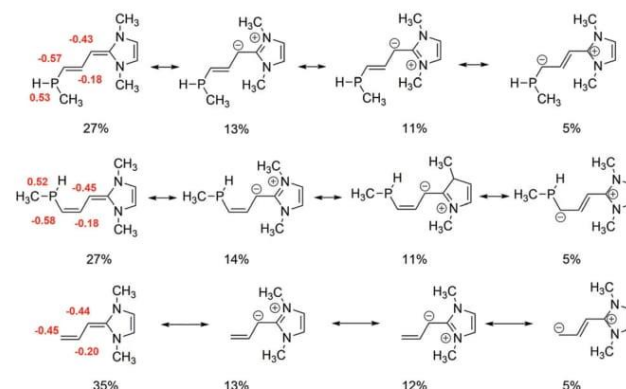


**Fig. 3** POV-ray depiction of the molecular structure of **17** and **18**. ORTEPs drawn at 50% probability, all H-atoms are omitted for clarity. Selected bond lengths (Å) and angles (°) of **17**: C1–C4 1.376(2), C4–C5 1.422(2), C5–C6 1.355(2), P1–C31 1.8623(16), P1–C6 1.8157(18); C31–P1–C6 97.74(8), P1–C6–C5 125.03(13), C6–C5–C4 127.50(16), C5–C4–C1 127.72(16); C1–C4–C5–C6 –178.81(17), C4–C5–C6–P1 –1.7(3); **18**: C1–C4 1.3734(16), C4–C5 1.4309(15), C5–C6 1.3483(16), P1–C31 1.8523(12), P1–C6 1.7876(12); C31–P1–C6 108.27(5), P1–C6–C5 123.74(9), C6–C5–C4 123.78(11), C5–C4–C1 128.19(10); C1–C4–C5–C6 –170.82(11), C4–C5–C6–P1 –175.64(9).



**Scheme 7** Natural resonance theory (NRT) performed on model compounds to investigate the allyl character in corresponding phosphines **17** and **18** in their *E*- (top) and *Z*-configuration (middle) compared to unsubstituted enediamines (bottom). Formula weights below 5% are not depicted and NPA-charges are given in red.

ment in **17** and **18** as judged by the dihedral angles (Fig. 3). In solution both **17** and **18** mainly exist as *E*-configured 1,3-dienes, with **17** showing the *Z*-configured diene as a minor isomer. An NRT analysis using the truncated model H<sub>3</sub>CP(H)C<sub>3</sub>H<sub>3</sub>Ime<sub>2</sub> revealed four major resonance structures, clearly showing effective  $\pi$ -delocalization into the imidazole ring system and the NPA charges suggest charge accumulation on the  $\gamma$ -C atom (Scheme 7). This delocalization is also evident from inspection of the Kohn–Sham orbitals of **17** and **18**, which show delocalization in the HOMO–1 and HOMO, the LUMO and LUMO+1, however, are localized on the flanking aryl groups (Fig. S78 and 79†).<sup>30</sup>

## Conclusions

In summary we have shown facile substitution of the phosphine in phospho-Wittig reagents for NHCs, affording a variety of novel NHC-phosphinidene adducts. When using NHOs a substitution of PMe<sub>3</sub> was observed in all cases, however, in a second reaction step a C(sp<sup>2</sup>)–H activation of the =CH<sub>2</sub> moiety in the NHO occurs to give P-substituted NHOs in a facile manner. This C–H activation was shown to be more general and P-substituted dienes were obtained when **1** or **2** were treated with the enediamine IDipC<sub>3</sub>H<sub>4</sub>. These reactions clearly show the potential of phospho-Wittig reagents beyond the formation of phosphoalkenes and offer access to bulky phosphines. Of particular interest will be the potential of **17** to act as a dianionic ligand scaffold through twofold deprotonation in the vinylic position and the P–H group. Studies utilizing P-substituted NHOs **13**–**16** as ligands are currently ongoing in this laboratory.

## Conflicts of interest

There are no conflicts to declare.



## Acknowledgements

C. H.-J. thanks Prof. M. Beller for his support, the Max Buchner-Foundation for a Scientific Fellowship and support by an Exploration Grant of the Boehringer Ingelheim Foundation (BIS) is acknowledged. We thank our technical and analytical staff for assistance, especially Dr Anke Spannenberg for her support regarding X-ray analysis. We thank Dr Alexander Villinger for his help with obtaining the molecular structure of **5** by SC-XRD. J.-E. S. wishes to thank Dr Jonas Bresien for helpful discussions and the ITMZ at the University of Rostock for access to the Cluster Computer and especially Malte Willert for technical support.

## Notes and references

- G. Wittig and G. Geissler, *Justus Liebigs Ann. Chem.*, 1953, **580**, 44–57.
- G. Wittig and U. Schöllkopf, *Chem. Ber.*, 1954, **87**, 1318–1330.
- H. Ernst, *Pure Appl. Chem.*, 2002, **74**, 2213.
- C. Mercier and P. Chabardes, *Pure Appl. Chem.*, 1994, **66**, 1509.
- K. C. Nicolaou, M. W. Härter, J. L. Gunzner and A. Nadin, *Liebigs Ann.*, 1997, **1997**, 1283–1301.
- A. B. Burg and W. Mahler, *J. Am. Chem. Soc.*, 1961, **83**, 2388–2389.
- A. H. Cowley and M. C. Cushner, *Inorg. Chem.*, 1980, **19**, 515–518.
- E. Urnezis, S. Shah and J. D. Protasiewicz, *Phosphorus, Sulfur Silicon Relat. Elem.*, 1999, **144**, 137–139.
- J. D. Protasiewicz, *Eur. J. Inorg. Chem.*, 2012, **2012**, 4539–4549.
- A. Marinetti and F. Mathey, *Angew. Chem., Int. Ed. Engl.*, 1988, **27**, 1382–1384.
- S. Shah and J. D. Protasiewicz, *Chem. Commun.*, 1998, 1585–1586.
- S. Shah, M. C. Simpson, R. C. Smith and J. D. Protasiewicz, *J. Am. Chem. Soc.*, 2001, **123**, 6925–6926.
- K. Takeuchi, H.-o. Taguchi, I. Tanigawa, S. Tsujimoto, T. Matsuo, H. Tanaka, K. Yoshizawa and F. Ozawa, *Angew. Chem., Int. Ed.*, 2016, **55**, 15347–15350.
- R. C. Smith and J. D. Protasiewicz, *J. Am. Chem. Soc.*, 2004, **126**, 2268–2269.
- R. C. Smith, S. Shah, E. Urnezis and J. D. Protasiewicz, *J. Am. Chem. Soc.*, 2003, **125**, 40–41.
- A. Schumann, F. Reiß, H. Jiao, J. Rabeah, J.-E. Siewert, I. Krummenacher, H. Braunschweig and C. Hering-Junghans, *Chem. Sci.*, 2019, **10**, 7859–7867.
- Y. Masaaki, S. Takahiro and I. Naoki, *Chem. Lett.*, 1988, **17**, 1735–1738.
- A. H. Cowley, F. Gabbai, R. Schluter and D. Atwood, *J. Am. Chem. Soc.*, 1992, **114**, 3142–3144.
- X. Li, D. Lei, M. Y. Chiang and P. P. Gaspar, *J. Am. Chem. Soc.*, 1992, **114**, 8526–8531.
- B. Twamley, C. D. Sofield, M. M. Olmstead and P. P. Power, *J. Am. Chem. Soc.*, 1999, **121**, 3357–3367.
- X. Chen, R. C. Smith and J. D. Protasiewicz, *Chem. Commun.*, 2004, 146–147.
- U. J. Kilgore, H. Fan, M. Pink, E. Urnezis, J. D. Protasiewicz and D. J. Mindiola, *Chem. Commun.*, 2009, 4521–4523.
- L. Liu, D. A. Ruiz, D. Munz and G. Bertrand, *Chem*, 2016, **1**, 147–153.
- M. M. Hansmann and G. Bertrand, *J. Am. Chem. Soc.*, 2016, **138**, 15885–15888.
- D. W. N. Wilson, J. Feld and J. M. Goicoechea, *Angew. Chem.*, 2020, **59**, 20914.
- D. W. N. Wilson, W. K. Myers and J. M. Goicoechea, *Dalton Trans.*, 2020, **49**, 15249.
- T. Krachko and J. C. Sloatweg, *Eur. J. Inorg. Chem.*, 2018, **2018**, 2734–2754.
- A. Doddi, M. Peters and M. Tamm, *Chem. Rev.*, 2019, **119**, 6994–7112.
- T. Krachko, M. Bispinghoff, A. M. Tondreau, D. Stein, M. Baker, A. W. Ehlers, J. C. Sloatweg and H. Grützmaier, *Angew. Chem., Int. Ed.*, 2017, **56**, 7948–7951.
- Experimental and computational details, and details on the X-ray diffraction studies are included in the ESI. CCDC 2046859–2046869<sup>†</sup> contain the supplementary crystallographic data for this paper.
- P. Pyykkö and M. Atsumi, *Chem. – Eur. J.*, 2009, **15**, 12770–12779.
- S. Shah, G. P. A. Yap and J. D. Protasiewicz, *J. Organomet. Chem.*, 2000, **608**, 12–20.
- O. Back, M. Henry-Ellinger, C. D. Martin, D. Martin and G. Bertrand, *Angew. Chem., Int. Ed.*, 2013, **52**, 2939–2943.
- N. Hayakawa, K. Sadamori, S. Tsujimoto, M. Hatanaka, T. Wakabayashi and T. Matsuo, *Angew. Chem., Int. Ed.*, 2017, **56**, 5765–5769.
- K. Pal, O. B. Hemming, B. M. Day, T. Pugh, D. J. Evans and R. A. Layfield, *Angew. Chem., Int. Ed.*, 2016, **55**, 1690–1693.
- C. M. E. Graham, C. R. P. Millet, A. N. Price, J. Valjus, M. J. Cowley, H. M. Tuononen and P. J. Ragnogna, *Chem. – Eur. J.*, 2018, **24**, 672–680.
- J. E. M. N. Klein and G. Knizia, *Angew. Chem., Int. Ed.*, 2018, **57**, 11913–11917.
- G. Knizia, *J. Chem. Theory Comput.*, 2013, **9**, 4834–4843.
- M. M. D. Roy and E. Rivard, *Acc. Chem. Res.*, 2017, **50**, 2017–2025.
- S. Naumann, *Chem. Commun.*, 2019, **55**, 11658–11670.
- K. Powers, C. Hering-Junghans, R. McDonald, M. J. Ferguson and E. Rivard, *Polyhedron*, 2016, **108**, 8–14.
- M. M. Hansmann, P. W. Antoni and H. Pesch, *Angew. Chem.*, 2020, **59**, 5782–5787.
- I. C. Watson, A. Schumann, H. Yu, E. C. Davy, R. McDonald, M. J. Ferguson, C. Hering-Junghans and E. Rivard, *Chem. – Eur. J.*, 2019, **25**, 9678–9690.
- A. Dumrath, X.-F. Wu, H. Neumann, A. Spannenberg, R. Jackstell and M. Beller, *Angew. Chem., Int. Ed.*, 2010, **49**, 8988–8992.

## Paper

## Dalton Transactions

- 45 A. Dumrath, C. Lübke, H. Neumann, R. Jackstell and M. Beller, *Chem. – Eur. J.*, 2011, **17**, 9599–9604.
- 46 D. Rottschäfer, M. K. Sharma, B. Neumann, H.-G. Stammler, D. M. Andrada and R. S. Ghadwal, *Chem. – Eur. J.*, 2019, **25**, 8127–8134.
- 47 N. R. Paisley, M. W. Lui, R. McDonald, M. J. Ferguson and E. Rivard, *Dalton Trans.*, 2016, **45**, 9860–9870.
- 48 C. C. Chong, B. Rao, R. Ganguly, Y. Li and R. Kinjo, *Inorg. Chem.*, 2017, **56**, 8608–8614.
- 49 R. S. Ghadwal, S. O. Reichmann, F. Engelhardt, D. M. Andrada and G. Frenking, *Chem. Commun.*, 2013, **49**, 9440–9442.
- 50 C. E. I. Knappke, A. J. Arduengo III, H. Jiao, J.-M. Neudörfl and A. Jacobi von Wangelin, *Synthesis*, 2011, 3784–3795.
- 51 C. E. I. Knappke, J. M. Neudörfl and A. Jacobi von Wangelin, *Org. Biomol. Chem.*, 2010, **8**, 1695–1705.
- 52 I. C. Watson, Y. Zhou, M. J. Ferguson, M. Kränzlein, B. Rieger and E. Rivard, *Z. Anorg. Allg. Chem.*, 2020, **646**, 547–551.



## **6.2 Synthesis, Coordination Chemistry, and Mechanistic Studies of P,N-Type Phosphaalkene-Based Rh(I) Complexes**

Priyanka Gupta, Tobias Taeufer, Jan-Erik Siewert, Fabian Reiß, Hans-Joachim Drexler, Jola Pospech, Torsten Beweries and Christian Hering-Junghans

*Inorg. Chem.* **2022**, *61*, 11639–11650

DOI: 10.1021/acs.inorgchem.2c01158

Reprinted with permission from *Inorg. Chem.* **2022**, *61*, 11639–11650. Copyright 2022 American Chemical Society.

Contribution to this paper is 60%





# Synthesis, Coordination Chemistry, and Mechanistic Studies of P,N-Type Phosphaalkene-Based Rh(I) Complexes

Priyanka Gupta, Tobias Taeufer, Jan-Erik Siewert, Fabian Reiß, Hans-Joachim Drexler, Jola Pospech, Torsten Beweries,\* and Christian Hering-Junghans\*



Cite This: *Inorg. Chem.* 2022, 61, 11639–11650



Read Online

ACCESS |



Metrics & More



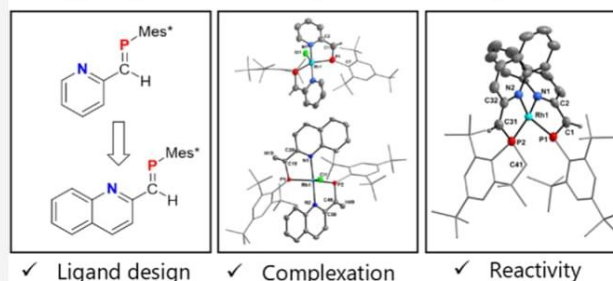
Article Recommendations



Supporting Information

**ABSTRACT:** The synthesis of P,N-phosphaalkene ligands, py-CH=PMe<sup>s\*</sup> (**1**, py = 2-pyridyl, Me<sup>s\*</sup> = 2,4,6-*t*Bu-C<sub>6</sub>H<sub>2</sub>) and the novel quin-CH=PMe<sup>s\*</sup> (**2**, quin = 2-quinolyl) is described. The reaction with [Rh(μ-Cl)cod]<sub>2</sub> produces Rh(I) bis(phosphaalkene) chlorido complexes **3** and **4** with distorted trigonal bipyramidal coordination environments. Complexes **3** and **4** show a pronounced metal-to-ligand charge transfer (MLCT) from Rh into the ligand P=C π\* orbitals. Upon heating, quinoline-based complex **4** undergoes twofold C–H bond activation at the *o*-*t*Bu groups of the Me<sup>s\*</sup> substituents to yield the cationic bis(phosphaindane) Rh(I) complex **5**, which could not be observed for the pyridine-based analogue **3**. Using sub- or superstoichiometric amounts of AgOTf the C–H bond activation at an *o*-*t*Bu group of one or at both Me<sup>s\*</sup> was detected, respectively. Density functional theory (DFT) studies suggest an oxidative proton shift pathway as an alternative to a previously reported high-barrier oxidative addition at Rh(I). The Rh(I) mono- and bis(phosphaindane) triflate complexes **6** and **7**, respectively, undergo deprotonation at the benzylic CH<sub>2</sub> group of the phosphaindane unit in the presence of KO<sup>t</sup>Bu to furnish neutral, distorted square-planar Rh(I) complexes **8** and **9**, respectively, with one of the P,N ligands being dearomatized. All complexes were fully characterized, including multinuclear NMR, vibrational, and ultraviolet–visible (UV–vis) spectroscopy, as well as single-crystal X-ray and elemental analysis.

## PN-type Quinoline Phosphaalkenes capture Rh(I)



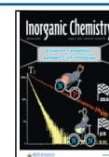
## INTRODUCTION

P,N-Phosphinopyridine and N,N-pyridineimine ligands have been extensively studied, and their applicability in catalytic processes has been demonstrated.<sup>1–5</sup> In contrast, reports on related pyridine-phosphaalkene P,N-ligands and their applications in coordination chemistry are less common. Phosphaalkene-based ligands are of interest for catalysis for various reasons. In contrast to imines in which the highest occupied molecular orbital (HOMO) is the nitrogen lone pair (LP), calculations and photoelectron spectroscopic investigations have revealed that the HOMO of phosphaalkenes is generally of π-type with an energetically nearly degenerate phosphorus lone pair orbital.<sup>6</sup> Compared to the sp<sup>2</sup>-type lone pair in imines, the lone pair on the P atom in phosphaalkenes has considerable s character and the polarity of the E=C double bond (E = P, N) is reversed as judged by the difference in the electronegativity (χ) between the heteroatoms (cf. χ(N) = 3.0, χ(P) = 2.1). Also, P is slightly more electropositive than carbon (cf. χ(C) = 2.5).<sup>7</sup> The polarity of the P=C bond can however be tuned by the judicious choice of substituents on both P and C, and amino-substitution on the C atom, for example, results in so-called inversely polarized phosphaalkenes.<sup>8</sup> These factors result in weaker σ coordination properties of the phosphorus

LP compared to that of the nitrogen in imines. However, the π\* orbital lowest unoccupied molecular orbital (LUMO) of phosphaalkenes is rather low in energy and thus enhances the acceptor properties in transition-metal complexes, resulting in more effective back-bonding.<sup>6</sup> Owing to their strong π-accepting nature and similar shape of the LUMO, phosphaalkenes are considered tunable homologues of the ubiquitous CO ligand.<sup>9</sup> In the last 50 years, the chemistry of phosphaalkenes has evolved into a vigorous field of inorganic and materials chemistry.<sup>10,11</sup> However, kinetic protection or delocalization of π electrons is necessary to stabilize the reactive P=C double bond. Numerous synthetic pathways toward phosphaalkenes have been presented in the literature, offering a variety of methods to construct these systems. In 1976, Becker presented the first acyclic phosphaalkene formed in the isomerization of silylacylphosphines R–P(SiMe<sub>3</sub>)–

Received: April 6, 2022

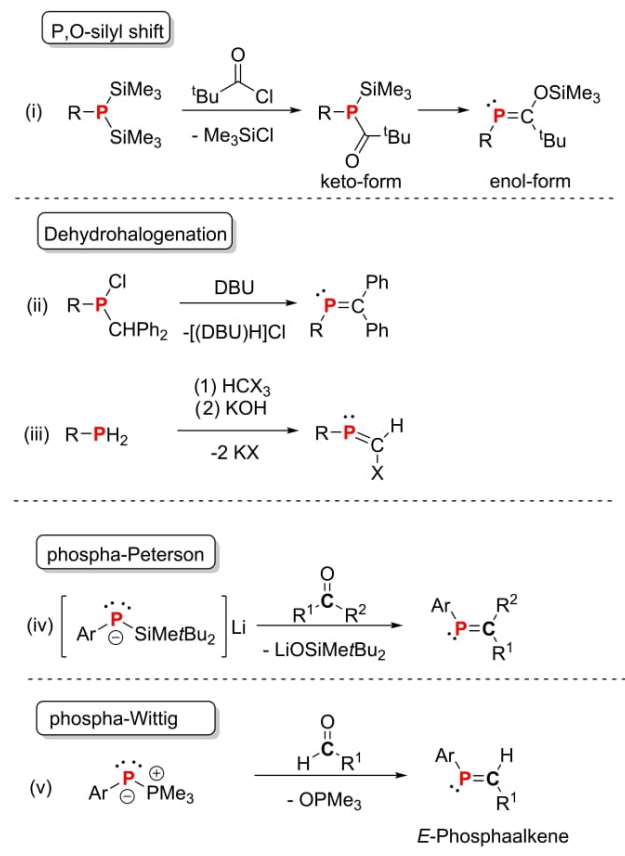
Published: July 20, 2022





(COCR<sub>3</sub>) (obtained from bis-silylphosphines and acylchlorides) into its enol-form at room temperature with the concomitant formation of a P=C double bond facilitated by a silyl shift to the oxygen of the keto-function (Scheme 1

**Scheme 1. Different Synthetic Strategies (i–v) toward Phosphaalkenes**



(i)).<sup>12</sup> Two years later, Bickelhaupt and co-workers reported the first localized, all-carbon-substituted P=C double bond. The synthesis was achieved by dehydrochlorination of a benzhydrol-substituted chlorophosphine R<sub>2</sub>PCl(CHPh<sub>2</sub>) in the presence of DBU as a scavenger of HCl (Scheme 1 (ii)).<sup>13</sup> An alternative route is the reaction of primary phosphines with geminal dihaloalkanes in the presence of a base as a scavenger for HX (Scheme 1 (iii)).<sup>14</sup> More recently, P=C double bonds have been constructed using silylphosphide lithium species in the reaction with ketones or aldehydes, affording the desired phosphaalkenes in mostly moderate yields after column chromatography (“phospho-Peterson” route; Scheme 1 (iv)).<sup>15</sup> The Gates group has further developed this synthetic route, using bis(silyl)phosphines as a starting material for the generation of reactive silyl phosphides. They have shown that starting from MesP(SiMe<sub>3</sub>)<sub>2</sub>, a variety of mesityl-substituted phosphaalkenes could be isolated, among them the P,N-type ligand MesP=C(Ph)(2-pyridyl).<sup>16</sup> In 1998, Protasiewicz et al. outlined the so-called “phospho-Wittig” reaction, using phosphanylidene-σ<sup>4</sup>-phosphoranes<sup>17</sup> of the type Ar-P(PMe<sub>3</sub>) (Mes\* = 2,4,6-*t*Bu<sub>3</sub>C<sub>6</sub>H<sub>2</sub>, Mes\*Ter = 2,6-(2,4,6-Me<sub>3</sub>C<sub>6</sub>H<sub>2</sub>)-C<sub>6</sub>H<sub>3</sub>) to construct a variety of phosphaalkenes in the reaction with aldehydes in an *E*-selective manner (Scheme 1 (v)).<sup>18</sup>

The “phospho-Wittig” concept has since been used to prepare a variety of P,N,P-,<sup>19</sup> P,P-,<sup>20</sup> and P,P,P,P-type phosphaalkene ligands (Scheme 2).<sup>21</sup> The first P,N-phosphaalkene ligand Mes\*P=C(H)Py was obtained in 45% yield using a “phospho-Peterson” protocol,<sup>22</sup> which was later improved by Bickelhaupt and co-workers, and the variant Mes\*P=C(SiMe<sub>3</sub>)Py was synthesized using a Pd-catalyzed route employing a phosphaalkene Grignard reagent.<sup>23</sup>

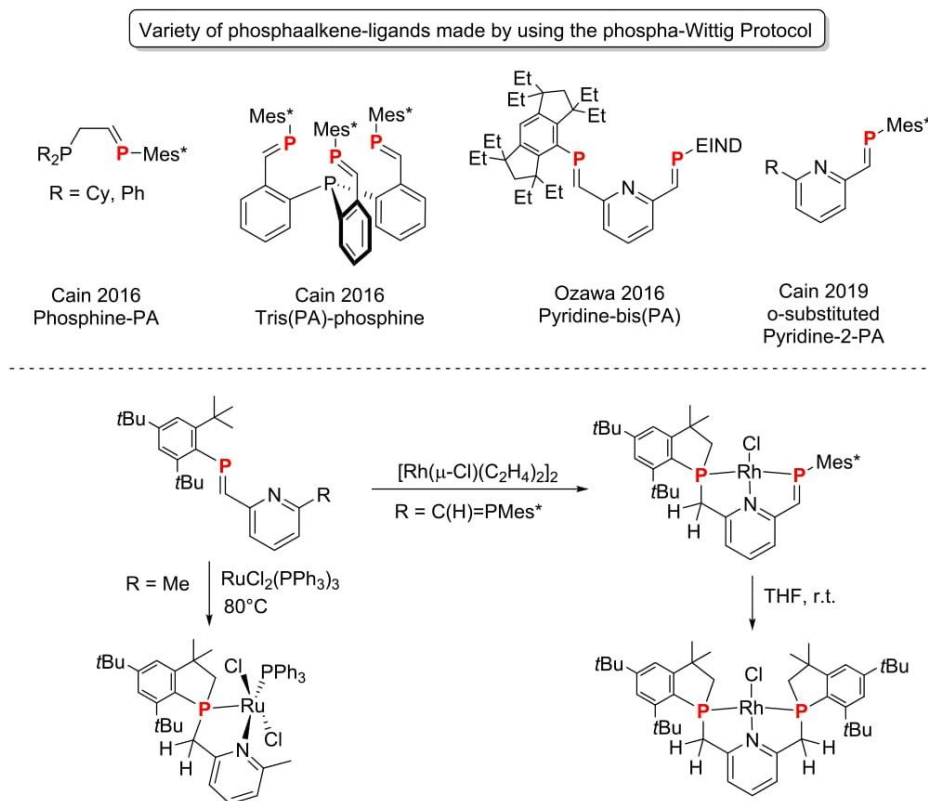
These ligands were then used to obtain η<sup>1</sup>,η<sup>1</sup>-[Mes\*P=C(SiMe<sub>3</sub>)Py]PdClX complexes. In general, the chemistry of platinum group metal phosphaalkene complexes is well established and several examples were studied over the last decade.<sup>24</sup> For example, Ozawa and co-workers presented various Rh, Ir, and Pt P,N,P-phosphaalkene systems with a pyridine backbone and sterically demanding Mes\* or EIND (EIND = 1,1,3,3,5,5,7,7-octaethyl-1,2,3,5,6,7-hexahydro-*s*-indacen-4-yl) substituents.<sup>25–27</sup> Metal–ligand cooperativity was observed for a mixed Ir(I) P,N,P-complex with phosphaalkene and phosphaindene units. This species undergoes dearomatization by deprotonation to produce an anionic complex that readily activates ammonia.<sup>28</sup> Apart from Geoffroy’s studies of a pyridine-based P,N-phosphaalkene Cu complex,<sup>29</sup> a series of Ru P,N-phosphaalkene complexes were reported by Cain and co-workers just recently. The latter complexes showed intramolecular C–H bond activation at the Mes\* groups to produce phosphaindene structures (Scheme 2 (bottom left)).<sup>30</sup> Similarly, Ozawa and co-workers showed that using the related Mes\*-substituted P,N,P-type ligand, twofold cyclization occurred to give the corresponding bis-phospholanyl RhCl-complex (Scheme 2 (bottom right)).<sup>31</sup> C–H bond activation is a common deactivation pathway for Mes\*-containing low-valent P-species.<sup>32,33</sup> Other P,N-type phosphaalkene ligands have been reported and include phosphaalkenes with pendant imine functions,<sup>34,35</sup> pyridine-bridged oxazoline phosphaalkenes,<sup>36</sup> chiral alkyl-bridged phosphaalkenes,<sup>37</sup> and OSiMe<sub>3</sub>-substituted phosphaalkenes in a pyridine-bridged P,N,P-bisphosphaalkene.<sup>38</sup> We have recently presented the convenient and large-scale synthesis of phospho-Wittig reagents, R–P(PMe<sub>3</sub>) with R = Mes\*, Mes\*Ter and Dip\*Ter (Dip\*Ter = 2,6-(2,6-*i*Pr<sub>2</sub>C<sub>6</sub>H<sub>3</sub>)-C<sub>6</sub>H<sub>3</sub>) and showed that PMe<sub>3</sub> can be displaced by NHCs or NHOs,<sup>39</sup> and furthermore serve as an interesting phosphinidene synthon for a variety of applications.<sup>40,41</sup> In the present study, these compounds are applied for the synthesis of a new π extended P,N-phosphaalkene ligand. We report the coordination chemistry at Rh(I) and give spectroscopic and theoretical insights into the observed intramolecular C–H bond activation sequences.

## RESULTS AND DISCUSSION

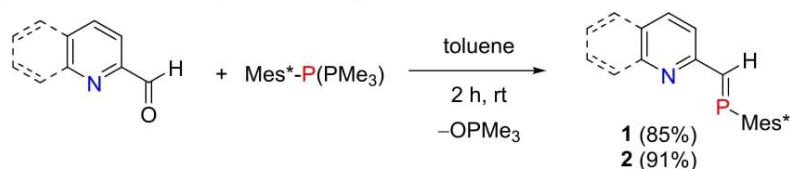
**Synthesis of Ligands.** The combination of 2-pyridine-carboxaldehyde or 2-quinolinecarboxaldehyde, respectively, with the phospho-Wittig reagent Mes\*–P(PMe<sub>3</sub>) in toluene at room temperature afforded, after removal of OPMe<sub>3</sub> by sublimation, the P,N-type phosphaalkene ligands py-CH=PMe\* (**1**, py = 2-pyridyl; 85%) and the novel quin-CH=PMe\* (**2**, quin = 2-quinolyl; 91%) as yellow, crystalline solids in excellent yields (Scheme 3). Our synthetic strategy provided better yields and a straightforward route in comparison to the previously reported synthesis of **1** (45%) using the “phospho-Peterson” methodology.<sup>22</sup>

Compounds **1** and **2** were identified by their diagnostic deshielded <sup>31</sup>P NMR signal of the P=C unit observed at 282.7 ppm (**1**) or 290.6 ppm (**2**), respectively. According to <sup>1</sup>H

**Scheme 2.** Variety of Phosphaalkene (PA) Ligands Prepared Using a “Phospha-Wittig” Approach (Top) and C–H Bond Activation and Cyclization in P,N- and P,N,P-Phosphaalkene Complexes of Ru(II) and Rh(I) (Bottom)



**Scheme 3.** *E*-Selective Synthesis of P,N-Phosphaalkene Ligands **1** and **2**



NMR spectroscopy, the phosphaalkene moieties adopt an *E*-configuration with the P=CH proton showing the expected doublet at 8.25 or 8.60 ppm, respectively, and a  $^2J_{P-H}$  coupling constant of approximately 25 Hz (cf. *E*-configured P,N-phosphaalkene ligands<sup>30</sup>  $^2J_{P-H}$  = ca. 25 Hz). Furthermore, **2** was characterized by  $^{13}C$  NMR spectroscopy, mass spectrometry, and elemental analysis. Crystals of **2** suitable for single-crystal X-ray diffraction (SC-XRD) were grown from a saturated *n*-hexane solution at  $-30$  °C and allowed to establish the molecular structure of **2** (Figure 1), which features a P–C atomic distance of 1.6705(13) Å, within the expected range for bidentate phosphaalkene-based ligands,<sup>25</sup> while the C–P–C angle ( $98.75(6)^\circ$ ) is consistent with a diffuse LP at the P atom, resulting in a decrease of the C–P–C angle in line with the VSEPR model. This was further rationalized by performing NBO<sup>42</sup> analyses (B3LYP/GD3BJ/def2tzvp) on both **1** and **2**. This revealed LPs on phosphorus with a high *s* character ( $sp^{0.6}$  hybridization), with both the  $\sigma$ - and  $\pi$ -components of the P=C double bond being polarized toward the C atom. In addition, the vertical electron affinities of **1** and **2** were theoretically determined and showed that **2** ( $E_{ea}$  = 22.5 kcal mol<sup>−1</sup>) has a higher electron affinity than **1** ( $E_{ea}$  = 17.3 kcal

mol<sup>−1</sup>; see Table S7 for details). The characterization data of **1** were in accordance with the literature values (see S7).

**Synthesis of Rh(I) Complexes.** In a next series of experiments, **1** and **2** were combined with  $[Rh(\mu-Cl)(cod)]_2$  in toluene in a 2:1 ratio (Scheme 4). For the reaction between **1** and  $[Rh(\mu-Cl)(cod)]_2$ , the ligand was consumed after stirring the mixture for 24 h, resulting in a color change from red to dark turquoise, and the appearance of a doublet at 262.2 ppm in the  $^{31}P\{^1H\}$  NMR spectrum with a  $^1J_{P-Rh}$  coupling constant of 217 Hz suggested the formation of a new Rh(I) complex (Table 1). SC-XRD experiments on intensively colored turquoise crystals grown by slow diffusion of *n*-pentane into a saturated CH<sub>2</sub>Cl<sub>2</sub> solution at room temperature showed the formation of the complex  $[(py-CH=PMes^*)_2RhCl]$  (**3**) (Figure 2 (left)), suggesting that a 4:1 ratio of the ligand and  $[Rh(\mu-Cl)(cod)]_2$  is needed to achieve full conversion of the rhodium precursor complex. Monitoring the reaction between **2** and  $[Rh(\mu-Cl)(cod)]_2$  in a 4:1 ratio by  $^{31}P\{^1H\}$  NMR spectroscopy at room temperature showed slow conversion into a new species, with a doublet at 270.1 ppm and a characteristic  $^1J_{P-Rh}$  coupling constant of 212 Hz (Table 1). SC-XRD analysis of crystals that precipitated from the



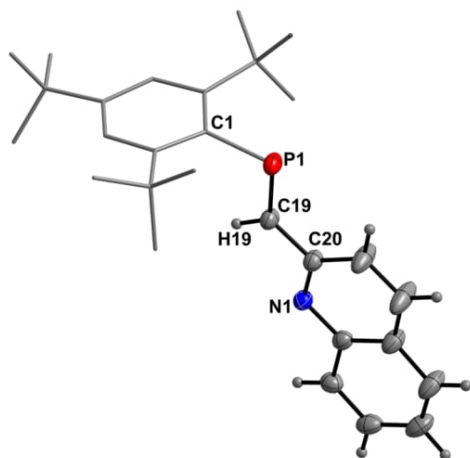


**Figure 1.** Molecular structure of **2**. ORTEPs drawn at 50% probability. Hydrogen atoms, except H19, are omitted for clarity. Selected bond lengths (Å) and angles (°) of **2**: P1–C1 1.8461(12), P1–C19 1.6705(13), C19–C20 1.4609(17), C20–N1 1.3275(16); C1–P1–C19 98.75(6), P1–C19–C20 125.85(10), P1–C19–H19 117.10.

reaction mixture showed the formation of  $[(\text{quin-CH}=\text{PMes}^*)_2\text{RhCl}]$  (**4**) (Figure 3). In both cases, the complexation results in shielding of the  $^{31}\text{P}$  NMR signal of the phosphalkene unit  $\Delta\delta(^{31}\text{P}\{^1\text{H}\}) \approx 20$  ppm).

The reaction between **2** and  $[\text{Rh}(\mu\text{-Cl})(\text{cod})]_2$  can be accelerated by heating to 80 °C over a period of 6 h, which is accompanied by a color change to blue and intensely blue-colored crystals of X-ray quality precipitate from the reaction mixture in good yield. The molecular structures of **3** and **4** adopt a distorted five-coordinate geometry around the metal in which the two P,N-ligands are arranged mutually *trans* to each other while the chlorido ligand occupies the fifth coordination site. Addition and co-workers introduced the  $\tau_5$  parameter to categorize five-coordinate metal complexes, with  $\tau_5 = 0$  indicating a perfect square-pyramidal  $C_{4v}$  geometry, while  $\tau_5 = 1$  indicates a perfect trigonal bipyramidal  $D_{3h}$  coordination environment. Both **3** and **4** show values of  $\tau_5 < 1$  (**3**: 0.77; **4**: 0.76) and are thus best described as distorted trigonal

bipyramidal complexes.<sup>43,44</sup> The two Mes\* groups are oriented nearly perpendicular to the coordination plane. The P–C bond lengths (**3**, P1–C1 1.681(9); **4**, P1–C19 1.6821(17), P2–C49 1.6810(18) Å) are typical for sustained P=C double bonds (Table 1) and are not affected upon complexation.

The Rh–P1, Rh–P2, Rh–N, and Rh–Cl lengths are comparable to those in  $[\text{RhCl}(\text{Mes}^*_2\text{-BPEP})]$  (BPEP = 2,6-bis(2-phosphaethenyl)pyridine).<sup>45</sup> Interestingly, a dinuclear  $\mu\text{-Cl}$  bridged Rh(III) complex **3a** (Figure 2 (right)) was co-crystallized with the desired complex **3**. Notably, a C–H bond cleavage of both *o*-*t*Bu substituents of the Mes\* ligand is observed. One hydrogen atom formally migrates from the *t*-Bu group to the carbon atom of the P=C bond to form a phosphaindane moiety, resulting in the loss of the P=C carbon double bond. The second *t*Bu group undergoes cyclometallation to the Rh center, resulting in an additional ligation of the rhodium center via a methylene bridge to the Mes\* substituent.

When studying the thermal stability of complex **4**, we discovered that heating of **4** at 80 °C for 6 h in toluene resulted in a red reaction mixture and formation of the C–H cyclized cationic bisphosphaindane complex **5** with an outer-sphere chloride counter-anion via intramolecular C–H addition of an *o*-*t*Bu-group to the P atoms of the P=C bond in both phosphalkene ligands along with unidentified decomposition products (Scheme 5). In complex **5**, both ligands are now mutually *cis*-oriented according to X-ray analysis on weakly diffracting crystals grown from a saturated dichloromethane solution at –30 °C (Figure S26). An orange solution of **5** featured a significantly shielded  $^{31}\text{P}\{^1\text{H}\}$  NMR resonance at 55.1 ppm ( $^1J_{\text{P-Rh}} = 174.4$  Hz) in accordance with other Rh 2-phospholene complexes.<sup>31</sup> Complex **5** could be isolated in 30% yield.

Interestingly, the phosphalkene unit in the pyridine-phosphalkene complex **3** remained unaffected even after heating at 80 °C for 2 days, as ascertained by  $^{31}\text{P}$  NMR spectroscopy. Upon prolonged heating (3 d), **3** started to decompose into various unidentified products. Having in mind that **3** decomposed in an unselective manner in  $\text{CH}_2\text{Cl}_2$  solution to give among others Rh(III) complex **3a**, we concluded that the pyridine-based phosphalkene system is less suitable for further reactivity studies.

#### Scheme 4. Synthesis of Rh(I) Complexes **3** and **4** Starting from the Respective P,N-Ligands **1** and **2**

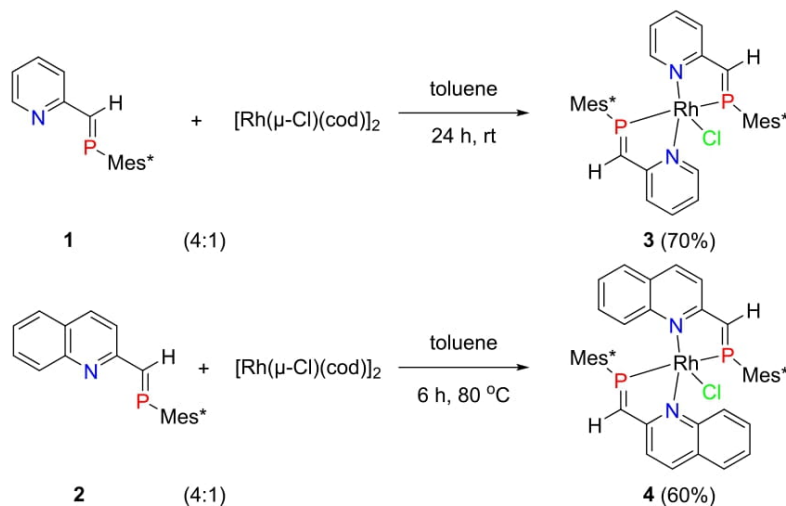
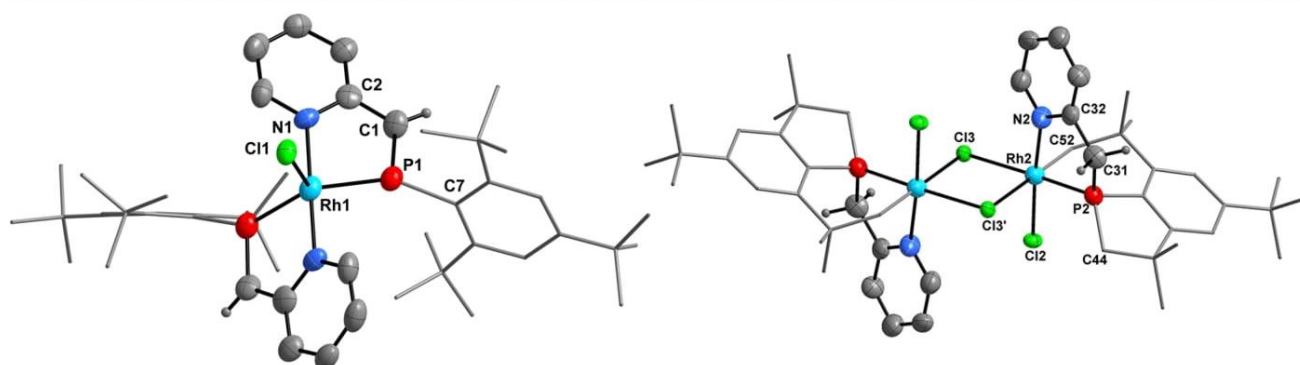


Table 1. Summary of Characteristic Spectroscopic and Structural Data of Compounds 1–9<sup>a</sup>

compound	$\delta^{31}\text{P}\{^1\text{H}\}$ [ppm]	$d(\text{P}-\text{C})$ [Å]	$d(\text{C}_{\text{PA}}-\text{C}_{\text{R}})$ [Å]	$d(\text{Rh}-\text{N})$ [Å]	$d(\text{Rh}-\text{P})$ [Å]
1 <sup>22</sup>	282.7	1.665(1)	1.46(1)		
2	290.6	1.6705(13)	1.4609(17)		
3	262.2 (d), $J_{\text{PRh}} = 217$ Hz	1.681(9)	1.431(12)	2.042(7)	2.214(2)
4	270.1 (d), $J_{\text{PRh}} = 212$ Hz	1.6821(17)	1.4230(2)	2.1256(14)	2.2542(4)
		1.6810(18)	1.4290(3)	2.1132(14)	2.1970(4)
5	55.1 (d), $J_{\text{PRh}} = 174$ Hz	n.a.	n.a.	n.a.	n.a.
6	245.2 (dd), $J_{\text{PRh}} = 212$ Hz, $J_{\text{PP}} = 33.5$ Hz	n.a.	n.a.	n.a.	n.a.
	55.7 (dd), $J_{\text{PRh}} = 144$ Hz, $J_{\text{PP}} = 32.4$ Hz				
7	55.1 (d), $J_{\text{PRh}} = 174$ Hz	1.859(3)	1.503(5)	2.143(3)	2.1908(9)
		1.855(3)	1.500(4)	2.155(3)	2.1887(9)
8	233.7 (dd), $J_{\text{PRh}} = 248.6$ , $J_{\text{PP}} = 34.7$ Hz	1.686(3)	1.422(4)	2.193(2)	2.1326(6)
	48.6 (dd), $J_{\text{PRh}} = 145.2$ , $J_{\text{PP}} = 34.6$ Hz	1.766(3)	1.375(4)	2.117(2)	2.2278(6)
9	56.8 (dd), $J_{\text{PRh}} = 174.4$ , $J_{\text{PP}} = 39.9$ Hz	n.a.	n.a.	n.a.	n.a.
	46.5 (dd), $J_{\text{PRh}} = 170.7$ , $J_{\text{PP}} = 40.0$ Hz				

<sup>a</sup>(C<sub>PA</sub>: C atom of the PA unit; C<sub>R</sub>: C atom of the py- or quin-C atom; n.a. = not available).





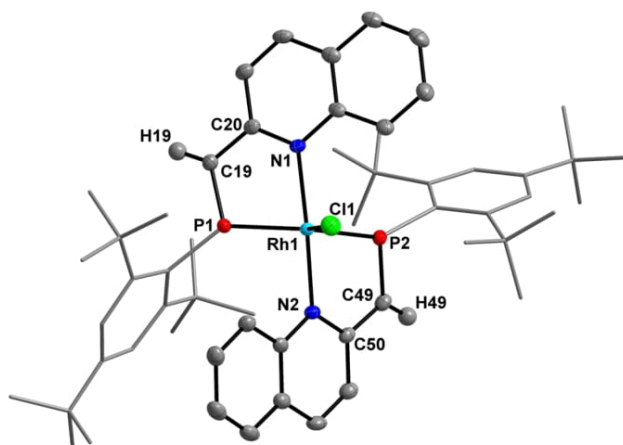


**Figure 3.** Molecular structure of complex 4. ORTEPs drawn at 50% probability. Hydrogen atoms, except on C19 and C49, are omitted for clarity. Selected bond lengths (Å) and angles (°) of 4: P1–C19 1.6821(17), P2–C49 1.6810(18), C19–C20 1.4230(2), C49–C50 1.4290(3), P1–Rh 2.1970(4), P2–Rh 2.2542(4), N1–Rh 2.1256(14), N2–Rh 2.1132(14), Rh–Cl 2.4755(4); C20–C19–P1 113.73(13), C50–C49–P2 115.41(13), P1–Rh–P2 128.33(16), N1–Rh–Cl 93.54(4), N2–Rh–Cl 92.44(4), P1–Rh–Cl 120.77(16), P2–Rh–Cl 110.88(16), N1–Rh–N2 173.89(5), P1–Rh–N1 80.52(4), P2–Rh–N2 80.68(4), C19–P1–Cl 113.91(8), C49–P2–Cl 105.38(8).

between TD-DFT and experimental data,<sup>47</sup> we found good agreement between spectroscopic and computational values. The blue color of the bis(phosphaalkene) complex 4 stems from a metal-to-ligand charge transfer (MLCT) band at  $\lambda_{\text{theor}} = 614$  nm, in which d electrons at Rh are excited into the ligand-based LUMO, which has significant P–C  $\pi^*$ -character (Table S4, excited state 3). Experimentally, this very intense band overlaps with a second absorption feature centered at 496 nm. For complex 6, the lowest energy absorptions are found at 449 and 546 nm (with a shoulder at ca. 650 nm), respectively, and can be assigned to MLCT into the P–C  $\pi^*$  of the intact phosphaalkene moiety ( $\lambda_{\text{theor}} = 517, 652$  nm). Orange-colored complex 7, containing two phosphaindane fragments, formed by twofold C–H bond activation, shows only weak absorption higher than 500 nm with the most important transitions at 400–450 nm that can be assigned to MLCT from the Rh center into the quinoline  $\pi^*$  orbitals (see Table S7 for details).

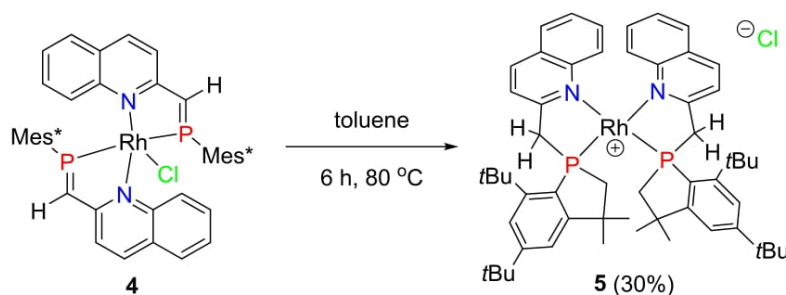
The formation of the triflate complex 6 was monitored by <sup>31</sup>P NMR spectroscopy, which revealed that the reaction proceeds via the formation of the cationic complex 4a, appearing as a doublet at 276.6 ppm with a <sup>1</sup>J<sub>P–Rh</sub> coupling constant of 210.4 Hz, followed by C–H addition/cyclization

exclusively at one of the Mes\*–P=CH groups (Scheme 6 and Figure S13). The <sup>31</sup>P{<sup>1</sup>H} NMR spectrum of complex 6 exhibits two doublet of doublets at 245.3 (<sup>1</sup>J<sub>P–Rh</sub> = 276.2, <sup>2</sup>J<sub>P–P</sub> = 33.5 Hz) and 55.7 ppm (<sup>1</sup>J<sub>P–Rh</sub> = 144.0, <sup>2</sup>J<sub>P–P</sub> = 32.4 Hz), suggesting that the two phosphorus nuclei are chemically inequivalent. Moreover, the small <sup>2</sup>J<sub>P–P</sub> coupling constant indicates that both ligands are *cis*-oriented in solution,<sup>48</sup> akin to a related square planar Rh(Cl)(PPh<sub>3</sub>) complex with an additional chiral isoquinoline phosphine P,N-type ligand (<sup>2</sup>J<sub>P–P</sub> = 41.6 Hz).<sup>49</sup> The two benzylic protons are diastereotopic, showing two sets of signals with a large <sup>2</sup>J<sub>H–H</sub> coupling of ca. 19.3 Hz, confirming that C–H activation and cyclization had occurred. The spectroscopic data of complex 7 are similar to those of complex 5, clearly indicating no interaction of the anions with the cationic Rh complex. Complex 7 was obtained in 75% isolated yield, and orange X-ray quality crystals were grown from a concentrated CH<sub>2</sub>Cl<sub>2</sub> solution exposed to *n*-pentane vapors at –30 °C. The molecular structure of 7 reveals that the cyclization of the Mes\* arms across the P=CH bond generates two new sp<sup>3</sup>-hybridized benzylic-type carbon atoms and P–C single bonds (1.859(3), 1.855(3) Å) (Figure 6), providing more flexibility in the chelate and opening up the bite angle to 83° (compared to ca 80° in 3 and 4), featuring *cis*-oriented P,N-ligands, with both P atoms on the same side. To gauge the geometries of four-coordinate transition-metal complexes, the  $\tau_4$  value has recently been introduced, with  $\tau_4 = 0$  indicating a perfect square planar, while  $\tau_4 = 1$  indicates a perfect tetrahedral geometry. With  $\tau_4 = 0.15$ , complex 7 can be classified as distorted square planar.<sup>50</sup>

C–H activation reactions at related phosphaalkene ligands were reported in the past. The rearrangement of the *t*Bu group of Mes\*P=CH was first reported by Gates et al. on the reactivity of Mes\*P=CH<sub>2</sub> toward MX<sub>3</sub> (M = Al, Ga), showing that, under catalytic conditions, an intramolecular C–H bond activation took place, which involves a phosphonium ion as a fleeting intermediate.<sup>51,52</sup> Later, Le Floch et al. reported another mechanism, supported largely by computations that involved coordination of the phosphaalkene to a phosphine ligated Pt(0) catalyst followed by stepwise C–H oxidative addition of the *t*Bu group.<sup>53</sup> To rationalize our experimental observations and to obtain further insights into this C–H bond activation sequence, we performed a DFT study of this process on the cation in complex 4a (as the anion is non-interacting), formed initially by halide abstraction from 4, to avoid the quantum mechanical problem of charge separation.

We optimized the structures on a double  $\zeta$  basis set, followed by triple  $\zeta$  basis set single-point calculations. All geometries were confirmed to be local minima or first-order

#### Scheme 5. C–H Activation/Cyclization of 4 upon Heating to Form 5



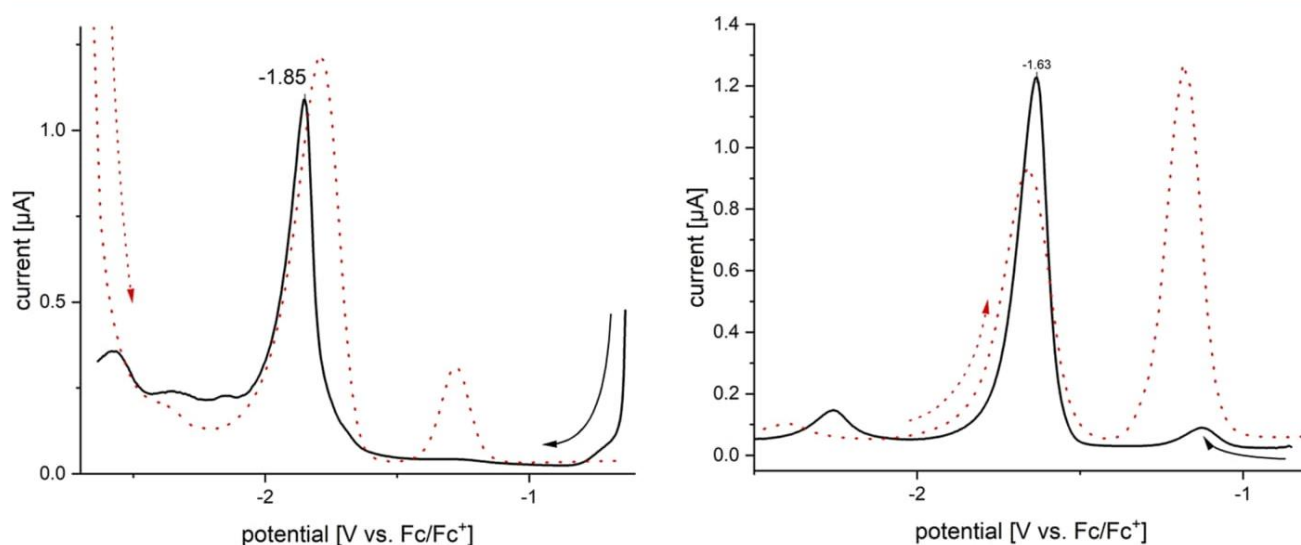
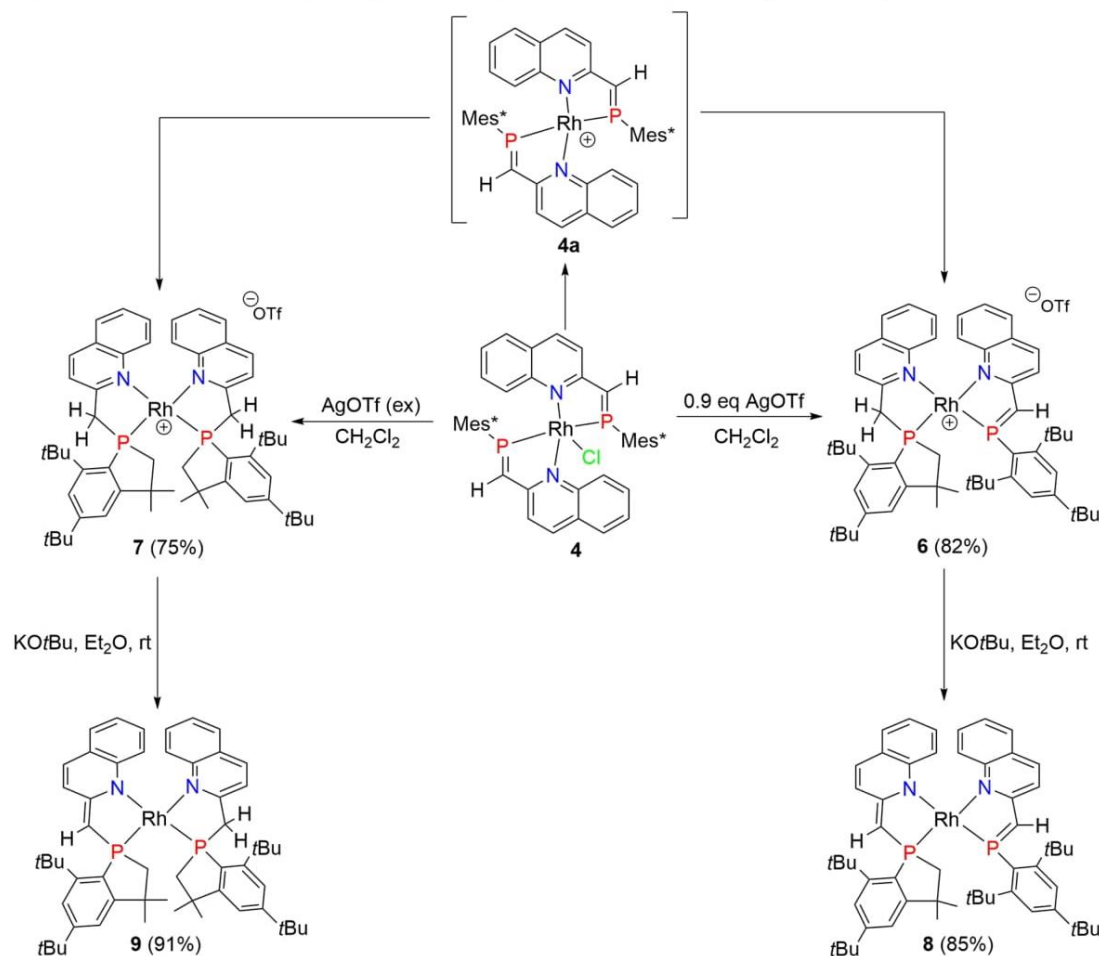


**Figure 4.** Differential pulse voltammograms for the reduction of complexes 3 (left) and 4 (right) in THF, 0.1 M [*n*Bu<sub>4</sub>N]PF<sub>6</sub>, obtained at 23 °C at a step potential of 25 mV s<sup>-1</sup>.

**Scheme 6. Synthesis of Cationic Rh(I) Complexes (6, 7) and Neutral Rh(I) Complexes (8, 9)**



saddle points (for transition states (TS)) on the potential energy surface by harmonic vibration frequency calculations on the same level of theory (B3LYP<sup>54–59</sup>/GD3B<sup>60,61</sup>/def2svp//def2tzvp<sup>62</sup>). Transition states were proven to be correct by

intrinsic reaction coordinate scans in both directions. First, we investigated the previously described pathway<sup>31</sup> by considering the oxidative addition of one methyl group of the *t*Bu unit to the rhodium center as the initial step. To our surprise, we



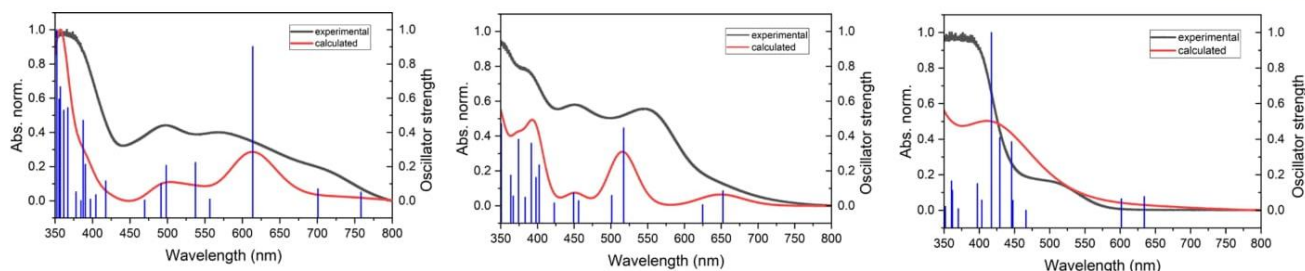


**Figure 5.** Comparison of experimental (black, 0.312 mM in  $\text{CH}_2\text{Cl}_2$ ) and calculated electronic absorption spectra (red) and oscillator strength of the transitions (blue) of complexes **4** (left), **6** (middle), and **7** (right).

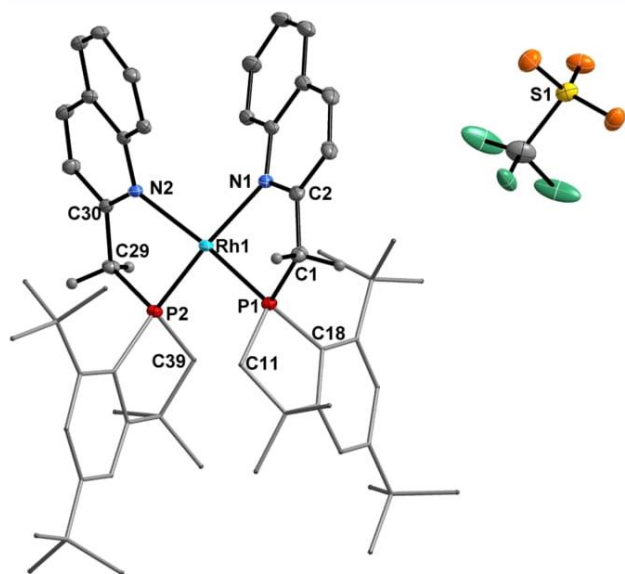


**Figure 6.** Molecular structure of complex **7**. ORTEPs drawn at 50% probability. Hydrogen atoms, except those on C1 and C28, are omitted for clarity. Selected bond lengths (Å) and angles ( $^\circ$ ) of **7**: P1–C1 1.859(3), P2–C29 1.855(3), C2–C1 1.503(5), C29–C30 1.500(4), P1–C11 1.830(3), P2–C39 1.830(3), P1–Rh 2.1908(9), P2–Rh 2.1887(9), N1–Rh 2.143(3), N2–Rh 2.155(3), P1–C18 1.850(3); C2–C1–P1 110.80(2), C30–C29–P2 111.40(2), P1–Rh–P2 96.98(3), N2–Rh–N1 99.51(10), N2–Rh–P2 82.64(8), N1–Rh–P1 82.69(8), P1–Rh–N2 170.20(8), P2–Rh–N1 169.28(8).

found a highly endergonic Gibbs free reaction enthalpy (see SI, page S32) and were not able to find the correct transition state for this pathway. Using a relaxed potential energy scan (PES), we were able to estimate the energy required for this transition state to be greater than 50 kcal/mol. Therefore, we investigated another stepwise pathway starting with a formal oxidative proton shift from the closest methyl group to the rhodium center (Scheme 7). This transition state (TS1) exhibits an activation barrier that is at the upper limit of a reaction that can be observed under ambient conditions ( $\Delta_R H = 30.6$  kcal/mol), which is reflected in the experimentally observed prolonged reaction time of 16 h. From TS1 we found the formal carbanion–phosphorus coupling to be exergonic by 40.5 kcal/mol, leading into a formally dearomatized and oxidized Rh(III) intermediate (Int1). The activation barrier for the formal hydride shift from the metal center to the ligand (TS2) is 12.0 kcal/mol, significantly lower than the first one. TS2 connects Int1 and the final cationic Rh(I) complex **6** via a reductive exergonic reaction step (−40.6 kcal/mol).

### Synthesis of Dearomatized Complexes **8** and **9**.

Pioneered by the Milstein group for pyridine–diphosphine PNP–pincer ligands, Ozawa and co-workers later demonstrated that pyridine-based phosphalkene PNP complexes undergo deprotonation at the benzylic carbon, which resulted in the dearomatization of the central pyridine ring.<sup>63,64</sup> In this study, we have succeeded for the first time in the preparation of dearomatized Rh complexes with simple, bidentate PN ligands. Treatment of mono and bis(phosphaindane) complexes **6** and **7**, respectively, with KOtBu in  $\text{Et}_2\text{O}$  resulted in the immediate deprotonation at the benzylic position with a notable color change from red to dark brown, to afford the neutral complexes **8** and **9** with the dearomatized PN\* ligand, which were isolated in 85 and 91% yields, respectively (Scheme 6 (bottom left and right)). The characteristic vinylic proton signal of **8** and **9** was observed at  $\delta$  4.27 and 4.54 ppm, respectively, as a doublet with a coupling constant of  $^2J_{\text{P-H}} = 3.4$  Hz in the  $^1\text{H}$  NMR spectrum. The  $^{31}\text{P}\{^1\text{H}\}$  NMR spectrum of **8** exhibited two sets of doublets of doublets at  $\delta$  233.7 ( $^1J_{\text{P-Rh}} = 248.6$ ,  $^2J_{\text{P-P}} = 34.7$  Hz) and 48.6 ( $^1J_{\text{P-Rh}} = 145.2$ ,  $^2J_{\text{P-P}} = 34.6$  Hz), which were assigned to the phosphalkene and phosphaindane units, respectively, while the two phosphaindane units in **9** appeared at 46.5 ( $^1J_{\text{P-Rh}} = 170.7$ ,  $^2J_{\text{P-P}} = 40.0$  Hz) and 56.8 ppm ( $^1J_{\text{P-Rh}} = 174.4$ ,  $^2J_{\text{P-P}} = 39.9$  Hz), respectively. These signals were clearly shifted upfield in comparison with the parent complexes **6** and **7**, and the small  $^2J_{\text{P-P}}$  coupling constants in both complexes indicate that the ligands are *cis*-oriented in solution.<sup>48</sup> In the  $^{13}\text{C}\{^1\text{H}\}$  NMR spectrum of **8** and **9**, a doublet for the vinylic carbon appeared at 84.2 ( $^1J_{\text{P-C}} = 52.7$  Hz) and 82.6 ppm ( $^1J_{\text{P-C}} = 48.6$  Hz), respectively. The structure of neutral complex **8** with a dearomatized quinoline ring was confirmed by SC-XRD experiments (Figure 7). The four-coordinate complex **8** can be classified as distorted square planar according to  $\tau_4 = 0.33$ .<sup>50</sup>

The P2–C31 bond in **8** (1.766(3) Å) is clearly shorter than normal P–C single bonds, whereas the C32–C31 bond length (1.375(4) Å) is between those expected for single and double bonds. These variations are characteristic of dearomatized PNP–pincer ligands.<sup>64–68</sup> On the other hand, the P1–C1 bond length (1.686(3) Å) is typical of P=C double bonds. Unlike previously reported anionic dearomatized Ir PNP\* complexes,<sup>28</sup> our neutral complexes **8** and **9** have so far not been able to facilitate the N–H bond cleavage of ammonia. Nevertheless, some preliminary experiments revealed that complexes **8** and **9** readily activate alcohols, and therefore, we are interested in further investigating the utility of our complexes **8** and **9** for the direct catalytic acceptor-free dehydrogenation of primary alcohols and test their potential in transfer hydrogenation reactions.<sup>66</sup>



Scheme 7. Considered C–H Bond Activation Sequence Supported by DFT Results (B3LYP/GD3BJ/def2svp//def2tzvp)

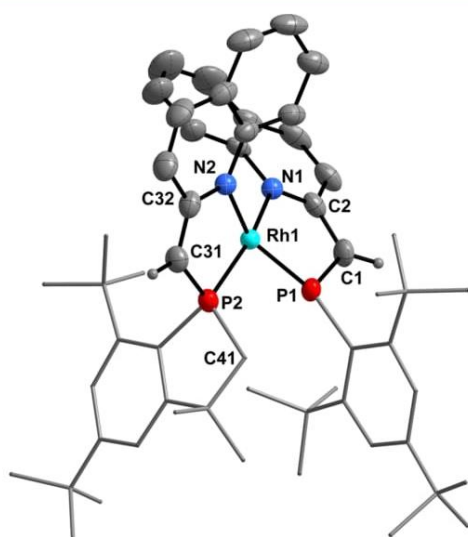
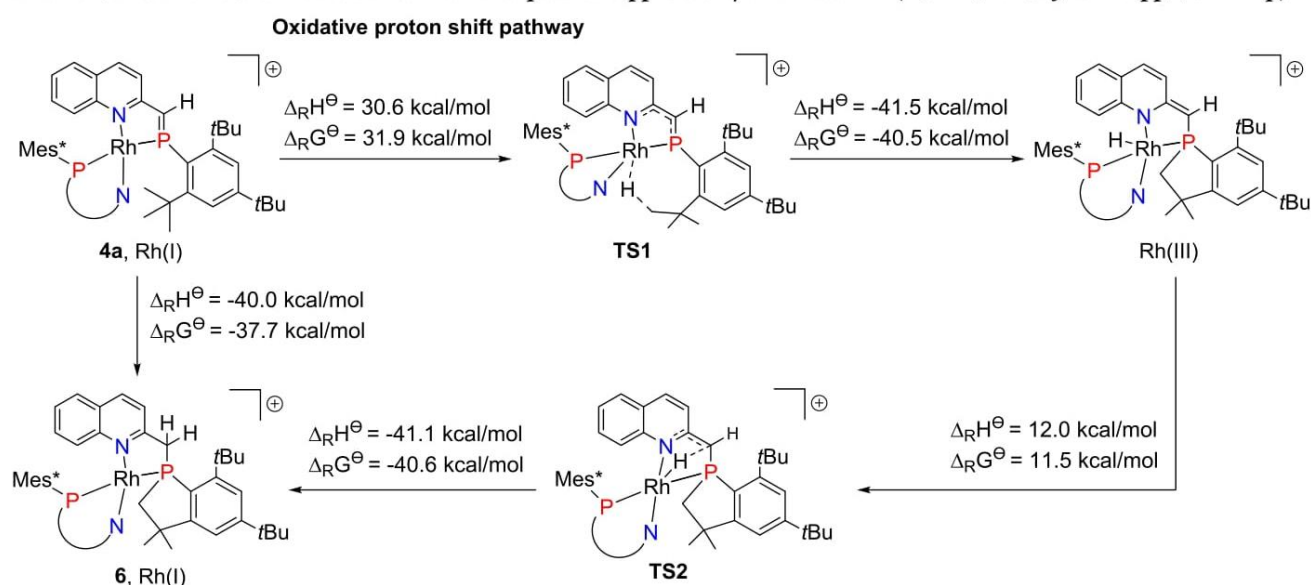


**Figure 7.** Molecular structure of complex 8. ORTEPs drawn at 50% probability. Hydrogen atoms, except those on C1 and C31, are omitted for clarity. Selected bond lengths (Å) and angles (°) of 8: P1–C1 1.686(3), P2–C31 1.766(3), C2–C1 1.422(4), C32–C31 1.375(4), P2–C41 1.841(3), P1–Rh 2.1326(6), P2–Rh 2.2278(6), N1–Rh 2.193(2), N2–Rh 2.117(2); C2–C1–P1 113.68(19), C32–C31–P2 115.4(2), P1–Rh–P2 100.66(2), N2–Rh–N1 106.07(8), N2–Rh–P2 82.85(6), N1–Rh–P1 79.41(6), P1–Rh–N2 150.48(6), P2–Rh–N1 162.03(5).

## CONCLUSIONS

In summary, we have presented the synthesis and characterization of the novel P,N-type quinoline-based phosphaphalkene ligand 2. When coordinated to Rh(I), 2 and the related pyridyl-substituted ligand 1 show a diverse coordination chemistry, ranging from simple twofold coordination, to give complexes 3 and 4, to C–H bond activation at the *o*-*t*Bu group of the Mes\*-substituted phosphaphalkenes in complex 4. Cationic complexes produced in salt metathesis reactions with AgOTf are not stable and undergo C–H bond activation at the Mes\* groups, resulting in the formation of cationic

mono (6) and bis(phosphaindane) (7) complexes. This type of ligand activation reactivity was described before for related systems with bidendate P,N,P-type Mes\*-substituted phosphaphalkene ligands; however, we have for the first time rationalized this for P,N-type ligands coordinated to Rh(I) by spectroscopic and computational analysis. We propose a new type of bond activation pathway that involves oxidative proton shift from the *t*Bu group to the Rh center along with the formation of a phosphaindane unit instead of initial oxidative addition of the *t*Bu group at Rh(I). Using these C–H bond activated complexes, we have demonstrated the selective deprotonation at the benzylic carbon to cause dearomatization of one of the quinoline rings, selectively. In the future, we will utilize these complexes in the stoichiometric and catalytic activation of small molecules. It is furthermore desirable to systematically extend this type of coordination chemistry to other metals and strongly  $\pi$  accepting P,N-phosphaphalkene architectures to unlock new types of organometallic reactivity that is unprecedented for related pyridinephosphine and pyridineimine ligands.

## ASSOCIATED CONTENT

### Supporting Information

The Supporting Information is available free of charge at <https://pubs.acs.org/doi/10.1021/acs.inorgchem.2c01158>.

General information; experimental methods; NMR spectra; electrochemical studies; computational details; and X-ray crystallographic data (PDF)

XYZ coordinates for the optimized geometries (xyz)

### Accession Codes

CCDC 2162622–2162626 contain the supplementary crystallographic data for this paper. These data can be obtained free of charge via [www.ccdc.cam.ac.uk/data\\_request/cif](http://www.ccdc.cam.ac.uk/data_request/cif), or by emailing [data\\_request@ccdc.cam.ac.uk](mailto:data_request@ccdc.cam.ac.uk), or by contacting The Cambridge Crystallographic Data Centre, 12 Union Road, Cambridge CB2 1EZ, UK; fax: +44 1223 336033.

## AUTHOR INFORMATION

### Corresponding Authors

**Torsten Beweries** – Leibniz-Institut für Katalyse e.V. (LIKAT), 18059 Rostock, Germany; [orcid.org/0000-0002-2416-8874](https://orcid.org/0000-0002-2416-8874); Phone: +49(0)381 1281 104; Email: [Torsten.beweries@catalysis.de](mailto:Torsten.beweries@catalysis.de)

**Christian Hering-Junghans** – Leibniz-Institut für Katalyse e.V. (LIKAT), 18059 Rostock, Germany; [orcid.org/0000-0003-4937-2625](https://orcid.org/0000-0003-4937-2625); Phone: +49(0)381 1281 260; Email: [Christian.hering-junghans@catalysis.de](mailto:Christian.hering-junghans@catalysis.de)

### Authors

**Priyanka Gupta** – Leibniz-Institut für Katalyse e.V. (LIKAT), 18059 Rostock, Germany

**Tobias Taeufer** – Leibniz-Institut für Katalyse e.V. (LIKAT), 18059 Rostock, Germany

**Jan-Erik Siewert** – Leibniz-Institut für Katalyse e.V. (LIKAT), 18059 Rostock, Germany

**Fabian Reiß** – Leibniz-Institut für Katalyse e.V. (LIKAT), 18059 Rostock, Germany; [orcid.org/0000-0002-1119-0343](https://orcid.org/0000-0002-1119-0343)

**Hans-Joachim Drexler** – Leibniz-Institut für Katalyse e.V. (LIKAT), 18059 Rostock, Germany

**Jola Pospech** – Leibniz-Institut für Katalyse e.V. (LIKAT), 18059 Rostock, Germany; [orcid.org/0000-0001-7794-2600](https://orcid.org/0000-0001-7794-2600)

Complete contact information is available at:

<https://pubs.acs.org/10.1021/acs.inorgchem.2c01158>

### Author Contributions

P.G. designed and performed the experiments. T.T., J.-E.S., and J.P. did the electrochemical measurements and analyzed the data. P.G., F.R., and C.H.-J. carried out the DFT calculations. H.-J.D. and C.H.-J. performed the X-ray experiments and analyzed the data. T.B. and C.H.-J. proposed and supervised the project. All of the authors were involved in discussing the results and writing the manuscript.

### Notes

The authors declare no competing financial interest.

## ACKNOWLEDGMENTS

The authors thank their technical and analytical staff for assistance. They also thank Nora Jannsen and Carmen Selle for assistance with UV–vis measurements. Financial support by LIKAT (PhD fellowship for P.G.) is gratefully acknowledged. C.H.-J. and J.-E.S. thank the Leibniz Association for funding within the scope of the Leibniz ScienceCampus Phosphorus Research Rostock ([www.sciencecampus-rostock.de](http://www.sciencecampus-rostock.de)). C.H.-J. (Material Allowance) and J.-E.S. (Kekulé Fellowship) wish to thank the Fonds der chemischen Industrie for financial support. F.R. wishes to thank the ITMZ at the University of Rostock for access to the Cluster Computer and especially M. Willert for technical support.

## REFERENCES

- (1) Speiser, F.; Braunstein, P.; Saussine, L. Nickel Complexes Bearing New P,N-Phosphinopyridine Ligands for the Catalytic Oligomerization of Ethylene. *Organometallics* **2004**, *23*, 2633–2640.
- (2) Dugal-Tessier, J.; Dake, G. R.; Gates, D. P. P,N-Chelate Complexes of Pd(II) and Pt(II) Based on a Phosphaalkene Motif: A Catalyst for the Overman–Claisen Rearrangement. *Organometallics* **2007**, *26*, 6481–6486.

- (3) Abo-Amer, A.; Boyle, P. D.; Puddephatt, R. J. Platinum complexes from pyridine-imine ligands with pendent functional groups. *Inorg. Chim. Acta* **2021**, 522, No. 120387.
- (4) Davies, D. L.; Lelj, F.; Lowe, M. P.; Ryder, K. S.; Singh, K.; Singh, S. Pyridine imines as ligands in luminescent iridium complexes. *Dalton Trans.* **2014**, 43, 4026–4039.
- (5) Daugulis, O.; Brookhart, M.; White, P. S. Phosphinidene-Palladium Complexes for the Polymerization and Oligomerization of Ethylene. *Organometallics* **2002**, *21*, 5935–5943.
- (6) Gilheany, D. G. Structure and Bonding in Organophosphorus-(III) Compounds. In *The Chemistry of Organophosphorus Compounds*; John Wiley & Sons, 1990; pp 9–49.
- (7) Nyulaszi, L.; Veszpremi, T.; Reffy, J. A new look at the similarities of the conjugative ability and reactivity of phosphorus-carbon and carbon-carbon double bonding. *J. Phys. Chem. A* **1993**, *97*, 4011–4015.
- (8) Weber, L. Phosphaalkenes with Inverse Electron Density. *Eur. J. Inorg. Chem.* **2000**, 2000, 2425–2441.
- (9) Doux, M.; Moores, A.; Mézailles, N.; Ricard, L.; Jean, Y.; Le Floch, P. The CO/PC analogy in coordination chemistry and catalysis. *J. Organomet. Chem.* **2005**, *690*, 2407–2415.
- (10) Bates, J. I.; Dugal-Tessier, J.; Gates, D. P. Phospha-organic chemistry: from molecules to polymers. *Dalton Trans.* **2010**, 39, 3151–3159.
- (11) Mathey, F. Phospha-Organic Chemistry: Panorama and Perspectives. *Angew. Chem., Int. Ed.* **2003**, *42*, 1578–1604.
- (12) Recker, G. Bildung und Eigenschaften von Acylphosphinen. I. Monosubstitutionsreaktionen an substituierten Disilylphosphinen mit Pivaloylchlorid. *Z. Anorg. Allg. Chem.* **1976**, *423*, 242–254.
- (13) Klebach, T. C.; Lourens, R.; Bickelhaupt, F. Synthesis of mesityldiphenylmethylenephosphine: a stable compound with a localized phosphorus:carbon bond. *J. Am. Chem. Soc.* **1978**, *100*, 4886–4888.
- (14) Appel, R.; Casser, C.; Immenkeppel, M.; Knoch, F. Easy Synthesis of Phosphaalkenes by a Phosphorus-Analogous Isocyanide Reaction and an Atypical Crystal Structure of a Tetracarbonyl-(phosphaalkene)iron Complex. *Angew. Chem., Int. Ed.* **1984**, *23*, 895–896.
- (15) Yoshifuji, M.; Toyota, K.; Inamoto, N. Photoisomerization of benzylidenephosphine containing phosphorus in low coordination state. *Tetrahedron Lett.* **1985**, *26*, 1727–1730.
- (16) Yam, M.; Chong, J. H.; Tsang, C.-W.; Patrick, B. O.; Lam, A. E.; Gates, D. P. Scope and Limitations of the Base-Catalyzed Phospha-Peterson PC Bond-Forming Reaction. *Inorg. Chem.* **2006**, *45*, 5225–5234.
- (17) Protasiewicz, J. D. Coordination-Like Chemistry of Phosphinidenes by Phosphanes. *Eur. J. Inorg. Chem.* **2012**, 2012, 4539–4549.
- (18) Shah, S.; Protasiewicz, J. D. 'Phospha-Wittig' reactions using isolable phosphoranylidenephosphines ArP=PR<sub>3</sub> (Ar = 2,6-Mes<sub>2</sub>C<sub>6</sub>H<sub>3</sub> or 2,4,6-But<sub>3</sub>C<sub>6</sub>H<sub>2</sub>). *Chem. Commun.* **1998**, 15, 1585–1586.
- (19) Nakajima, Y.; Okamoto, Y.; Chang, Y.-H.; Ozawa, F. Synthesis, Structures, and Reactivity of Ruthenium Complexes with PNP-pincer Type Phosphaalkene Ligands. *Organometallics* **2013**, *32*, 2918–2925.
- (20) Magnuson, K. W.; Oshiro, S. M.; Gurr, J. R.; Yoshida, W. Y.; Gembicky, M.; Rheingold, A. L.; Hughes, R. P.; Cain, M. F. Streamlined Preparation and Coordination Chemistry of Hybrid Phosphine–Phosphaalkene Ligands. *Organometallics* **2016**, *35*, 855–859.
- (21) Miura-Akagi, P. M.; Nakashige, M. L.; Maile, C. K.; Oshiro, S. M.; Gurr, J. R.; Yoshida, W. Y.; Royappa, A. T.; Krause, C. E.; Rheingold, A. L.; Hughes, R. P.; Cain, M. F. Synthesis of a Tris(phosphaalkene)phosphine Ligand and Fundamental Organometallic Reactions on Its Sterically Shielded Metal Complexes. *Organometallics* **2016**, *35*, 2224–2231.
- (22) Jouaiti, A.; Geoffroy, M.; Bernardinelli, G. Synthesis of new chelating agents: Association of a phosphaalkene moiety with a pyridine. *Tetrahedron Lett.* **1992**, *33*, 5071–5074.
- (23) van der Sluis, M.; Beverwijk, V.; Termaten, A.; Gavrilova, E.; Bickelhaupt, F.; Koosijman, H.; Veldman, N.; Spek, A. L. Synthesis of



2-(2-Pyridyl)phosphaalkenes [Mes\*PC(R)Py] (R = H, SiMe<sub>3</sub>) and Their Complexes  $\eta^1, \eta^1$ -[Mes\*PC(R)Py]XPdCl (X = Cl, Me, Ac). *Organometallics* **1997**, *16*, 1144–1152.

(24) Takeuchi, K.; Minami, A.; Nakajima, Y.; Ozawa, F. Synthesis and Structures of Nickel Complexes with a PN-Chelate Phosphaalkene Ligand. *Organometallics* **2014**, *33*, 5365–5370.

(25) Taguchi, H.-o.; Sasaki, D.; Takeuchi, K.; Tsujimoto, S.; Matsuo, T.; Tanaka, H.; Yoshizawa, K.; Ozawa, F. Unsymmetrical PNP-Pincer Type Phosphaalkene Ligands Protected by a Fused-Ring Bulky Eind Group: Synthesis and Applications to Rh(I) and Ir(I) Complexes. *Organometallics* **2016**, *35*, 1526–1533.

(26) Chang, Y.-H.; Nakajima, Y.; Ozawa, F. A Bis(phosphaethenyl)-pyridine Complex of Iridium(I): Synthesis and Catalytic Application to N-Alkylation of Amines with Alcohols. *Organometallics* **2013**, *32*, 2210–2215.

(27) Takeuchi, K.; Taguchi, H.-o.; Tanigawa, I.; Tsujimoto, S.; Matsuo, T.; Tanaka, H.; Yoshizawa, K.; Ozawa, F. A Square-Planar Complex of Platinum(0). *Angew. Chem., Int. Ed.* **2016**, *55*, 15347–15350.

(28) Chang, Y.-H.; Nakajima, Y.; Tanaka, H.; Yoshizawa, K.; Ozawa, F. Facile N–H Bond Cleavage of Ammonia by an Iridium Complex Bearing a Noninnocent PNP-Pincer Type Phosphaalkene Ligand. *J. Am. Chem. Soc.* **2013**, *135*, 11791–11794.

(29) Jouaiti, A.; Geoffroy, M.; Bernardinelli, G. Mono- and bidentate phosphaalkene ligands: structures of their copper(I) chloride complexes. *J. Chem. Soc., Dalton Trans.* **1994**, *11*, 1685–1688.

(30) Nakashige, M. L.; Lorigo, J. I. P.; Wong, L. S.; Gurr, J. R.; O'Donnell, T. J.; Yoshida, W. Y.; Rheingold, A. L.; Hughes, R. P.; Cain, M. F. E-Selective Synthesis and Coordination Chemistry of Pyridine-Phosphaalkenes: Five Ligands Produce Four Distinct Types of Ru(II) Complexes. *Organometallics* **2019**, *38*, 3338–3348.

(31) Taguchi, H.-o.; Chang, Y.-H.; Takeuchi, K.; Ozawa, F. Catalytic Synthesis of an Unsymmetrical PNP-Pincer-Type Phosphaalkene Ligand. *Organometallics* **2015**, *34*, 1589–1596.

(32) Liang, H.; Ito, S.; Yoshifuji, M. Preparation, structure and coordination properties of 3,3-bis(diisopropylamino)-3-thioxo-1-(2,4,6-tri-tert-butylphenyl)-1,3-diphosphapropene. *Org. Biomol. Chem.* **2003**, *1*, 3054–3058.

(33) Yoshifuji, M.; Sato, T.; Inamoto, N. Wavelength- and Temperature-dependent Photolysis of a Diphosphene. Generation of 2,4,6-Tri-tert-butylphenylphosphinidene and E/Z Isomerization. *Chem. Lett.* **1988**, *17*, 1735–1738.

(34) Clausing, S. T.; Salazar, D. M.; Orthaber, A. Preparation, photo- and electrochemical studies of a homoleptic imine-phosphaalkene Cu(I) complex. *Inorg. Chim. Acta* **2020**, *513*, No. 119958.

(35) Salazar, D. M.; Gupta, A. K.; Orthaber, A. Reactivity studies of an imine-functionalised phosphaalkene; unusual electrostatic and supramolecular stabilisation of a  $\sigma^2\lambda^3$ -phosphorus motif via hydrogen bonding. *Dalton Trans.* **2018**, *47*, 10404–10409.

(36) Serin, S. C.; Pick, F. S.; Dake, G. R.; Gates, D. P. Copper(I) Complexes of Pyridine-Bridged Phosphaalkene-Oxazoline Pincer Ligands. *Inorg. Chem.* **2016**, *55*, 6670–6678.

(37) Dugal-Tessier, J.; Dake, G. R.; Gates, D. P. Chiral Ligand Design: A Bidentate Ligand Incorporating an Acyclic Phosphaalkene. *Angew. Chem., Int. Ed.* **2008**, *47*, 8064–8067.

(38) Orthaber, A.; Belaj, F.; Pietschnig, R. Synthesis, structure and  $\pi$ -delocalization of a phosphaalkenyl based neutral PNP-pincer. *Inorg. Chim. Acta* **2011**, *374*, 211–215.

(39) Gupta, P.; Siewert, J.-E.; Wellnitz, T.; Fischer, M.; Baumann, W.; Beweries, T.; Hering-Junghans, C. Reactivity of phospha-Wittig reagents towards NHCs and NHOs. *Dalton Trans.* **2021**, *50*, 1838–1844.

(40) Fischer, M.; Reiß, F.; Hering-Junghans, C. Titanocene pnicinidene complexes. *Chem. Commun.* **2021**, *57*, 5626–5629.

(41) Fischer, M.; Hering-Junghans, C. On 1,3-phosphaazaaalkenes and their diverse reactivity. *Chem. Sci.* **2021**, *12*, 10279–10289.

(42) Glendening, E. D.; Badenhoop, J. K.; Reed, A. E.; Carpenter, J. E.; Bohmann, J. A.; Morales, C. M.; Landis, C. R.; Weinhold, F. NBO

6.0; Theoretical Chemistry Institute, University of Wisconsin-Madison, 2013.

(43) The  $\tau_5$  is defined as:  $\tau_5 = (\beta - \alpha)/60^\circ$ .  $\alpha$  and  $\beta$  refer to the two largest  $\theta$  bond angles in a five-coordinate complex. In an ideal square pyramidal structure ( $\tau_5 = 0$ ),  $\alpha = \beta = 180^\circ$ ; while in an ideal trigonal bipyramidal structure ( $\tau_5 = 1$ ),  $\alpha = 120^\circ$  and  $\beta = 180^\circ$ . For more details see: Blackman, A. G.; Schenk, E. B.; Jelley, R. E.; Krenske, E. H.; Gahan, L. R. Five-coordinate transition metal complexes and the value of  $\tau_5$ : observations and caveats. *Dalton Trans.* **2020**, *49*, 14798–14806.

(44) Addison, A. W.; Rao, T. N.; Reedijk, J.; van Rijn, J.; Verschoor, G. C. Synthesis, structure, and spectroscopic properties of copper(II) compounds containing nitrogen–sulphur donor ligands; the crystal and molecular structure of aqua[1,7-bis(N-methylbenzimidazol-2'-yl)-2,6-dithiaheptane]copper(II) perchlorate. *J. Chem. Soc., Dalton Trans.* **1984**, *7*, 1349–1356.

(45) Hayashi, A.; Okazaki, M.; Ozawa, F.; Tanaka, R. Synthesis, Structures, and Catalytic Properties of Late-Transition-Metal 2,6-Bis(2-phosphaethenyl)pyridine Complexes. *Organometallics* **2007**, *26*, 5246–5249.

(46) Svyaschenko, Y. V.; Orthaber, A.; Ott, S. Tuning the Electronic Properties of Acetylenic Fluorenes by Phosphaalkene Incorporation. *Chem. - Eur. J.* **2016**, *22*, 4247–4255.

(47) Foresman, J.; Frisch, A. *Exploring Chemistry With Electronic Structure Methods*, 3rd ed.; Gaussian, Inc.: 2015.

(48) Viviente, E. M.; Pregosin, P. S.; Schott, D. NMR Spectroscopy and Homogeneous Catalysis. In *Mechanisms in Homogeneous Catalysis*; John Wiley & Sons, 2005; pp 1–80.

(49) Katona, D.; Lu, Y.; Li, Y.; Pullarkat, S. A.; Leung, P.-H. Catalytic Approach toward Chiral P,N-Chelate Complexes Utilizing the Asymmetric Hydrophosphination Protocol. *Inorg. Chem.* **2020**, *59*, 3874–3886.

(50) The  $\tau_4$  is defined as:  $\tau_4 = [360^\circ - (\alpha + \beta)]/141^\circ$ .  $\alpha$  and  $\beta$  refer to the two largest  $\theta$  bond angles in a four-coordinate complex. In an ideal tetrahedral structure ( $\tau_4 = 1$ ),  $\alpha = \beta = 109.5^\circ$ , while in an ideal square planar structure ( $\tau_4 = 0$ ),  $\alpha = \beta = 180^\circ$ . For more details see: Yang, L.; Powell, D. R.; Houser, R. P. Structural variation in copper(i) complexes with pyridylmethylamide ligands: structural analysis with a new four-coordinate geometry index,  $\tau_4$ . *Dalton Trans.* **2007**, 955–964.

(51) Tsang, C.-W.; Rohrick, C. A.; Saini, T. S.; Patrick, B. O.; Gates, D. P. Reactions of Electrophiles with the Phosphaalkene Mes\*PCH<sub>2</sub>: Mechanistic Studies of a Catalytic Intramolecular C–H Bond Activation Reaction. *Organometallics* **2002**, *21*, 1008–1010.

(52) Tsang, C.-W.; Rohrick, C. A.; Saini, T. S.; Patrick, B. O.; Gates, D. P. Destiny of Transient Phosphenium Ions Generated from the Addition of Electrophiles to Phosphaalkenes: Intramolecular C–H Activation, Donor–Acceptor Formation, and Linear Oligomerization. *Organometallics* **2004**, *23*, 5913–5923.

(53) Houdard, R.; Mézailles, N.; Le Goff, X.-F.; Le Floch, P. Platinum(0)-Catalyzed Intramolecular Addition of a C–H Bond onto the P=C Bond of a Phosphaalkene. *Organometallics* **2009**, *28*, 5952–5959.

(54) Becke, A. D. Density-functional exchange-energy approximation with correct asymptotic behavior. *Phys. Rev. A* **1988**, *38*, 3098–3100.

(55) Vosko, S. H.; Wilk, L.; Nusair, M. Accurate spin-dependent electron liquid correlation energies for local spin density calculations: a critical analysis. *Can. J. Phys.* **1980**, *58*, 1200–1211.

(56) Perdew, J. P. Density-functional approximation for the correlation energy of the inhomogeneous electron gas. *Phys. Rev. B* **1986**, *33*, 8822–8824.

(57) Lee, C.; Yang, W.; Parr, R. G. Development of the Colle-Salvetti correlation-energy formula into a functional of the electron density. *Phys. Rev. B* **1988**, *37*, 785–789.

(58) Miehlich, B.; Savin, A.; Stoll, H.; Preuss, H. Results obtained with the correlation energy density functionals of Becke and Lee, Yang and Parr. *Chem. Phys. Lett.* **1989**, *157*, 200–206.

(59) Becke, A. D. Density-functional thermochemistry. III. The role of exact exchange. *J. Chem. Phys.* **1993**, *98*, 5648–5652.

(60) Grimme, S.; Ehrlich, S.; Goerigk, L. Effect of the damping function in dispersion corrected density functional theory. *J. Comput. Chem.* **2011**, *32*, 1456–1465.

(61) Grimme, S.; Antony, J.; Ehrlich, S.; Krieg, H. A consistent and accurate ab initio parametrization of density functional dispersion correction (DFT-D) for the 94 elements H–Pu. *J. Chem. Phys.* **2010**, *132*, No. 154104.

(62) Weigend, F.; Ahlrichs, R. Balanced basis sets of split valence, triple zeta valence and quadruple zeta valence quality for H to Rn: Design and assessment of accuracy. *Phys. Chem. Chem. Phys.* **2005**, *7*, 3297–3305.

(63) Khaskin, E.; Iron, M. A.; Shimon, L. J. W.; Zhang, J.; Milstein, D. N–H Activation of Amines and Ammonia by Ru via Metal–Ligand Cooperation. *J. Am. Chem. Soc.* **2010**, *132*, 8542–8543.

(64) Feller, M.; Diskin-Posner, Y.; Shimon, L. J. W.; Ben-Ari, E.; Milstein, D. N–H Activation by Rh(I) via Metal–Ligand Cooperation. *Organometallics* **2012**, *31*, 4083–4101.

(65) Zhang, J.; Gandelman, M.; Shimon, L. J. W.; Rozenberg, H.; Milstein, D. Electron-Rich, Bulky Ruthenium PNP-Type Complexes. Acceptorless Catalytic Alcohol Dehydrogenation. *Organometallics* **2004**, *23*, 4026–4033.

(66) Zhang, J.; Leitus, G.; Ben-David, Y.; Milstein, D. Facile Conversion of Alcohols into Esters and Dihydrogen Catalyzed by New Ruthenium Complexes. *J. Am. Chem. Soc.* **2005**, *127*, 10840–10841.

(67) Zhang, J.; Leitus, G.; Ben-David, Y.; Milstein, D. Efficient Homogeneous Catalytic Hydrogenation of Esters to Alcohols. *Angew. Chem., Int. Ed.* **2006**, *45*, 1113–1115.

(68) Anaby, A.; Butschke, B.; Ben-David, Y.; Shimon, L. J. W.; Leitus, G.; Feller, M.; Milstein, D. B–H Bond Cleavage via Metal–Ligand Cooperation by Dearomatized Ruthenium Pincer Complexes. *Organometallics* **2014**, *33*, 3716–3726.

## Recommended by ACS

### Metal–Ligand Cooperative Proton Transfer as an Efficient Trigger for Rhodium–NHC–Pyridonato Catalyzed *gem*-Specific Alkyne Dimerization

María Galiana-Cameo, Ricardo Castarlenas, *et al.*

JUNE 09, 2021  
ACS CATALYSIS

READ 

### Photoconductive Properties and Electronic Structure in 3,5-Disubstituted 2-(2'-Pyridyl)Pyrroles Coordinated to a Pd(II) Salicylideneimine Synthon

Andreea Ionescu, Iolinda Aiello, *et al.*

JUNE 14, 2021  
INORGANIC CHEMISTRY

READ 

### Pathways to Metal–Ligand Cooperation in Quinoline-Based Titanium(IV) Pincers: Nonelectrophilic N-methylation, Deprotonation, and Dihydropyridine Formation

Rosa Fandos, Eleuterio Álvarez, *et al.*

JUNE 07, 2021  
ORGANOMETALLICS

READ 

### Expanding the Range of Pyrenylphosphines and Their Derived Ru(II)-Arene Complexes

Laia Rafols, Arnald Grabulosa, *et al.*

AUGUST 07, 2020  
ORGANOMETALLICS

READ 

Get More Suggestions >

### **6.3 Metal-Free N-H Bond Activation by Phospha-Wittig Reagents**

Fabian Dankert, Jan-Erik Siewert, Priyanka Gupta, Florian Weigend, Christian Hering-Junghans

*Angew. Chem.Int. Ed.* **2022**, *61*, e20220706

DOI: 10.1002/anie.202207064

Reprinted (adapted) with permission from *Angewandte Chemie International Edition*.  
Copyright 2022 John Wiley and Sons.

Contribution to this paper is 10%





## Phosphorus

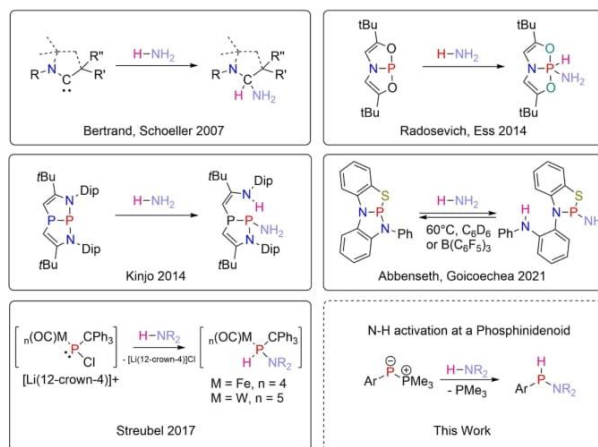
How to cite: *Angew. Chem. Int. Ed.* **2022**, 61, e202207064  
 International Edition: doi.org/10.1002/anie.202207064  
 German Edition: doi.org/10.1002/ange.202207064

## Metal-Free N–H Bond Activation by Phospha-Wittig Reagents\*\*

Fabian Dankert, Jan-Erik Siewert, Priyanka Gupta, Florian Weigend,\* and Christian Hering-Junghans\*

Dedicated to Professor Holger Braunschweig on the occasion of his 60<sup>th</sup> birthday

**Abstract:** N-containing molecules are mostly derived from ammonia (NH<sub>3</sub>). Ammonia activation has been demonstrated for single transition metal centers as well as for low-valent main group species. Phosphinidenes, mono-valent phosphorus species, can be stabilized by phosphines, giving so-called phosphanylidene phosphoranes of the type RP(PR'<sub>3</sub>). We demonstrate the facile, metal-free NH<sub>3</sub> activation using ArP(PMe<sub>3</sub>), affording for the first time isolable secondary aminophosphines ArP(H)NH<sub>2</sub>. DFT studies reveal that two molecules of NH<sub>3</sub> act in concert to facilitate an NH<sub>3</sub> for PMe<sub>3</sub> exchange. Furthermore, H<sub>2</sub>NR and HNR<sub>2</sub> activation is demonstrated.



**Scheme 1.** Key examples of NH<sub>3</sub>-activation. At a single carbon center, at geometrically constrained P-atoms, at Li/Cl phosphinidenoid metal complexes and outline of this study.

Ammonia (NH<sub>3</sub>) is the most ubiquitously used source of nitrogen in the synthesis of N-containing molecules. However, NH<sub>3</sub> activation is challenging and oxidative addition at a single metal center using Ir-pincer complexes was first shown in 2005 by Hartwig et al. and by Turculet and co-workers in 2009.<sup>[1]</sup> This challenge stems from the N–H bond dissociation enthalpy (106.12(6) kcal mol<sup>−1</sup>)<sup>[2]</sup> and from the formation of unreactive Werner-type complexes with NH<sub>3</sub>.<sup>[3]</sup> Strictly metal-free NH<sub>3</sub> activation was reported by Bertrand, Schoeller et al. using (alkyl)(amino) carbenes (AACs), resulting in the oxidative addition at a dicoordinate carbon center (Scheme 1, top).<sup>[4]</sup> Since this report a variety of low valent group 13<sup>[5]</sup> and 14<sup>[6]</sup> compounds have been shown to oxidatively add NH<sub>3</sub>. In 1987 Arduengo and co-workers described the addition of ECl<sub>3</sub> to HN(CH<sub>2</sub>CH<sub>2</sub>C(O)R) to

give planar T-shaped pnictogen species, which in case of E = P oxidatively activated CH<sub>3</sub>OH as well as facilitated the coupling of alkynes.<sup>[7]</sup> Radosevich and Ess revisited these geometrically constrained P-species and used them in the activation of RNH<sub>2</sub> (R = H, alkyl, aryl), affording N-functionalized P<sup>V</sup> compounds (Scheme 1, top).<sup>[8]</sup> The application of P<sup>III</sup> species in unusual non-trigonal coordination environments in NH<sub>3</sub> activation has since attracted considerable interest,<sup>[9]</sup> and was recently reviewed.<sup>[10]</sup> Moreover, reversible NH<sub>3</sub>-activation using NNS-type ligands on P<sup>III</sup> was reported in 2021 (Scheme 1, middle right).<sup>[11]</sup> In this regard the reversible H<sub>2</sub> activation and NH<sub>3</sub> activation to give azadiphosphiridines by the neutral biradicaloid [P(μ-N<sup>Mes</sup>Ter)]<sub>2</sub> (<sup>Mes</sup>Ter = 2,6-(2,4,6-Me<sub>3</sub>-C<sub>6</sub>H<sub>2</sub>)<sub>2</sub>C<sub>6</sub>H<sub>3</sub>) is noteworthy.<sup>[12]</sup> In contrast to geometrically constrained P<sup>III</sup> compounds the activation of NH<sub>3</sub> at a metal-free P<sup>I</sup> center has not been reported to date.

Phosphinidenes, the isovalent analogues of carbenes, are in most cases transient species and possess two lone pairs of electrons (LP), along with one unoccupied valence (singlet state) or two unpaired electrons (triplet state).<sup>[13]</sup> Using a combination of electronic and kinetic stabilization, a singlet phosphinidene was recently isolated.<sup>[14]</sup> Most phosphinidenes are either stabilized by coordination to a transition metal fragment,<sup>[15]</sup> or by cycloaddition reactions to (conjugated) multiple bond systems, releasing the R–P fragment via

[\*] Dr. F. Dankert, J.-E. Siewert, P. Gupta, Dr. C. Hering-Junghans  
 Leibniz-Institut für Katalyse e.V. (LIKAT)  
 Albert-Einstein-Straße 3a, 18059 Rostock (Germany)  
 E-mail: christian.hering-junghans@catalysis.de

Prof. Dr. F. Weigend  
 Fachbereich Chemie, Philipps-Universität Marburg  
 Hans-Meerwein-Straße 4, 35032 Marburg (Germany)  
 E-mail: florian.weigend@chemie.uni-marburg.de

[\*\*] A previous version of this manuscript has been deposited on a preprint server (https://doi.org/10.26434/chemrxiv-2022-w5xvh).

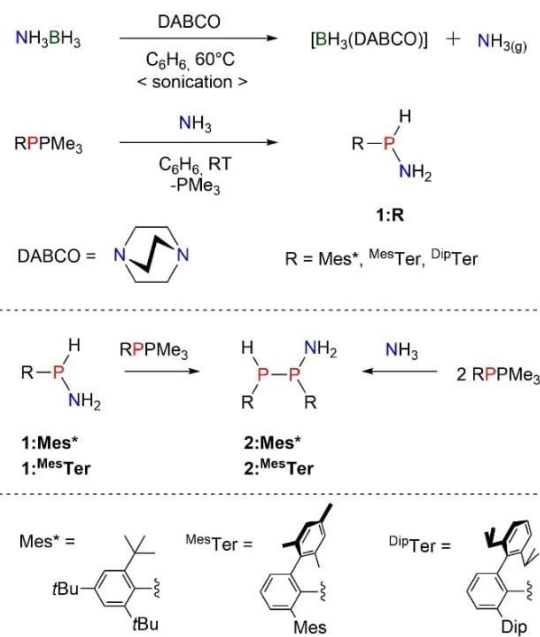
© 2022 The Authors. Angewandte Chemie International Edition published by Wiley-VCH GmbH. This is an open access article under the terms of the Creative Commons Attribution Non-Commercial NoDerivs License, which permits use and distribution in any medium, provided the original work is properly cited, the use is non-commercial and no modifications or adaptations are made.

cyclo-reversion.<sup>[16]</sup> With the emergence of Na(dioxane)<sub>2</sub>-(PCO),<sup>[17]</sup> elementyl phosphaketenes [E]-PCO became feasible and thermal or photochemical CO liberation was shown to unlock phosphinidene-type reactivity.<sup>[18]</sup> Phosphanylidene phosphoranes, Lewis base stabilized phosphinidenes, often referred to as Phospha-Wittig reagents,<sup>[19]</sup> of the type ArP(PMe<sub>3</sub>), have been shown to be phosphinidene transfer reagents.<sup>[20]</sup>

A PMe<sub>3</sub> for NHO (NHO=N-heterocyclic olefin) exchange followed by C(sp<sup>2</sup>)-H-activation was demonstrated.<sup>[21]</sup> The activation of strong E–H bonds with metal-free phosphinidenes remains largely elusive, though. For example, it has been a long-standing challenge to isolate secondary aminophosphines RP(H)–NR<sub>2</sub> as α-elimination of the amine results in the formation of the phosphinidene [R–P].<sup>[22]</sup> Stabilization by coordination of the phosphorus to a transition metal fragment (M) has been shown to render [R–P(H)NR<sub>2</sub>]M stable.<sup>[23]</sup> Using phosphanorbornadiene Cr and W complexes, Mathey and co-workers showed that upon diene cleavage amines, water and methanol can be activated at phosphorus.<sup>[24]</sup> Streubel and co-workers have shown that complexes of the type [(CO)<sub>n</sub>M–P(Cl)R][Li(12-crown-4)(thf)<sub>n</sub>] (M=Fe, W) unlock phosphinidenoid reactivity upon LiCl elimination and the functionalization of E–H bonds (E=N, O) at the metal-coordinated phosphorus atom has been documented (Scheme 1, bottom left).<sup>[25]</sup> Herein we report the facile N–H bond activation in NH<sub>3</sub> and amines using simple, metal-free ArP(PMe<sub>3</sub>), affording isolable Ar–P(H)NH<sub>2</sub> for the first time (Scheme 1, bottom right).

First, we found that treating H<sub>3</sub>BNH<sub>3</sub> with DABCO in a 1:1 ratio in benzene under sonication at 60 °C gave NH<sub>3</sub> in stoichiometric fashion. Next Mes\*P(PMe<sub>3</sub>) (Mes\*=2,4,6-*t*Bu<sub>3</sub>-C<sub>6</sub>H<sub>2</sub>) was treated with 10 equiv NH<sub>3</sub> in benzene for 3 h giving Mes\*P(H)NH<sub>2</sub> (**1:Mes\***) (Scheme 2).

**1:Mes\*** showed a doublet of triplets in the <sup>31</sup>P NMR spectrum at –24.35 ppm (<sup>1</sup>J<sub>PH</sub>=240.0, <sup>2</sup>J<sub>PH</sub>=8.5 Hz), collapsing into a singlet upon proton decoupling. In the <sup>1</sup>H NMR spectrum the PH proton is detected as a doublet of triplets at 6.52 ppm. IR spectroscopy revealed N–H and P–H bands at 3432 and 2387 cm<sup>–1</sup>, respectively. **1:Mes\*** is formed quantitatively and was isolated as a colourless crystalline powder. Next, <sup>Mes\*</sup>TerP(PMe<sub>3</sub>) and <sup>Dip</sup>TerP(PMe<sub>3</sub>) (<sup>Dip</sup>Ter=2,6-(2,6-*i*Pr<sub>2</sub>-C<sub>6</sub>H<sub>3</sub>)<sub>2</sub>C<sub>6</sub>H<sub>3</sub>) were exposed to an excess of NH<sub>3</sub> and the quantitative formation of **1:<sup>Mes\*</sup>Ter** and **1:<sup>Dip</sup>Ter**, was observed (Scheme 2). Compounds **1:R** represent the first isolable secondary aminophosphines of the type R–P(H)NH<sub>2</sub>. Aminophosphines of the type R–PH(NR<sub>2</sub>) have been postulated to be prone to eliminate HNR<sub>2</sub>. The first free secondary aminophosphine (Me<sub>3</sub>Si)<sub>2</sub>N–P(H)–N(H)SiMe<sub>3</sub> was shown to be thermally stable with respect to an α-elimination of H<sub>2</sub>NSiMe<sub>3</sub>.<sup>[26]</sup> Attempting to crystallize **1:Mes\*** or **1:<sup>Mes\*</sup>Ter** from concentrated benzene solutions yielded minimal amounts of colourless crystals for single crystal X-Ray diffraction (SC-XRD) experiments.<sup>[27]</sup> These were identified as the diphosphines RP(H)P(NH<sub>2</sub>)R (**2:R**; R=Mes\*, <sup>Mes\*</sup>Ter) (Figure 1). **2:R** were then rationally synthesized by either treatment of RP(PMe<sub>3</sub>) with 0.5 equiv of NH<sub>3</sub> or by addition of a second eq. of RP(PMe<sub>3</sub>) to a



**Scheme 2.** Synthesis of RP(H)NH<sub>2</sub> (**1:R**) and formation of diphosphines **2:R**.

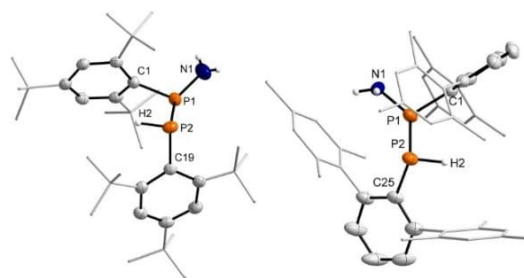


**Figure 1.** Molecular structures of **2:Mes\*** (left) and **2:<sup>Mes\*</sup>Ter** (right). Ellipsoids drawn at 50% probability with C–H atoms omitted, *t*Bu- and Mes-groups rendered as wire-frame for clarity. Selected bond lengths [Å] and angles [°] (**2:Mes\***): N1–P1 1.6587(30), P1–P2 2.2498(10); C1–P1–P2 101.80(7), N1–P1–P2 105.08(10), P1–P2–C19 99.37(7); **2:<sup>Mes\*</sup>Ter**: N1–P1 1.6935(35), P1–P2 2.222(8); N1–P1–P2 103.21(10), P1–P2–C25 103.56(65), C1–P1–P2 104.067(63).

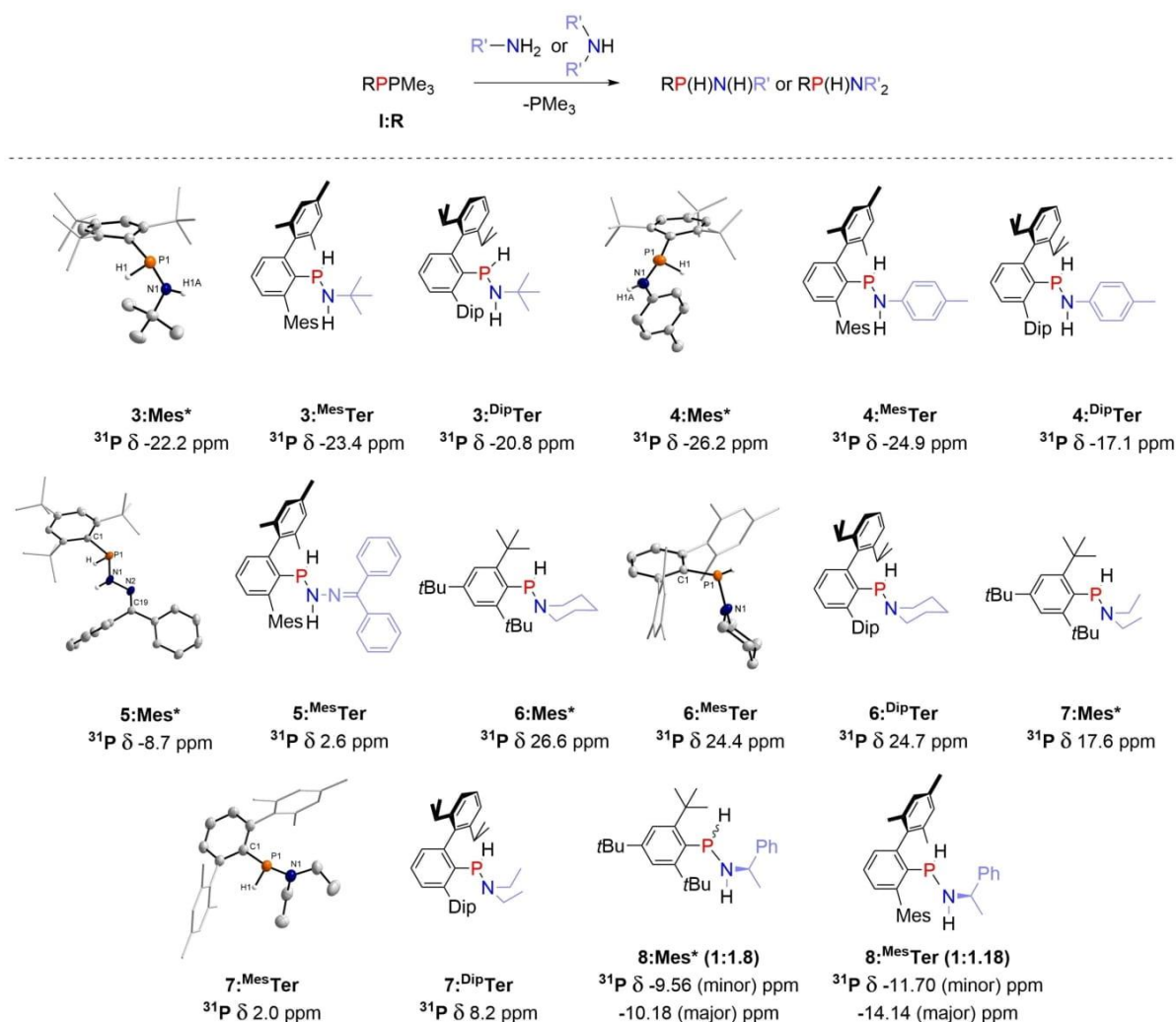
benzene solution of **1:R** (see Supporting Information). **1:Mes\*** and **1:<sup>Mes\*</sup>Ter** are stable and undergo α-elimination, which was found to be energetically feasible by theoretical means (Table S9), to afford **2:R** only in highly concentrated solutions over an extended period of time. Moreover, **2:Mes\*** was exposed to NH<sub>3</sub> and the formation of **1:Mes\*** was not detected, excluding **2:Mes\*** as possible intermediate in the formation of **1:Mes\***. **2:<sup>Dip</sup>Ter** could not be synthesized, thus indicating the steric protection of the <sup>Dip</sup>Ter-substituent.

**2:Mes\*** shows two doublets (<sup>1</sup>J<sub>PP</sub>=238.5 Hz) in the <sup>31</sup>P{<sup>1</sup>H} NMR spectrum at 30.82 (PNH<sub>2</sub>) and at –30.92 ppm (PH), indicating a P–P single bond and a single diastereomer in solution. Interestingly, in the <sup>31</sup>P{<sup>1</sup>H} NMR spec-



trum of **2<sup>Mes</sup>Ter** two sets of doublets in close proximity are detected in a 2:3 ratio, indicating two diastereomers in solution, which might arise from the sterically more flexible environment provided by the <sup>Mes</sup>Ter-substituent. While the *PH* proton of **2<sup>Mes</sup>\*** at 5.01 ppm gives a doublet of doublets in the <sup>1</sup>H NMR spectrum, two *PH* resonances are detected for **2<sup>Mes</sup>Ter** at 3.88 and 3.49 ppm in a 2:3 ratio. **2<sup>Mes</sup>\*** crystallizes as its *R,R*-diastereomer with the <sup>Mes</sup>-substituents being located on the same side of the P1–P2 axis (2.2498(10) Å) with a dihedral angle (C1–P1–P2–C19) of 106.36° (Figure 1), agreeing with the structure of the related diphosphine <sup>Mes</sup>\*P(H)P(CN–B(C<sub>6</sub>F<sub>5</sub>)<sub>3</sub>)<sup>Mes</sup>\* (cf. d(P–P) = 2.2461(8) Å, > (C1–P1–P2–C19) = 106.65°).<sup>[20c]</sup> Whereas in solution two diastereomers of **2<sup>Mes</sup>Ter** prevail, only the *S,S*-diastereomer is detected in the solid state with NH<sub>2</sub> and H being disordered (Figure S2). The dihedral angle (C1–P1–P2–C25) of 138.54° is considerably wider compared to **2<sup>Mes</sup>\***, which can be attributed to the 2,6-substituents of

the <sup>Mes</sup>Ter groups, see above. Next, RP(PMe<sub>3</sub>) and the primary amine H<sub>2</sub>N*t*Bu were combined to give RP(H)N–(H)*t*Bu (**3<sup>R</sup>**; R = <sup>Mes</sup>\*, <sup>Mes</sup>Ter, <sup>Dip</sup>Ter). **3<sup>Mes</sup>\*** shows a doublet of doublets in the <sup>1</sup>H NMR spectrum at 6.39 ppm (*PH*: <sup>1</sup>*J*<sub>PH</sub> = 211.1; <sup>3</sup>*J*<sub>HH</sub> = 3.5 Hz) as well as a doublet of doublets at 1.12 ppm (*NH*: <sup>2</sup>*J*<sub>PH</sub> = 5.2; <sup>3</sup>*J*<sub>HH</sub> = 3.5 Hz). **3<sup>Mes</sup>Ter** contained trace amounts of the diphosphine (<sup>Mes</sup>TerP)<sub>2</sub> (ca. 10 %).<sup>[20c]</sup> The clean formation of **3<sup>Dip</sup>Ter** was achieved in benzene at 80 °C and the characteristic <sup>31</sup>P NMR data of compounds **3<sup>R</sup>** are summarized in Scheme 3. The molecular structures of **3<sup>Mes</sup>\*** and **3<sup>Dip</sup>Ter** revealed both enantiomers represented by disorder of the whole –P(H)N(H)R unit, with P1–N1 distances (**3<sup>Mes</sup>\*** 1.6917(13), **3<sup>Dip</sup>Ter** 1.6646(48) Å) in the range of contracted single bonds (Σ*r*<sub>cov</sub>(P–N) = 1.82 Å).<sup>[28]</sup> a trigonal pyramidal P and planar N atoms. To further expand the scope to aniline derivatives, *p*-toluidine was combined in benzene with the respective phosphazene Wittig reagents. After sonication overnight at 60 °C or



**Scheme 3.** NH-activation of primary and secondary amines at ArP(PMe<sub>3</sub>).

stirring at room temperature, Mes\*P(H)N(H)Tol (**4Mes\***) and Mes\*TerP(H)N(H)Tol (**4Mes\*Ter**) were obtained as beige powders. With Ph<sub>2</sub>C=N–NH<sub>2</sub> Mes\*P(PMe<sub>3</sub>) cleanly reacted to give Mes\*P(H)N(H)NCPh<sub>2</sub> (**5Mes\***) in 58 % isolated yield. **5Mes\*** is a colorless crystalline solid, with a characteristic doublet of doublets at 7.02 ppm (PH), a pseudo-triplet at 5.88 ppm (NH) in the <sup>1</sup>H NMR spectrum and a singlet in the <sup>31</sup>P{<sup>1</sup>H} NMR spectrum at –8.8 ppm. **5Mes\*** shows short P1–N1 (1.709(1) Å) and N1–N2 (1.360(18) Å) as well as N2–C19 (1.2900(13) Å) distances in the expected range for a hydrazone derivative (cf. Ph<sub>2</sub>C=NN(H)PPh<sub>2</sub> P–N 1.697(2), N–N 1.373(2), C=N 1.292(2) Å).<sup>[29]</sup> The PH and NH protons reside on the same side according to SC-XRD experiments.

Then we investigated whether piperidine or HNET<sub>2</sub> could be NH-activated, as secondary amine activation was previously only reported for NNS-substituted P<sup>III</sup> system in dipolar fashion.<sup>[11]</sup> RP(PMe<sub>3</sub>) reacted cleanly with piperidine in C<sub>6</sub>H<sub>6</sub> under sonication for 4 h at elevated temperatures, to give RP(H)N(C<sub>5</sub>H<sub>10</sub>) (**6R**, R = Mes\*, Mes\*Ter, Dip\*Ter) quantitatively as colorless solids. **6R** show characteristic <sup>31</sup>P{<sup>1</sup>H} NMR signals at ca. 25 ppm, deshielded compared to **3R** and **4R**. RP(PMe<sub>3</sub>) also reacted cleanly with HNET<sub>2</sub> under the same conditions outlined above to give RP(H)NEt<sub>2</sub> (**7R**, R = Mes\*, Mes\*Ter, Dip\*Ter), with <sup>31</sup>P{<sup>1</sup>H} NMR shifts between 17.6 ppm (**7Mes\***) and 1.97 ppm (**7Mes\*Ter**), which is shielded significantly compared to Mes\*TerP(NEt<sub>2</sub>)<sub>2</sub> (cf. δ(<sup>31</sup>P) = 100.2 ppm).<sup>[30]</sup> X-Ray quality crystals of **6R** and **7R** (except for **6Mes\***) were grown and their molecular structures show trigonal pyramidal P atoms with P–N bond lengths of ca. 1.68 Å. The value agrees well with that within the metal complex [(CO)<sub>5</sub>W](P(H)(CPh<sub>3</sub>NBn<sub>2</sub>)) (cf. d(P–N) = 1.6877(19) Å).<sup>[25a]</sup> Using (*R*)-(+)-1-phenylethylamine we succeeded in the synthesis of a diastereomeric mixture of the chiral phosphines *R,R*-**8Mes\*** and *R,S*-**8Mes\***, with one of the diastereomers being formed preferentially (1:1.8 ratio). Using Mes\*TerP(PMe<sub>3</sub>) a 1:1.2 mixture of both isomers was obtained. This clearly shows the potential of rapidly accessing a new class of chiral phosphines through NH-activation at phospho-Wittig reagents.

We next investigated the underlying reaction mechanism for the metal-free N–H activation at ArP(PMe<sub>3</sub>). Reaction pathways were identified with a chain-of-states method under the sole constraint of equally spaced structures<sup>[31]</sup> at the PBE/def2-TZVP DFT level, followed by full optimization of the stationary points (see Supporting Information for computational details).<sup>[32]</sup> Mes\*P(PMe<sub>3</sub>) was used as the phosphanylidene phosphorane and akin to the NH-bond activation mechanism proposed by Streubel and Espinosa for [(CO)<sub>4</sub>Fe](P(NH<sub>3</sub>)Me) in which four NH<sub>3</sub> molecules facilitate the NH transfer,<sup>[25b]</sup> we employed two NH<sub>3</sub> molecules in our calculations (Figure 2).

The reaction pathway from Mes\*P(PMe<sub>3</sub>) + 2NH<sub>3</sub> to Mes\*P(H)NH<sub>2</sub> + PMe<sub>3</sub> + NH<sub>3</sub> is shown in Figure 2. The two NH<sub>3</sub> molecules form a dimer, which is adsorbed by a hydrogen bridge (H2...P1), coming with an overall gain of 14 kJ mol<sup>–1</sup> (LM1). It is followed by a transition state (TS1) where the P–P bond is weakened and the P...H contact is released in favour of a P...N contact with the N atom of the

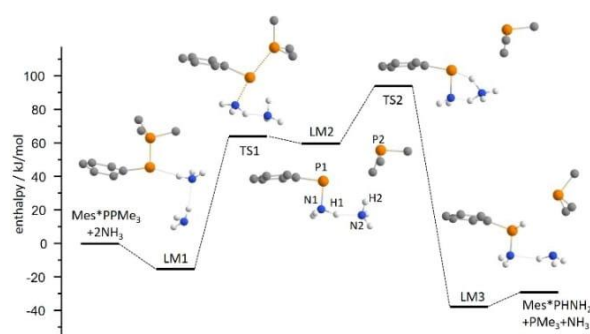


**Figure 2.** Enthalpy profile for the proposed reaction pathway from Mes\*P(PMe<sub>3</sub>) and 2 NH<sub>3</sub> (Mes\* represented by central C<sub>6</sub>) at the PBE/def2-TZVP DFT level.

other NH<sub>3</sub> unit of the dimer (P1...N1), which requires 77 kJ mol<sup>–1</sup>. Next, the P–P bond is cleaved in favour of the P–N bond (LM2, gain 2 kJ mol<sup>–1</sup>). LM2 features a hydrogen bridge N1–H1...N2. The formation of favourable Mes\*P–(H)NH<sub>2</sub> with weakly adsorbed NH<sub>3</sub> and PMe<sub>3</sub> (LM3) is achieved via a second transition state, TS2, which is higher in enthalpy than LM2 by 35 kJ mol<sup>–1</sup>. This transition state differs from LM2 in two respects: It consists of rather an NH<sub>2</sub><sup>(–)</sup> and an NH<sub>4</sub><sup>(+)</sup> unit (NBO charges –0.31 and +0.53) connected by a H bond (N1...H1–N2), and a second H bond from the NH<sub>4</sub> unit to the P atom. The latter becomes the P–H bond in LM3 (energy gain 134 kJ mol<sup>–1</sup> with respect to TS2). Final removal of PMe<sub>3</sub> and NH<sub>3</sub> requires 11 kJ mol<sup>–1</sup>. Thus, the overall gain is 27 kJ mol<sup>–1</sup>, and with barrier heights of 77 and 36 kJ mol<sup>–1</sup> the reaction is feasible under ambient conditions. Matters are completely different for the reaction with a single NH<sub>3</sub> molecule. Here, the transition state for an intramolecular direct H-shift from N to P was found to be 172 kJ mol<sup>–1</sup> above the initial state; further, the analogue to LM2 shows vibration modes close to zero (7 and 9 cm<sup>–1</sup>, see Supporting Information for details) and converges to the analogue of LM1 if only weakly distorted. Also, all attempts to optimize a transition state between these two local minima ended in the analogue of LM1. These features are not in line with the reaction going to completion at room temperature (see Supporting Information for details). It is thus evident, that smooth changes from N–H...N to N...H–N (and similarly for P) make this reaction feasible at room temperature. Based on these theoretical studies it would be expected that the formation of secondary aminophosphines is generally dependent on the amine concentration. In order to probe this the 1:1 reaction of Mes\*P(PMe<sub>3</sub>) and *p*-toluidine was followed by <sup>1</sup>H NMR spectroscopy at different concentrations at room temperature. This clearly showed that the reaction is faster at higher amine concentrations (Figure S95). In addition, we found that a Mes\*P(PMe<sub>3</sub>) to *p*-toluidine ratio of 1:2 resulted in full conversion to give **4Mes\*** in less than 5 min at room temperature. Even though the conversion time plots did not allow to extract the reaction order, the amine concentration clearly affects the outcome of the reaction.



It has been shown earlier that the transamination of  $\text{P}(\text{NEt}_2)_3$  with primary aromatic di- and polyamines gave rise to the formation of a variety of structurally stabilized aminophosphines, with the concomitant formation of  $\text{HNEt}_2$ .<sup>[33]</sup> We thus tested whether **6-Mes\*** would undergo transamination in the presence of an excess of *p*-toluidine. Heating a mixture of **6-Mes\*** and *p*-toluidine (1:3 ratio) over a period of 2 weeks at 80 °C gave rise to the formation **4-Mes\*** and piperidine, with a conversion of ca. 75 % based on  $^{31}\text{P}$  NMR spectroscopy (Figure S96). This clearly illustrates the synthetic potential of secondary aminophosphines.<sup>[34]</sup>

In summary, the facile activation of  $\text{NH}_3$  with the aid of phospho-Wittig reagents of the type  $\text{ArP}(\text{PMe}_3)$  has been demonstrated to give for the first time secondary aminophosphanes of the type  $\text{ArP}(\text{H})\text{NH}_2$  (**1-R**). The activation of primary and secondary amines was likewise achieved. This novel reactivity of phospho-Wittig reagents is a straightforward way towards P–N-bonds from a variety of substrates, including chiral amines. Efforts to utilize this concept in the design of new P-containing materials are currently underway. For example, we strive to construct multidentate ligand architectures and to explore the synthesis of chiral phosphine ligands.

## Acknowledgements

C.H.-J. thanks the Boehringer Ingelheim Foundation for support through an Exploration Grant. F.D. and C.H.-J. thank the Leibniz Association for funding within the scope of the Leibniz ScienceCampus Phosphorus Research Rostock ([www.sciencecampus-rostock.de](http://www.sciencecampus-rostock.de)). F.D. thanks C.H.-J. for his ongoing support. J.-E.S. wishes to thank the Fonds der chemischen Industrie for financial support. We want to thank Eszter Baráth and Torsten Beweries for helpful discussions. Open Access funding enabled and organized by Projekt DEAL.

## Conflict of Interest

The authors declare no conflict of interest.

## Data Availability Statement

The data that support the findings of this study are available in the Supporting Information of this article.

**Keywords:** Amines • Bond Cleavage • N–H Activation • Phosphorus • Small Molecule Activation

- [1] a) J. Zhao, A. S. Goldman, J. F. Hartwig, *Science* **2005**, *307*, 1080–1082; b) E. Morgan, D. F. MacLean, R. McDonald, L. Turculet, *J. Am. Chem. Soc.* **2009**, *131*, 14234–14236.
- [2] D. H. Mordant, M. N. R. Ashfold, R. N. Dixon, *J. Chem. Phys.* **1996**, *104*, 6460–6471.

- [3] A. Werner, *Z. Anorg. Chem.* **1893**, *3*, 267–330.
- [4] G. D. Frey, V. Lavallo, B. Donnadieu, W. W. Schoeller, G. Bertrand, *Science* **2007**, *316*, 439–441.
- [5] a) J. A. B. Abdalla, I. M. Riddlestone, R. Tirfoin, S. Aldridge, *Angew. Chem. Int. Ed.* **2015**, *54*, 5098–5102; *Angew. Chem.* **2015**, *127*, 5187–5191; b) J. Feld, D. W. N. Wilson, J. M. Goicoechea, *Angew. Chem. Int. Ed.* **2021**, *60*, 22057–22061; *Angew. Chem.* **2021**, *133*, 22228–22232; c) M. K. Sharma, C. Wölper, S. Schulz, *Dalton Trans.* **2022**, *51*, 1612; d) Z. Zhu, X. Wang, Y. Peng, H. Lei, J. C. Fetting, E. Rivard, P. P. Power, *Angew. Chem. Int. Ed.* **2009**, *48*, 2031–2034; *Angew. Chem.* **2009**, *121*, 2065–2068.
- [6] a) M. E. Alberto, N. Russo, E. Sicilia, *Chem. Eur. J.* **2013**, *19*, 7835–7846; b) D. C. H. Do, A. V. Protchenko, M. Á. Fuentes, J. Hicks, P. Vasko, S. Aldridge, *Chem. Commun.* **2020**, *56*, 4684–4687; c) A. Jana, C. Schulzke, H. W. Roesky, *J. Am. Chem. Soc.* **2009**, *131*, 4600–4601; d) A. Meltzer, S. Inoue, C. Präsang, M. Driess, *J. Am. Chem. Soc.* **2010**, *132*, 3038–3046; e) Y. Peng, B. D. Ellis, X. Wang, P. P. Power, *J. Am. Chem. Soc.* **2008**, *130*, 12268–12269; f) A. V. Protchenko, J. I. Bates, L. M. A. Saleh, M. P. Blake, A. D. Schwarz, E. L. Kolychev, A. L. Thompson, C. Jones, P. Mountford, S. Aldridge, *J. Am. Chem. Soc.* **2016**, *138*, 4555–4564; g) D. Reiter, P. Frisch, D. Wendel, F. M. Hörmann, S. Inoue, *Dalton Trans.* **2020**, *49*, 7060–7068.
- [7] A. J. Arduengo, C. A. Stewart, F. Davidson, D. A. Dixon, J. Y. Becker, S. A. Culley, M. B. Mizen, *J. Am. Chem. Soc.* **1987**, *109*, 627–647.
- [8] S. M. McCarthy, Y.-C. Lin, D. Devarajan, J. W. Chang, H. P. Yennawar, R. M. Rioux, D. H. Ess, A. T. Radosevich, *J. Am. Chem. Soc.* **2014**, *136*, 4640–4650.
- [9] a) J. Cui, Y. Li, R. Ganguly, A. Inthirarajah, H. Hirao, R. Kinjo, *J. Am. Chem. Soc.* **2014**, *136*, 16764–16767; b) T. P. Robinson, D. M. De Rosa, S. Aldridge, J. M. Goicoechea, *Angew. Chem. Int. Ed.* **2015**, *54*, 13758–13763; *Angew. Chem.* **2015**, *127*, 13962–13967; c) T. P. Robinson, S.-K. Lo, D. De Rosa, S. Aldridge, J. M. Goicoechea, *Chem. Eur. J.* **2016**, *22*, 15712–15724; d) S. Volodarsky, R. Dobrovetsky, *Chem. Commun.* **2018**, *54*, 6931–6934.
- [10] J. Abbeneth, J. M. Goicoechea, *Chem. Sci.* **2020**, *11*, 9728–9740.
- [11] J. Abbeneth, O. P. E. Townrow, J. M. Goicoechea, *Angew. Chem. Int. Ed.* **2021**, *60*, 23625–23629; *Angew. Chem.* **2021**, *133*, 23817–23821.
- [12] A. Hinz, A. Schulz, A. Villinger, *Angew. Chem. Int. Ed.* **2016**, *55*, 12214–12218; *Angew. Chem.* **2016**, *128*, 12402–12406.
- [13] M. T. Nguyen, A. Van Keer, L. G. Vanquickenborne, *J. Org. Chem.* **1996**, *61*, 7077–7084.
- [14] L. Liu, David A. Ruiz, D. Munz, G. Bertrand, *Chem* **2016**, *1*, 147–153.
- [15] A. H. Cowley, *Acc. Chem. Res.* **1997**, *30*, 445–451.
- [16] a) A. Velian, C. C. Cummins, *J. Am. Chem. Soc.* **2012**, *134*, 13978–13981; b) W. J. Transue, A. Velian, M. Nava, C. García-Iriepa, M. Temprado, C. C. Cummins, *J. Am. Chem. Soc.* **2017**, *139*, 10822–10831; c) M. B. Geeson, W. J. Transue, C. C. Cummins, *J. Am. Chem. Soc.* **2019**, *141*, 13336–13340.
- [17] J. M. Goicoechea, H. Grützmacher, *Angew. Chem. Int. Ed.* **2018**, *57*, 16968–16994; *Angew. Chem.* **2018**, *130*, 17214–17240.
- [18] a) M. M. Hansmann, G. Bertrand, *J. Am. Chem. Soc.* **2016**, *138*, 15885–15888; b) M. M. Hansmann, R. Jazsar, G. Bertrand, *J. Am. Chem. Soc.* **2016**, *138*, 8356–8359; c) D. W. N. Wilson, J. Feld, J. M. Goicoechea, *Angew. Chem. Int. Ed.* **2020**, *59*, 20914–20918; *Angew. Chem.* **2020**, *132*, 21100–21104; d) M. K. Sharma, C. Wölper, G. Haberhauer, S. Schulz, *Angew. Chem. Int. Ed.* **2021**, *60*, 6784–6790; *Angew. Chem.* **2021**, *133*, 6859–6865.
- [19] J. D. Protasiewicz, *Eur. J. Inorg. Chem.* **2012**, 4539–4549.



- [20] a) M. Fischer, F. Reiß, C. Hering-Junghans, *Chem. Commun.* **2021**, 57, 5626–5629; b) M. Fischer, S. Nees, T. Kupfer, J. T. Goettel, H. Braunschweig, C. Hering-Junghans, *J. Am. Chem. Soc.* **2021**, 143, 4106–4111; c) M. Fischer, C. Hering-Junghans, *Chem. Sci.* **2021**, 12, 10279–10289; d) U. J. Kilgore, H. Fan, M. Pink, E. Urnezus, J. D. Protasiewicz, D. J. Mindiola, *Chem. Commun.* **2009**, 4521–4523.
- [21] P. Gupta, J.-E. Siewert, T. Wellnitz, M. Fischer, W. Baumann, T. Beveries, C. Hering-Junghans, *Dalton Trans.* **2021**, 50, 1838–1844.
- [22] A. B. Burg, P. J. Slota, *J. Am. Chem. Soc.* **1958**, 80, 1107–1109.
- [23] G. Huttner, H.-D. Müller, *Angew. Chem. Int. Ed. Engl.* **1975**, 14, 571–572; *Angew. Chem.* **1975**, 87, 595–596.
- [24] a) A. Marinetti, F. Mathey, *Organometallics* **1982**, 1, 1488–1492; b) A. Marinetti, F. Mathey, J. Fischer, A. Mitschler, *J. Am. Chem. Soc.* **1982**, 104, 4484–4485.
- [25] a) R. Streubel, A. Schmer, A. W. Kyri, G. Schnakenburg, *Organometallics* **2017**, 36, 1488–1495; b) A. Schmer, T. Terschüren, G. Schnakenburg, A. Espinosa Ferao, R. Streubel, *Eur. J. Inorg. Chem.* **2019**, 1604–1611.
- [26] E. Niecke, G. Ringel, *Angew. Chem. Int. Ed. Engl.* **1977**, 16, 486–487; *Angew. Chem.* **1977**, 89, 500–501.
- [27] See Supporting Information for all experimental details. Deposition Numbers 2141957, 2141958, 2141959, 2141960, 2141961, 2141962, 2141963, 2141964, 2141965, 2141966, 2141967 and 2141968 contain the supplementary crystallographic data for this paper. These data are provided free of charge by the joint Cambridge Crystallographic Data Centre and Fachinformationszentrum Karlsruhe Access Structures service.
- [28] P. Pyykkö, M. Atsumi, *Chem. Eur. J.* **2009**, 15, 12770–12779.
- [29] Y. S. Panova, A. V. Sheyanova, V. V. Sushev, N. V. Zolotarova, A. V. Cherkasov, A. N. Kornev, *Russ. Chem. Bull.* **2020**, 69, 1897–1906.
- [30] J.-E. Siewert, A. Schumann, M. Fischer, C. Schmidt, T. Taeufer, C. Hering-Junghans, *Dalton Trans.* **2020**, 49, 12354–12364.
- [31] P. Plessow, *J. Chem. Theory Comput.* **2013**, 9, 1305–1310.
- [32] a) S. G. Balasubramani, G. P. Chen, S. Coriani, M. Diedenhofen, M. S. Frank, Y. J. Franzke, F. Furche, R. Grotjahn, M. E. Harding, C. Hättig, A. Hellweg, B. Helmich-Paris, C. Holzer, U. Huniar, M. Kaupp, A. M. Khah, S. K. Khani, T. Müller, F. Mack, B. D. Nguyen, S. M. Parker, E. Perlt, D. Rappoport, K. Reiter, S. Roy, M. Rückert, G. Schmitz, M. Sierka, E. Tapavicza, D. P. Tew, C. V. Wüllen, V. K. Voora, F. Weigend, A. Wodyński, J. M. Yu, *J. Chem. Phys.* **2020**, 152, 184107; b) F. Weigend, R. Ahlrichs, *Phys. Chem. Chem. Phys.* **2005**, 7, 3297–3305; c) J. P. Perdew, K. Burke, M. Ernzerhof, *Phys. Rev. Lett.* **1996**, 77, 3865–3868.
- [33] a) J. Gopalakrishnan, *Appl. Organomet. Chem.* **2009**, 23, 291–318; b) J. M. Barendt, E. G. Bent, R. C. Haltiwanger, A. D. Norman, *Inorg. Chem.* **1989**, 28, 2334–2339.
- [34] a) T. L. Chan, Z. Xie, *Chem. Commun.* **2016**, 52, 7280–7283; b) M. M. Olmstead, P. P. Power, G. A. Sigel, *Inorg. Chem.* **1988**, 27, 2045–2049.

Manuscript received: May 13, 2022

Accepted manuscript online: May 20, 2022

Version of record online: July 4, 2022

## **6.4 Deoxygenation of chalcogen oxides $EO_2$ ( $E = S, Se$ ) with phospho-Wittig reagents**

Fabian Dankert, Priyanka Gupta, Tim Wellnitz, Wolfgang Baumann, Christian Hering-Junghans

*Dalton Trans.*, **2022**, 51, 18642

DOI: 10.1039/D2DT03703C

Reprinted (adapted) with permission from *Dalton Trans.*

© The Royal Society of Chemistry 2022

Contribution to this paper is 10%





## PAPER

View Article Online

View Journal



Cite this: DOI: 10.1039/d2dt03703c

Deoxygenation of chalcogen oxides EO<sub>2</sub> (E = S, Se) with phospho-Wittig reagents†Fabian Dankert,  Priyanka Gupta,  Tim Wellnitz, Wolfgang Baumann and Christian Hering-Junghans \*

In here we present the deoxygenation of the chalcogen oxides EO<sub>2</sub> (E = S, Se) with R-P(PMe<sub>3</sub>), so-called phospho-Wittig reagents. The reaction of DABSO (DABCO·2SO<sub>2</sub>) with R-P(PMe<sub>3</sub>) (R = Mes\*, 2,4,6-tBu<sub>3</sub>-C<sub>6</sub>H<sub>2</sub>; <sup>Me</sup>Ter, 2,6-(2,4,6-Me<sub>3</sub>-C<sub>6</sub>H<sub>2</sub>)<sub>2</sub>-C<sub>6</sub>H<sub>3</sub>) resulted in the formation of thiadiphosphiranes (RP)<sub>2</sub>S (**1:R**), while selenadiphosphiranes (RP)<sub>2</sub>Se (**2:R**) were afforded with SeO<sub>2</sub>, both accompanied by the formation of OPMe<sub>3</sub>. Utilizing the sterically more encumbered <sup>Dip</sup>Ter-P(PMe<sub>3</sub>) (<sup>Dip</sup>Ter = 2,6-(2,6-iPr<sub>2</sub>-C<sub>6</sub>H<sub>3</sub>)<sub>2</sub>-C<sub>6</sub>H<sub>3</sub>) a different selectivity was observed and (<sup>Dip</sup>TerP)<sub>2</sub>Se (**2:<sup>Dip</sup>Ter**) along with [Se(μ-P<sup>Dip</sup>Ter)]<sub>2</sub> (**3:<sup>Dip</sup>Ter**) were isolated as the Se-containing species in the reaction with SeO<sub>2</sub>. Interestingly, the reaction with DABSO (or with equimolar ratios of SeO<sub>2</sub> at elevated temperatures) gave rise to the formation of the OPMe<sub>3</sub>-stabilized dioxophosphorane (phosphinidene dioxide) <sup>Dip</sup>TerP(O)<sub>2</sub>-OPMe<sub>3</sub> (**4:<sup>Dip</sup>Ter**) as the main product. This contrasting reactivity can be rationalized by two potential pathways in the reaction with EO<sub>2</sub>: (i) a Wittig-type pathway and (ii) a pathway involving oxygenation of the phospho-Wittig reagents and release of SO. Thus, phospho-Wittig reagents are shown to be useful synthetic tools for the metal-free deoxygenation of EO<sub>2</sub> (E = S, Se).

Received 17th November 2022,  
Accepted 23rd November 2022

DOI: 10.1039/d2dt03703c

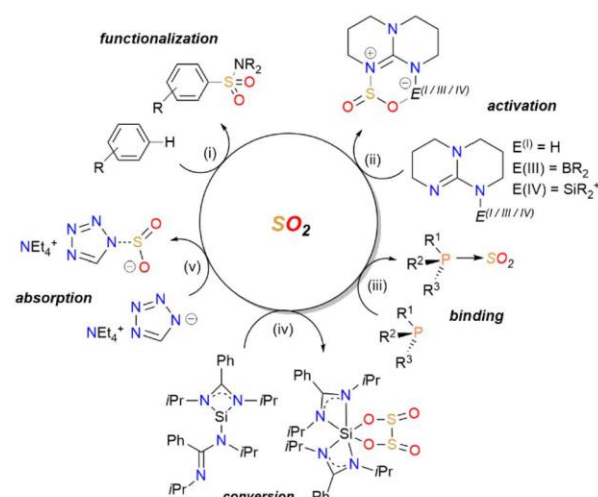
rsc.li/dalton

## Introduction

Sulphur dioxide, SO<sub>2</sub>, is among the main pollutants in the flue gas from the combustion of fossil fuels.<sup>1–3</sup> Most industrial combustion units are scrubbers and typically desulfurization procedures are based on aqueous alkaline solutions and/or various wet-sulfuric-acid processes. A drawback of these techniques is for instance the high amount of wastewater.<sup>4</sup> Flue gas desulfurization requires effective interactions of a certain material with SO<sub>2</sub> and several strategies have been developed to sequester SO<sub>2</sub> at ambient conditions. From the perspective of a main-group chemist, SO<sub>2</sub> binding<sup>5–15</sup> and activation,<sup>16–21</sup> conversion and/or reduction,<sup>22–28</sup> but also sorption<sup>29–33</sup> have been realized.

Furthermore, the functionalization with SO<sub>2</sub> building blocks has been achieved in various small organic molecules over time.<sup>38–43</sup> A selection of recent (yet arbitrarily) examples of SO<sub>2</sub> capture and functionalization are depicted in Scheme 1. Waldvogel and co-workers presented a simple electrochemical

setup for the synthesis of sulfonamides using SO<sub>2</sub>, Hünig's base and activated anisols (Scheme 1, i).<sup>34</sup> With the aid of 1,5,7-triazabicyclo[4.4.0]dec-5-ene (TBD) reversible SO<sub>2</sub> capture



**Scheme 1** Different approaches in SO<sub>2</sub> capture and conversion with main-group compounds (recent examples). (i) HNR<sub>2</sub>, SO<sub>2</sub>, DIPEA, electrochemical setup (see ref. 34); (ii) CD<sub>2</sub>Cl<sub>2</sub> or THF-d<sub>8</sub> frozen solution to ambient temperature;<sup>35</sup> (iii) –78 °C or ambient temperature;<sup>36</sup> THF; (iv) –78 °C to –20 °C;<sup>24</sup> (v) ethylene glycol additive, ambient temperature.<sup>37</sup>

Leibniz Institut für Katalyse e.V. (LIKAT), A.-Einstein-Str.3a, 18059 Rostock, Germany. E-mail: christian.hering-junghans@catalysis.de; <https://www.catalysis.de/forschung/aktivierung-kleiner-molekuele/>

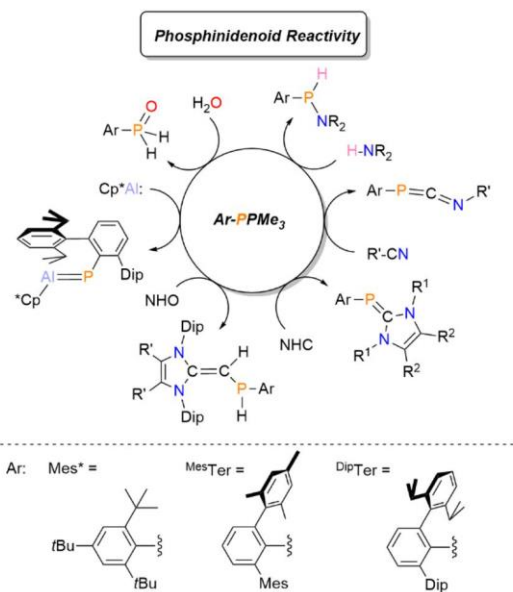
† Electronic supplementary information (ESI) available: Synthesis and characterization of compounds, NMR spectra, crystallographic, and computational details. CCDC 2174939–2174945. For ESI and crystallographic data in CIF or other electronic format see DOI: <https://doi.org/10.1039/d2dt03703c>

## Paper

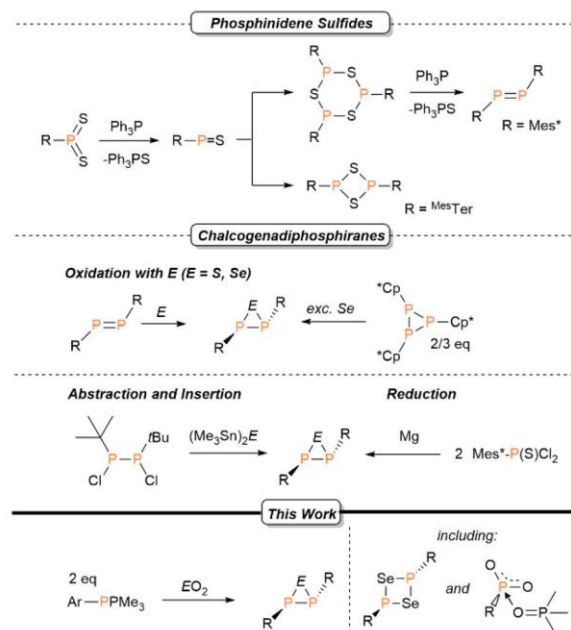
was achieved and could be extended to boryl- and silylium-functionalized TBD systems (Scheme 1, ii).<sup>35</sup> The reactivity of functionalized TBD systems can be classified as FLP-type and follows reports by Erker *et al.* using P/B-,<sup>18</sup> and M/P- (M = Zr, Hf),<sup>44</sup> while Mitzel and co-workers reported a P/Si-FLP capable of SO<sub>2</sub> capture.<sup>45</sup> Investigations on the reduction of SO<sub>2</sub> with phosphines date back to the seminal work of Fluck and Binder in the 1960s,<sup>27,28</sup> though partially very harsh conditions had to be employed to reach oxidation of various phosphines. SO<sub>2</sub> binding and conversion under mild conditions with electron-rich phosphanes was realized by Dielmann and co-workers just recently (Scheme 1, iii).<sup>36</sup> The reaction of highly nucleophilic, predominantly imidazolin-2-imine substituted phosphanes were found to yield stable R<sub>3</sub>P → SO<sub>2</sub> adducts, which were further converted into a mixture of phosphine-oxides, -sulfides and R<sub>3</sub>P → SO<sub>3</sub> adducts. Theoretical studies point to the intermediate formation of sulfur monoxide SO in these reactions, which disproportionates into S and SO<sub>2</sub>. Using bis(guanidinato)silylenes the reaction with SO<sub>2</sub> in hexane resulted in the formation of a six-coordinate sulfitosilicon(IV) species whereas in liquid SO<sub>2</sub> a dithionosilicon(IV) complex was obtained, in which S–S-coupling was achieved (Scheme 1, iv).<sup>46</sup> The potential of ionic liquids in SO<sub>2</sub> capture has been thoroughly investigated. For example, using tetraethylammonium tetrazolate and ethylene glycol at a molar ratio of 1 : 2, effective SO<sub>2</sub> capture at low SO<sub>2</sub> concentrations was documented (Scheme 1, v).<sup>37</sup>

In our group we are interested in the reactivity of phosphanylidene-σ<sup>4</sup>-phosphoranes, R-P(PMe<sub>3</sub>), also termed as phospho-Wittig reagents.<sup>47</sup> These compounds can be classified as “masked” phosphinidenes, showing phosphinidenoid reactivity upon PMe<sub>3</sub> release. We have demonstrated the facile NH<sup>−</sup><sub>4</sub> as well as OH-bond<sup>49</sup> activation at the P(i) center as well as the cleavage of the terminal C(sp<sup>2</sup>)-H bonds of N-heterocyclic olefins (NHO) to give P-substituted NHOs.<sup>50</sup>

Utilizing phospho- and arsa-Wittig reagents as pnictinidene transfer reagents, phospho- as well as arsaaluminenes<sup>51</sup> – compounds showing E<sup>13</sup>-E<sup>15</sup> multiple bonding<sup>52</sup> – could be generated in the reaction with (Cp\*Al)<sub>4</sub> (Scheme 2). The initially published key reactivity of these systems, however, mainly focused on the phospho-Wittig type reactivity towards aldehydes.<sup>53</sup> Aldehydes can be deoxygenated forming various phosphoalkenes (with a P=C double bond) in *E*-selective fashion. The driving force for these reactions is the formation of PMe<sub>3</sub>O making R-P(PMe<sub>3</sub>) effective deoxygenation reagents. Furthermore, the dicoordinate phosphanylidene P atom is electron-rich, akin to the imidazolin-2-imine substituted phosphanes reported to effectively bind SO<sub>2</sub>.<sup>36</sup> The diverse phospho-Wittig reactivity and the electron-rich character of R-P(PMe<sub>3</sub>) prompted us to examine the reactivity of such systems towards chalcogen oxides and elucidate whether SO<sub>2</sub> (and also SeO<sub>2</sub>) can be deoxygenated. This might give access to a variety of PCh-species (Ch = S, Se), among them the oligomers of phosphinidene chalcogenides R-PCh,<sup>54</sup> phosphinidene dichalcogenides R-PCh<sub>2</sub>,<sup>55–57</sup> and three-membered chalcogenadiphosphiranes R-P(Ch)P-R (Scheme 3, top). In general, the oxi-



Scheme 2 Phospho-Wittig reagents as phosphinidene precursors and their diverse reactivity toward selected nucleophiles.



Scheme 3 Pathways for the generation of phosphinidene sulfides (top) and various routes for the generation of thia- and selenadiphosphiranes (middle) and summary of this study.

dation of diphosphenes with elemental sulphur (or selenium) is the most established route to synthesize P<sub>2</sub>Ch (Ch = S, Se) rings (Scheme 3).<sup>58–66</sup> A handful of other routes have also been reported,<sup>67–71</sup> among them a combined dechlorination–elementation strategy using (Me<sub>3</sub>Sn)<sub>2</sub>E and (tBuPCL)<sub>2</sub> to access (tBuP)<sub>2</sub>E (E = S, Se) (Scheme 3, middle).<sup>72</sup> In here we show that



phospha-Wittig reagents reduce SO<sub>2</sub> (and SeO<sub>2</sub>) under mild conditions to form a series of thia- and selenadiphosphiranes as the main products (Scheme 3, bottom).

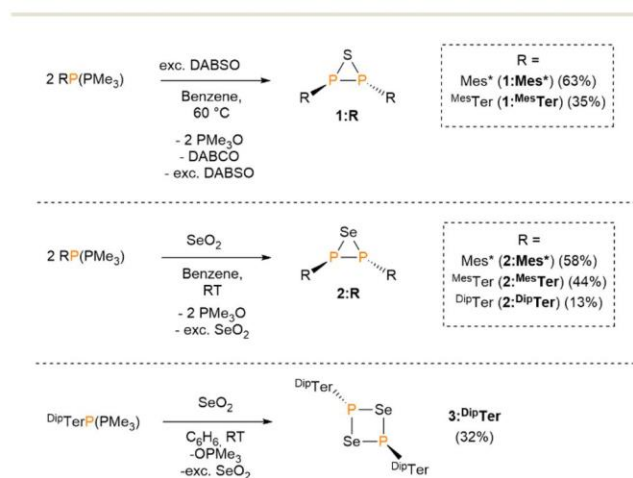
## Results and discussion

We started to investigate the reactivity of phospho-Wittig reagents towards EO<sub>2</sub> (E = S, Se) and chose DABSO (DABCO·2SO<sub>2</sub>) as a safe surrogate for SO<sub>2</sub>. The adduct is bench-top stable and stoichiometric amounts of SO<sub>2</sub> can thus be generated.<sup>73</sup> Conversion of R-P(PMe<sub>3</sub>) (R = Mes\*, 2,4,6-*t*Bu<sub>3</sub>-C<sub>6</sub>H<sub>2</sub>; Mes\*Ter, 2,6-(2,4,6-Me<sub>3</sub>-C<sub>6</sub>H<sub>2</sub>)<sub>2</sub>-C<sub>6</sub>H<sub>3</sub>) with 1 eq. of SO<sub>2</sub> (0.5 eq. of DABSO) yielded a brown solution at first which decolourised upon heating to 60 °C overnight. NMR spectroscopic investigation showed a single resonance at −66.01 ppm in the <sup>31</sup>P{<sup>1</sup>H} NMR spectrum (R = Mes\*) along with the presence of OPMe<sub>3</sub> (δ(<sup>31</sup>P) ≈ 30 ppm, δ(<sup>1</sup>H) = 0.87) (Scheme 4, top). Recrystallization of the crude product from a MeCN/benzene solution at 6 °C yielded crystals suitable for single crystal X-ray diffraction (SC-XRD) analysis, which revealed the formation of the thiadiphosphirane (Mes\*P)<sub>2</sub>S (**1:Mes\***), which was first described by Yoshifuji *et al.* in the reduction of Mes\*P(S)Cl<sub>2</sub>

with Mg.<sup>74</sup> The same observation was made for the conversion of Mes\*Ter-P(PMe<sub>3</sub>) with one equivalent of SO<sub>2</sub>, which revealed a single resonance at −112.53 ppm in the <sup>31</sup>P{<sup>1</sup>H} NMR spectrum (Scheme 3, top). Recrystallization from a hot MeCN solution yielded colourless needles suitable for SC-XRD experiments and verified the formation of the related, yet novel thiadiphosphirane (Mes\*TerP)<sub>2</sub>S (**1:Mes\*Ter**). The P–P bond length of 223.42(8) pm in **1:Mes\***,<sup>75</sup> and equal P–S atom distances of 211.45(10) pm indicate a C<sub>2</sub> symmetric structure in the solid state. Tilting of the P<sub>2</sub>S moiety causes disorder in the crystal structure of **1:Mes\*Ter**. This precludes a detailed discussion of bond lengths, which nevertheless are similar to those in **1:Mes\***. The atom distances and angles detected in **1:R** (R = Mes\*, Mes\*Ter; Table 1) are in agreement with known thiadiphosphiranes (*cf.* (Fc'-P)<sub>2</sub>S;<sup>76</sup> P–P = 219.03(12); P–S = 212.81(13)–213.48(13) pm; Fc' = 2,5-bis(3,5-*t*Bu<sub>2</sub>-C<sub>6</sub>H<sub>3</sub>)-ferrocenyl). In seemingly similar manner, the deoxygenation and thus reduction of SeO<sub>2</sub> with R-P(PMe<sub>3</sub>) (R = Mes\*, Mes\*Ter) is accomplished at ambient temperature and selenadiphosphiranes are obtained (Scheme 4, middle). After workup, the <sup>31</sup>P{<sup>1</sup>H} NMR spectra show singlet resonances at −49.12 ppm (**2:Mes\***) and −100.39 ppm (**2:Mes\*Ter**). Furthermore, characteristic triplets are observed at 43.1 (**2:Mes\***) and −90.4 (**2:Mes\*Ter**) ppm in the <sup>77</sup>Se{<sup>1</sup>H} NMR spectra with <sup>1</sup>J<sub>PSe</sub> coupling constants of 138.6 and 114.8 Hz, respectively (Table 1). The <sup>77</sup>Se{<sup>1</sup>H} NMR shift differs significantly in **2:R**, but the detected values are in the range expected for selenadiphosphiranes (*cf.* δ(<sup>77</sup>Se) (2,4,6-CF<sub>3</sub>-C<sub>6</sub>H<sub>2</sub>)<sub>2</sub>P<sub>2</sub>Se<sup>63</sup> 127.8 (<sup>1</sup>J<sub>PSe</sub> = 135 Hz); (IDipCPh)<sub>2</sub>P<sub>2</sub>Se<sup>58</sup> −24.3 ppm (<sup>1</sup>J<sub>PSe</sub> = 74 Hz)) and are supported by the characteristic <sup>1</sup>J<sub>PSe</sub> coupling constants. Moreover, DFT studies showed theoretical <sup>77</sup>Se NMR shifts for **2:Mes\*** (δ<sub>calc</sub>(<sup>77</sup>Se) 35.5 ppm) and **2:Mes\*Ter** (δ<sub>calc</sub>(<sup>77</sup>Se) −98.1 ppm), which were in good agreement with the experimental values.<sup>75</sup> Even though Yoshifuji reported the synthesis of **2:Mes\*** in the reaction of (Mes\*P)<sub>2</sub> with elemental selenium,<sup>65</sup> no crystal structure was reported to date. In the herein provided crystal structures of **1:R** as well as of **2:R** the organic ligand frameworks are arranged *trans* to each other with respect to the P<sub>2</sub> unit.

Both species **2:R** show C–P–P angles of around 106°, demonstrating that similar arrangements for both substituent environments, Mes\* and Mes\*Ter, are favourable (Fig. 1).

All other metrics agree with known thia- and selenadiphosphiranes.<sup>58–66</sup> A notable side-reaction for the syn-



**Scheme 4** Synthesis of thia- (**1:R**) and selenadiphosphiranes (**2:R**) from phospho-Wittig reagents and DABSO (top) and SeO<sub>2</sub> (middle). Synthesis of **3:DipTer** from DipTer-P(PMe<sub>3</sub>) and 1 eq. SeO<sub>2</sub> (bottom).

**Table 1** <sup>31</sup>P{<sup>1</sup>H} and <sup>77</sup>Se{<sup>1</sup>H} NMR shifts, along with <sup>1</sup>J<sub>PSe</sub> coupling constants and selected bond lengths [Å] and angles [°] of compounds **1:R**, **2:R** and four-membered species **3:DipTer** as well as of the literature known species [Se(μ-P<sup>Mes\*Ter</sup>)<sub>2</sub>]<sup>55</sup>

Compound	δ <sup>31</sup> P{ <sup>1</sup> H} <sup>a</sup>	δ <sup>77</sup> Se{ <sup>1</sup> H} <sup>a</sup>	d (P–P) <sup>b</sup>	d (P–E) <sup>b</sup>	<P–E–P <sup>c</sup>
<b>1:Mes*</b>	−66.0		223.42(8)	211.45(10)	63.783(22)
<b>1:Mes*Ter</b>	−112.5		218.7(26)	211.1(15)/212.4(13)	62.17(52)
<b>2:Mes*</b>	−49.1	43.1 <sup>1</sup> J <sub>PSe</sub> = 138.6 Hz	225.02(8)	226.14(6)	59.673(17)
<b>2:Mes*Ter</b>	−100.4	−90.4 <sup>1</sup> J <sub>PSe</sub> = 114.8 Hz	219.85(17)	227.05(10)/227.01(13)	57.919(41)
<b>2:DipTer</b>	−86.8	−13.1 <sup>1</sup> J <sub>PSe</sub> = 117.5 Hz	223.30(25)	226.26(19)/225.61(16)	59.230(61)
<b>3:DipTer</b>	70.1	−22.7 <sup>1</sup> J <sub>PSe</sub> = 14.1 Hz	323.78(7)	228.02(5)/228.20(5)	90.420(18)
[Se(μ-P <sup>Mes*Ter</sup> ) <sub>2</sub> ] <sup>55</sup>	23.1	484.6 <sup>1</sup> J <sub>PSe</sub> = 45.9 Hz	302.59(20)	2.3113(14)/2.3060(16)	82.17(6)/82.06(5)

<sup>a</sup> Chemical shifts given in ppm. <sup>b</sup> Atomic distances in pm. <sup>c</sup> Angles in °.

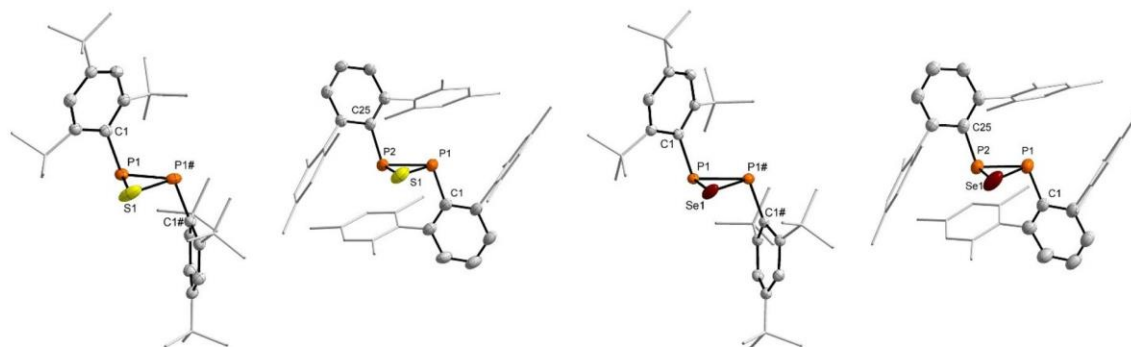


**Fig. 1** Molecular structures of **1:R** (left) and **2:R** (right) in the crystal ( $R = \text{Mes}^*, \text{MesTer}$ ). Ellipsoids drawn at 50% with C–H-atoms omitted and tBu- and Mes-groups rendered as wire-frame for clarity. Atoms depicted with # are symmetry generated over  $1 - x, y, 3/2 - z$ . Selected bond lengths [pm] and angles [°] (from left to right): **1:Mes\***: P1–P1# 223.42(8), C1–P1 188.33(18), P1–S1 211.45(10), P1–S1–P1# 63.783(22), S1–P1–P1# 58.108(20), C1–P1–S1 99.748(62), C1–P1–P1# 106.622(66); **1:MesTer**: P1–P2 218.7(26), P1–S1 211.1(15), C1–P1 187.5(13), P2–S1 212.4(13), C25–P2 186.6(15), P1–S1–P2 62.17(52), S1–P1–P2 59.18(53), C1–P1–S1 101.72(57), C25–P2–P1 105.57(65), C25–P2–S1 102.80(63); **2:Mes\***: P1–P1# 225.02(8), C1–P1 188.12(18), P1–Se1 226.14(6), P1–Se1–P1# 59.673(17), Se1–P1–P1# 60.163(18), C1–P1–Se1 99.599(58), C1–P1–P1# 105.988(64); **2:MesTer**: P1–P2 219.85(17), P1–Se1 227.01(13), C1–P1 186.95(38), P2–Se1 227.05(10), C25–P2 186.33(37), P1–Se1–P2 57.919(41), Se1–P1–P2 61.050(42), C1–P1–Se1 100.79(11), C25–P2–P1 105.18(10), C25–P2–S1 102.47(10).

thesis of **2:Mes\*** can be observed, when the stoichiometry is *ca.* 1 eq. of  $\text{SeO}_2$  and the solution is heated up while being sonicated. A green rather than colourless solution is obtained on this occasion and, according to  $^{31}\text{P}$  NMR spectroscopy, this side product can be observed at around 270 ppm in the  $^{31}\text{P}$  NMR spectrum. According to previous reports by Yoshifuji<sup>65</sup> and Tokitoh,<sup>76</sup> this green side product is assigned to the diselenophosphorane  $\text{Mes}^*\text{PSe}_2$  ( $\delta(^{31}\text{P}\{^1\text{H}\}) = 273$  ppm). For comparison see also  $\text{BbtPSe}_2$  ( $\delta(^{31}\text{P}\{^1\text{H}\}) = 273$  ppm; Bbt = 2,6-bis[bis(trimethylsilyl)-methyl]-4-[tris(trimethylsilyl)-methyl]phenyl). Unfortunately, our efforts to crystallize this compound failed so far, but the formation of  $\text{Mes}^*\text{PSe}_2$  hints at the formation of elemental selenium in this reaction.

Surprisingly, treatment of  $\text{DipTerP}(\text{PMe}_3)$  with 0.5 eq. of  $\text{SeO}_2$  at room temperature resulted in a mixture of products of which the expected selenadiphosphirane ( $\text{DipTerP})_2\text{Se}$  (**2:DipTer**) was obtained after recrystallization from MeCN/benzene in the form of X-ray quality crystals (isolated yield

13%). Isolated **2:DipTer** showed a resonance at  $-87$  ppm in the  $^{31}\text{P}\{^1\text{H}\}$  NMR spectrum and a  $^{77}\text{Se}$  NMR signal as a characteristic triplet at  $-13.1$  ppm with  $^1J_{\text{PSe}} = 117.5$  Hz, in line with the  $^{77}\text{Se}$  satellites detected in the  $^{31}\text{P}\{^1\text{H}\}$  NMR spectrum. In the  $^1\text{H}$  NMR spectrum of **2:DipTer** two sets of signals are detected for the  $\text{DipTer}$ -moiety indicating hindered rotation in solution. The molecular structure showed the expected  $\text{P}_2\text{Se}$  cyclic core with P–Se atom distances of 226.26(19) pm and a P–P atom distance of 223.30(25) pm (Fig. 2, left), in good agreement with the values found for **2:R** ( $R = \text{Mes}^*, \text{MesTer}$ ) and various selenadiphosphiranes with bulky substituents on phosphorus (*cf.*  $(\text{Bbt-P})_2\text{Se}$ ;  $d(\text{P–P}) = 223.9(4)–225.0(3)$  pm,  $d(\text{P–Se}) = 225.0(3)–227.0(3)$  pm).<sup>76</sup> Interestingly, the crude reaction mixture after conversion of  $\text{DipTer-P}(\text{PMe}_3)$  with 1 eq.  $\text{SeO}_2$  at room temperature overnight revealed another resonance in the  $^{31}\text{P}\{^1\text{H}\}$  NMR spectrum at 70 ppm, shifted towards lower field excluding a selenadiphosphirane or diselenophosphorane (Scheme 4, bottom).

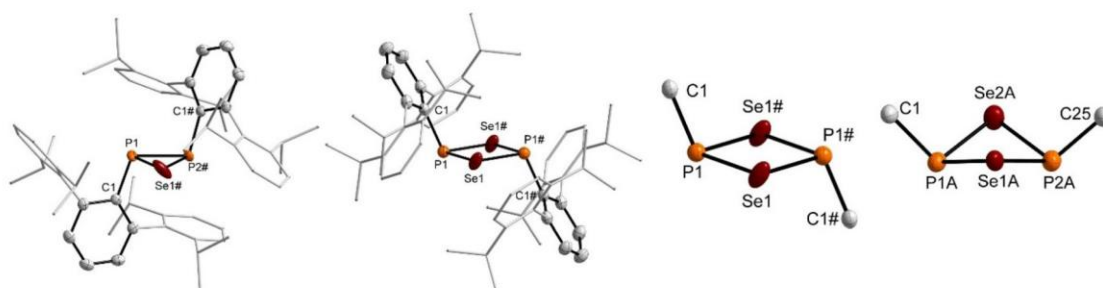


**Fig. 2** Molecular structures of **2:DipTer** and **3:DipTer** in the crystal (left) and cut-out of the C–P<sub>2</sub>Se<sub>2</sub>–C fragments of **3:DipTer** and previously published  $[\text{Se}(\mu\text{-P}^{\text{MesTer}})_2]$  (right).<sup>55</sup> Ellipsoids drawn at 50% with C–H-atoms omitted and Dip-groups rendered as wire-frame for clarity. Selected bond lengths [pm] and angles [°]: **2:DipTer**: C1–P1 186.29(24), P1–P2# 223.30(25), P1–Se1# 226.26(19), P2#–Se1# 225.61(16), C1–P1–Se1# 95.867(82), C1–P1–P2# 109.226(93); **3:DipTer**: C1–P1 184.70(19), P1...P2 323.78(7), Se1...Se1# 321.42(4), P1–Se1 228.02(5), C1–P1–Se1 105.942(62);  $[\text{Se}(\mu\text{-P}^{\text{MesTer}})_2]$ :<sup>55</sup> C1–P1A 184.60(36), P1A–Se1A 231.03(19), P1A–Se2A 230.60(13), Se1A...Se2A 323.40(15), P1A...P2A 302.59(20), P2A–C25 185.45(65), P2A–Se1A 229.34(13), P2A–Se2A 230.24(16).

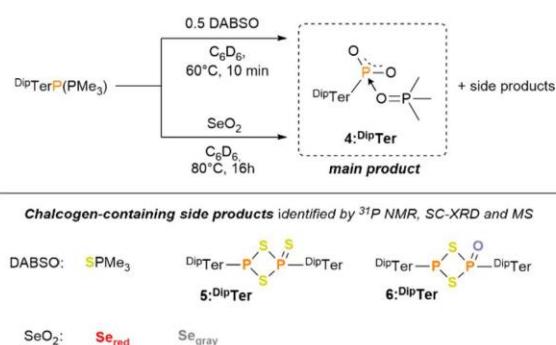


Tuononen, Ragogna and co-workers have recently reported on four-membered rings of the general formula  $[\text{Ch}(\mu\text{-P}^{\text{Mes}}\text{Ter})_2]$  ( $\text{Ch} = \text{S}, \text{Se}$ ),<sup>55</sup> with the  $^{31}\text{P}$  NMR shift of the Se species at 23.1 (Table 1) and the S species at 126.4 ppm, suggesting that the species detected at 70 ppm corresponded to  $[\text{Se}(\mu\text{-P}^{\text{Dip}}\text{Ter})_2]$  (**3:DipTer**). **3:DipTer** could be isolated by adding a MeCN/*n*-hexane mixture (1:4 ratio) to the crude product. After phase separation the MeCN phase was discarded, and the *n*-hexane phase was worked-up. After removal of the solvent, recrystallization of the residue from benzene at 6 °C verified our assumption of a four membered  $\text{P}_2\text{Se}_2$  ring within  $[\text{Se}(\mu\text{-P}^{\text{Dip}}\text{Ter})_2]$  (**3:DipTer**) (Scheme 4, bottom), which was isolated as a yellow crystalline solid (isolated yield 32%). The  $^{77}\text{Se}$  NMR shift of  $[\text{Se}(\mu\text{-P}^{\text{Mes}}\text{Ter})_2]$  was determined at 484.6 ppm as a triplet with  $^1J_{\text{PSe}} = 45.9$  Hz.<sup>55</sup>

However, the  $^{77}\text{Se}$  NMR chemical shift of **3:DipTer** at  $-22.70$  ppm with a  $^1J_{\text{PSe}}$  coupling constant of 14.1 Hz did not match the values reported for  $[\text{Se}(\mu\text{-P}^{\text{Mes}}\text{Ter})_2]$ , with structural differences most likely causing the discrepancies in the  $^{77}\text{Se}$  NMR chemical shift. Determination of the molecular structure of **3:DipTer** showed that the organic ligands were oriented *trans* to each other, whereas a *cis* orientation is present in  $[\text{Se}(\mu\text{-P}^{\text{Mes}}\text{Ter})_2]$  (Fig. 2). Second, the  $\text{P}_2\text{Se}_2$  moiety in **3:DipTer** is planar compared to the butterfly-shaped central  $\text{P}_2\text{Se}_2$ -ring in  $[\text{Se}(\mu\text{-P}^{\text{Mes}}\text{Ter})_2]$  (folded along the Se–Se axis by *ca.* 45°). The experimental  $^{77}\text{Se}$  chemical shifts were in reasonable agreement with the theoretical values obtained at the PBE0-D3/def2-TZVP//PBE0-D3/def2-SVP level of theory for  $[\text{Se}(\mu\text{-P}^{\text{Mes}}\text{Ter})_2]$  ( $\delta_{\text{calc}}(^{77}\text{Se})$  401.0 ppm) and **3:DipTer** ( $\delta_{\text{calc}}(^{77}\text{Se})$   $-98.3$  ppm).<sup>75</sup> Hence, we show that ligand conformation as well as the positioning of the Se atoms within P<sub>2</sub>Se<sub>2</sub>-heterocycles can significantly alter the  $^{77}\text{Se}$  NMR chemical shift.

Interestingly,  $\text{DipTer-P}(\text{PMe}_3)$  bearing the bulkier  $\text{DipTer}$ -substituent ( $\text{DipTer} = 2,6\text{-}(2,6\text{-iPr}_2\text{-C}_6\text{H}_3)_2\text{-C}_6\text{H}_3$ ), showed a unique reactivity towards DABSO as a different deoxygenation product was obtained in this case and (partially) characterized. We first treated  $\text{DipTer-P}(\text{PMe}_3)$  with DABSO at 60 °C in  $\text{C}_6\text{D}_6$  solution (Scheme 5), which after 10 min afforded a crude product mixture showing two doublets in the  $^{31}\text{P}\{^1\text{H}\}$  NMR spectrum

as the main component at 74.7 ppm and 11.7 ppm (Fig. S42†) with a  $J_{\text{PP}}$  coupling constant of 18.6 Hz, not in line with the singlet resonances of thiadiphosphiranes **1:R** (*vide supra*). Upon proton coupling, the doublet at 74.7 ppm split into a decett of doublets in the  $^{31}\text{P}$  NMR spectrum, indicating the presence of a  $\text{PMe}_3$ -containing moiety. The same species was obtained when  $\text{DipTer-P}(\text{PMe}_3)$  was treated with 1 eq. of  $\text{SeO}_2$  and the mixture was heated to 80 °C overnight (Fig. S43†). After removal of the solvent and recrystallization of the crude reaction mixture from toluene at  $-30$  °C, few crystals suitable for SC-XRD experiments were obtained (see chapter 3.7 in the ESI†), which revealed that  $[(\text{DipTerPO}_2)\text{OPMe}_3]$  (**4:DipTer**) had formed (Fig. 3). **4:DipTer** can be classified as  $\text{OPMe}_3$ -stabilized dioxophosphorane, or phosphinidenedioxide. Species of the general formula  $\text{R-PO}_2$  are generally prone to oligomerize giving cyclic oligophosphonates of the formula  $(\text{R-PO}_2)_n$ ,<sup>77</sup> which can be thermally treated to give inorganic polymers with a  $\text{P}^{\text{V}}\text{-O}$  main chain.<sup>78</sup> Very recently, the dimer of  $\text{DipTerPO}_2$ ,  $[\text{DipTerPO}_2]_2$ , a lighter congener of Lawssons<sup>79</sup> and Woolins reagents,<sup>80</sup> respectively, was reported.<sup>81</sup> Moreover, the parent phenylphosphinidenedioxide  $\text{PhPO}_2$  could be trapped in an argon matrix and characterized by means of vibrational spectroscopy.<sup>82</sup> The central P atom of **4:DipTer** is highly Lewis acidic, according to NBO analyses with a natural charge of 2.35 and a net charge transfer from  $\text{OPMe}_3$  of  $0.3e$  to the  $\text{DipTerPO}_2$  unit. With 146.41(19) and 147.21(17) pm the P1–O1/O2 atom distances are similar to those in the related, DMAP-stabilized phosphinidene dioxide  $[(\text{DipTerPO}_2)\text{DMAP}]$  ( $\text{P-O} = 147.38(8)$ , 147.81(8) pm).<sup>81</sup> The P1–O3 atom distance is considerably larger at 169.03(13) pm, which is a comparably long P–O–P bridging bond (*cf.*  $[\text{Ph-P}(\text{O})_2]_6$ ;  $\text{O}(\text{P-O}) = 160.1$  pm)<sup>78</sup> but still matches the covalent P–O single bond covalent radius of 174 pm.<sup>83</sup> The Wiberg bond index of the P1–O3 bond of 0.45 is indicative of dative bonding, which is further supported by the sum of angles at P1 ( $\sum\langle\text{P1}\rangle = 342.91^\circ$ ), indicating only a minimally perturbed  $\text{DipTerPO}_2$  unit, in line with  $[(\text{RPO}_2)\text{DMAP}]$  ( $\text{R} = \text{Ph}, \text{Mes}$ )<sup>75</sup> and  $(\text{DipTerPO}_2)\text{DMAP}$ . According to



**Scheme 5** Reactivity of  $\text{DipTer-P}(\text{PMe}_3)$  towards DABSO, yielding **4:DipTer** and side-products, which were examined by  $^{31}\text{P}$  NMR spectroscopy, SC-XRD and MS experiments.

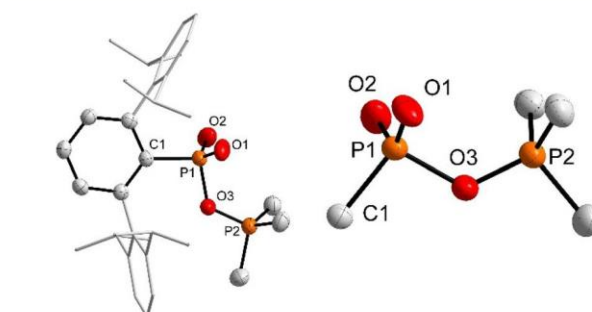


**Fig. 3** Molecular structure of **4:DipTer** in the crystal (left) and cutout of the  $\text{C-P}(\text{O})_2\text{-OPMe}_3$  fragment (right). Ellipsoids drawn at 50% with solvent molecules and C–H-atoms omitted as well as Dip-groups rendered as wire-frame for clarity. Selected bond lengths [pm] and angles [°]: C1–P1 182.42(17), O1–P1 146.41(19), O2–P1 147.21(17), O3–P1 169.03(13), O2–P2 152.00(14), C1–P1–O3 101.33(8), P1–O3–P2 125.84(9).



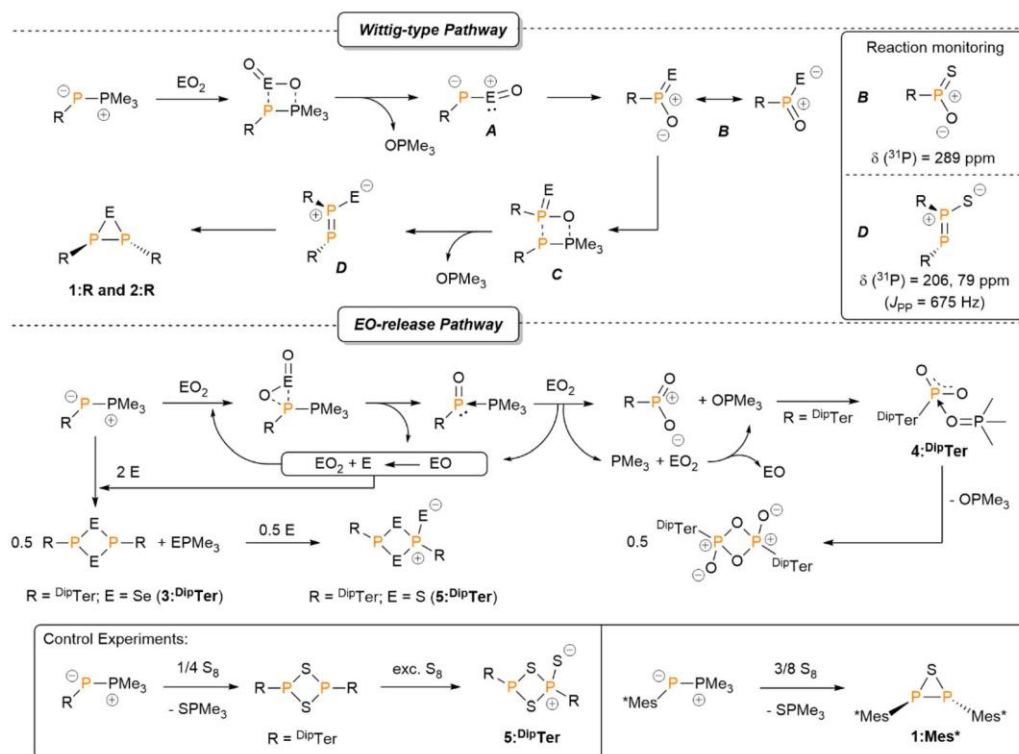
## Paper

second order perturbation analysis the bonding between  $\text{OPMe}_3$  and  $\text{DipTerPO}_2$  is best described as interaction of a  $\text{sp}^{2.8}$  lone pair of electrons on O3 with a p-type vacancy on P1, resulting in a stabilization energy of  $239.03 \text{ kcal mol}^{-1}$ . Unfortunately, the characterization of **4:DipTer** was restricted to X-ray, NMR and mass spectrometric (MS) investigations, due to its rather labile nature and the presence of by-products.

The formation of **4:DipTer** suggested that in the case of  $\text{DipTerP}(\text{PMe}_3)$  the reaction with  $\text{EO}_2$  proceeded differently than with  $\text{RP}(\text{PMe}_3)$  ( $\text{R} = \text{Mes}^*, \text{Mes}^*\text{Ter}$ ). It seemed puzzling that no sulfur or selenium containing species were observed. Close inspection of the  $^{31}\text{P}$  NMR spectrum of the reaction mixture of  $\text{DipTerP}(\text{PMe}_3)$  with 1 eq. of  $\text{SO}_2$  (0.5 eq. DABSO) showed that beside the major doublets for **4:DipTer** a variety of minor signals between 40 and 5 ppm were observed. One of these species was identified as  $\text{SPMe}_3$  with a characteristic  $^{31}\text{P}$  NMR shift of 27.2 ppm.<sup>84</sup>

Two sets of doublets at 38.6 and 16.1 ppm, and 12.6 and 5.1 ppm, respectively, indicated the formation of two unsymmetric species containing two different phosphorus environments, respectively. A singlet signal at 17.4 ppm was assigned to  $[\text{DipTerPO}_2]_2$ ,<sup>81</sup> which should form upon release of  $\text{OPMe}_3$  from **4:DipTer**. Work-up of the crude product mixture (see chapter 3.8 in the ESI†) and recrystallization from toluene at  $-78^\circ\text{C}$  gave platelet-shaped single crystals beside crystals of  $\text{OPMe}_3$ . SC-XRD experiments revealed a compound of the general formula  $(\text{DipTerP})_2\text{S}_{3-x}\text{O}_x$  with a four-membered  $\text{P}_2\text{E}_2$ -

ring as well as one of the P atoms being oxidized further, as derived from a preliminary, purposely not CCDC-deposited, structural model (see Fig. S8†). The respective individual molecular components are present with different occupancies in combination with disorder around a crystallographically imposed center of inversion. Using ESI<sup>+</sup> MS the conclusions drawn from the SC-XRD experiment were partially verified and agreed with the side-products observed by  $^{31}\text{P}$  NMR spectroscopy as three components were identified:  $\text{DipTerP}(\text{O})(\mu_2\text{-O})(\mu_2\text{-S})\text{P}^{\text{DipTer}}$  or  $\text{DipTerP}(\text{S})(\mu_2\text{-O})(\mu_2\text{-O})\text{P}^{\text{DipTer}}$ ,  $\text{DipTerP}(\text{O})(\mu_2\text{-S})(\mu_2\text{-S})\text{P}^{\text{DipTer}}$  or  $\text{DipTerP}(\text{S})(\mu_2\text{-O})(\mu_2\text{-S})\text{P}^{\text{DipTer}}$  and  $\text{DipTerP}(\text{S})(\mu_2\text{-S})(\mu_2\text{-S})\text{P}^{\text{DipTer}}$  (**5:DipTer**). Furthermore, with  $\text{DipTerP}(\text{OH})(\mu_2\text{-O})(\text{OH})\text{P}^{\text{DipTer}}$  a fourth species was detected, which is most likely a hydrolysis product due to acidic MS conditions, though (Fig. S46–S49†). Theoretical studies on the potential isomers of  $[\text{DipTer}_2\text{P}_2\text{S}_2\text{O}]$  and on **5:DipTer** allowed to determine their respective theoretical  $^{31}\text{P}$  NMR shifts, which clearly showed that the doublets at 38.6 and 16.1 ppm ( $\delta_{\text{calc}}(^{31}\text{P}) = 59.3, 29.4 \text{ ppm}$ ) in the  $^{31}\text{P}$  NMR spectrum of the reaction mixture can be attributed to **5:DipTer** and the doublets and 12.6 and 5.1 ppm ( $\delta_{\text{calc}}(^{31}\text{P}) = 30.0, 22.1 \text{ ppm}$ ) were assigned to  $\text{DipTerP}(\text{O})(\mu_2\text{-S})(\mu_2\text{-S})\text{P}^{\text{DipTer}}$  (**6:DipTer**). Taking these observations into account the surprising formation of **4:DipTer** as the major product can be rationalized by initial oxygenation of  $\text{DipTerP}(\text{PMe}_3)$  by  $\text{SO}_2$  and tentatively the release of metastable SO (Scheme 6, bottom; EO-release pathway). SO then disproportionates in solution to give S and  $\text{SO}_2$ .<sup>85–87</sup> An independent



**Scheme 6** Proposed pathways for the formation of **1:R** and **2:R** via a Wittig-type reaction (top) and rationalization of the formation of **4:DipTer** via an EO-release pathway (bottom).



reaction of  $\text{DipTer-P}(\text{PMe}_3)$  with 2 eq. of elemental sulfur clearly showed the formation of  $\text{SPMe}_3$  and  $[\text{S}(\mu\text{-P}^{\text{DipTer}})_2]$  ( $\delta(^{31}\text{P}) = 142.6$  ppm) (Fig. S52†), the sulfur congener of  $3\text{:DipTer}$ . Treatment of  $3\text{:DipTer}$  with an excess of sulfur (>2 eq.) indicated formation of  $5\text{:DipTer}$ , providing another hint that elemental sulfur is responsible for the formation of  $\text{SPMe}_3$  and  $5\text{:DipTer}$  (Fig. S53†). Having established the sulfur-containing by-products we next turned our attention to the reaction of  $\text{DipTer-P}(\text{PMe}_3)$  with  $\text{SeO}_2$  and noted the formation of a reddish precipitate, which was assumed to be red selenium. This was verified by isolation of the red residue and subsequent reaction with  $\text{PPh}_3$  in  $\text{C}_6\text{D}_6$ . This afforded a mixture of  $\text{SePPh}_3$  and  $\text{OPPh}_3$  (2.3 : 1) after heating to 80 °C over a period of 24 h. Hence, the red residue indeed contained elemental selenium (presumably a mixture of  $\text{Se}_{(\text{red})}$  and  $\text{Se}_{(\text{gray})}$ ) as well as minor  $\text{SeO}$ -species (indicated by the formation of  $\text{OPPh}_3$ , see Fig. S50†).

In order to better understand why the reaction of  $\text{R-P}(\text{PMe}_3)$  ( $\text{R} = \text{Mes}^*, {}^{\text{Mes}}\text{Ter}$ ) afforded the thiadiphosphiranes **1:R** as the major products, the reaction of  $\text{Mes}^*\text{-P}(\text{PMe}_3)$  and 0.5 eq. DABSO was followed by  $^{31}\text{P}$  NMR spectroscopy at room temperature over a period of 5 h. Over this period characteristic intermediates could be observed. A signal at 285 ppm was assigned to the mixed dichalcogenaphosphorane  $\text{Mes}^*\text{P}(\text{S})\text{O}$  (cf.  $\text{Mes}^*\text{PS}_2$   $\delta(^{31}\text{P}) = 298$  ppm), which should be more shielded compared to  $\text{Mes}^*\text{PS}_2$  according to theoretical studies ( $\delta_{\text{calc}}(^{31}\text{P})$   $\text{Mes}^*\text{PS}_2$  349.4;  $\text{Mes}^*\text{P}(\text{S})\text{O}$  250.3 ppm).<sup>56</sup> Moreover, a set of doublets at 208 and 66 ppm ( $J_{\text{PP}} = 670$  Hz) indicated a species with a direct P–P bond, which was assigned to  $\text{Mes}^*\text{P}=\text{P}(\text{S})\text{Mes}^*$ , in which the  $\text{Mes}^*$ -substituents are *cis*-oriented (cf. *trans*- $\text{Mes}^*\text{P}=\text{P}(\text{S})\text{Mes}^*$   $\delta(^{31}\text{P}) = 255.8, 247.8$  ppm;  $J_{\text{PP}} = 629.9$  Hz).<sup>66</sup> A second set of doublets at 195 and 28 ppm ( $J_{\text{PP}} = 30$  Hz) indicated the formation of species comprising two P atoms and was assigned to the  $\text{OPMe}_3$  (or possibly also  $\text{SPMe}_3$ ) adduct of  $\text{Mes}^*\text{P}(\text{S})\text{O}$ . Surprisingly, the reaction mixture also contained free  $\text{PMe}_3$  ( $\delta(^{31}\text{P}) = -62.6$  ppm) and  $\text{SPMe}_3$  ( $\delta(^{31}\text{P}) = 27.2$  ppm), as well as  $\text{OPMe}_3$ . Unreacted starting material slowly decreased in concentration over 5 h and the amount of product **1:Mes\*** gradually increased with respect to  $\text{Mes}^*\text{-P}(\text{PMe}_3)$ . Full conversion of  $\text{Mes}^*\text{-P}(\text{PMe}_3)$  was only achieved upon heating the reaction mixture overnight. This indicates that in case of  $\text{Mes}^*\text{-P}(\text{PMe}_3)$  and  ${}^{\text{Mes}}\text{Ter-P}(\text{PMe}_3)$  a second, Wittig-type pathway is plausible (Scheme 6, top). After formation of a loose adduct between  $\text{SO}_2$  and  $\text{RP}(\text{PMe}_3)$ , deoxygenation gives  $\text{R-PSO}$  (**A**), which isomerizes to  $\text{RP}(\text{S})\text{O}$  (**B**), with the concomitant formation of  $\text{OPMe}_3$ . The mixed phosphorane species **B** ( $\text{R} = \text{Mes}^*, \text{E} = \text{S}$ ) was found to be thermodynamically favoured by 204.6 kJ mol<sup>-1</sup> (see chapter 4.3 in the ESI†).<sup>49</sup>  $\text{RP}(\text{S})\text{O}$  can then react with a second equivalent of  $\text{R-P}(\text{PMe}_3)$  to give again  $\text{OPMe}_3$  and the diphosphene-monosulfide  $\text{RP}=\text{P}(\text{S})\text{R}$ , in which the R-groups are *cis*-oriented. Upon heating  $\text{RP}=\text{P}(\text{S})\text{R}$  is then transformed into the observed thiadiphosphiranes. It needs to be pointed out that the EO-release pathway (Scheme 6, bottom) might be operative in this case as well. This assumption stems from an individual reaction of  $\text{Mes}^*\text{-P}(\text{PMe}_3)$  with an excess of elemental sulfur, which

gave **1:Mes\*** as the major product, with minimal amounts of  $\text{Mes}^*\text{PS}_2$  and  $\text{SPMe}_3$  being present in solution as well, which was also observed in the formation of **1:Mes\*** (Fig. S54†). This gives a rationale for the formation of  $\text{SPMe}_3$  also in the case of **1:Mes\***.

Interestingly, the stoichiometry of the reaction is of minor importance for the conversion of  $\text{R-P}(\text{PMe}_3)$  ( $\text{R} = \text{Mes}^*, {}^{\text{Mes}}\text{Ter}$ ) with  $\text{EO}_2$ . 0.5 as well as 1 eq. of  $\text{EO}_2$  both yield chalcogenadiphosphiranes as the main product after thorough work-up procedures. The concomitant formation of  $\text{OPMe}_3$  and  $\text{SPMe}_3$ , which are difficult to separate, lowered isolated yields to moderate values (Scheme 4). Nevertheless, a practical pathway for the effective deoxygenation of  $\text{SO}_2$  and  $\text{SeO}_2$  aided by  $\text{R-P}(\text{PMe}_3)$  ( $\text{R} = \text{Mes}^*, {}^{\text{Mes}}\text{Ter}$ ) to give three-membered chalcogenadiphosphiranes has been established herein.

## Conclusions

In here we have described the reactivity of phospho-Wittig reagents towards  $\text{SO}_2$ , by using DABSO as a  $\text{SO}_2$  source, and  $\text{SeO}_2$ . We could show that the phospho-Wittig reagents  $\text{R-P}(\text{PMe}_3)$  ( $\text{R} = \text{Mes}^*, {}^{\text{Mes}}\text{Ter}$ ) selectively yield the respective thia- as well as selenadiphosphiranes **1:R** and **2:R**. In addition,  $\text{DipTer-P}(\text{PMe}_3)$  can afford the four-membered ring species **3:DipTer** in the reaction with  $\text{SeO}_2$  and is a rare example of a compound with a  $\text{P}_2\text{Se}_2$  core. Furthermore, we have systematically examined the reactivity of  $\text{DipTer-P}(\text{PMe}_3)$  towards  $\text{SO}_2$  and  $\text{SeO}_2$  regarding different reaction conditions. As evident from the crystal structure of **4:DipTer** it can be seen that  $\text{DipTer-P}(\text{PMe}_3)$  can be oxidized to the dioxophosphorane  $\text{DipTer-P}(\text{O})_2$ , which is kinetically stabilized through the bulkiness of the  $\text{DipTer}$  moiety and additional  $\text{OPMe}_3$  coordination. This represents the first example of a phosphineoxide-stabilized dioxophosphorane, which is labile. Furthermore, the sulfur containing side-products were determined to be rare asymmetric P–O and P–S heterocycles, which could be detected *via*  $^{31}\text{P}$  NMR spectroscopy and mass spectrometry when converting  $\text{SO}_2$  and  $\text{DipTer-P}(\text{PMe}_3)$ . Two potential pathways for the formation of chalcogenadiphosphiranes and dioxophosphoranes are presented herein. First, a Wittig-type pathway for the formation of thia- and selenadiphosphiranes and second, an EO-release pathway for the formation of **4:DipTer**.

Taking all observations and characterized compounds into account, a considerable structural diversity was discovered after deoxygenation of chalcogen oxides depending on different reaction conditions and ligand-bulkiness. We believe that an even higher steric bulk might serve for the successful isolation of free phosphinidene-sulfides, -selenides as well as -oxides. These species are expected to be useful tools for bond activation chemistry and further studies are currently underway. In how far further Lewis-base stabilized  $\text{R-P}(\text{O})_2$  or even the free dioxophosphoranes are accessible will be part of future studies.



## Author contributions

F. D. and C. H.-J. designed the experiments and carried out most of the experimental work with help from P. G. and T. W. F. D. and C. H.-J. characterized the compounds and analyzed the data. W. B. performed the  $^{77}\text{Se}\{^1\text{H}\}$  NMR studies and analyzed the data. C. H.-J. carried out computational studies, proposed and supervised the project. The manuscript was written through contributions of all authors. All authors have given approval to the final version of the manuscript.

## Conflicts of interest

There are no conflicts to declare.

## Acknowledgements

C. H.-J. thanks the Boehringer Ingelheim Foundation for support through an Exploration Grant. F. D. and C. H.-J. thank the Leibniz Association for funding within the scope of the Leibniz ScienceCampus Phosphorus Research Rostock (<https://www.sciencecampus-rostock.de>). Financial support by LIKAT (PhD fellowship for P. G.) and the GSO through a KT-Boost fund is gratefully acknowledged. F. D. thanks C. H.-J. for his ongoing support. We furthermore thank Andreas Koch for his valuable help with mass spectrometry.

## References

- 1 X. Li, J. Han, Y. Liu, Z. Dou and T.-a. Zhang, *Sep. Purif. Technol.*, 2022, **281**, 119849–119849.
- 2 A. Poullikkas, *Energy Technol. Policy*, 2015, **2**, 92–103.
- 3 R. del Valle-Zermeno, J. Formosa and J. M. Chimenos, *Rev. Chem. Eng.*, 2015, **31**, 303–327.
- 4 R. K. Srivastava, W. Jozewicz and C. Singer, *Environ. Prog.*, 2001, **20**, 219–228.
- 5 R. Wei, X. Chen and Y. Gong, *Inorg. Chem.*, 2020, **59**, 4703–4710.
- 6 F. Dankert, A. Feyh and C. von Hänisch, *Eur. J. Inorg. Chem.*, 2020, **2020**, 2744–2756.
- 7 K. Reuter, S. S. Rudel, M. R. Buchner, F. Kraus and C. von Hänisch, *Chem. – Eur. J.*, 2017, **23**, 9607–9617.
- 8 M. Malischewski, D. V. Peryshkov, E. V. Bukovsky, K. Seppelt and S. H. Strauss, *Inorg. Chem.*, 2016, **55**, 12254–12262.
- 9 A. Kumar, G. S. McGrady, J. Passmore, F. Grein and A. Decken, *Z. Anorg. Allg. Chem.*, 2012, **638**, 744–753.
- 10 J. Derendorf, M. Kessler, C. Knapp, M. Rühle and C. Schulz, *Dalton Trans.*, 2010, **39**, 8671–8678.
- 11 T. S. Cameron, G. B. Nikiforov, J. Passmore and J. M. Rautiainen, *Dalton Trans.*, 2010, **39**, 2587–2596.
- 12 I. Nagasawa, H. Amita and H. Kitagawa, *Chem. Commun.*, 2009, 204–205.
- 13 M. K. Denk, K. Hatano and A. J. Lough, *Eur. J. Inorg. Chem.*, 2003, **2003**, 224–231.
- 14 J. K. Brask, T. Chivers and M. Parvez, *Angew. Chem., Int. Ed.*, 2000, **39**, 958–960.
- 15 M. R. Snow and J. A. Ibers, *Inorg. Chem.*, 1973, **12**, 224–229.
- 16 N. Szykiewicz, J. Chojnacki and R. Grubba, *Inorg. Chem.*, 2020, **59**, 6332–6337.
- 17 N. Aders, L. Keweloh, D. Pleschka, A. Hepp, M. Layh, F. Rogel and W. Uhl, *Organometallics*, 2019, **38**, 2839–2852.
- 18 M. Sajid, A. Klose, B. Birkmann, L. Liang, B. Schirmer, T. Wiegand, H. Eckert, A. J. Lough, R. Fröhlich, C. G. Daniliuc, S. Grimme, D. W. Stephan, G. Kehr and G. Erker, *Chem. Sci.*, 2013, **4**, 213–219.
- 19 F. Lavigne, E. Maerten, G. Alcaraz, V. Branchadell, N. Saffon-Merceron and A. Baceiredo, *Angew. Chem., Int. Ed.*, 2012, **51**, 2489–2491.
- 20 A. Kraft, N. Trapp, D. Himmel, H. Böhrer, P. Schlüter, H. Scherer and I. Krossing, *Chem. – Eur. J.*, 2012, **18**, 9371–9380.
- 21 M. Kessler, C. Knapp, V. Sagawe, H. Scherer and R. Uzun, *Inorg. Chem.*, 2010, **49**, 5223–5230.
- 22 A. J. Boutland, I. Pernik, A. Stasch and C. Jones, *Chem. – Eur. J.*, 2015, **21**, 15749–15758.
- 23 A. C. Schmidt, F. W. Heinemann, C. E. Kefalidis, L. Maron, P. W. Roesky and K. Meyer, *Chem. – Eur. J.*, 2014, **20**, 13501–13506.
- 24 K. Junold, F. M. Mück, C. Kupper, J. A. Baus, C. Burschka and R. Tacke, *Chem. – Eur. J.*, 2014, **20**, 12781–12785.
- 25 T. Chivers, T. J. Clark, M. Parvez and G. Schatte, *Dalton Trans.*, 2003, 2107–2108.
- 26 S. I. A. El Sheikh, B. C. Smith and M. E. Sobeir, *Angew. Chem., Int. Ed. Engl.*, 1970, **9**, 308.
- 27 E. Fluck and H. Binder, *Z. Anorg. Allg. Chem.*, 1967, **354**, 139–148.
- 28 E. Fluck and H. Binder, *Angew. Chem., Int. Ed. Engl.*, 1965, **4**, 359.
- 29 E. Martínez-Ahumada, D. He, V. Berryman, A. López-Olvera, M. Hernandez, V. Jancik, V. Martis, M. A. Vera, E. Lima, D. J. Parker, A. I. Cooper, I. A. Ibarra and M. Liu, *Angew. Chem., Int. Ed.*, 2021, **60**, 17556–17563.
- 30 G. Zhu, C. D. Hoffman, Y. Liu, S. Bhattacharyya, U. Tumuluri, M. L. Jue, Z. Wu, D. S. Sholl, S. Nair, C. W. Jones and R. P. Lively, *Chem. – Eur. J.*, 2016, **22**, 10743–10747.
- 31 G. Cui, F. Zhang, X. Zhou, H. Li, J. Wang and C. Wang, *Chem. – Eur. J.*, 2015, **21**, 5632–5639.
- 32 D. Yang, M. Hou, H. Ning, J. Ma, X. Kang, J. Zhang and B. Han, *ChemSusChem*, 2013, **6**, 1191–1195.
- 33 W. Wu, B. Han, H. Gao, Z. Liu, T. Jiang and J. Huang, *Angew. Chem., Int. Ed.*, 2004, **43**, 2415–2417.
- 34 S. P. Blum, T. Karakaya, D. Schollmeyer, A. Klapars and S. R. Waldvogel, *Angew. Chem., Int. Ed.*, 2021, **60**, 5056–5062.
- 35 A. Adenot, N. von Wolff, G. Lefèvre, J. C. Berthet, P. Thuéry and T. Cantat, *Chem. – Eur. J.*, 2019, **25**, 8118–8126.



- 36 F. Buß, P. Rotering, C. Mück-Lichtenfeld and F. Dielmann, *Dalton Trans.*, 2018, **47**, 10420–10424.
- 37 G. Cui, D. Yang and H. Qi, *Ind. Eng. Chem. Res.*, 2021, **60**, 4536–4541.
- 38 H. Chen, R. Ding, H. Tang, Y. Pan, Y. Xu and Y. Chen, *Chem. – Asian J.*, 2019, **14**, 3264–3268.
- 39 N. von Wolff, J. Char, X. Frogneux and T. Cantat, *Angew. Chem., Int. Ed.*, 2017, **56**, 5616–5619.
- 40 T. Liu, D. Zheng, Y. Ding, X. Fan and J. Wu, *Chem. – Asian J.*, 2017, **12**, 465–469.
- 41 D. Zheng, Y. An, Z. Li and J. Wu, *Angew. Chem., Int. Ed.*, 2014, **53**, 2451–2454.
- 42 D. Markovic, E. Roversi, R. Scoppelliti, P. Vogel, R. Meana and J. A. Sordo, *Chem. – Eur. J.*, 2003, **9**, 4911–4915.
- 43 E. Roversi, R. Scoppelliti, E. Solari, R. Estoppey, P. Vogel, P. Braña, B. Menéndez and J. A. Sordo, *Chem. – Eur. J.*, 2002, **8**, 1336–1355.
- 44 X. Xu, G. Kehr, C. G. Daniliuc and G. Erker, *J. Am. Chem. Soc.*, 2014, **136**, 12431–12443.
- 45 B. Waerder, M. Pieper, L. A. Körte, T. A. Kinder, A. Mix, B. Neumann, H. G. Stammler and N. W. Mitzel, *Angew. Chem., Int. Ed.*, 2015, **54**, 13416–13419.
- 46 F. M. Mück, J. A. Baus, R. Bertermann and R. Tacke, *Eur. J. Inorg. Chem.*, 2016, **2016**, 3240–3245.
- 47 J. D. Protasiewicz, *Eur. J. Inorg. Chem.*, 2012, **2012**, 4539–4549.
- 48 F. Dankert, J.-E. Siewert, P. Gupta, F. Weigend and C. Hering-Junghans, *Angew. Chem., Int. Ed.*, 2022, e202207064.
- 49 F. Dankert, M. Fischer and C. Hering-Junghans, *Dalton Trans.*, 2022, **51**, 11267–11276.
- 50 P. Gupta, J. E. Siewert, T. Wellnitz, M. Fischer, W. Baumann, T. Beweries and C. Hering-Junghans, *Dalton Trans.*, 2021, **50**, 1838–1844.
- 51 M. Fischer, S. Nees, T. Kupfer, J. T. Goettel, H. Braunschweig and C. Hering-Junghans, *J. Am. Chem. Soc.*, 2021, **143**, 4106–4111.
- 52 F. Dankert and C. Hering-Junghans, *Chem. Commun.*, 2022, **58**, 1242–1262.
- 53 S. Shah and J. D. Protasiewicz, *Chem. Commun.*, 1998, 1585–1586.
- 54 B. Cetinkaya, P. B. Hitchcock, M. F. Lappert, A. J. Thorne and H. Goldwhite, *J. Chem. Soc., Chem. Commun.*, 1982, 691–693.
- 55 C. M. E. Graham, T. E. Pritchard, P. D. Boyle, J. Valjus, H. M. Tuononen and P. J. Ragoon, *Angew. Chem., Int. Ed.*, 2017, **56**, 6236–6240.
- 56 Y. Masaaki, T. Kozo, A. Kaori and I. Naoki, *Chem. Lett.*, 1984, **13**, 317–318.
- 57 J. Navech, M. Revel and R. Kraemer, *Tetrahedron Lett.*, 1985, **26**, 207–210.
- 58 D. Rottschäfer, M. K. Sharma, B. Neumann, H. G. Stammler, D. M. Andrada and R. S. Ghadwal, *Chem. – Eur. J.*, 2019, **25**, 8127–8134.
- 59 C. Mitrofan, T. Gust, A. Zanin, R. M. Bîrzo, P. G. Jones, W. W. du Mont, S. Hayashi, W. Nakanishi and H. C. Marsmann, *Eur. J. Inorg. Chem.*, 2017, **2017**, 1526–1536.
- 60 T. L. Chan and Z. Xie, *Chem. Commun.*, 2016, **52**, 7280–7283.
- 61 T. Sasamori, M. Sakagami and N. Tokitoh, *J. Sulphur Chem.*, 2013, **34**, 677–683.
- 62 A. Tsurusaki, N. Nagahora, T. Sasamori, K. Matsuda, Y. Kanemitsu, Y. Watanabe, Y. Hosoi, Y. Furukawa and N. Tokitoh, *Bull. Chem. Soc. Jpn.*, 2010, **83**, 456–478.
- 63 H. Voelker, U. Pieper, H. W. Roesky and G. M. Sheldrick, *Z. Naturforsch., B: J. Chem. Sci.*, 1994, **49**, 255–257.
- 64 M. Abe, K. Toyota and M. Yoshifuji, *Chem. Lett.*, 1992, **21**, 2349–2352.
- 65 M. Yoshifuji, K. Shibayama and N. Inamoto, *Chem. Lett.*, 1984, **13**, 603–606.
- 66 M. Yoshifuji, K. Shibayama, N. Inamoto, K. Hirotsu and T. Higuchi, *J. Chem. Soc., Chem. Commun.*, 1983, 862–863.
- 67 N. Nagahora, T. Sasamori, Y. Hosoi, Y. Furukawa and N. Tokitoh, *J. Organomet. Chem.*, 2008, **693**, 625–632.
- 68 W.-W. du Mont, T. Gust, J. Mahnke, R. M. Bîrzo, L. Barra, D. Bugnariu, F. Ruthe, C. Wismach, P. G. Jones, K. Karaghiosoff, L. Nyulászi and Z. Benkő, *Angew. Chem., Int. Ed.*, 2007, **46**, 8682–8685.
- 69 G. Jochem, K. Karaghiosoff, S. Plank and S. D. U. A. Schmidpeter, *Chem. Ber.*, 1995, **128**, 1207–1219.
- 70 P. Jutzi, N. Brusdeilins, H. G. Stammler and B. Neumann, *Chem. Ber.*, 1994, **127**, 997–1001.
- 71 E. Niecke and R. Rüger, *Angew. Chem., Int. Ed. Engl.*, 1983, **22**, 155–156.
- 72 M. Baudler, H. Suchomel, G. Fürstenberg and U. Schings, *Angew. Chem., Int. Ed. Engl.*, 1981, **20**, 1044–1045.
- 73 H. Woolven, C. González-Rodríguez, I. Marco, A. L. Thompson and M. C. Willis, *Org. Lett.*, 2011, **13**, 4876–4878.
- 74 M. Yoshifuji, K. Ando, K. Shibayama, N. Inamoto, K. Hirotsu and T. Higuchi, *Angew. Chem., Int. Ed. Engl.*, 1983, **22**, 418–419.
- 75 See ESI† for all experimental and computational details.
- 76 T. Sasamori, N. Takeda and N. Tokitoh, *J. Phys. Org. Chem.*, 2003, **16**, 450–462.
- 77 S. Fuchs and H. Schmidbaur, *Z. Naturforsch., B: J. Chem. Sci.*, 1995, **50**, 855–858.
- 78 M. I. Arz, V. T. Annibale, N. L. Kelly, J. V. Hanna and I. Manners, *J. Am. Chem. Soc.*, 2019, **141**, 2894–2899.
- 79 B. S. Pedersen, S. Scheibye, K. Clausen and S.-O. Lawesson, *Bull. Soc. Chim. Belg.*, 1978, **87**, 293–297.
- 80 J. C. Fitzmaurice, D. J. Williams, P. T. Wood and J. D. Woollins, *J. Chem. Soc., Chem. Commun.*, 1988, 741–743.
- 81 L. E. English, A. Pajak, C. L. McMullin, J. P. Lowe, M. F. Mahon and D. J. Liptrot, *Chem. – Eur. J.*, 2022, **28**, e202200376.
- 82 A. Mardukov, D. Niedek and P. R. Schreiner, *J. Am. Chem. Soc.*, 2017, **139**, 5019–5022.
- 83 P. Pykkö and M. Atsumi, *Chem. – Eur. J.*, 2009, **15**, 12770–12779.

Paper

Dalton Transactions

- 84 R. García-Rodríguez and H. Liu, *J. Am. Chem. Soc.*, 2012, **134**, 1400–1403.
- 85 D. J. Meschi and R. J. Myers, *J. Am. Chem. Soc.*, 1956, **78**, 6220–6223.
- 86 F. J. Lovas, E. Tiemann and D. R. Johnson, *J. Chem. Phys.*, 1974, **60**, 5005–5010.
- 87 J. T. Herron and R. E. Huie, *Chem. Phys. Lett.*, 1980, **76**, 322–324.



## **6.5 P,N-Type Phosphaalkene-based Ir(I) Complexes: Synthesis, Coordination Chemistry, and Catalytic Applications**

Priyanka Gupta, Hans-Joachim-Drexler, Richard Wingad, Duncan Wass, Torsten Beweries, Christian Hering-Junghans

*Inorg. Chem. Front.*, **2023**, *10*, 2285.

Contribution to this paper is 70%



## RESEARCH ARTICLE

View Article Online  
View Journal | View IssueCite this: *Inorg. Chem. Front.*, 2023, 10, 2285**P,N-type phosphalkene-based Ir(I) complexes: synthesis, coordination chemistry, and catalytic applications†**Priyanka Gupta,<sup>a,b</sup> Hans-Joachim Drexler,<sup>a</sup> Richard Wingad,<sup>b</sup> Duncan Wass,<sup>b</sup> Eszter Baráth,<sup>a</sup> Torsten Beweries<sup>a\*</sup> and Christian Hering-Junghans<sup>a\*</sup>

Phosphaalkenes are an emerging class of ligands with unique electronic properties that can be regarded as tuneable variants of the ubiquitous CO ligand. Our group has recently reported the synthesis of the P, N-type phosphalkene ligand quin-CH=PMes\* (**1**, quin = 2-quinoliny) and its coordination chemistry with Rh(I) was investigated. In this study, we present the synthesis and characterisation of iridium(I) complex [(quin-CH=PMes\*)<sub>2</sub>IrCl] (**5**), which showed a versatile reactivity upon chloride abstraction with AgOTf in different coordinating solvents affording pyridine-coordinated cationic Ir(I) complex [(quin-CH=PMes\*)<sub>2</sub>Ir(py)][OTf] (**6**) and C–H bond activated cyclometallated Ir(III)-hydrido complex **8**. Treatment of complex **5** with CO, (CH<sub>3</sub>)<sub>2</sub>Mg or NaN<sub>3</sub>, respectively, produced three types of five-coordinate Ir(I) complexes **9**, **10** and **11** in excellent yields. Complex **6** was found to be less active as a catalyst in the *N*-alkylation of aniline with benzyl alcohol than complex **5**, likely due to the instability of Ir complex **6** in the presence of base at higher temperatures. Complex **5** has also been tested as a catalyst in the Guerbet-type coupling of methanol and ethanol to iso-butanol, which is a promising biofuel candidate, and showed good conversion and selectivity towards the desired iso-butanol.

Received 19th January 2023,

Accepted 21st March 2023

DOI: 10.1039/d3qi00142c

rsc.li/frontiers-inorganic

**Introduction**

Over the past three decades, there has been a growing interest to incorporate phosphalkenes (PAs) in transition metal catalysts. This interest is based on the energetically low-lying  $\pi^*$  orbitals in PAs, thereby serving as effective  $\pi$ -acceptors towards transition metals.<sup>1,2</sup> The lone pair on phosphorus in PAs possesses high *s*-character and thus, their  $\sigma$ -donating ability can be compared to carbon monoxide rather than to imines. The lone pair on carbon ( $n_C$ ) in C=O is formally in an *sp*-hybrid orbital (50% 2*s*), similar in *s*-character to the lone pair of the parent PA HP=CH<sub>2</sub> (66% 3*s*). In addition to the similar  $\sigma$ -donor properties, the analogy between PAs and carbon monoxide extends to their excellent  $\pi$ -accepting ability (Fig. 1a).<sup>3</sup> This particular ligand property is useful, as it should in principle

facilitate the reductive elimination step in a given catalytic cycle, leading to efficient systems for a wide range of catalytic organic transformations in conjunction with group

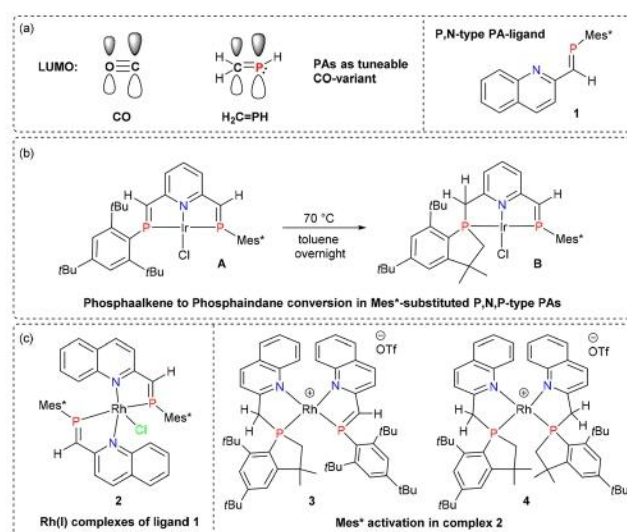


**Fig. 1** (a) Illustration of the analogy between CO and phosphalkenes; ligand activation in (b) previously reported Ir P,N,P phosphalkene pincer complexes<sup>29</sup> and (c) Rh P,N phosphalkene complexes.<sup>32</sup>

<sup>a</sup>Leibniz Institut für Katalyse e.V. (LIKAT), A.-Einstein-Str. 29a, 18059 Rostock, Germany. E-mail: torsten.beweries@catalysis.de, christian.hering-junghans@catalysis.de

<sup>b</sup>Cardiff Catalysis Institute, Cardiff University, Translational Research Hub, Maindy Road, Cathays, Cardiff, Wales, CF24 4HQ, UK

† Electronic supplementary information (ESI) available: Synthesis and characterisation of compounds, NMR and IR spectra, crystallographic, and computational details. CCDC 2235638–2235640. For ESI and crystallographic data in CIF or other electronic format see DOI: <https://doi.org/10.1039/d3qi00142c>



## Research Article

## Inorganic Chemistry Frontiers

8–10 metals.<sup>4–6</sup> Representative examples, in which PA-containing metal complexes were utilised, include the hydroamination of 1,3-dienes (Pd),<sup>7</sup> the dehydrative allylation with allylic alcohols (Pd),<sup>8,9</sup> the *Z*-selective hydrosilylation of alkynes (Ru),<sup>10,11</sup> the hydroamidation of enones (Rh)<sup>12</sup> and the *N*-alkylation of amines with alcohols (Ir).<sup>13</sup> *N*-Alkylation of amines with alcohols is an environmentally benign process of preparing amines, which produces water as the sole byproduct.<sup>14–16</sup> Although both heterogeneous and homogeneous catalysts have been reported to promote the reaction, ruthenium<sup>17–19</sup> and iridium<sup>20–23</sup> complexes have constituted a vast majority of the homogeneous catalysts. While this area of research is still growing, the field of PA-based ligands remains underexplored compared with the ubiquitously used related phosphine- or imine-based P,N ligands, which have been at the forefront of development in various areas of catalysis research.<sup>24,25</sup> The groups of Geoffroy and Yoshifuji reported a series of kinetically protected mono-, di- and tridentate PA-ligands following the “phospha-Peterson” route that involves the reaction of a silylated phosphide-anion of the type  $\text{RP}^{(-)}\text{Si}(t\text{Bu})\text{Me}_2$  with an aldehyde or ketone.<sup>26,27</sup> Later, Bickelhaupt and co-workers improved the “phospha-Peterson” protocol and the variant  $\text{Mes}^*\text{P}=\text{C}(\text{SiMe}_3)\text{Py}$  ( $\text{Mes}^* = 2,4,6\text{-}t\text{Bu}_3\text{C}_6\text{H}_2$ ) was synthesised using a Pd catalysed route employing a phosphalkene Grignard reagent.<sup>28</sup> So far, PA-based P,N,P-pincer complexes of late transition metal complexes have been comparably well-studied while the reports on related bidentate PA-based P,N-ligands are still limited. In particular, Ozawa *et al.* have demonstrated that one of the  $\text{P}=\text{C}$  bonds installed in a P,N,P-pincer type iridium complex,  $[\text{IrCl}(\text{BPEP-H})]$  ( $\text{BPEP} = 2,6\text{-bis}[2\text{-(}2,4,6\text{-tri-}t\text{butylphenyl)-2-phosphaethenyl}]\text{pyridine}$ ; **A** (Fig. 1b), undergoes intramolecular C–H activation at one of the  $\text{Mes}^*$ -substituents on P and cyclisation to afford a modified, unsymmetric P,N,P-pincer featuring phospholane, pyridine, and phosphalkene donor sites (**B**, Fig. 1b). P,N,P-pincer iridium complexes with a phosphanylmethyl group (**B**) on the pyridine core undergo deprotonation at the benzylic position, resulting in dearomatisation of the pyridine ring. The dearomatised complexes have shown potential in the activation of small molecules in a heterolytic manner, particularly towards N–H bond activation of ammonia and amines *via* metal-ligand cooperativity.<sup>29</sup> Mixed bidentate P,N-ligands, featuring a phosphalkene moiety and an imine donor, on reaction with  $[\text{Pd}(\text{cod})\text{MeCl}]$  ( $\text{cod} = 1,5\text{-cyclooctadiene}$ ) have been reported to give bimetallic macrocyclic derivatives.<sup>30</sup> We have recently reported on the synthesis and characterisation of the P,N-type quinoline-based phosphalkene ligand  $\text{quin-CH}=\text{PMes}^*$  (**1**,  $\text{quin} = 2\text{-quinolinyl}$ ), synthesised by the combination of the phosphawittig reagent  $\text{Mes}^*\text{P}(\text{PMe}_3)$ <sup>31</sup> with 2-quinolinecarboxaldehyde and investigated its coordination chemistry with Rh(i), giving complex **2**, with Rh in a distorted trigonal bipyramidal coordination mode and two ligands of **1** being mutually *trans*-oriented.<sup>32</sup> **2** was shown to undergo a selective cyclisation of one or two of the P,N-ligands by using sub- or superstoichiometric amounts of  $\text{AgOTf}$  ( $\text{OTf}^- = \text{O}_3\text{SCF}_3^-$ ) resulting in the formation of complexes **3** and **4** (Fig. 1c). Also, we proposed a

new type of bond activation pathway that involves an oxidative proton shift from the *t*Bu group to the Rh centre along with formation of a phosphaindane unit instead of initial oxidative addition of the *t*Bu group at Rh(i).

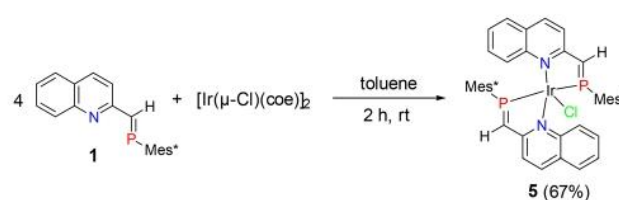
Intrigued by the general question of reactivity differences between 4d and 5d metals, we have now investigated structurally related iridium systems. In this paper, we report the multifaceted coordination chemistry of the P,N-phosphalkene ligand  $\text{quin-CH}=\text{PMes}^*$  (**1**,  $\text{quin} = 2\text{-quinolinyl}$ ) at Ir(i) and highlight the reactivity of these complexes using spectroscopic methods. Moreover, these complexes were tested as catalysts in the *N*-alkylation of aniline with benzyl alcohol and in the Guerbet-type upgrading of ethanol to iso-butanol. Ruthenium complexes are active for the Guerbet-type synthesis of both *n*- and iso-butanol,<sup>33–39</sup> Homogeneous iridium systems have been previously reported for the Guerbet reaction of ethanol to *n*-butanol.<sup>40–43</sup> The only example of an iridium system for the upgrading of ethanol/methanol to iso-butanol was reported by Xu and Mu using iridium complexes immobilised on *N*-functionalised carbon materials.<sup>44</sup> Therefore, we turned our attention to investigate the efficacy of our iridium complex **5** in the co-condensation of ethanol and methanol to produce iso-butanol.

## Results and discussion

### Synthesis of Ir(i) complexes

The reaction of  $\text{quin-CH}=\text{PMes}^*$  (**1**) with  $[\text{Ir}(\mu\text{-Cl})(\text{coe})_2]_2$  ( $\text{coe} = \text{cyclooctene}$ ) in toluene in a 4:1 ratio afforded  $[(\text{quin-CH}=\text{PMes}^*)_2\text{IrCl}]$  (**5**), which precipitated from the reaction mixture as a dark blue solid and was isolated on a 0.2 g scale (isolated yield: 67%; Scheme 1). Single crystal X-ray diffraction (SC-XRD) analysis of crystals grown from a saturated  $\text{CH}_2\text{Cl}_2$  solution at  $-30^\circ\text{C}$  confirmed the formation of complex **5**.

The molecular structure (Fig. 2) of **5** adopts a distorted trigonal bipyramidal geometry with a  $\tau_5$  value of 0.75 (the  $\tau_5$  parameter is used to categorise five-coordinate metal complexes, with  $\tau_5 = 0$  indicating a perfect square-pyramidal  $C_{4v}$  geometry, while  $\tau_5 = 1$  indicates a perfect trigonal bipyramidal  $D_{3h}$  coordination environment).<sup>45,46</sup> The quinoline N atoms occupy the axial positions, whereas both P atoms as well as the  $\text{Cl}^-$  ligand lie in the trigonal plane, with both ligands being *trans*-oriented with respect to the  $\text{Mes}^*$ -substituent. The P–C bond lengths (P1–C10 1.685(4), P2–C40 1.680(4) Å) are nearly identical to those in its rhodium analogue **2** (1.6821(17), 1.6810(18) Å).<sup>32</sup>



**Scheme 1** Synthesis of Ir(i) complex **5** starting from P,N-ligand **1**.



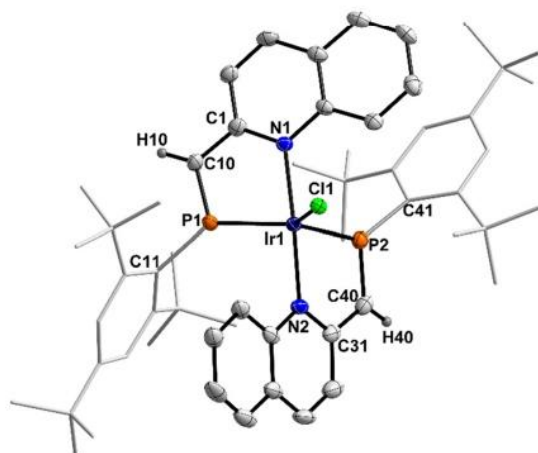


**Fig. 2** Molecular structure of complex 5. Thermal ellipsoids drawn at 50% probability. Hydrogen atoms, except on the phosphaalkene unit (C10 and C40), are omitted for clarity. Selected bond lengths (Å) and angles (°) of 5: P1–C10 1.685(4), P2–C40 1.680(4), C10–C1 1.412(5), C40–C31 1.415(6), P1–Ir 2.1959(9), P2–Ir 2.2030(10), N1–Ir 2.116(3), N2–Ir 2.114(3), Ir–Cl 2.4579(10); C1–C10–P1 113.2(3), C31–C40–P2 114.0(3), P1–Ir–P2 129.32(4), N1–Ir–Cl 91.31(8), N2–Ir–Cl 94.10(9), P1–Ir–Cl 116.19(4), P2–Ir–Cl 114.49(3), N1–Ir–N2 174.50(12), P1–Ir–N1 80.48(8), P2–Ir–N2 80.42(9), C10–P1–C11 116.86(17), C40–P2–C41 116.90(19).

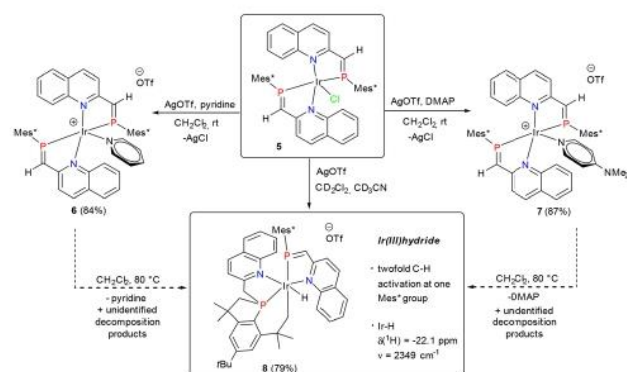
The Ir–N distances (2.116(3), 2.114(3) Å) are slightly longer than the typical range for P,N,P-pincer iridium(i) complexes (2.05–2.09 Å).<sup>47–49</sup>

The asymmetric stretching mode of the P=C bonds is clearly identified in the IR spectrum ( $\nu_{\text{P=C}}$ ) at 939 cm<sup>−1</sup> (Table 1). In the <sup>31</sup>P{<sup>1</sup>H} NMR spectrum the two phosphorus atoms are equivalent giving a singlet for 5 at 250.8 ppm (*cf.* 2  $\delta(^{31}\text{P}\{^1\text{H}\})$  262.5 ppm). Interestingly, unlike [IrCl(Mes\*<sub>2</sub>-BPEP)] (A),<sup>29</sup> the phosphaalkene unit in the bis-quinoline-PA complex 5 remained unaffected upon heating at 80 °C and only starts to decompose into some unidentified side products after two days of continuous heating, as ascertained by <sup>31</sup>P{<sup>1</sup>H} NMR spectroscopy. Complex 5 is stable in CD<sub>2</sub>Cl<sub>2</sub> solution in air, *i.e.*, in the presence of traces of water, and is still present after addition of water and heating, making this species a promis-

ing platform for the study of catalytic reactions requiring thermal activation.

### Effect of coordinating solvents

Following our recent observation of C–H bond activation at the *o*-*t*Bu group of the Mes\*<sup>+</sup>-substituents in Rh complex 2 during salt metathesis reactions (Fig. 1c),<sup>32</sup> we decided to study the corresponding reaction of Ir P,N-complex 5 with AgOTf. To our surprise, we found that the reaction of complex 5 with AgOTf in non-coordinating solvent such as CD<sub>2</sub>Cl<sub>2</sub> at room temperature resulted in the formation of a mixture of products, as observed by <sup>31</sup>P{<sup>1</sup>H} NMR spectroscopy. In contrast, upon using a 2 : 1 mixture of CH<sub>2</sub>Cl<sub>2</sub> and pyridine as a N-donor coordinating solvent, the <sup>31</sup>P{<sup>1</sup>H} NMR spectrum featured a slightly shielded singlet resonance at 244.9 ppm indicating the formation of moisture stable pyridine coordinated Ir(i) complex [(quin-CH=PMes\*)<sub>2</sub>Ir(py)]OTf (6) (Scheme 2). This was corroborated by the molecular structure that was determined from blue-coloured single crystals obtained from a saturated THF solution layered with *n*-hexane (Fig. 3). Dative coordination of the pyridine to Ir(i) is characterised by the Ir1–N3 distance of 2.157(5) Å, which is minimally longer than the Ir1–N1, Ir1–N2 (2.122(4), 2.115(5) Å) distances to the quinoline N atoms in the axial positions of the distorted trigonal pyramid around the



**Scheme 2** Synthesis of cationic Ir(i) complexes 6 and 7 and formation of the Ir(III) complex 8.

**Table 1** Summary of characteristic spectroscopic and structural data of compounds 5–11 (C<sub>PA</sub>: C atom of the phosphaalkene unit; C<sub>R</sub>: C atom of the quin-C atom; n.a. = not available)

	$\delta(^{31}\text{P})$ [ppm]	$d(\text{P}-\text{C})$ [Å]	$d(\text{C}_{\text{PA}}-\text{C}_{\text{R}})$ [Å]	$d(\text{Ir}-\text{N})$ [Å]	$d(\text{Ir}-\text{P})$ [Å]	$\tilde{\nu}(\text{P}=\text{C})$ [cm <sup>−1</sup> ]
5	250.8	1.685(4) 1.680(4)	1.412(5) 1.415(6)	2.116(3) 2.114(3)	2.1959(9) 2.2030(10)	939
6	244.9	1.678(6) 1.699(7)	1.419(8) 1.407(12)	2.122(4) 2.115(5) 2.157(5)	2.2097(16) 2.2032(15)	941
7	245.5 285.5 (t)	n.a.	n.a.	n.a.	n.a.	939
8	6.8 (t, $J = 11.3$ Hz)	n.a.	n.a.	n.a.	n.a.	n.a.
9	271.4	n.a.	n.a.	n.a.	n.a.	957
10	250.0	1.696(2) 1.697(2)	1.403(3) 1.401(4)	2.1121(17) 2.1070(18)	2.1987(5) 2.2010(6)	919
11	243.0	n.a.	n.a.	n.a.	n.a.	933



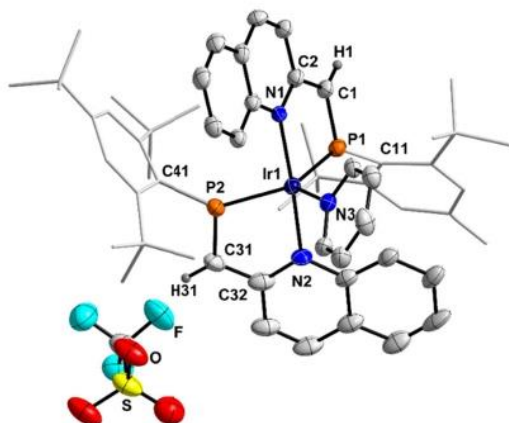


**Fig. 3** Molecular structure of complex **6**. Thermal ellipsoids drawn at 30% probability. Hydrogen atoms, except on the phosphalkene unit (C1 and C31), are omitted for clarity. Selected bond lengths (Å) and angles (°) of **6**: P1–C1 1.678(6), P2–C31 1.699(7), C1–C2 1.419(8), C31–C32 1.407(12), P1–Ir 2.2097(16), P2–Ir 2.2032(15), N1–Ir 2.122(4), N2–Ir 2.115(5), Ir–N3 2.157(5); C2–C1–P1 113.8(5), C32–C31–P2 112.5(5), P1–Ir–P2 127.21(6), N1–Ir–N3 91.97(19), N2–Ir–N3 93.88(19), P1–Ir–N3 115.27(13), P2–Ir–N3 117.51(14), N1–Ir–N2 174.1(2), P1–Ir–N1 80.65(13), P2–Ir–N2 80.32(16), C1–P1–C11 115.6(3), C31–P2–C41 117.0(3).

central Ir atom ( $\tau_5 = 0.78$ ). In order to show that pyridine coordination is general, complex **5** was treated with 4-(dimethylamino)pyridine (DMAP) in the presence of AgOTf in  $\text{CH}_2\text{Cl}_2$ , producing complex  $[(\text{quin-CH=PMes}^*)_2\text{Ir}(\text{dmap})]\text{OTf}$  (**7**) in 87% isolated yield (Scheme 2), which was fully characterised by elemental analysis, NMR spectroscopy ( $\delta(^{31}\text{P}\{^1\text{H}\})$  245.5 ppm), and infrared spectroscopy. As expected, the spectroscopic data of the DMAP complex **7** are similar to those of complex **6**.

Next, we observed that upon using acetonitrile, the reaction proceeded differently. Upon adding AgOTf to a  $\text{CH}_2\text{Cl}_2$ /acetonitrile (2 : 1) solution of complex **5**, the colour of the reaction mixture slowly changed from blue to red after stirring overnight at room temperature. The  $^{31}\text{P}\{^1\text{H}\}$  NMR spectrum featured two new doublets at 285.5 and 6.8 ppm, respectively, with a  $^2J_{\text{P-P}}$  coupling constant of approximately 11 Hz and an additional singlet at 246.7 ppm, which was assigned to the acetonitrile coordinated Ir(I) complex  $[(\text{quin-CH=PMes}^*)_2\text{Ir}(\text{NCMe})]\text{OTf}$  (**8a**).

Although strongly coordinating to group 9 metals,<sup>50</sup> acetonitrile is known to undergo replacement by stronger donors such as pyridine,<sup>51</sup> and complex **8a** slowly converted into the complex showing the two doublets at 285.5 and 6.8 ppm. The reaction can be accelerated by heating over a period of 12 h at 60 °C. SC-XRD experiments on weakly diffracting red crystals grown from a saturated dichloromethane solution layered with *n*-hexane revealed an unexpected C–H bond cleavage of both *o*-*t*Bu substituents on one of the Mes<sup>\*</sup>-substituents of the P,N-ligand (Fig. S10†). One hydrogen atom formally migrates from the *t*Bu group to the carbon atom of the P=C bond to form a phosphaindane moiety,<sup>29,52</sup> resulting in the loss of the P=C double bond. The second *t*Bu group undergoes cyclometalla-

tion to the Ir centre, resulting in the formation of Ir(III) hydride complex **8** (Scheme 2) that is characterised by a triplet signal in the  $^1\text{H}$  NMR spectrum at  $-22.1$  ppm for the Ir–H. Moreover, the presence of a terminal Ir–H was further supported by its stretching vibration at  $2349\text{ cm}^{-1}$  in the IR spectrum ( $\nu_{\text{calc}} = 2347\text{ cm}^{-1}$ ). In contrast, pyridine coordinated Ir(I) complex **6** and DMAP coordinated Ir(I) complex **7** remained intact upon heating overnight at 60 °C and start converting into complex **8** only upon prolonged heating at 80 °C along with the formation of some unidentified decomposition products (Fig. S25†).

UV-vis spectroscopic and computational analysis of the electronic structure of the Ir phosphalkene complexes (Fig. 4) indicates that the deep blue colour of the bis(phosphalkene) complex **5** stems from two longest wavelength absorptions ( $\lambda_{\text{calc}} = 692.0, 661.9\text{ nm}$ ), which are mainly local excitations at Ir, with partial metal to ligand charge transfer (MLCT) from Ir into the  $\pi^*$  of the P=C bonds. Both transitions are HOMO to LUMO or HOMO–1 to LUMO transitions, respectively. For complex **6**, the lowest energy absorption is found at 620 nm and can be assigned to similar local excitations found in complex **5**. However, the presence of pyridine significantly stabilises the HOMO, resulting in a widening of the HOMO–LUMO gap, which explains the blue-shift of the longest wavelength absorption. In the case of complex **8**, we found very good agreement between spectroscopic and computational values. Red coloured complex **8**, containing phosphaindane and cyclometallated fragments, formed by twofold C–H activation, shows intense band overlap at 521 nm, which can be attributed to a MLCT from Ir mainly into the  $\pi^*$  orbital of the intact phosphalkene.

### Ligand exchange reactions

Complex **5** was reacted with CO (1 atm) at room temperature in the presence of  $\text{NaBF}_4$  to form a turquoise solution of  $[(\text{quin-CH=PMes}^*)_2\text{Ir}(\text{CO})]\text{OTf}$  (**9**).

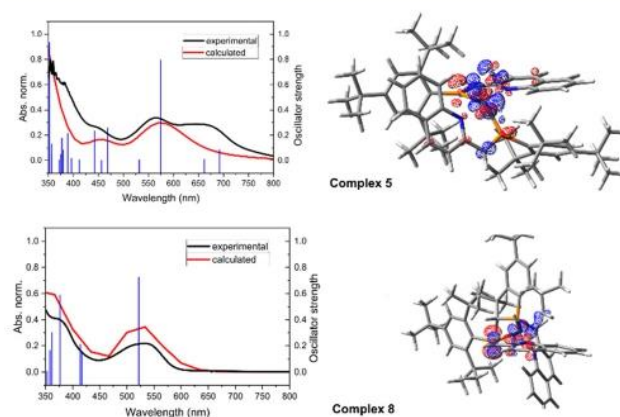


**Fig. 4** Left: comparison of experimental (black, 0.2 mM in  $\text{CH}_2\text{Cl}_2$ ) and calculated electronic absorption spectra (red) and oscillator strength of the transitions (blue) of complexes **5** (top) and **8** (bottom). Right: charge density difference between the ground state and the first excited state (red regions correspond to the electron, whereas blue regions indicate the electron hole).



$\text{CH}=\text{PMes}^*)_2\text{Ir}(\text{CO})\text{]} \text{BF}_4$  (**9**), which was found to exhibit a  $\nu_{\text{CO}}$  band at  $1978\text{ cm}^{-1}$  in the IR spectrum (Scheme 3). This value is higher than that of the neutral complex  $[\text{Ir}(\text{CO})(\text{PPEP}^*)]$  ( $\text{PPEP}^* = \text{deprotonated } 2\text{-(phospholanylmethyl)-6-(2-phosphaethenyl)pyridine}$ )<sup>29</sup> ( $\nu_{\text{CO}} = 1958\text{ cm}^{-1}$ ) and of the cationic species  $[\text{Ir}(\text{CO})(\text{PNP})]^+$  ( $\text{PNP} = 2,6\text{-bis}[(\text{di-}t\text{-tert-butylphosphino})\text{methyl}]\text{pyridine}$ )<sup>53</sup> ( $\nu_{\text{CO}} = 1962\text{ cm}^{-1}$ ). Hence, the iridium centre in **9** is more electron-deficient than in the related complexes. The presence of the carbonyl ligand was further evident from the  $^{13}\text{C}$  NMR triplet resonance at  $\delta$  168.9 ppm with a  $^2J_{\text{P-C}}$  coupling constant of 6.9 Hz. The molecular structure of carbonyl ligated iridium complex **9** was confirmed by SC-XRD analysis of a single crystal grown at room temperature from a saturated 1,2-difluorobenzene solution layered with *n*-hexane (Fig. S14†). However, the crystals were of poor quality and helped to only verify the connectivity but did not permit a discussion of structural parameters.

Transition-metal methyl complexes can be arguably considered the most important family of compounds with  $\sigma\text{-M-C}$  bonds. The chemistry of mononuclear methyl derivatives of iridium is largely dominated by the presence of tridentate P,C, P-,<sup>54,55</sup> P,N,P-,<sup>56–58</sup> N,N,P-,<sup>59</sup> and O,N,O-<sup>60</sup> ligands whereas reports on related bidentate ligand coordinated iridium methyl complexes are still rare. We attempted to synthesise methyl complex  $[(\text{quin-CH}=\text{PMes}^*)_2\text{IrCH}_3]$  (**10**) by nucleophilic methylation of the  $\text{Ir}(\text{i})$  precursor (**5**). An excess of  $(\text{CH}_3)_2\text{Mg}$  was added to a  $\text{CH}_2\text{Cl}_2$  solution of complex **5**, resulting in a turquoise-coloured solution of complex **10** (Scheme 3). The  $^1\text{H}$  NMR spectrum in  $\text{CD}_2\text{Cl}_2$  showed the expected three *t*Bu resonances of the  $\text{Mes}^*$  groups (18H each), and an upfield singlet at  $\delta$  0.91 (3H) in the alkyl region. Complex **10** was isolated as a crystalline solid, suitable for X-ray diffraction analysis (Fig. 5), in 68% yield. The  $\text{Ir-CH}_3$  distance ( $2.133(2)\text{ \AA}$ ) falls into the range of other reported  $\text{Ir-CH}_3$  distances ( $2.03\text{--}2.22\text{ \AA}$ ).<sup>61</sup>

To further evaluate the capability of complex **5** to engage in metathesis reactions, this species was stirred with an excess of sodium azide in THF at room temperature. The addition of lithium chloride as a phase-transfer catalyst<sup>62</sup> to solubilise

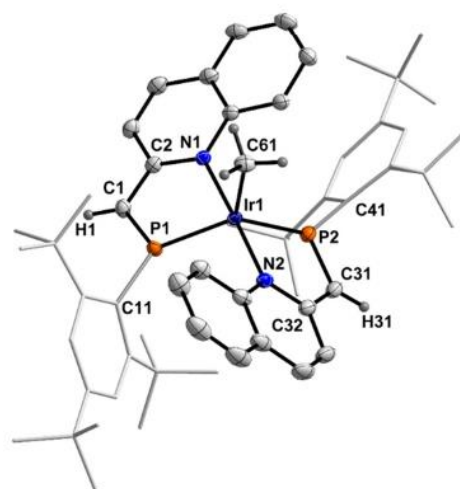
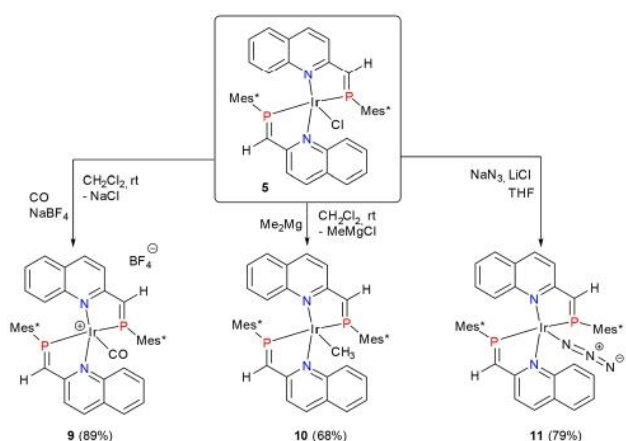


**Fig. 5** Molecular structure of complex **10**. Thermal ellipsoids drawn at 50% probability. Hydrogen atoms, except on the phosphalkene unit (C1 and C31), are omitted for clarity. Selected bond lengths ( $\text{\AA}$ ) and angles ( $^\circ$ ) of **10**: P1–C1 1.696(2), P2–C31 1.697(2), C1–C2 1.403(3), C31–C32 1.401(4), P1–Ir 2.1987(5), P2–Ir 2.2010(6), N1–Ir 2.1121(17), N2–Ir 2.1070(18), Ir–C61 2.133(2); C2–C1–P1 113.34(16), C32–C31–P2 113.67(17), P1–Ir–P2 131.77(2), N1–Ir–C61 90.30(8), N2–Ir–C61 91.92(8), P1–Ir–C61 115.17(7), P2–Ir–C61 113.06(7), N1–Ir–N2 177.53(7), P1–Ir–N1 80.63(5), P2–Ir–N2 80.53(5), C1–P1–C11 116.53(10), C31–P2–C41 116.66(11).

azide ions through conversion of insoluble  $\text{NaN}_3$  into soluble  $\text{LiN}_3$  and  $\text{NaCl}$  proved to be efficient in reducing the reaction time to 7–10 days, allowing for the isolation of iridium azide complex **11** as a dark green solid in an isolated yield of 79% after workup (Scheme 3). Single crystals grown from a saturated THF solution layered with *n*-hexane were characterised in a SC-XRD experiment, confirming the structural motif with an azide group in the trigonal plane of an overall distorted bipyramidal structure (Fig. S21†). The found connectivity is in line with a strong IR band for the terminal azide at  $\nu_{\text{NN}} = 2020\text{ cm}^{-1}$  and a single signal in the  $^{31}\text{P}\{^1\text{H}\}$  NMR spectrum at 243 ppm. For a comparison of the most important structural and spectroscopic data of all Ir P,N phosphalkene complexes discussed in this manuscript see Table 1.

#### N-Alkylation of aniline with benzyl alcohol catalysed by **5** and **6**

Having a set of new P,N-type phosphalkene-based  $\text{Ir}(\text{i})$  complexes in hand, we next wanted to evaluate their activity in the catalytic *N*-alkylation of aniline with benzyl alcohol using  $\text{KOtBu}$  as an external base. Kempe and co-workers have developed novel iridium(*i*) complexes coordinated with P,N chelate ligands, which exhibit high catalytic performance in the *N*-alkylation of aromatic primary amines, in conjunction with a stoichiometric amount of  $\text{KOtBu}$ .<sup>63–65</sup> The use of iridium(*i*) bearing a P,N,P pincer-type phosphalkene ligand (BPEP-H) toward *N*-alkylation of primary and secondary amines with alcohols is well-precedented.<sup>13</sup> We have tested the catalytic activity of complex **5** and pyridine-coordinated cationic Ir complex **6**. The model reaction of aniline and benzyl alcohol was performed at  $100\text{ }^\circ\text{C}$  for 24 h in THF using 1 mmol of each



**Scheme 3** Synthesis of  $\text{Ir}(\text{i})$  complexes (**9**, **10** and **11**).



## Research Article

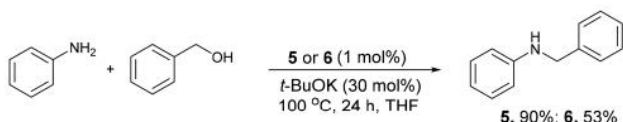
## Inorganic Chemistry Frontiers

substrate, 30 mol% of *t*BuOK and 1 mol% of precatalyst **5** and **6**, respectively (Scheme 4).

The catalytic reaction successfully proceeded with complete conversion to obtain *N*-benzylaniline (90% yield) catalysed by **5**, whereas no formation of PhN(CH<sub>2</sub>Ph)<sub>2</sub> as a dialkylation product was detected. On the other hand, the reaction catalysed by **6** afforded *N*-benzylaniline in only 53% yield in addition to PhN=CHPh (16%). The reduced catalytic activity of complex **6** towards *N*-alkylation of aniline with benzyl alcohol can be attributed to the instability of the complex at higher temperatures. As discussed above, prolonged heating of complex **6** transforms this species into doubly C–H activated Ir (III) complex **8**, which is not catalytically active.

### Upgrading of ethanol and methanol to iso-butanol catalysed by **5**

The Guerbet-type upgrading of ethanol to *n*-butanol and ethanol/methanol to iso-butanol is of considerable recent interest because of the use of these C<sub>4</sub> alcohols as advanced biofuels.<sup>66–69</sup> Upon using 0.1 mol% of catalyst **5**, a rather low conversion (30%) of ethanol and a low yield of the desired iso-butanol although high selectivity in the liquid fraction (93%) was obtained after two hours (Table 2, entry 1). The discrepancy between conversion of ethanol and product yield is due to the formation of solid and gaseous side products *via* competing pathways as observed in previous studies.<sup>55</sup> Extending the reaction time to 20 h led to a small increase in iso-butanol yield (36%) with high selectivity (91%) (entry 2). The addition



**Scheme 4** *N*-Alkylation of aniline (1 mmol) with benzyl alcohol (1 mmol) catalysed by complexes **5** or **6**.

**Table 2** Iridium catalysed conversion of ethanol and methanol to iso-butanol (A)

Entry	[ <b>5</b> ] [mol%]	<i>t</i> [h]	Conversion EtOH <sup>a</sup> [%]	Yield (A) i-BuOH <sup>b,c</sup> [%]	Yield (B) n-PrOH <sup>b,c</sup> [%]
1	0.1	2	30	19 (93)	1.5 (7)
2	0.1	20	74	36 (91)	2.5 (6)
3 <sup>d</sup>	0.1	20	65	33 (90)	2.5 (7)
4	0.25	20	80	60 (93)	2.3 (4)
5	0.25	2	47	35 (88)	3.0 (7)

<sup>a</sup>Total conversion of ethanol as determined by GC analysis of the reaction mixture revealed the presence of some unidentified side products.

<sup>b</sup>Yield and selectivity in the liquid fraction determined by GC using hexadecane as internal standard. <sup>c</sup>Selectivities for the respective alcohol are given in parentheses. <sup>d</sup>0.1 mol% of PPh<sub>3</sub> was also added.

of triphenylphosphine had little effect on the catalysis (entry 3). Interestingly, use of 0.25 mol% of **5** achieved 80% conversion of ethanol in 60% yield of iso-butanol with high selectivity after 20 h of reaction (entry 4). Reducing the reaction time to 2 h led to a decrease in both iso-butanol yield (35%) and selectivity (88%) (entry 5).

As a likely mechanistic scenario, methanol and ethanol are dehydrogenated to formaldehyde and acetaldehyde *via* a transient iridium alkoxide species, producing a metal hydride complex. Aldol coupling yields, after rehydrogenation, *n*-propanol. A further dehydrogenation, aldol coupling, re-hydrogenation cycle with a second equivalent of methanol yields iso-butanol.<sup>70,71</sup> The facile β elimination of aldehyde to produce Ir hydrides was probed in a control experiment where NaOEt was added to precatalyst **5** at room temperature, yielding a mixture of hydride species that could not be isolated (Fig. S27†). These preliminary results showed the potential of complex **5** as an effective precatalyst for the upgrading of ethanol/methanol mixtures to iso-butanol. This demonstrates the first use of a P,N-type phosphalkene based iridium complex in Guerbet-type catalysis.

## Conclusion

In summary, we have presented the synthesis and characterisation of iridium(I) complex **5** bearing two P,N-type phosphalkene ligands, which produces cationic complexes **6**, **7**, and **8** in salt metathesis reactions with AgOTf in different coordinating solvents. In the presence of acetonitrile, the unexpected cyclo-metallation of the second *o*-*t*Bu substituent of the Mes\* ligand to afford the Ir(III) monohydride species (**8**) was observed. We have for the first time rationalised such ligand activation reactivity for P,N-type ligands coordinated to Ir(I) by spectroscopic and computational analysis. Complex **5** showcases a diverse coordination chemistry, ranging from carbonyl coordination, to give electron-deficient Ir complex **9**, to nucleophilic methylation using organometallic reagent, (CH<sub>3</sub>)<sub>2</sub>Mg, affording Ir–CH<sub>3</sub> complex **10**. Additionally, we have demonstrated the catalytic activity of complexes **5** and **6** towards *N*-alkylation of aniline with benzyl alcohol. While the catalytic activity of complex **6** is rather low, complex **5** has proven to be reactive towards aniline. Complex **5** was also an effective pre-catalyst for the upgrading of ethanol/methanol mixtures to iso-butanol in 60% yield and 93% selectivity over 20 hours. Future studies will aim at further evaluating their catalytic potential towards *N*-alkylation of amines with a variety of primary and secondary alcohols and other alcohol upgrading processes such as ethanol homocoupling to *n*-butanol. Of particular interest will be the potential of Ir(III)-hydrido complex **8** to act as a catalyst in catalytic dehydrogenation reactions.

## Author contributions

P.G. designed and performed the experiments. H.-J.D. and C. H.-J. performed the X-ray experiments and analysed the data.



P.G. carried out the DFT calculations. R.W. and D.W. supervised the Guerbet catalytic reaction. P.G., H.-J.D., R.W., D.W., E.B., T.B. and C.H.-J. discussed the data. T.B. and C.H.-J. proposed and supervised the project. P.G., T.B. and C.H.-J. prepared and revised the manuscript.

## Conflicts of interest

There are no conflicts to declare.

## Acknowledgements

We thank our technical and analytical staff for assistance. Financial support by LIKAT (PhD fellowship for P. G.) is gratefully acknowledged. C. H.-J. thanks the Leibniz Association for funding within the scope of the Leibniz ScienceCampus Phosphorus Research Rostock (<https://www.sciencecampus-rostock.de>). C. H.-J. (Material Allowance) wishes to thank the Fonds der Chemischen Industrie for financial support. P. G. wishes to thank the ITMZ at the University of Rostock for access to the Cluster Computer and especially M. Willert for technical support.

## References

- 1 L. Weber, Recent developments in the chemistry of metallo-phosphaalkenes, *Coord. Chem. Rev.*, 2005, **249**, 741–763.
- 2 P. L. Floch, Phosphaalkene, phospholyl and phosphinine ligands: New tools in coordination chemistry and catalysis, *Coord. Chem. Rev.*, 2006, **250**, 627–681.
- 3 M. Doux, A. Moores, N. Mézailles, L. Ricard, Y. Jean and P. L. Floch, The CO/PC analogy in coordination chemistry and catalysis, *J. Organomet. Chem.*, 2005, **690**, 2407–2415.
- 4 B. Deschamps, X. Le Goff, L. Ricard and P. Le Floch, Phosphaalkenes palladium(II) complexes in the Suzuki and Sonogashira cross-coupling reactions, *Heteroat. Chem.*, 2007, **18**, 363–371.
- 5 F. Ozawa and M. Yoshifuji, Catalytic applications of transition-metal complexes bearing diphosphinidenecyclobutenes (DPCB), *Dalton Trans.*, 2006, 4987–4995.
- 6 A. Ziolkowska, J. Doroszkuk and Ł. Ponikiewski, *Organometallics*, 2023, DOI: <https://doi.org/10.1021/acs.organomet.2c00379>.
- 7 T. Minami, H. Okamoto, S. Ikeda, R. Tanaka, F. Ozawa and M. Yoshifuji, ( $\eta^3$ -Allyl)palladium complexes bearing diphosphinidenecyclobutene ligands: Highly active catalysts for the hydroamination of 1,3-dienes, *Angew. Chem., Int. Ed.*, 2001, **40**, 4501–4503.
- 8 F. Ozawa, H. Okamoto, S. Kawagishi, S. Yamamoto, T. Minami and M. Yoshifuji, ( $\pi$ -Allyl)palladium complexes bearing diphosphinidenecyclobutene ligands (DPCB): Highly active catalysts for direct conversion of allylic alcohols, *J. Am. Chem. Soc.*, 2002, **124**, 10968–10969.
- 9 F. Ozawa, T. Ishiyama, S. Yamamoto, S. Kawagishi, H. Murakami and M. Yoshifuji, Catalytic C–O bond cleavage of allylic alcohols using diphosphinidenecyclobutene-coordinated palladium complexes. A mechanistic study, *Organometallics*, 2004, **23**, 1698–1707.
- 10 M. Nagao, K. Asano, K. Umeda, H. Katayama and F. Ozawa, Highly (Z)-selective hydrosilylation of terminal alkynes catalyzed by a diphosphinidenecyclobutene-coordinated ruthenium complex: Application to the synthesis of (Z,Z)-bis(2-bromoethenyl)arenes, *J. Org. Chem.*, 2005, **70**, 10511–10514.
- 11 A. Hayashi, T. Yoshitomi, K. Umeda, M. Okazaki and F. Ozawa, Synthesis and reactions of diphosphinidenecyclobutene ruthenium complexes relevant to catalytic hydrosilylation of terminal alkynes, *Organometallics*, 2008, **27**, 2321–2327.
- 12 A. Hayashi, M. Okazaki, F. Ozawa and R. Tanaka, Synthesis, structures, and catalytic properties of late-transition-metal 2,6-bis(2-phosphaethenyl)pyridine complexes, *Organometallics*, 2007, **26**, 5246–5249.
- 13 Y.-H. Chang, Y. Nakajima and F. Ozawa, A bis(phosphaethenyl)pyridine complex of iridium(III): Synthesis and catalytic application to N-alkylation of amines with alcohols, *Organometallics*, 2013, **32**, 2210–2215.
- 14 M. H. S. Hamid, P. A. Slatford and J. M. Williams, Borrowing hydrogen in the activation of alcohols, *Adv. Synth. Catal.*, 2007, **349**, 1555–1575.
- 15 G. Guillena, D. J. Ramon and M. Yus, Hydrogen autotransfer in the N-alkylation of amines and related compounds using alcohols and amines as electrophiles, *Chem. Rev.*, 2010, **110**, 1611–1641.
- 16 S. Bähn, S. Imm, L. Neubert, M. Zhang, H. Neumann and M. Beller, The catalytic amination of alcohols, *ChemCatChem*, 2011, **3**, 1853–1864.
- 17 D. Hollmann, A. Tillack, D. Michalik, R. Jackstell and M. Beller, An improved ruthenium catalyst for the environmentally benign amination of primary and secondary alcohols, *Chem. – Asian J.*, 2007, **2**, 403–410.
- 18 A. Tillack, D. Hollmann, D. Michalik and M. Beller, A novel ruthenium-catalyzed amination of primary and secondary alcohols, *Tetrahedron Lett.*, 2006, **47**, 8881–8885.
- 19 M. Zhang, S. Imm, S. Bähn, H. Neumann and M. Beller, Synthesis of  $\alpha$ -amino acid amides: Ruthenium-catalyzed amination of  $\alpha$ -hydroxy amides, *Angew. Chem.*, 2011, **123**, 11393–11397.
- 20 M. Onoda and K.-i. Fujita, Iridium-catalyzed C-alkylation of methyl group on N-heteroaromatic compounds using alcohols, *Org. Lett.*, 2020, **22**, 7295–7299.
- 21 A. JohnáBlacker and M. Jonathan, Iridium-catalysed amine alkylation with alcohols in water, *Chem. Commun.*, 2010, **46**, 1541–1543.
- 22 N. Andrushko, V. Andrushko, P. Roose, K. Moonen and A. Börner, Amination of aliphatic alcohols and diols with an iridium pincer catalyst, *ChemCatChem*, 2010, **2**, 640–643.



## Research Article

## Inorganic Chemistry Frontiers

- 23 F. Li, H. Shan, L. Chen, Q. Kang and P. Zou, Direct N-alkylation of amino-azoles with alcohols catalyzed by an iridium complex/base system, *Chem. Commun.*, 2011, **48**, 603–605.
- 24 M. P. Carroll and P. J. Guiry, P, N ligands in asymmetric catalysis, *Chem. Soc. Rev.*, 2014, **43**, 819–833.
- 25 J. Margalef, M. Biosca, P. de la Cruz Sánchez, J. Faiges, O. Pamies and M. Dieguez, Evolution in heterodonor PN, PS and PO chiral ligands for preparing efficient catalysts for asymmetric catalysis. From design to applications, *Coord. Chem. Rev.*, 2021, **446**, 214120.
- 26 A. Jouaiti, M. Geoffroy, G. Terron and G. Bernardinelli, Synthesis, structure and ligand-centred reduction of an orthometallated complex of palladium containing two phosphalkene groups, *J. Chem. Soc., Chem. Commun.*, 1992, 155–156.
- 27 H. Kawanami, K. Toyota and M. Yoshifuji, Preparation and Palladium Complex Formation of Several (2-Phosphaethenyl)benzenes, *Chem. Lett.*, 1996, **25**, 533–534.
- 28 M. van der Sluis, V. Beverwijk, A. Termaten, E. Gavrilova, F. Bickelhaupt, H. Kooijman, N. Veldman and A. L. Spek, Synthesis of 2-(2-Pyridyl)phosphaalkenes [Mes\*PC(R)Py] (R = H, SiMe<sub>3</sub>) and Their Complexes  $\eta^1, \eta^1$ -[Mes\*PC(R)Py]XPdCl (X = Cl, Me, Ac), *Organometallics*, 1997, **16**, 1144–1152.
- 29 Y.-H. Chang, Y. Nakajima, H. Tanaka, K. Yoshizawa and F. Ozawa, Facile N–H Bond Cleavage of Ammonia by an Iridium Complex Bearing a Noninnocent PNP-Pincer Type Phosphaalkene Ligand, *J. Am. Chem. Soc.*, 2013, **135**, 11791–11794.
- 30 M. van der Sluis, V. Beverwijk, A. Termaten, F. Bickelhaupt, H. Kooijman and A. L. Spek, Synthesis of Novel Phosphaalkene-Based Bidentate Ligands Mes\*PCH(3-R-Ar) (R = Pyridyl, Carbaldimino) and Formation of Three-Membered Palladacycles Mes\*(Me)P–CH(3-R-Ar)–PdCl by Carbapalladation of the PC Double Bond, *Organometallics*, 1999, **18**, 1402–1407.
- 31 P. Gupta, J.-E. Siewert, T. Wellnitz, M. Fischer, W. Baumann, T. Beweries and C. Hering-Junghans, Reactivity of phospho-Wittig reagents towards NHCs and NHOs, *Dalton Trans.*, 2021, **50**, 1838–1844.
- 32 P. Gupta, T. Taeufer, J.-E. Siewert, F. Reiß, H.-J. Drexler, J. Pospech, T. Beweries and C. Hering-Junghans, Synthesis, Coordination Chemistry, and Mechanistic Studies of P, N-Type Phosphaalkene-Based Rh(i) Complexes, *Inorg. Chem.*, 2022, **61**, 11639–11650.
- 33 G. R. Dowson, M. F. Haddow, J. Lee, R. L. Wingad and D. F. Wass, Catalytic conversion of ethanol into an advanced biofuel: unprecedented selectivity for n-butanol, *Angew. Chem., Int. Ed.*, 2013, **52**, 9005–9008.
- 34 R. L. Wingad, P. J. Gates, S. T. Street and D. F. Wass, Catalytic conversion of ethanol to n-butanol using ruthenium P–N ligand complexes, *ACS Catal.*, 2015, **5**, 5822–5826.
- 35 K.-N. T. Tseng, S. Lin, J. W. Kampf and N. K. Szymczak, Upgrading ethanol to 1-butanol with a homogeneous air-stable ruthenium catalyst, *Chem. Commun.*, 2016, **52**, 2901–2904.
- 36 Y. Xie, Y. Ben-David, L. J. Shimon and D. Milstein, Highly efficient process for production of biofuel from ethanol catalyzed by ruthenium pincer complexes, *J. Am. Chem. Soc.*, 2016, **138**, 9077–9080.
- 37 A. M. Davies, Z.-Y. Li, C. R. Stephenson and N. K. Szymczak, Valorization of Ethanol: Ruthenium-Catalyzed Guerbet and Sequential Functionalization Processes, *ACS Catal.*, 2022, **12**, 6729–6736.
- 38 R. L. Wingad, E. J. Bergström, M. Everett, K. J. Pellow and D. F. Wass, Catalytic conversion of methanol/ethanol to isobutanol—a highly selective route to an advanced biofuel, *Chem. Commun.*, 2016, **52**, 5202–5204.
- 39 K. J. Pellow, R. L. Wingad and D. F. Wass, Towards the upgrading of fermentation broths to advanced biofuels: a water tolerant catalyst for the conversion of ethanol to isobutanol, *Catal. Sci. Technol.*, 2017, **7**, 5128–5134.
- 40 K. Koda, T. Matsu-ura, Y. Obora and Y. Ishii, Guerbet reaction of ethanol to n-butanol catalyzed by iridium complexes, *Chem. Lett.*, 2009, **38**, 838–839.
- 41 G. Xu, T. Lammens, Q. Liu, X. Wang, L. Dong, A. Caiazzo, N. Ashraf, J. Guan and X. Mu, Direct self-condensation of bio-alcohols in the aqueous phase, *Green Chem.*, 2014, **16**, 3971–3977.
- 42 S. Chakraborty, P. E. Piszal, C. E. Hayes, R. T. Baker and W. D. Jones, Highly selective formation of n-butanol from ethanol through the Guerbet process: A tandem catalytic approach, *J. Am. Chem. Soc.*, 2015, **137**, 14264–14267.
- 43 M. Wilklow-Marnell and W. W. Brennessel, A POCO type pincer complex of iridium: Synthesis, characterization, and catalysis, *Polyhedron*, 2019, **160**, 83–91.
- 44 Q. Liu, G. Xu, X. Wang and X. Mu, Selective upgrading of ethanol with methanol in water for the production of improved biofuel—isobutanol, *Green Chem.*, 2016, **18**, 2811–2818.
- 45 A. G. Blackman, E. B. Schenk, R. E. Jelley, E. H. Krensch and L. R. Gahan, Five-coordinate transition metal complexes and the value of  $\tau_5$ : observations and caveats, *Dalton Trans.*, 2020, **49**, 14798–14806.
- 46 A. W. Addison, T. N. Rao, J. Reedijk, J. van Rijn and G. C. Verschoor, Synthesis, structure, and spectroscopic properties of copper(II) compounds containing nitrogen-sulphur donor ligands; the crystal and molecular structure of aqua[1,7-bis(N-methylbenzimidazol-2'-yl)-2,6-dithiaheptane]copper(II) perchlorate, *J. Chem. Soc., Dalton Trans.*, 1984, 1349–1356.
- 47 E. Ben-Ari, G. Leitun, L. J. Shimon and D. Milstein, Metal–Ligand Cooperation in C–H and H<sub>2</sub> Activation by an Electron-Rich PNP Ir(i) System: Facile Ligand Dearomatization–Aromatization as Key Steps, *J. Am. Chem. Soc.*, 2006, **128**, 15390–15391.
- 48 E. Ben-Ari, R. Cohen, M. Gandelman, L. J. Shimon, J. M. Martin and D. Milstein, ortho C–H Activation of



- Haloarenes and Anisole by an Electron-Rich Iridium(I) Complex: Mechanism and Origin of Regio- and Chemoselectivity. An Experimental and Theoretical Study, *Organometallics*, 2006, **25**, 3190–3210.
- 49 W. H. Bernskoetter, S. K. Hanson, S. K. Buzak, Z. Davis, P. S. White, R. Swartz, K. I. Goldberg and M. Brookhart, Investigations of Iridium-Mediated Reversible C–H Bond Cleavage: Characterization of a 16-Electron Iridium(III) Methyl Hydride Complex, *J. Am. Chem. Soc.*, 2009, **131**, 8603–8613.
- 50 N. Jannsen, C. Fischer, C. Selle, C. Pribbenow, H.-J. Drexler, F. Reiß, T. Beweries and D. Heller, How solvents affect the stability of cationic Rh(I) diphosphine complexes: a case study of MeCN coordination, *Dalton Trans.*, 2022, **51**, 18068–18076.
- 51 L. Palacios, A. Di Giuseppe, R. Castarlenas, F. J. Lahoz, J. J. Pérez-Torrente and L. A. Oro, Pyridine versus acetonitrile coordination in rhodium–N-heterocyclic carbene square-planar complexes, *Dalton Trans.*, 2015, **44**, 5777–5789.
- 52 S. Shah, M. C. Simpson, R. C. Smith and J. D. Protasiewicz, Three Different Fates for Phosphinidenes Generated by Photocleavage of Phospha-Wittig Reagents ArP PMe<sub>3</sub>, *J. Am. Chem. Soc.*, 2001, **123**, 6925–6926.
- 53 L. Schwartzburd, M. A. Iron, L. Konstantinovski, Y. Diskin-Posner, G. Leitun, L. J. W. Shimon and D. Milstein, Synthesis and Reactivity of an Iridium(I) Acetyl PNP Complex. Experimental and Computational Study of Metal–Ligand Cooperation in H–H and C–H Bond Activation via Reversible Ligand Dearomatization, *Organometallics*, 2010, **29**, 3817–3827.
- 54 J. J. Adams, N. Arulsamy and D. M. Roddick, Acceptor PCP Pincer Iridium(I) Chemistry: Stabilization of Nonmeridional PCP Coordination Geometries, *Organometallics*, 2011, **30**, 697–711.
- 55 S. Kundu, J. Choi, D. Y. Wang, Y. Choliy, T. J. Emge, K. Krogh-Jespersen and A. S. Goldman, Cleavage of Ether, Ester, and Tosylate C(sp<sup>3</sup>)–O Bonds by an Iridium Complex, Initiated by Oxidative Addition of C–H Bonds. Experimental and Computational Studies, *J. Am. Chem. Soc.*, 2013, **135**, 5127–5143.
- 56 M. D. Walter, P. S. White, C. K. Schauer and M. Brookhart, The quest for stable  $\sigma$ -methane complexes: computational and experimental studies, *New J. Chem.*, 2011, **35**, 2884–2893.
- 57 J. Campos, S. Kundu, D. R. Pahls, M. Brookhart, E. Carmona and T. R. Cundari, Mechanism of Hydrogenolysis of an Iridium–Methyl Bond: Evidence for a Methane Complex Intermediate, *J. Am. Chem. Soc.*, 2013, **135**, 1217–1220.
- 58 J. G. Melnick, A. T. Radosevich, D. Villagrán and D. G. Nocera, Decarbonylation of ethanol to methane, carbon monoxide and hydrogen by a [PNP]Ir complex, *Chem. Commun.*, 2010, **46**, 79–81.
- 59 N. G. Leonard, P. G. Williard and W. H. Bernskoetter, Synthesis and coordination chemistry of organoiridium complexes supported by an anionic tridentate ligand, *Dalton Trans.*, 2011, **40**, 4300–4306.
- 60 R. Fu, J. E. Bercaw and J. A. Labinger, Intra- and Intermolecular C–H Activation by Bis(phenolate)pyridineiridium(III) Complexes, *Organometallics*, 2011, **30**, 6751–6765.
- 61 C. L. Pitman and A. J. M. Miller, Photochemical Production of Ethane from an Iridium Methyl Complex, *Organometallics*, 2017, **36**, 1906–1914.
- 62 M. Gediga, S. Burck, J. Bender, D. Förster, M. Nieger and D. Gudat, Specific and Reversible Alkynyl Transfer Reactions of an N-Heterocyclic Phosphane, *Eur. J. Inorg. Chem.*, 2014, **2014**, 1818–1825.
- 63 S. Michlik, T. Hille and R. Kempe, The Iridium-Catalyzed Synthesis of Symmetrically and Unsymmetrically Alkylated Diamines under Mild Reaction Conditions, *Adv. Synth. Catal.*, 2012, **354**, 847–862.
- 64 B. Blank, M. Madalska and R. Kempe, An Efficient Method for the Selective Iridium-Catalyzed Monoalkylation of (Hetero)aromatic Amines with Primary Alcohols, *Adv. Synth. Catal.*, 2008, **350**, 749–758.
- 65 B. Blank, S. Michlik and R. Kempe, Synthesis of Selectively Mono-N-Arylated Aliphatic Diamines via Iridium-Catalyzed Amine Alkylation, *Adv. Synth. Catal.*, 2009, **351**, 2903–2911.
- 66 (a) H. Aitchison, R. L. Wingad and D. F. Wass, Homogeneous Ethanol to Butanol Catalysis- Guerbet Renewed, *ACS Catal.*, 2016, **6**, 7125–7132; (b) Y. Xie, Y. Ben-David, L. J. W. Shimon and D. Milstein, Highly Efficient Process for Production of Biofuel from Ethanol Catalyzed by Ruthenium Pincer Complexes, *J. Am. Chem. Soc.*, 2016, **138**, 9077–9080.
- 67 J. T. Kozłowski and R. J. Davis, Heterogeneous catalysts for the Guerbet coupling of alcohols, *ACS Catal.*, 2013, **3**, 1588–1600.
- 68 A. Galadima and O. Muraza, Catalytic upgrading of bioethanol to fuel grade biobutanol: a review, *Ind. Eng. Chem. Res.*, 2015, **54**, 7181–7194.
- 69 D. Gabriëls, W. Y. Hernández, B. Sels, P. Van Der Voort and A. Verberckmoes, Review of catalytic systems and thermodynamics for the Guerbet condensation reaction and challenges for biomass valorization, *Catal. Sci. Technol.*, 2015, **5**, 3876–3902.
- 70 M. H. S. A. Hamid, P. A. Slatford and J. M. J. Williams, Borrowing Hydrogen in the Activation of Alcohols, *Adv. Synth. Catal.*, 2007, **349**, 1555–1575.
- 71 L. M. Kabadwal, S. Bera and D. Banerjee, Recent advances in sustainable organic transformations using methanol: expanding the scope of hydrogen-borrowing catalysis, *Org. Chem. Front.*, 2021, **8**, 7077–7096.



## 7 References

- [1] K. B. Dillon, F. Mathey, J. F. Nixon, *Phosphorus: the carbon copy: from organophosphorus to phospho-organic chemistry*, Wiley-Blackwell, **1998**.
- [2] F. Mathey, *Phosphorus-carbon heterocyclic chemistry*, Elsevier, **2001**.
- [3] T. Gier, *Journal of the American Chemical Society* **1961**, *83*, 1769-1770.
- [4] K. Dimroth, P. Hoffmann, *Chem. Ber.* **1966**, *99*, 1325-1331.
- [5] G. Märkl, *Angew. Chem.* **1966**, *78*, 907-908.
- [6] A. J. Ashe III, *Journal of the American Chemical Society* **1971**, *93*, 3293-3295.
- [7] G. Becker, **1976**.
- [8] T. C. Klebach, R. Lourens, F. Bickelhaupt, *Journal of the American Chemical Society* **1978**, *100*, 4886-4888.
- [9] J. I. Bates, J. Dugal-Tessier, D. P. Gates, *Dalton Trans.* **2010**, *39*, 3151-3159.
- [10] F. Ozawa, M. Yoshifuji, *Dalton Trans.* **2006**, 4987-4995.
- [11] P. Le Floch, *Coord. Chem. Rev.* **2006**, *250*, 627-681.
- [12] D. P. Gates, *New Aspects in Phosphorus Chemistry V* **2005**, 107-126.
- [13] L. Weber, *Coord. Chem. Rev.* **2005**, *249*, 741-763.
- [14] F. Mathey, *Angew. Chem. Int. Ed.* **2003**, *42*, 1578-1604.
- [15] S. Shah, J. D. Protasiewicz, *Coord. Chem. Rev.* **2000**, *210*, 181-201.
- [16] P. L. Floch, *Coord. Chem. Rev.* **2006**, *250*, 627-681.
- [17] M. Regitz, O. J. Scherer, R. Appel, *Multiple bonds and low coordination in phosphorus chemistry*, Thieme Medical Publishers, **1990**.
- [18] M. W. Schmidt, P. N. Truong, M. S. Gordon, *Journal of the American Chemical Society* **1987**, *109*, 5217-5227.
- [19] P. v. R. Schleyer, D. Kost, *Journal of the American Chemical Society* **1988**, *110*, 2105-2109.
- [20] M. Doux, A. Moores, N. Mézailles, L. Ricard, Y. Jean, P. Le Floch, *J. Organomet. Chem.* **2005**, *690*, 2407-2415.
- [21] G. Recker, *Z. Anorg. Allg. Chem.* **1976**, *423*, 242-254.
- [22] R. Appel, C. Casser, M. Immenkeppel, F. Knoch, *Angewandte Chemie International Edition in English* **1984**, *23*, 895-896.
- [23] A. Jouaiti, M. Geoffroy, G. Bernardinelli, *Tetrahedron Letters* **1992**, *33*, 5071-5074.
- [24] H. Kawanami, K. Toyota, M. Yoshifuji, *Chem. Lett.* **1996**, *25*, 533-534.
- [25] M. Yam, J. H. Chong, C.-W. Tsang, B. O. Patrick, A. E. Lam, D. P. Gates, *Inorg. Chem.* **2006**, *45*, 5225-5234.
- [26] O. Riant, O. Samuel, H. B. Kagan, *Journal of the American Chemical Society* **1993**, *115*, 5835-5836.
- [27] H.-o. Taguchi, D. Sasaki, K. Takeuchi, S. Tsujimoto, T. Matsuo, H. Tanaka, K. Yoshizawa, F. Ozawa, *Organometallics* **2016**, *35*, 1526-1533.
- [28] J. D. Protasiewicz, *Eur. J. Inorg. Chem.* **2012**, *2012*, 4539-4549.
- [29] S. Shah, J. D. Protasiewicz, *Chem. Commun.* **1998**, 1585-1586.
- [30] Y. Nakajima, Y. Okamoto, Y.-H. Chang, F. Ozawa, *Organometallics* **2013**, *32*, 2918-2925.
- [31] K. W. Magnuson, S. M. Oshiro, J. R. Gurr, W. Y. Yoshida, M. Gembicky, A. L. Rheingold, R. P. Hughes, M. F. Cain, *Organometallics* **2016**, *35*, 855-859.
- [32] P. M. Miura-Akagi, M. L. Nakashige, C. K. Maile, S. M. Oshiro, J. R. Gurr, W. Y. Yoshida, A. T. Royappa, C. E. Krause, A. L. Rheingold, R. P. Hughes, *Organometallics* **2016**, *35*, 2224-2231.
- [33] H.-o. Taguchi, D. Sasaki, K. Takeuchi, S. Tsujimoto, T. Matsuo, H. Tanaka, K. Yoshizawa, F. Ozawa, *Organometallics* **2016**, *35*, 1526-1533.
- [34] M. L. Nakashige, J. I. Loristo, L. S. Wong, J. R. Gurr, T. J. O'Donnell, W. Y. Yoshida, A. L. Rheingold, R. P. Hughes, M. F. Cain, *Organometallics* **2019**, *38*, 3338-3348.
- [35] P. Gupta, T. Taeufer, J.-E. Siewert, F. Reiß, H.-J. Drexler, J. Pospech, T. Beweries, C. Hering-Junghans, *Inorg. Chem.* **2022**, *61*, 11639-11650.
- [36] A. Marinetti, F. Mathey, *Angewandte Chemie International Edition in English* **1988**, *27*, 1382-1384.



- [37] R. C. Smith, S. Shah, E. Urnezis, J. D. Protasiewicz, *Journal of the American Chemical Society* **2003**, *125*, 40-41.
- [38] A. Schumann, F. Reiß, H. Jiao, J. Rabeah, J.-E. Siewert, I. Krummenacher, H. Braunschweig, C. Hering-Junghans, *Chemical Science* **2019**, *10*, 7859-7867.
- [39] Rhett C. Smith, T. Ren, John D. Protasiewicz, *Eur. J. Inorg. Chem.* **2002**, 2002, 2779-2783.
- [40] S. Shah, M. C. Simpson, R. C. Smith, J. D. Protasiewicz, *Journal of the American Chemical Society* **2001**, *123*, 6925-6926.
- [41] P. Gupta, J.-E. Siewert, T. Wellnitz, M. Fischer, W. Baumann, T. Beweries, C. Hering-Junghans, *Dalton Transactions* **2021**, *50*, 1838-1844.
- [42] C. Smit, T. A. Van der Knaap, F. Bickelhaupt, *Tetrahedron Lett.* **1983**, *24*, 2031-2034.
- [43] L. Weber, *Chem. Rev.* **1992**, *92*, 1839-1906.
- [44] P. Pyykkö, M. Atsumi, *Chemistry—A European Journal* **2009**, *15*, 186-197.
- [45] Y. Masaaki, S. Takahiro, I. Naoki, *Chem. Lett.* **1988**, *17*, 1735-1738.
- [46] U. J. Kilgore, H. Fan, M. Pink, E. Urnezis, J. D. Protasiewicz, D. J. Mindiola, *Chem. Commun.* **2009**, 4521-4523.
- [47] M. Fischer, F. Reiß, C. Hering-Junghans, *Chemical Communications* **2021**, *57*, 5626-5629.
- [48] T. Krachko, J. C. Sootweg, *Eur. J. Inorg. Chem.* **2018**, 2018, 2734-2754.
- [49] A. Doddi, M. Peters, M. Tamm, *Chem. Rev.* **2019**, *119*, 6994-7112.
- [50] K. Powers, C. Hering-Junghans, R. McDonald, M. J. Ferguson, E. Rivard, *Polyhedron* **2016**, *108*, 8-14.
- [51] M. M. Roy, E. Rivard, *Acc. Chem. Res.* **2017**, *50*, 2017-2025.
- [52] C. E. Knappke, J. M. Neudörfl, A. J. von Wangelin, *Organic & Biomolecular Chemistry* **2010**, *8*, 1695-1705.
- [53] M. Fischer, C. Hering-Junghans, *Chemical science* **2021**, *12*, 10279-10289.
- [54] H. Sitzmann, M. F. Lappert, C. Dohmeier, C. Üffing, H. Schnöckel, *J. Organomet. Chem.* **1998**, *561*, 203-208.
- [55] A. Hofmann, T. Tröster, T. Kupfer, H. Braunschweig, *Chemical science* **2019**, *10*, 3421-3428.
- [56] M. Fischer, S. Nees, T. Kupfer, J. T. Goettel, H. Braunschweig, C. Hering-Junghans, *Journal of the American Chemical Society* **2021**, *143*, 4106-4111.
- [57] F. Dankert, C. Hering-Junghans, *Chem. Commun.* **2022**, *58*, 1242-1262.
- [58] F. Dankert, J.-E. Siewert, P. Gupta, F. Weigend, C. Hering-Junghans, *Angew. Chem. Int. Ed.* **2022**, *61*, e202207064.
- [59] S. Holand, C. Charrier, F. Mathey, J. Fischer, A. Mitschler, *Journal of the American Chemical Society* **1984**, *106*, 826-828.
- [60] T. A. Van der Knaap, F. Bickelhaupt, J. G. Kraaykamp, G. Van Koten, J. P. Bernards, H. T. Edzes, W. S. Veeman, E. De Boer, E. J. Baerends, *Organometallics* **1984**, *3*, 1804-1811.
- [61] R. Apfel, C. Casser, F. Knoch, *J. Organomet. Chem.* **1985**, *293*, 213-217.
- [62] I.-P. Lorenz, W. Pohl, H. Nöth, M. Schmidt, *J. Organomet. Chem.* **1994**, *475*, 211-221.
- [63] K. Knoll, G. Huttner, M. Wasiucionek, L. Zsolnai, *Angewandte Chemie International Edition in English* **1984**, *23*, 739-740.
- [64] H. Eshtiagh-Hosseini, H. W. Kroto, J. F. Nixon, M. J. Maah, M. J. Taylor, *J. Chem. Soc., Chem. Commun.* **1981**, 199-200.
- [65] T. C. Klebach, R. Lourens, F. Bickelhaupt, C. H. Stam, A. Van Herk, *J. Organomet. Chem.* **1981**, *210*, 211-221.
- [66] H. W. Kroto, J. F. Nixon, M. J. Taylor, A. A. Frew, K. W. Muir, *Polyhedron* **1982**, *1*, 89-95.
- [67] F. Ozawa, M. Yoshifuji, *Comptes Rendus Chimie* **2004**, *7*, 747-754.
- [68] Q. Knijnenburg, S. Gambarotta, P. H. M. Budelaar, *Dalton Trans.* **2006**, 5442-5448.
- [69] V. C. Gibson, S. K. Spitzmesser, *Chem. Rev.* **2003**, *103*, 283-316.
- [70] K. Hayashi, M. Nakatani, A. Hayashi, M. Takano, M. Okazaki, K. Toyota, M. Yoshifuji, F. Ozawa, *Organometallics* **2008**, *27*, 1970-1972.
- [71] Y. Nakajima, M. Nakatani, K. Hayashi, Y. Shiraishi, R. Takita, M. Okazaki, F. Ozawa, *New J. Chem.* **2010**, *34*, 1713-1722.

- [72] Y. Nakajima, Y. Nakao, S. Sakaki, Y. Tamada, T. Ono, F. Ozawa, *Journal of the American Chemical Society* **2010**, *132*, 9934-9936.
- [73] Y. Nakajima, Y. Shiraishi, T. Tsuchimoto, F. Ozawa, *Chem. Commun.* **2011**, *47*, 6332-6334.
- [74] Y. Nakajima, T. Tsuchimoto, Y.-H. Chang, K. Takeuchi, F. Ozawa, *Dalton Trans.* **2016**, *45*, 2079-2084.
- [75] Y.-H. Chang, Y. Nakajima, F. Ozawa, *Organometallics* **2013**, *32*, 2210-2215.
- [76] Y.-H. Chang, Y. Nakajima, H. Tanaka, K. Yoshizawa, F. Ozawa, *Journal of the American Chemical Society* **2013**, *135*, 11791-11794.
- [77] P. Gupta, T. Taeufer, J.-E. Siewert, F. Reiß, H.-J. Drexler, J. Pospech, T. Beweries, C. Hering-Junghans, *Inorganic Chemistry* **2022**, *61*, 11639-11650.
- [78] A. Jouaiti, M. Geoffroy, G. Terron, G. Bernardinelli, *J. Chem. Soc., Chem. Commun.* **1992**, 155-156.
- [79] L. Weber, *Angew. Chem. Int. Ed.* **2002**, *41*, 563-572.
- [80] S. D. Ittel, L. K. Johnson, M. Brookhart, *Chem. Rev.* **2000**, *100*, 1169-1204.
- [81] S. Ikeda, F. Ohhata, M. Miyoshi, R. Tanaka, T. Minami, F. Ozawa, M. Yoshifuji, *Angew. Chem. Int. Ed.* **2000**, *39*, 4512-4513.
- [82] F. Ozawa, S. Kawagishi, T. Ishiyama, M. Yoshifuji, *Organometallics* **2004**, *23*, 1325-1332.
- [83] O. Daugulis, M. Brookhart, P. S. White, *Organometallics* **2002**, *21*, 5935-5943.
- [84] A. Ionkin, W. Marshall, *Chem. Commun.* **2003**, 710-711.
- [85] A. De Meijere, F. Diederich, A. de Meijere, *Metal-catalyzed cross-coupling reactions, Vol. 1*, Wiley-VCH Weinheim, **2004**.
- [86] E.-i. Negishi, L. Anastasia, *Chem. Rev.* **2003**, *103*, 1979-2018.
- [87] N. Miyaara, A. Suzuki, *Chem. Rev.* **1995**, *95*, 2457-2483.
- [88] P. Espinet, A. M. Echavarren, *Angew. Chem. Int. Ed.* **2004**, *43*, 4704-4734.
- [89] W. JP, *Buchwald SL. Acc. Chem. Res* **1998**, *31*, 805.
- [90] J. Hartwig, *Acc. Chem. Res* **1998**, *31*, 852.
- [91] S. V. Ley, A. W. Thomas, *Angew. Chem. Int. Ed.* **2003**, *42*, 5400-5449.
- [92] K. Toyota, K. Masaki, T. Abe, M. Yoshifuji, *Chem. Lett.* **1995**, *24*, 221-222.
- [93] H. Liang, K. Nishide, S. Ito, M. Yoshifuji, *Tetrahedron Lett.* **2003**, *44*, 8297-8300.
- [94] H. Liang, S. Ito, M. Yoshifuji, *Org. Lett.* **2004**, *6*, 425-427.
- [95] K. Nishide, H. Liang, S. Ito, M. Yoshifuji, *J. Organomet. Chem.* **2005**, *690*, 4809-4815.
- [96] S. Ito, H. Liang, *J. Organometal. Chem.* **2005**, *690*, 2531.
- [97] B. Deschamps, X. Le Goff, L. Ricard, P. Le Floch, *Heteroat. Chem* **2007**, *18*, 363-371.
- [98] K. Toyota, J. Ujita, S. Kawasaki, K. Abe, N. Yamada, M. Yoshifuji, *Tetrahedron Lett.* **2004**, *45*, 7609-7612.
- [99] A. S. Gajare, R. S. Jensen, K. Toyota, M. Yoshifuji, F. Ozawa, *Synlett* **2005**, *2005*, 144-148.
- [100] R. S. Jensen, A. S. Gajare, K. Toyota, M. Yoshifuji, F. Ozawa, *Tetrahedron Lett.* **2005**, *46*, 8645-8647.
- [101] M. Sundermeier, A. Zapf, M. Beller, *Angew. Chem. Int. Ed.* **2003**, *42*, 1661-1664.
- [102] F. Jin, P. N. Confalone, *Tetrahedron Lett.* **2000**, *41*, 3271-3273.
- [103] A. S. Gajare, K. Toyota, M. Yoshifuji, F. Ozawa, *The Journal of organic chemistry* **2004**, *69*, 6504-6506.
- [104] A. S. Gajare, K. Toyota, M. Yoshifuji, F. Ozawa, *Chem. Commun.* **2004**, 1994-1995.
- [105] A. Hayashi, T. Yoshitomi, K. Umeda, M. Okazaki, F. Ozawa, *Organometallics* **2008**, *27*, 2321-2327.
- [106] F. OZAWA, S. YAMAMOTO, S. KAWAGISHI, M. HIRAOA, S. IKEDA, T. MINAMI, S. ITO, M. YOSHIFUJI, *Chem. Lett.* **2001**, *2001*, 972-973.
- [107] T. E. Muller, K. C. Hultsch, M. Yus, F. Foubelo, M. Tada, *Chem. Rev.* **2008**, *108*, 3795-3892.
- [108] R. S. Jensen, K. Umeda, M. Okazaki, F. Ozawa, M. Yoshifuji, *J. Organomet. Chem.* **2007**, *692*, 286-294.
- [109] J. Dugal-Tessier, G. R. Dake, D. P. Gates, *Organometallics* **2007**, *26*, 6481-6486.
- [110] F. Ozawa, H. Okamoto, S. Kawagishi, S. Yamamoto, T. Minami, M. Yoshifuji, *Journal of the American Chemical Society* **2002**, *124*, 10968-10969.

- [111] H. Murakami, Y. Matsui, F. Ozawa, M. Yoshifuji, *J. Organomet. Chem.* **2006**, *691*, 3151-3156.
- [112] H. Murakami, T. Minami, F. Ozawa, *The Journal of Organic Chemistry* **2004**, *69*, 4482-4486.
- [113] R. Takita, Y. Takada, R. S. Jensen, M. Okazaki, F. Ozawa, *Organometallics* **2008**, *27*, 6279-6285.
- [114] J. Dugal-Tessier, G. R. Dake, D. P. Gates, *Org. Lett.* **2010**, *12*, 4667-4669.

# PRIYANKA GUPTA

Ph.D. Student

DOB : 26-09-1995

Place: Ghaziabad, UP, India



## RESEARCH EXPERIENCE

### Ph.D. Work | LIKAT, Rostock

**Project 1:** Exploring the utility of Phosphanylidene phosphoranes as Phosphinidene-Sources.

**Publication :** Reactivity of Phospha-Wittig Reagents towards NHCs and NHOs.

Priyanka Gupta, Jan-Erik Siewert, Tim Wellnitz, Malte Fischer, Wolfgang Baumann, Torsten Beweries, Christian Hering-Junghans, *Dalton Trans.*

**2021**, 50, 1838-1844.

DOI: <https://doi.org/10.1039/D1DT00071C>

**Project 2:** Designing Phosphaalkene based ligands and coordinating with late transition metals for their applications in homogeneous catalysis.

**Publication :** Synthesis, Coordination Chemistry, and Mechanistic Studies of P,N-Type Phosphaalkene-Based Rh(I) Complexes

Priyanka Gupta, Tobias Taeufer, Jan-Erik Siewert, Fabian Reiß, Hans-Joachim Drexler, Jola Pospech, Torsten Beweries, Christian Hering-Junghans, *Inorg. Chem.* **2022**, 61, 11639.

DOI: <https://doi.org/10.1021/acs.inorgchem.2c01158>

**Publication :** P,N-Type Phosphaalkene-based Ir(I) Complexes: Synthesis, Coordination Chemistry, and Catalytic Applications

Priyanka Gupta, Hans-Joachim-Drexler, Richard Wingad, Duncan Wass, Torsten Beweries, Christian Hering-Junghans, *Inorg. Chem. Front.*, **2023**, 10, 2285.

DOI: <https://doi.org/10.1039/D3QI00142C>

### Other Publications :

DOI: <https://doi.org/10.1002/anie.202207064>

DOI: <https://doi.org/10.1039/D2DT03703C>

### Master Dissertation | Guide - Prof. R Murugavel, IIT Bombay

**Project:** Synthesis of C3 -symmetry Urea and Thiourea linked Triphenylbenzene based Covalent Organic Frameworks and their application in Catalysis.


- Synthesized covalent organic frameworks and analyzed for surface properties using BET.
- Applied as efficient catalysts in Knoevenagel condensation reaction.

### Internship | Guide - Prof. S. Mukherjee, IISc Bengaluru [17]

**Project:** Synthesis of  $\alpha$ -fluoro nitroalkane and cinchona-derived organocatalyst.

- Synthesized cinchona-derived bifunctional organocatalyst.
- Characterized samples using nuclear magnetic resonance (NMR) and mass spectrometry.

## CONTACT

 +49 0176 83874598

 [priyanka.gupta@catalysis.de](mailto:priyanka.gupta@catalysis.de)

## EDUCATION

2020-2023

**Leibniz Institute for Catalysis,  
Rostock, Germany**  
Ph.D. in Chemistry

2016-2018

**IIT Bombay, India**  
Master in Chemistry

2013-2016

**Delhi University, Delhi, India**  
Bachelor in Chemistry

## SKILLSET

### Laboratory skills | Softwares

- Schlenk techniques.
- Synthesis of organic and inorganic products.
- Characterisation using NMR, IR, UV-VIS, SCXRD.
- Mnova, Origin, Diamond
- DFT Calculations

### Other Skills

- Blog Writing on wordpress
- You tube Channel called 'chemmunicate'
- Painting



## WORK EXPERIENCE

**HPL Additives Ltd.** | [July 2019 – Dec 2019]

- Recruited as a Research Executive for the R&D plant in Faridabad, India.
- Worked for the optimization process of chain extender and cross linking agents.

**RAO Educational Services Ltd.** | [Jan 2019 – June 2019]

- Worked as a Lecturer of chemistry for senior secondary high school students.
- Tutored them for the preparation of IIT-JEE entrance exam preparation.

## PROJECTS AND CONFERENCES

**Conferences** | Talks | Poster Presentations

- Delivered a talk at 44th International Conference on Coordination Chemistry.
- Delivered a talk at 18th European Workshop on P-Chemistry'21.
- Designed and conferred a poster at AGICHEM'21.
- Participated in the poster presentation at ACS Spring Meeting'21.
- Presented a poster at FG Wöhler Association for Inorganic Chemistry Online conference'20.
- Volunteered for a poster presentation at the Symposium on Chemical Bond Activation'20.

**28th Mid-Year Meeting** | IISC Bangaluru ['17]

- Attended a lecture on 'Killing Thrombus with Nano Bullets' by Debabrata Dash, BHU Varanasi.
- Participated in a conference with Dr. V Subramanian, CLRI, Chennai on 'Exploring the changes in the structure of peptides adsorbed on carbon and boron nitride nanomaterials.'

**Annual Chemistry Seminar** | Kirorimal college, Delhi University ['15]

- Achieved **1st position** in poster presentation on 'Edge of Ruthenium over other Elements'.
- Presented the unusual facts and anticancer properties of ruthenium.

**Gyanodya Educational Project** | Project on Wheels, Delhi University ['14]

- Project on 'Utilization of Waste Material and Urbanization' selected out of 3000+ students.
- Worked in a team of 15 students and visited five major cities of India.
- Analyzed the methodology and techniques used by Garbage Management Plant, Kanpur and Municipal Corporation House, Surat for their planning towards a smart city.

## SCHOLASTIC ACHIEVEMENTS

- Secured **All India Rank - 21** in the prestigious examination of IIT - JAM Chemistry'16.
- Felicitated by college for being in **top-3** out of 300 students in CONTECH-15 conducted by TIFR'15.
- Bestowed with a scholarship by school for securing **CGPA 10/10** in secondary CBSE Exam'11.
- Awarded a **Certificate of Merit** in All India Talent Search Examination conducted nationwide.

## EXTRA- CURRICULAR

**Department placement coordinator** | Institute Placement Team, IIT Bombay [Mar 2017 – May 2018]

- Worked as a representative & communication medium between the placement office and students.
- Conducted pre placement activities like GDs, personal interview & skill development workshops.

**Sports secretary** | Hostel 11, IIT Bombay [July 2016 -17]

- Won the overall rolling trophy in General Championship of Sports'16-17.
- Maintained sports culture in the hostel by enthusiastic participation of inmates in various sports activities.

**Social activities**

- Volunteered to teach underprivileged children at a student-driven organization, Abhyasika, IITBombay.
- Engaged into a social cause of electrifying houses of a small village 'Khapi', Gujrat powered by PEPSI.